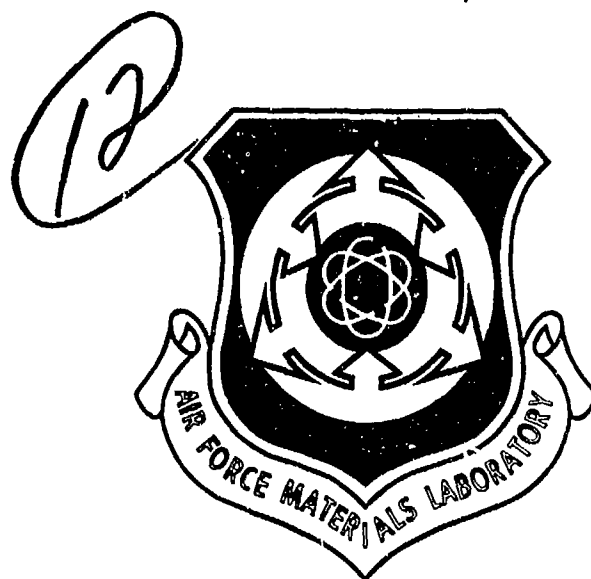


AD A 039864

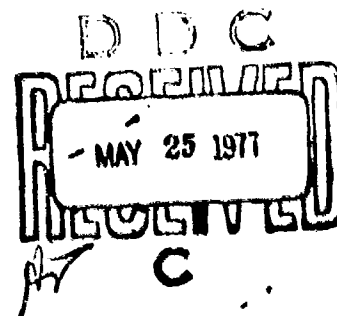
AFML-TR-76-173



## EXPLORATORY DEVELOPMENT ON DURABILITY OF ADHESIVE BONDED JOINTS

BOEING COMMERCIAL AIRPLANE COMPANY  
P.O. BOX 3707  
SEATTLE, WASHINGTON 98124

OCTOBER 1976



TECHNICAL REPORT AFML-TR-76-173  
FINAL REPORT FOR PERIOD FEBRUARY 1974 - OCTOBER 1976

Approved for public release; distribution unlimited

AD NO. \_\_\_\_\_  
DDC FILE COPY

Prepared for  
AIR FORCE MATERIALS LABORATORY  
AIR FORCE SYSTEMS COMMAND  
WRIGHT-PATTERSON AIR FORCE BASE, OHIO 45433


## NOTICE

When Government drawings, specifications, or other data are used for any purpose other than in connection with a definitely related Government procurement operation, the United States Government thereby incurs no responsibility nor any obligation whatsoever; and the fact that the government may have formulated, furnished, or in any way supplied the said drawings, specifications, or other data, is not to be regarded by implication or otherwise as in any manner licensing the holder or any other person or corporation, or conveying any rights or permission to manufacture, use, or sell any patented invention that may in any way be related thereto.

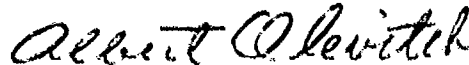
The data in this report is merely a factual presentation of the results of the particular tests performed and is not to be used, copied, or referenced for advertisement purposes.


This report has been reviewed by the Information Office (IO) and is releasable to the National Technical Information Service (NTIS). At NTIS, it will be available to the general public, including foreign nations.

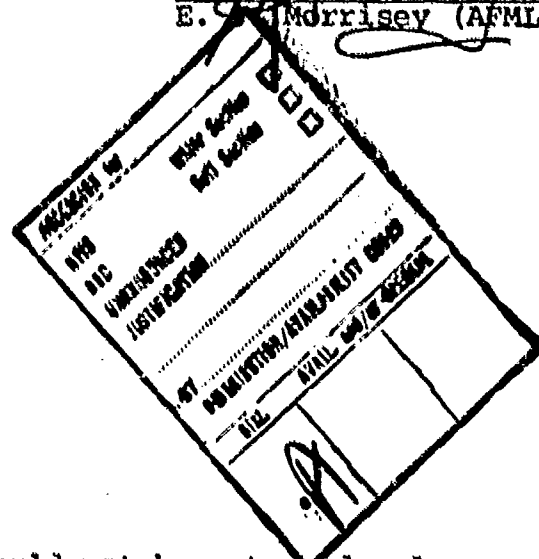
This technical report has been reviewed and is approved for publication.

  
W. M. Scardino (AFML/MXE)  
Project Engineer

FOR THE COMMANDER

  
ALBERT OLEVITCH, Chief  
Materials Engineering Branch  
Systems Support Division

  
E. J. Morrissey (AFML/MXE)



Copies of this report should not be returned unless return is required by security considerations, contractual obligations, or notice on a specific document.

UNCLASSIFIED

SECURITY CLASSIFICATION OF THIS PAGE (When Data Entered)

REPORT DOCUMENTATION PAGE		READ INSTRUCTIONS BEFORE COMPLETING FORM	
1. REPORT NUMBER AFML-TR-76-173	2. GOVT ACCESSION NO.	3. RECIPIENT'S CATALOG NUMBER	
4. TITLE (and Subtitle) Exploratory Development on Durability of Adhesive Bonded Joints.		5. TYPE OF REPORT & PERIOD COVERED Final Report, 1 Feb 74 - Oct 76,	
6. AUTHOR(s) J. A. Marceau J. C. McMillan		7. PERFORMING ORG. REPORT NUMBER D6-41317-2	
9. PERFORMING ORGANIZATION NAME AND ADDRESS Boeing Commercial Airplane Company P.O. Box 3707 Seattle, Washington 98124		8. CONTRACT OR GRANT NUMBER(s) Air Force AF 33615-74-C-5065	
11. CONTROLLING OFFICE NAME AND ADDRESS Air Force Materials Laboratory Air Force Systems Command Wright-Patterson AFB, Ohio 45433		10. PROGRAM ELEMENT, PROJECT, TASK AREA & WORK UNIT NUMBERS Project 7381/Task 738106 W.O. No. 73810682	
14. MONITORING AGENCY NAME & ADDRESS (if different from Controlling Office)		12. REPORT DATE Oct 76	
		13. NUMBER OF PAGES 12 164p.	
		15. SECURITY CLASSIFICATION UNCLASSIFIED	
		15a. DECLASSIFICATION/DOWNGRADING SCHEDULE NA	
16. DISTRIBUTION STATEMENT (of this Report) Approved for public release; distribution unlimited.			
17. DISTRIBUTION STATEMENT (of the abstract entered in Block 20, if different from Report)			
18. SUPPLEMENTARY NOTES			
19. KEY WORDS (Continue on reverse side if necessary and identify by block number) Adhesives Thick-adherend lap shear Durability Thick-adherend double cantilever beam Test methods Thick-adherend single cantilever beam Surface preparation Wedge test Adherend Stressed-durability -Static and Cyclic			
20. ABSTRACT (Continue on reverse side if necessary and identify by block number) The objectives of the program were to evaluate stressed durability test methods, to use these methods to test adhesive bonding materials and processes, and to develop a correlation between laboratory test results and in-service performance. The test method evaluation was completed early in the program and results were published in an interim technical report, AFML-TR-75-3, Durability of Adhesive Bonded Joints, February 1975.			

DD FORM 1 JAN 73 1473

EDITION OF 1 NOV 65 IS OBSOLETE

UNCLASSIFIED

SECURITY CLASSIFICATION OF THIS PAGE (When Data Entered)

CTB 314115

UNCLASSIFIED

SECURITY CLASSIFICATION OF THIS PAGE(When Data Entered)

20. ABSTRACT (Continued)

Four stressed durability test methods were selected for the test program:

- (1) A thick-adherend lap-shear specimen (Mode I and Mode II loading);
- (2) A thick-adherend double cantilever beam (DCB) specimen (Mode I loading);
- (3) A thin adherend DCB specimen (wedge test, Mode I loading);
- (4) A thick adherend single cantilever beam (SCB) specimen for honeycomb sandwich evaluation (Mode I and Mode II loading).

Alloy, adherend surface treatment, adhesive primer, and adhesive interactions were evaluated.

The materials and processes used were:

- (1) Alloys: 2024-T3, 2024-T3 clad (1230 alloy), 7075-T6, and 7075-T6 clad (7072 alloy);
- (2) Adhesives: FM 123-2 and EA 9628 250°F curing adhesives, and AF 143 and PL 729-3 350°F curing adhesives;
- (3) Primers: BR 123 non-corrosion-inhibiting primer, BR 127 corrosion-inhibiting primer, and EC 3917 and PL 728 corrosion-inhibiting primers for use with the two 350°F curing adhesives;
- (4) Adherend surface treatment processes: Optimized FPL etch, chromic acid anodize, and phosphoric acid anodize;
- (5) Aluminum honeycomb core: Standard core, Dura-Core and CR III corrosion-resistant cores, and phosphoric acid anodized core.

Results of this investigation have shown that:

1. Two basically different test specimen configurations are required to assess adhesive bonded joint durability performance, one that emphasizes combined Mode I and II loading and one that evaluated Mode I loading only.
2. Cyclic loading of bonded joints is more damaging to the bondlines than steady-state loading.
3. Phosphoric acid anodized adherend surfaces showed the best over-all durability performance in both metal-to-metal bonds and honeycomb core bonds.
4. The presence of clad in the bondline increases the tendency for crevice corrosion.
5. Corrosion-inhibiting primers (CIAP) improved the stressed durability performance of bonded specimens over that of the non-corrosion-inhibiting primer. CIAP did not prevent crevice corrosion.
6. A laboratory test/in-service performance correlation has been demonstrated under Mode I loading conditions.

Continued study of stressed durability has been recommended to better understand how this information can be applied to design of critical load-carrying aircraft structure.

\*Mode I: Opening mode (cleavage)

Mode II: Forward shear (edge sliding)

SECURITY CLASSIFICATION OF THIS PAGE(When Data Entered)

## FOREWORD

This technical report was prepared by the Boeing Materials Technology Unit, Boeing Commercial Airplane Company, Renton, Washington, under USAF contract F33615-74-C-5065, Project FY-1457-00616/7381. The program was administered by the Systems Support Division of the Air Force Materials Laboratory, with Mr. W. M. Seardino (AFML/MXE) as project engineer. An interim technical report under the same contract covering the period 1 February 1974 to 1 July 1974 was published in February 1975 as AFML-TR-75-3 "Durability of Adhesive Bonded Joints."

Mr. J. A. Marceau is the principal investigator and Mr. J. C. McMillan is the program manager. The authors wish to acknowledge the efforts of F. E. Coverson and T. Gaines of Boeing Materials Technology and T. Kane of Boeing Structural Testing Laboratory.

## TABLE OF CONTENTS

	Page
1.0 INTRODUCTION . . . . .	1
2.0 SYNOPSIS OF PHASE I AND PHASE II RESULTS . . . . .	6
2.1 Stressed Durability Test Methods . . . . .	6
2.2 Adherend Surface Preparation . . . . .	7
3.0 PHASE III RESULTS . . . . .	9
3.1 Nondestructive Inspection (NDI) of Bonded Assemblies . . . . .	11
3.2 Verification of Test Methods (Task 1) . . . . .	11
3.2.1 Sustained-Stress Thick-Adherend Lap-Shear Tests . . . . .	11
3.2.2 Sustained-Stress Thick-Adherend DCB Tests . . . . .	16
3.2.3 Final Justification of Test Methods . . . . .	18
3.3 Influence of Test Temperature (Task 6) . . . . .	19
3.4 Effect of Test Duration on Sustained-Stress Tests (Tasks 2, 3, 5, and 10) . . . . .	20
3.4.1 Thick-Adherend Lap-Shear Tests (Task 2) . . . . .	20
3.4.2 Thick-Adherend DCB Tests . . . . .	22
3.4.3 Honeycomb SCB Tests (Tasks 5 and 10) . . . . .	23
3.5 Cyclic Stress Tests (Tasks 4 and 8) . . . . .	26
3.5.1 Thick-Adherend Lap-Shear Cyclic Load Tests . . . . .	26
3.5.2 Thick-Adherend DCB Cyclic Load Tests (Task 8) . . . . .	30
3.6 Durability Testing in Salt Spray (Task 9) . . . . .	33
3.7 Lab Test/In-Service Correlation (Task 7) . . . . .	38
3.7.1 Durability Testing of Commercial Aircraft . . . . .	38
3.7.2 Durability Testing of Air Force Aircraft . . . . .	41
4.0 PHASE IV, SPECIMENS FOR OUTDOOR EXPOSURE . . . . .	47
5.0 DISCUSSION . . . . .	48
5.1 Stressed Durability Test Methods . . . . .	48
5.2 Long-Term Environmental Effects . . . . .	48
5.3 Stressed Durability of Clad and Bare Alloys . . . . .	51
5.4 Inservice Behavior and Stressed Durability Test Correlations . . . . .	53
5.5 Optimum Temperature for Stressed Durability Tests . . . . .	53
5.6 Documenting Test Methods . . . . .	54
5.7 General Discussion . . . . .	55
5.7.1 Durability of Honeycomb Sandwich Construction . . . . .	55
5.7.2 Corrosion-Inhibiting Adhesive Primers . . . . .	55
5.7.3 Adherend Surfaces . . . . .	56
5.7.4 Adhesives . . . . .	56
6.0 CONCLUSIONS . . . . .	57
6.1 Stressed Durability Test Methods . . . . .	57
6.2 Long-Term Environmental Effects . . . . .	57

PRECEDING PAGE BLANK NOT FILMED

## TABLE OF CONTENTS (Continued)

	Page
6.3 Stressed Durability of Clad and Bare Alloys . . . . .	58
6.4 Inservice Behavior and Stressed Durability Test Correlations . . . . .	58
6.5 Optimum Temperature for Stressed Durability Tests . . . . .	58
6.6 Documenting Test Methods . . . . .	58
6.7 General Conclusions . . . . .	59
 7.0 RECOMMENDATIONS . . . . .	 60
7.1 Stressed Durability Test Methods . . . . .	60
7.2 Stressed Durability of Clad and Bare Alloys . . . . .	60
 8.0 REFERENCES . . . . .	 61
 GLOSSARY . . . . .	 63
 APPENDIX A NONDESTRUCTIVE INSPECTION (NDI) OF BONDED TEST ASSEMBLIES . . . . .	 139
 APPENDIX B LOADING VALIDITY OF MODIFIED STRESS CORROSION JIG	 144
 APPENDIX C WEDGE TEST FOR ADHESIVE BONDED SURFACE DURABILITY OF ALUMINUM . . . . .	 151

## LIST OF ILLUSTRATIONS

No.		Page
1	Loading Modes Possible in Bonded Materials . . . . .	65
2	Thick-Adherend Machined Lap-Shear Specimen . . . . .	65
3	Thick-Adherend DCB Specimens . . . . .	66
4	Thin-Adherend DCB Specimen (Wedge Test) . . . . .	68
5	Thick-Adherend SCB Specimen . . . . .	69
6	Thick-Adherend Lap-Shear Modified Loading Fixture . . . . .	70
7	Environmental Exposure Chamber for 140° F/Condensing Humidity, Showing Arrangement of DCB and Stressed Lap-Shear Specimens . . . . .	70
8	Typical Thick-Adherend Lap-Shear Specimen Failures for Sustained-Stress Tests Exposed to 140° F/Condensing Humidity . . . . .	71
9	DCB Specimen Exposure Results . . . . .	72
10	Opened DCB Specimens Bonded with PL 729-3/PL 728 . . . . .	78
11	Opened DCB Specimens Bonded With AF 143/EC 3917 System . . . . .	80
12	Opened DCB Specimens Bonded With FM 123-2/BR 127 System . . . . .	82
13	Opened DCB Specimens Bonded With EA 9628/BR 127 System . . . . .	84
14	Influence of Test Temperature on DCB Specimen . . . . .	86
15	Influence of Long-Term Exposure on DCB Specimen . . . . .	88
16	Influence of Adhesive Primers on DCB Specimen . . . . .	91
17	Typical Failure Modes and Filiform Corrosion in Bondlines of DCB Specimens Comparing CIAP and non-CIAP Primers After 82 Weeks Exposure to 40° F/Condensing Humidity . . . . .	93
18	Influence of Honeycomb Core and Face Sheet Surface Treatments on Environmental Durability . . . . .	94
19	Failure Modes in the Pretest, Test, and Posttest Areas of SCB Specimens Bonded with EA 9628 and Exposed to 140° F/Condensing Humidity . . . . .	97
20	Load Profiles for Slow Cyclic Loading of Lap-Shear Specimens . . . . .	99
21	Cyclic Load Machine for Lap-Shear Durability Testing . . . . .	100
22	Typical Examples of Failure Modes for Slow Cycle Fatigue (0.8 and 10 cph) . . . . .	100
23	Comparisons of Slow Cyclic Fatigue for 0.8 cph (Bell) and 10 cph . . . . .	101
24	Fatigue Test Arrangement for Thick-Adherend Lap-Shear Specimens (Environmental Chamber Surrounds the Specimen.) . . . . .	102
25	Fast Cycle Stress Results . . . . .	103
26	Failure Mode Characteristics of Thick Adherend Lap Shear Specimens Tested at 1800 cpm, R = 0.06, . . . . .	108
27	Typical Lap-Shear Failures at 1800 cpm, 2024-T3 Bare Bonded With EA 9628/BR 127, . . . . .	109
28	Topographical Features Which Appear To Be Fatigue Striations at Adhesive-Primer Interface Zone . . . . .	110
29	Fast Cyclic Load Machine for DCB Specimens . . . . .	111
30	Slow Cyclic Load Machine for DCB Specimens . . . . .	112
31	Cyclic Crack Growth Rate Data . . . . .	113
32	Fracture Appearances From Cyclic Loading of DCB Specimens EA 9628/ BR 127 Adhesive Primer System, . . . . .	118

## LIST OF ILLUSTRATIONS (Continued)

No.		Page
33	Wedge Test Specimens Exposed to 5% Salt Spray . . . . .	119
34	Specimen Configuration for Commercial Aircraft A . . . . .	124
35	Specimen Configuration for Commercial Aircraft B . . . . .	125
36	Specimen Configuration for Commercial Aircraft C . . . . .	126
37	Specimen Configuration for Commercial Aircraft D . . . . .	127
38	Sustained-Stress Lap-Shear Results of Specimens Machined From Aircraft A and B Components . . . . .	128
39	Wedge Test Results of Specimens Machined From Aircraft A and B Components . . . . .	129
40	Section of Aircraft C Component Showing Areas Where Test Specimens Were Taken . . . . .	130
41	Wedge Test Results of Specimens Machined From Aircraft C and D Components . . . . .	131
42	Typical Wedge Test and Peel Test Specimens From Aircraft C . . . . .	131
43	Typical Bonded Honeycomb Panel With Closeouts From Air Force Aircraft . . . . .	132
44	Typical Cross Section of Honeycomb Structure With Tapered Closeout . . . . .	132
45	Configurations of Specimens Fabricated From Air Force Aircraft Details . . . . .	133
46	Wedge Test Results of Specimens Machined From Air Force Aircraft . . . . .	134
47	Sustained-Stress Thick-Adherend Lap-Shear Time-to-Failure Results . . . . .	136
48	Comparison of Bonded Aluminum Fatigue Crack Growth Data With Published Data for Fatigue Crack Growth in Aluminum Alloys . . . . .	137
A-1	Neutron Radiograph of Laminated 2024-T3 Clad Panel Section for Thick-Adherend DCB Specimens Showing Voids in One or More Bondlines . . . . .	140
B-1	Lap-Shear Loading Fixture for Sustained Stress Durability Testing . . . . .	144
B-2	Strain Gage Location on Thick-Adherend Lap-Shear Specimen . . . . .	145
B-3	Thick-Adherend Lap-Shear Modified Loading Fixture . . . . .	147
C-1	Crack Extension Specimen Configuration . . . . .	153

## LIST OF TABLES

No.		Page
1	Phase III Test Matrix . . . . .	3
2	Rationale for Selection of Materials, Processes, and Test Environments . . . . .	9
3	Detailed Processing Description . . . . .	10
4	Baseline Shear Strengths - Room Temperature . . . . .	12
5	Sustained Stress Test Results: Thick-Adherend Lap-Shear Specimens, Phosphoric Acid Anodize . . . . .	13
6	Sustained Stress Test Results: Thick-Adherend Lap-Shear Specimens, Chromic Acid Anodize . . . . .	14
7	Sustained Stress Test Results: Thick-Adherend Lap Shear Specimens, FPL Etch . . . . .	15
8	Long-Term Sustained Stress Test Results (9 Months)-Thick-Adherend Lap-Shear Specimens, Phosphoric Acid Anodize . . . . .	21
9	Materials and Processes Used for Single Cantilever Beam (SCB) Specimens . . . . .	24
10	Slow Cyclic Stress Test Results: Thick-Adherend Lap-Shear Specimens, Phosphoric Acid Anodize . . . . .	27
11	Slow Cyclic Stress Test Results: Thick-Adherend Lap-Shear Specimens, Phosphoric Acid Anodize . . . . .	28
12	Bondment Variables for Salt Spray Tests . . . . .	33
13	Durability Testing in Salt Spray, Surface Preparation: Phosphoric Acid Anodize . . . . .	35
14	Durability Testing in Salt Spray, Surface Preparation: Chromic Acid Anodize . . . . .	36
15	Durability Testing in Salt Spray, Surface Preparation: FPL Etch . . . . .	37
16	Commercial Aircraft Bonded Details . . . . .	38
17	Test Results: Commercial Aircraft . . . . .	40
18	Air Force Aircraft Bonded Details . . . . .	41
19	Residual Room Temperature Peel and Shear Strength: Air Force Aircraft Bondments . . . . .	43
20	Thick-Adherend DCB Test Results: Air Force Aircraft Bonded Details . . . . .	45
21	Materials and Processes for Phase IV Specimens . . . . .	47
22	Comparisons of Potential Differences Between Cladding and Core for 2024 and 7075 . . . . .	52
A-1	Nondestructive Inspection (NDI) of Bonded Metal-to-Metal Assemblies . . . . .	141
A-2	Nondestructive Inspection (NDI) of Bonded Honeycomb Sandwich Assemblies . . . . .	143
B-1	Strain Gage Measurements of Thick-Adherend Lap-Shear Specimens . . . . .	146
B-2	Strain Gage Measurements of Lap-Shear Specimens in Modified Loading Fixture . . . . .	148
B-3	Bending Moments of Lap-Shear Specimens at 750 lb Load . . . . .	150

## 1.0 INTRODUCTION

The performance of bonded joints in aircraft structure has varied in both military and commercial applications. For the most part, bonded structure has provided excellent service performance over many years; however, some bonded parts have experienced disbond with varying degrees of subsequent bondline corrosion after relatively short service exposure.

Traditional test and performance evaluation methods have not been capable of precluding disbonding and corrosion in service, and as a result serious questions concerning the reliability of bonding have been raised. The traditional test methods generally encompass three areas: (1) lap-shear testing as a function of temperature, (2) peel testing as a function of temperature, and (3) exposure of unstressed lap-shear specimens to various environments for relatively short periods of time (e.g., 30 days) before testing. An examination of the fractured traditional test specimens shows that these tests do not duplicate the features characteristic of service disbands.

In recent years, it has been found that testing bonded joints under a sustained stress while simultaneously exposing the specimens to warm/wet environments results in failures of the bond at stresses far below the ultimate stress measured at the exposure temperature. This type of stressed durability test is capable of showing differences in performance between adhesive systems and various process parameters. In addition, the failure modes of improperly processed bondments tested in this manner have an appearance characteristic of service disbands; i.e., interfacial failures.

The objectives of this contract were to:

1. Determine a sound method of evaluating stressed durability of adhesively bonded structural aluminum materials, including an assessment of the merits of cyclic versus steady-state stress testing and of the effect load profile has on stressed durability testing.
2. Evaluate the long-term effects of environment on stressed adhesive bonds in metal-to-metal (aluminum-to-aluminum) and aluminum honeycomb sandwich constructions.
3. Determine the difference in stressed environmental durability between clad and bare aluminum alloys.
4. Assess the correlation between inservice behavior of adhesively bonded aircraft assemblies and stressed durability tests.
5. Determine the optimum temperature for performing stressed durability tests of structural aerospace adhesives.
6. Develop or perfect stressed durability tests for metal-to-metal and sandwich specimens and document these in ASTM test method format.

The program was conducted in four phases:

- Phase I Literature survey
- Phase II Selection of durability test methods
- Phase III Stressed durability testing of metal-to-metal bonds and metal honeycomb sandwich
- Phase IV Specimens for outdoor exposure

Phases I and II were completed early in the program, and these results have been published in Air Force Technical Report AFML-TR-75-3 (ref 1).

Phase III consisted of 10 tasks, which were the main effort of the program and were designed to meet the preceding objectives. The specific tasks were as follows:

- Task 1 Verification of test methods
- Task 2 Influence of test duration
- Task 3 Verification of corrosion-inhibiting primer (CIAP) contribution
- Task 4 Influence of cyclic loading
- Task 5 Application of test method to honeycomb sandwich
- Task 6 Influence of test temperature
- Task 7 Lab test/in-service correlation
- Task 8 Cyclic stress durability of bonded systems
- Task 9 Durability testing in salt spray
- Task 10 Additional honeycomb cores for honeycomb sandwich tests

The test matrix for each of these tasks, including the total number of specimens tested, is shown in table 1.

Phase IV consisted of providing the Air Force with test specimens.

The following sections present a brief summary of the Phase I and Phase II results (reported in ref. 1), and detailed results of Phase III, with a discussion of these results.

Table 1.—Phase III Test Matrix

Phase III—Stress relaxation testing of metal-to-metal and metal-to-polymer bonds	Adhesive/ primer	Surface preparations	Adherends	Specimen configurations	Stress levels psi	Static or cyclic load profile	Environment	Specimen replication	Total number of specimens
<b>Task 1</b> Verification of test method	1 FM 123.2/ER 127 2 EA 9628/ER 127 3 AF 143.1C 3917 4 PL 728.3/PL 728	1 FPL etch 2 Chromic acid anodize 3 Phosphoric acid anodize	1 2024-T3 clad 2 2024-T3 bare 3 7075-T6 clad 4 7075-T6 bare	1 Thick-adherend lap shear 2 Thick-adherend double cantilever beam, DCB	1 900 2 1500	Static	140°F/condensing humidity (CH)	3	288
<b>Task 2</b> Verification of test method	1 FM 123.2/ER 127 2 EA 9628/ER 127 3 AF 143.1C 3917 4 PL 728.3/PL 728	Phosphoric acid anodize	1 2024-T3 clad 2 2024-T3 bare	1 Thick-adherend lap shear	1 600 2 900 3 1200 4 1500	Static	140°F/condensing humidity (CH)	6	192
<b>Task 3</b> Verification of OAP primer specification	1 FM 123.2/ER 127 2 FM 123.7/ER 123 (metal OAP)	1 Chromic acid anodize 2 Phosphoric acid anodize	1 2024-T3 clad 2 2024-T3 bare	2 Thick-adherend DCB		Static	140°F/CH	6	48
<b>Task 4</b> Verification of cyclic load	1 EA 9628/ER 127 2 AF 143.1C 3917	Phosphoric acid anodize	1 2024-T3 clad 2 2024-T3 bare	Thick-adherend lap shear	1 600 2 900 3 1200 4 1500	1 Bell Cycle 1 1/4 hr un- loaded 2 Boeing Cycle (0.8 cph) 4 min loaded 2 min un- loaded (10 cph)	1 140°F/CH (adhesive 1) 2 160°F/CH (adhesive 2)	6	160
<b>Task 5</b> Verification of test method for metal-to-metal bonds	1 FM 123.2/ER 127 2 EA 9628/ER 127 3 AF 143.1C 3917	Face Sheet 1 Chromic acid anodize 2 Phosphoric acid anodize H.C. Core 1 Dura Core 1 2 Phosphoric acid anodize core	Face Sheet 2024-T3 bare H.C. Core 5052	Thick-adherend single cantilever beam, SCB		Static	1 140°F/CH (adhesives 1 and 2) 2 160°F/CH (adhesives 3 and 4)	2	24
<b>Task 6</b> Verification of test method	1 FM 123.2/ER 127 2 EA 9628/ER 127 3 AF 143.1C 3917	Phosphoric acid anodize	2024-T3 bare	Thick-adherend DCB		Static	1 120°F/CH 2 160°F/CH	6	48

Table 1.—(Continued)

Phase III—Strength durability testing of metal to metal and metal to polymer	Adhesive/ primer	Surface preparations	Adherends	Specimen configurations	Stress levels psi	Static or cyclic load profile	Environment	Specimen replication	Total number of specimens
<p><b>Task 2</b> Lab test on test piece conformity</p>	<p><b>Commercial Adhesive:</b> 1 AF 125EC 2320 2 F10 123-2/BR 123</p>	<p>FPL etch</p>	<p>2024-T3 clad</p>	1 Thin-adherent lap shear	1 Ultimate		Room temperature		22
				2 Ports shear	2 300	Static	140°F/CH		23
				3 Climbing drum peel	Ultimate		Room temperature		47
				4 Thin-adherent DCB, wedge test	Ultimate	Static	Room temperature 120°F and 140°F CH		2
	<p><b>A-1 Force Augment:</b> 1 AF 110 2 F10 52 3 F10 123-2</p>	<p>FPL etch</p>	<p>2024 T3 clad</p>	1 Thick-adherent lap; shear	1 Ultimate		Room temperature		48
				2 Thick-adherent DCB	2 1500	Static	1 140°F/CH (adhesive 1) 2 160°F/CH (adhesive 2)		7
				3 Thin-adherent DCB, wedge test		Static	1 140°F/CH (adhesive 1) 2 160°F/CH (adhesive 2)		9
				4 Climbing drum peel		Static	1 140°F/CH (adhesive 1) 2 160°F/CH (adhesive 2)		30
	<p><b>EA 9670-BR 127</b></p>	<p>1 Chromic acid anodize 2 Phosphoric acid anodize 3 Phosphoric FPL etch</p>	<p>1 2024 T3 bare 2 7075 T6 bare</p>	1 Thick-adherent lap shear	Ultimate		Room temperature		16
				2 Thin-adherent DCB	2000 to 3300	1800 cpm at R = 0.06	1 75°F/dry 2 75°F/wet 3 140°F/dry 4 140°F/wet		80
<p><b>Task 1</b> Cyclic stress durability and endurance systems</p>	<p>EA 9670-BR 127</p>	<p>1 Chromic acid anodize 2 Phosphoric acid anodize 3 Phosphoric FPL etch</p>	<p>1 2024 T3 bare 2 7075 T6 bare</p>	1 Thick-adherent DCB		1 Bell Cycle 1 hr loaded 1/4 hr un- loaded (0.8 cph) 2 Boering Cycle 3 sec loaded 3 sec un- loaded (10 cpm) 3 1800 cpm	1 75°F/dry 2 75°F/wet 3 140°F/dry 4 140°F/wet		66

Table 1.-(Continued)

Specimen description and material properties	Adhesives	Surface preparations	Adherends	Specimen configurations	Stress levels psi	Static or cyclic load profile	Environment	Specimen replication	Total number of specimens
Type 9 Corrosive testing in salt spray	1 FM 123 2 BR 123 2 FM 123 2 BR 123 3 EA 9028 2R 123	1 Q-simulated EPL etch 2 Chromic acid anodize 3 Phosphoric acid anodize	1 2024-T3 clad 2 2024-T3 bare 3 7075-T6 clad 4 7075-T6 bare	Thin adherend DCB, wedge test		Static	5% salt spray at 95°F	5	120
Type 10 Acetic acid honeycombs coated for test methods of honeycombs standards	EA 9028 BR 123	Face Sheet Phosphoric acid anodize H.C. Core 1 CR III core 2 Standard core	Face Sheet 2024-T3 bare H.C. Core 5052	Thick adherend SCB		Static	140°F/CH	2	4

\* FM 123 2 1250°F cure, old technology adhesive  
BR 123 1250°F cure, new technology primer  
EA 9028 1250°F cure, old technology primer  
FM 123 1250°F cure, old technology adhesive  
EA 9028 1250°F cure, new technology adhesive

AF 143 1250°F cure, new technology adhesive  
EC 3317 1250°F cure, new technology primer  
AF 123 1250°F cure, old technology adhesive  
EC 2228 1250°F cure, old technology primer  
AF 123 1250°F cure, old technology adhesive  
PL 123 1250°F cure, new technology adhesive  
PL 123 1250°F cure, new technology primer

b Dual Cure 1 Contamination-resistant core from American Cyanamid Co.  
CR III core Contamination-resistant core from Hexion Corp., Dublin, California 94566  
Surface 3 core Non-corrosion resistant core from American Cyanamid Co. or Hexion Corp.  
Phosphoric acid anodize core Standard core that has been anodized

American Cyanamid Company, Bloomington Department,  
Huntsville, Alabama 35894

Hycol Division of the Dexter Corporation,  
2850 Wilson Pike Road, Pittsburg, California 94565

Minnesota Mining and Manufacturing Company,  
St. Paul, Minnesota 55101

B.F. Goodrich General Products Co., A Division of the B.F. Goodrich Co.,  
500 South Main Street, Akron, Ohio 44318

## 2.0 SYNOPSIS OF PHASE I AND PHASE II RESULTS<sup>1</sup>

The purpose of Phase I was to review the literature and to survey adhesive manufacturers, prime aerospace contractors, and any other pertinent sources to determine currently used methods of stressed exposure durability testing and practices relative to the types of aluminum adherends presently being used or contemplated for use in adhesively bonded aerospace structure. The purpose of Phase II was to assess the various durability test methods and select the methods for use in Phase III of this program. In addition, surface preparation processes were to be assessed and three selected for use in Phase III.

More than 700 references (articles and abstracts) were reviewed. These references included such categories as test methods, specimen stress analyses, failure mechanisms, adherend surface preparation, environmental effects on bonds and adhesives, corrosion, and service failure analyses.

### 2.1 STRESSED DURABILITY TEST METHODS

Assessment of the reported test results revealed that a sustained stress applied to the bondline when the specimen is simultaneously exposed to an aqueous environment causes some degree of damage to occur. The degree of damage within the bond is a function of the stress level, availability of water, temperature, and adhesive system.

Assessment of the test methods described in the literature revealed that all the specimen configurations, when stressed, have a load component normal to the bond plane present at the load transfer edge of the joint. This loading mode is known as Mode I (opening mode). (See fig. 1.) Most specimen configurations that are cantilevered, peeled, or under flatwise tension are exposed primarily to Mode I. Most other configurations have shear as the primary loading mode and Mode I as the secondary mode. This type of shear is known as Mode II (forward shear). (See fig. 1.) A third loading mode known as Mode III (sidewise shear, fig. 1) is not present in any of the test configurations reviewed.

Selection of test methods and specimen configurations for Phase III was based on the following criteria:

1. The test specimens must relate to real structure loading modes.
2. Mode I loading must be controllable.
3. Mode II loading must be controllable.
4. The test method must yield quantitative results and not be subjective. A secondary goal was to provide a specimen that might be used in the future to relate a finite element stress analysis of the test specimen configuration to a similar analysis of real structure.

<sup>1</sup>Reported in AFML-TR-75-3 (ref 1)

5. Fabrication of specimens must be reasonable, i.e., specimens must be relatively simple, must not require unusually close dimensional tolerances, and fabrication costs must be low for programs involving large numbers of test specimens.

Based on these criteria, the four following specimens were selected as the most suitable for meeting the objectives of the program. These configurations relate best to the two loading modes present in most test specimen configurations and in real structure.

- Thick-adherend machined lap-shear specimen.—These specimens are machined from two bonded 1/4-in.-thick aluminum plates. The specimens are 1 in. wide and 7 in. long, with a 1/2-in. overlap machined in the middle. (See fig. 2.)
- Thick-adherend double cantilever beam (DCB) specimen.—These specimens are machined from two bonded 1/2-in.-thick aluminum plates (or four bonded 1/4-in. plates for clad alloys, which are commonly available only up to 1/4-in. thick). The specimens are 1 by 1 by approximately 14 in. (See fig. 3.)
- Thin-adherend DCB specimen ("wedge test").<sup>1</sup> These specimens are cut from 6- by 6-by 1/8-in. panels bonded together. The specimens are 1 by 6 by 1/4 in. (See fig. 4.)
- Thick-adherend single cantilever beam (SCB) specimen.—These specimens are cut from bonded sandwich assemblies. The specimens are 3 in. wide and approximately 14 in. long with a 1/2-in.-thick test face sheet. (See fig. 5.)

With the exception of the thick-adherend lap-shear specimen, the preceding specimens do not require fixtures or external loading to maintain the sustained stress; i.e., they are self-contained. To apply the desired sustained stress to the lap-shear specimen, a portable loading fixture was used. (See fig. 6.)

## 2.2 ADHEREND SURFACE PREPARATION

The criteria used in assessing and selecting the surface preparation processes for use in this program were:

1. Processes which have gained acceptance throughout the industry after many years of service history.
2. Processes which represent new technology as related to environmental durability performance of bonded systems.

Based on these criteria, the following three surface treatments were selected for the program:

1. Boeing FPL etch process, BAC 5514, revision F

<sup>1</sup>The thin-adherend wedge test specimen was not accepted during Phase II but was subsequently added to the program because of the need for a very inexpensive, qualitative test specimen.

2. Bell Helicopter chromic acid anodize process, BPS FW 4352, revision G
3. Boeing-developed phosphoric acid anodize process, BAC 5555

The FPL etch and the chromic acid anodize processes have gained wide acceptance throughout the industry and have many years of service history. It should be noted, however, that the FPL etch specified in the BAC 5514, revision F process includes process controls and test requirements that are in excess of those normally applied in the industry. This process is sometimes called "optimized" FPL etch. The parameters for the "optimized" FPL etch have been submitted to ASTM for membership approval to update ASTM standard D2651-67 (1973), "Standard Recommended Practice for Preparation of Metal Surfaces for Adhesive Bonding." The phosphoric acid anodize process is an example of new technology surface preparation.

### 3.0 PHASE III RESULTS

Specimen configurations, with the exception of the thin-adherend wedge specimen, and prebond surface preparations to be used in Phase III were selected in Phases I and II. At the onset of Phase III, alloys, adhesives, and test environments were selected. These are listed in table 2 along with the criteria for their selection. Details of processes used in curing adhesives and primers and applying surface preparations are described in table 3.

*Table 2.—Rationale for Selection of Materials, Processes, and Test Environments*

Subject	Criteria	Selection
<u>Materials</u> Aluminum alloys	Representative of alloys commonly used in aerospace bonding	2024-T3 clad (1230 cladding alloy) 2024-T3 bare 7075-T6 clad (7072 cladding alloy) 7075-T6 bare
Adhesives	250°F cure current technology 250°F cure new technology with improved stressed durability 350°F cure new technology of current interest to the Air Force	FM 123-2 (10 mil film thickness) EA 9628 (10 mil film thickness) AF 143 (15 mil film thickness) PL 729-3 (15 mil film thickness)
Primers	250°F use non-CIAP primer, old technology 250°F cure corrosion-inhibiting adhesive primer (CIAP), new technology 350°F cure CIAP new technology	BR 123 for use with FM 123-2 BR 127 for use with FM 123-2 and EA 9628 EC 3917 for use with AF 143 PL 728 for use with PL 729-3
<u>Processes</u> Metal prebond surface treatments	Processes that have gained acceptance throughout the industry with years of service history  Processes that represent new technology related to durability performance of bonded systems	FPL etch, Boeing, BAC 5514, Rev. F  Chromic acid anodize, Bell Helicopter, BPS FW 43-62, Rev. G, Method 1A Phosphoric acid anodize, Boeing, BAC 5555
<u>Environments</u> Warm, wet test exposure conditions  Corrosive	Representative of moderate to severe conditions that exist in aircraft environments, e.g., elevated temperature and high humidity  Corrosive environment	120°F/condensing humidity 140°F/condensing humidity 160°F/condensing humidity  5% salt spray at 95°F

Table 3.—Detailed Processing Description

Material/process	Processing details	
<u>Adhesives</u> FM 123-2 EA 9628	Temperature rise:	5-6°F/min
	Cure:	225°-250°F for 90 min
	Pressure:	Metal-to-metal, 50 and 100 psi <sup>a</sup> Honeycomb, 35 psi
AF 143 PL 729-3	Temperature rise:	5-6°F/min
	Cure:	340° to 360°F for 60 min
	Pressure:	Metal-to-metal, 50 and 100 psi <sup>a</sup> Honeycomb, 35 psi
<u>Primers</u> BR 123	Application:	Spray
	Cure:	(Noncuring) air dry a minimum of 1 hr at room temperature
	Thickness:	Less than 0.0002 in. but visible
BR 127	Application:	Spray
	Cure:	Air dry 1/2 hr, then cure at 250°F for 1 hr
	Thickness:	0.0001-0.0004 in.
EC 3917	Application:	Spray
	Cure:	Air dry 1/2 hour, then cure at 250°F for 1 hr
	Thickness:	0.0001-0.0004 in.
PL 728	Application:	Spray
	Cure:	Air dry 2 hr minimum at room temperature
	Thickness:	0.0001-0.0004 in.
<u>Surface preparation</u> FPL etch	1	Alkaline clean 10 min and rinse 5 min in tap water, 110°F minimum <sup>b</sup>
	2	Deoxidize 12-15 min at 150°-160°F in: Na <sub>2</sub> Cr <sub>2</sub> O <sub>7</sub> · 2H <sub>2</sub> O - 4.1 to 12.0 oz/gal H <sub>2</sub> SO <sub>4</sub> 66° BE - 38.5 to 41.5 oz/gal Aluminum (2024 bare) - 0.20 oz/gal of dissolved aluminum minimum Water - balance
	3	Rinse 5 min in tap water and dry at 140°F maximum <sup>b</sup>
Chromic acid anodize (Bell)	1	Degrease and alkaline clean 5-10 min, then rinse
	2	Deoxidize 5-10 min at 140°-160°F in: Na <sub>2</sub> Cr <sub>2</sub> O <sub>7</sub> · 2H <sub>2</sub> O - 2 to 3 wt % H <sub>2</sub> SO <sub>4</sub> - 22 to 28 wt % Water - balance Rinse thoroughly
	3	Anodize at 40-12 V for 30-35 min in 6-10 wt % chromic acid solution at 95-121°F, rinse
	4	Seal in 75-120 ppm chromic acid solution for 7-9 min at 180°-185°F, dry
Phosphoric acid anodize (Boeing)	1	Vapor degrease and alkaline clean 10 minutes; rinse 5 min in tap water, 110°F minimum
	2	Deoxidize 10-15 min at room temperature in Amchem 6-10 deoxidizer <sup>c,d</sup> Amchem 6-10 - 4 to 9 vol % Nitric acid - 10 to 20 oz/gal Water - balance 5 min
	3	Anodize in 8-12 wt % phosphoric acid for 20-15 min at 10-11 V and 65° to 85°F. Rinse 5 min in tap water and dry at 160°F maximum

<sup>a</sup>100 psi used for thick adherend DCU assemblies  
50 psi used for all others

<sup>b</sup>Spray rinse all surfaces simultaneously with their withdrawal from solution

<sup>c</sup>Amchem Products, Inc., Ambler, Pennsylvania

<sup>d</sup>FPL etch may be used as a deoxidizer step.

### 3.1 NONDESTRUCTIVE INSPECTION (NDI) OF BONDED ASSEMBLIES

Nondestructive inspection of all bonded assemblies was carried out prior to fabricating test specimens. NDI methods used were ultrasonic through-transmission and low-voltage X-ray (25 to 50 kV), with selected panels inspected by neutron radiography. The radiographic techniques were most effective in showing details of voids and porosity, neutron radiography being superior to low-voltage X-ray. A discussion of the correlation of NDI results with the stressed durability results is presented in appendix A.

There is no correlation between adverse durability and voids/porosity observed by NDI.

### 3.2 VERIFICATION OF TEST METHODS (TASK 1)

#### 3.2.1 SUSTAINED-STRESS THICK-ADHEREND LAP-SHEAR TESTS

Thick-adherend lap-shear specimens representing the four alloys, four adhesives, three surface treatment processes, and three corrosion-inhibiting adhesive primers (CIAP) were fabricated by machining specimens (fig. 2) from large area bonded assemblies. Ten specimens for each system were randomly selected and tested as room-temperature controls. (See table 4.)

Shear strengths for clad specimens were generally a few hundred psi lower than for the corresponding bare specimens, as shown in table 4. Shear strengths of the PL 729-3/PL 728 system were lower for the two anodized surface treatments than for the FPL surface treatment, which was particularly evident on anodized clad alloys. Failure modes for all three surface treatments were cohesive within the primer. For the anodized specimens, the crack path was within the primer but very near the oxide surface, while on the FPL-etched specimens, more primer was left on the adherend.

This phenomenon of reduced shear strengths with cohesive fractures very near the oxide surface has been observed with other similar primers during tests conducted independent of this program. The fracture starts near the oxide/primer interface and is somehow related to the thick anodic oxide and some specific polymer species in the primer, since this strength reduction was not observed with all 350° F primer systems. This phenomenon requires additional investigation for complete understanding. It should be emphasized that the reduced strength is not reflected in reduced environmental durability.

Three specimens for each system were loaded at two different levels (900 and 1500 psi) in the modified testing fixture (note app. A) shown in figure 6. The stressed specimens were exposed to a 140°F/condensing humidity environment for 140 days. (The test period was limited by the contract duration). One of the environmental chambers with loaded fixtures is shown in figure 7. Time to failure was recorded for those specimens that failed. Those that did not fail in the 140-day period were tested for residual shear strength at room temperature. Time to failure and residual shear strength results are given in tables 5, 6, and 7.

Table 4.—Baseline Shear Strengths—Room Temperature

Surface treatment	Alloy	FM 123-2/BR 127		EA 9628/BR 127		AF 143/EC 3917		PL 729-3/PL 728	
		psi	S <sup>a</sup>	psi	S	psi	S	psi	S
Phosphoric acid anodize	2024-T3 clad	5498	399	5575	72	5513	140	4856	297
	2024-T3 bare	6136	89	5751	207	6152	239	7160	197
	7075-T6 clad	5976	132	5730	280	5815	99	5554	530
	7075-T6 bare	6226	114	5704	198	6029	204	7112	170
Chromic acid anodize	2024-T3 clad	5404	143	5705	58	5205	139	4323	186
	2024-T3 bare	6140	103	5806	81	5861	113	5807	321
	7075-T6 clad	5640	83	5731	60	5482	154	5324	418
	7075-T6 bare	5765	b-760	5502	152	5660	283	5506	326
FPL etch	2024-T3 clad	5760	139	5492	53	5616	66	6162	138
	2024-T3 bare	6367	141	5630	138	6242	160	7320	238
	7075-T6 clad	6065	196	5812	113	5833	117	6833	261
	7075-T6 bare	6275	74	5815	394	6107	112	6709	355

<sup>a</sup>Standard deviation, S, for 10 specimens

<sup>b</sup>Voids in three specimens (see app. A)

Table 5.—Sustained Stress Test Results—Thick-Adherend Lap-Shear Specimens,  
Phosphoric Acid Anodize

140 Days at 140° F/Condensing Humidity

250° F Cure Adhesives

Alloy	Sustained stress, psi	FM 123-2/BR 127				EA 9628/BR 127			
		$\bar{x}$ (avg)		S <sub>a</sub>	$\bar{x}$ (avg)	$\bar{x}$ (avg)		S	$\bar{x}$ (avg)
		Days to failure	Residual strength, psi			Baseline strength, psi	Days to failure		
2024-T3 clad	1500 900	31.0 —	— 4753	2.6 260	— 5498	— —	— —	292 220	5575
2024-T3 bare	1500 900	35.7 —	— 5486	14.6 16.0	— 6136	— —	— —	220 172	5751
7075-T6 clad	1500 900	28.0 35 (1) <sup>b</sup>	— 4220 (2)	7.2 573	— 5976	— —	— —	240 138	5730
7075-T6 bare	1500 900	39.7 —	— 5326	8.1 336	6226	34.6 (1) —	353 378	5704	

350° F Cure Adhesives

Alloy	Sustained stress, psi	AF 143/EC 3917				PL 729-3/PL 728			
		$\bar{x}$ (avg)		S	$\bar{x}$ (avg)	$\bar{x}$ (avg)		S	$\bar{x}$ (avg)
		Days to failure	Residual strength, psi			Baseline strength, psi	Days to failure		
2024-T3 clad	1500 900	— —	4846 4906	120 205	— 5513	— —	— —	210 220	4856
2024-T3 bare	1500 900	— —	4800 4920	471 465	— 6152	— —	— —	70 192	7160
7075-T6 clad	1500 900	— —	4733 5073	185 41	— 5815	— —	— —	120 75	5554
7075-T6 bare	1500 900	— —	5160 5090 (2)	260 382	6029	— —	— —	381 518	7112

<sup>a</sup>Standard deviation, S, days or psi as applicable

<sup>b</sup>( ) represents number of specimens for x if other than 3

Table 6. - Sustained Stress Test Results - Thick-Adherend Lap-Shear Specimens,  
Chromic Acid Anodize

140 Days at 140° F/Condensing Humidity<sup>a</sup>

250° F Cure Adhesives

Alloy	Sustained stress psi	FM 123-2/BR 127			EA 9628/BR 127		
		$\bar{x}$ (avg)		S <sub>a</sub>	$\bar{x}$ (avg)		S
		Days to failure	Residual strength, psi		Days to failure	Residual strength, psi	
2024-T3 clad	1500 900	25.7 104 (1)	- 4750 (2)	4.2 127	121 (1) <sup>b</sup> -	4045 (2) 5173	516 64
2024-T3 bare	1500 900	38.7 (2) 70 (2)	- 4280 (1)	8.1 34.0	34 (1)	4430 (2) 6073	127 253
7075-T6 clad	1500 900	30.0 50 (1)	- 4620 (2)	3.6 0	76 (1) -	3620 (2) 5533	282 555
7075-T6 bare	1500 900	34.0 35 (1)	- 5430 (2)	0 70	34 (2) -	5240 (1) 6206	0 499

350° F Cure Adhesives

Alloy	Sustained stress psi	AF 143/EC 3917			PL 729-3PL 728		
		$\bar{x}$ (avg)		S	$\bar{x}$ (avg)		S
		Days to failure	Residual strength, psi		Days to failure	Residual strength, psi	
2024-T3 clad	1500 900	- -	4360 4353	120 128	- -	2966 3093	211 140
2024-T3 bare	1500 900	- -	4360 5226	196 133	- -	4140 3760	314 124
7075-T6 clad	1500 900	- -	4473 4546	219 438	- -	5813 3040	316 386
7075-T6 bare	1500 900	- -	4933 4813	370 219	- -	3866 4316	318 273

<sup>a</sup>Standard deviation, S, days or psi as applicable

<sup>b</sup>( ) represents number of specimens for  $\bar{x}$  if other than 3

Table 7.—Sustained Stress Test Results—Thick-Adherend Lap Shear Specimens,  
FPL Etch

140 Days at 140° F/Condensing Humidity

250° F Cure Adhesives

Alloy	Sustained stress, psi	FM 123-2/BR 127				EA 9628/BR 127			
		$\bar{x}$ (avg)		S <sup>a</sup>	$\bar{x}$ (avg)	$\bar{x}$ (avg)		S	$\bar{x}$ (avg)
		Days to failure	Residual strength, psi			Days to failure	Residual strength, psi		
2024-T3 clad	1500 900	70.7	—	49.5 160	5760	—	5506 5600	136 160	5492
2024-T3 bare	1500 900	34.0 91.5 (2)	—	0 17.7	6367	67.0 (2)	4900 (1) <sup>b</sup> 6066	12.7 41	5630
7075-T6 clad	1500 900	41.0 102	—	9.6 18.1	6065	76 (2)	3760 (1) 5833	39.6 219	5812
7075-T6 bare	1500 900	51.0 36 (1)	—	1.7 551	6275	93 (1)	5730 (2) 6266	268 90	5815

350° F Cure Adhesives

Alloy	Sustained stress, psi	AF 143/EC 3917				PL 729-3/PL 728			
		$\bar{x}$ (avg)		S	$\bar{x}$ (avg)	$\bar{x}$ (avg)		S	$\bar{x}$ (avg)
		Days to failure	Residual strength, psi			Days to failure	Residual strength, psi		
2024-T3 clad	1500 900	—	4726 4813	119 120	5616	—	5800 5593	170 151	6162
2024-T3 bare	1500 900	—	4900 4933	274 94	6242	—	6026 5933	421 397	7320
7075-T6 clad	1500 900	—	4800 4833	211 241	5833	—	5813 5510 (2)	316 269	6833
7075-T6 bare	1500 900	—	4526 4640	98 14	6107	—	6080 (1) 6200 (1)	—	6709

<sup>a</sup>Standard deviation, S, days or psi as applicable

<sup>b</sup>( ) represents number of specimens for  $\bar{x}$  if other than 3

Residual shear strengths for the EA 9628/BR 127 system are typically higher for specimens stressed at 900 psi than for those stressed at 1500 psi. These residual strengths tend to be equal to or higher than the control shear specimens—particularly higher with the bare alloy.

This test method discriminates between adhesive systems; i.e., most of the failures occurred with the FM 123-2/BR 127 adhesive/primer system, some failures occurred with the new technology adhesive/primer system EA 9628/BR 127, but no failures occurred with either of the two 350° F cure adhesive/primer systems. Surface treatments and alloys did not have a significant effect on the time to failure or the failure modes. Typical failure modes are shown in figure 8.

In conducting this first task, inconsistent results were encountered with the original loading fixture and the thick-adherend lap-shear specimen. The problem was traced to nonaxial loading of the test specimen. After a brief test program, the loading fixture was modified to eliminate the nonaxial loads. The problem and solution are presented in appendix B. The modified loading fixture was used for all tests reported.

Conclusions that can be drawn from these tests are:

1. Sustained-stress testing of thick-adherend lap-shear specimens will discriminate between different adhesive/primer systems in terms of their stressed durability performance.
2. There is an inherently high degree of scatter in the time-to-failure data due to the many unavoidable variables involved, e.g., stress level variations, nonaxial loading, specimen flaws, bondline thickness variations or bondline flaws.

### 3.2.2 SUSTAINED-STRESS THICK-ADHEREND DCB TESTS

Thick-adherend DCB specimens for each of the four alloys, four adhesives, three surface treatment processes, and three corrosion-inhibiting primers were fabricated by cutting specimens from large bonded assemblies and milling the cut sides to produce smooth surfaces (fig. 3). DCB specimens for each of the clad alloys were fabricated by bonding four 1/4-in.-thick plates to make up the 1-in.-thick specimen. This was necessary since 1/2-in.-thick clad plate could not be purchased at an acceptable cost. The specimens were stressed by tightening two 1/4-28 bolts into one end until a displacement of 0.10 in. was obtained (fig. 3). This displacement was chosen for convenience to standardize specimen configuration. After waiting 1 day for equilibrium to be established, the tip of the crack front created in the bondline was marked.

Pairs of specimens representing each bonded system were then placed in a 140° F/condensing humidity environment for periods up to 6 months and removed periodically to measure any change in crack tip location. The data, crack length from point of loading vs time, were recorded and reduced to an energy term,  $G_I$ , or strain energy release rate. This is a measurement of the fracture toughness of the joint or its ability to contain a crack under stress in a given environment. By knowing the length of the crack from the point of loading to the crack tip, the displacement, and the dimensions of the specimen,  $G_I$  can be calculated from the following formula (ref. 2):

$$G_I = \frac{y^2 E h^3 [3(a + 0.6h)^2 + h^2]}{16 [(a + 0.6h)^3 + ah^2]^2} \quad (1)$$

where

y = displacement at load point (inches)

a = crack length from load point (inches)

h = specimen half height (inches)

E = modulus of elasticity of adherends (psi  $\times 10^6$ )

Plots of  $G_I$  vs exposure time for each bonded system are shown in figure 9. There is no significant difference in durability behavior between surface treatments and alloys in terms of crack growth equilibrium resulting from the environmental exposure, i.e., the stress corrosion cracking threshold,  $G_{ISCC}$ , except for the failure modes within the stressed zone. After opening one set of specimens for each bonded system, it was observed that the FPL-etched specimens had a higher frequency of adhesive failures within the stressed zone than did the two anodized treatment specimens, primarily with the 250°F cure epoxy systems. This was not reflected in the crack growth data. For instance, the  $G_I$  vs time data in figure 9g show no significant difference between surface treatments, but the FPL-etched specimens had at least 50% adhesive-type failure in the area of crack growth while the two anodized surfaces had less than 5% adhesive failure. The apparent variations in  $G_I$  vs time between the three surface preparations are within the normal variations one would expect of this test method. Typical failure modes are shown in figures 10 through 13.

The DCB specimens did not reveal any significant difference between the two 250°F cure epoxy adhesives, in contrast to the stressed lap-shear tests. This implies that the combined Mode I and Mode II loading of the lap-shear specimen has a different effect on the stressed durability than does Mode I loading only.

The more brittle 350°F cure epoxies were not as tough initially as the 250°F cure systems, but time in the environment for these systems resulted in little crack extension. A difference in the initial fracture toughness was evident between the two 350°F cure systems, with the AF 143/EC 3917 system exhibiting the higher values.

The AF 143/EC 3917 system performed quite consistently on all three surface treatments and four alloys, whereas the PL 729-3/PL 728 system varied considerably in fracture toughness, particularly with the two anodized surface treatments on the two clad alloys. In those cases,  $G_{Ia}$  values of about 1 in-lb/in<sup>2</sup> were achieved. Higher values of  $G_{Ia}$  for PL 729-3 were obtained on bare alloys with phosphoric acid anodize. Failure modes of the PL 729-3/PL 728 DCB specimens were all primer-oriented, including the FPL-etched specimens, except for adhesive failure in the stressed area for some specimens (fig. 10). Failure modes of the AF 143/EC 3917 bonded specimens were all cohesive within the adhesive (fig. 11).

Half of the specimens were opened after 20 weeks and the other half at the end of the program. Longest exposure times were 86 weeks. Extensive crevice corrosion (filiform appearance) occurred in the unstressed area (posttest zone) of the bondline after more than 77 weeks' exposure to 140°F/condensing humidity for those specimens bonded with FM 123-2 adhesive (fig. 12). Comparable specimens bonded with EA 9628 adhesive did not have corrosion in the bondline (fig. 13).

The two 350°F cure adhesives did not have bondline corrosion either. The anodized specimens bonded with the PL 729-3/PL 728 system did exhibit brittle fracture behavior in the pretest and posttest fracture areas, with the fracture failures occurring near the oxide surface but apparently in the primer. This phenomenon seemed to be unique to the PL 728 primer and the two anodized surfaces, although this did not have any effect on the durability performance of the bond.

Conclusions that can be drawn from these tests are:

1. The stressed DCB specimen does not discriminate between adhesive/primer systems in the same way as the stressed lap-shear specimens; i.e., the DCB specimens demonstrated differences in  $G_I$  between the 250°F cure systems and the 350°F cure systems tested, but not between the two 250°F cure adhesives.
2. Exposures of more than 77 weeks to 140°F/condensing humidity resulted in a crevice-type corrosion (filiform) in the bondline of the FM 123-2/BR 127 adhesive/primer system for all surface treatments and alloys tested.
3. The Mode I loading caused a brittle fracture to occur in the PL 728 primer on the anodized adherend surfaces in the pretest and posttest zones, but excellent stressed durability was exhibited.

### 3.2.3 FINAL JUSTIFICATION OF TEST METHODS

Final selection and justification of the test methods to be used for the remainder of Phase III were made at this point, based on the preceding results and prior experience.

- *Thick-adherend lap-shear specimen.* The decision to continue the use of this specimen was based on the rationale presented in the Phase I and II study (ref. 1) and the results of the preceding tests. The rationale was that thick adherends will transfer shear loads more uniformly through the test bondline and reduce the bending moment at the loading edge, thereby minimizing large adhesive strains at this point. (Solution of the nonaxial load problem encountered with this specimen and the static loading fixture as described in app. A supported the continued use of this specimen.) Results from verification tests also indicated that differences in stressed adhesive durability could be detected.
- *Thick-adherend DCB specimen.* This configuration allows a quantitative evaluation of the fracture toughness characteristics of adhesive systems in addition to qualitative information; e.g., adherend surface/adhesive durability and bondline corrosion interactions.

- *Thin-adherend DCB specimen (wedge test).*—This configuration was rejected in Phase II because it was not quantitative. However, it was subsequently added to this program because of a need for a simple, inexpensive test specimen that provided useful qualitative data.
- *Thick-adherend SCB specimen.*—This specimen configuration was not included in the verification tests because it was similar to the DCB specimen in many respects, in that it was a self-contained, stressed specimen that could yield quantitative data. The configuration is especially designed to assess face sheet and/or core surface quality and therefore was required to meet the objectives of the program.

### 3.3 INFLUENCE OF TEST TEMPERATURE (TASK 6)

The purpose of this group of tests was to determine the significance of temperature in conjunction with water on the durability of bonded joints. This effect was assessed using the bonded DCB specimen.

DCB specimens were fabricated as described in section 3.2.2 by using the 2024-T3 bare alloy with the phosphoric acid anodize surface treatment. The adhesive/primer systems used were FM 123-2/BR 127, EA 9628/BR 127, AF 143/EC 3917, and PL 729-3/PL 728.

Six specimens representing each bonded system were precracked and exposed to two environments: 120° and 160°F/condensing humidity. Data for the 140°F environment were developed in the tests described in section 3.2.2. Crack growth was monitored periodically, and at the end of 20 weeks' exposure two specimens from each group were opened for visual assessment. The remaining four specimens from each group were opened at the conclusion of the program (86 weeks).

Plots of  $G_I$  vs exposure time to the three temperatures at condensing humidity conditions are shown in figure 14. The crack containment capability of the two 250°F cure epoxy systems, FM 123-2 and EA 9628, was reduced at higher temperatures (fig. 14, a and b). There was some difference in performance between these two adhesives, but the significance of the difference was not apparent in this test. The effect of temperature on the two 350°F cure adhesives was insignificant in this test (fig. 14, c and d).

The failure modes of the specimens tested in 120° and 160°F environments were basically the same as those shown for the 140°F tests (figs. 10 through 13). The only significant difference was the general absence of corrosion in the bondline of those specimens bonded with FM 123-2/BR 127 adhesive when exposed to 120°F/condensing humidity environment.

The 140°F/condensing humidity environment was originally chosen for the test method verification tests, section 3.2, because it was considered both a severe environment that could shorten test periods and also one that aircraft could realistically expect to be exposed to during their service life. However, the DCB specimen results for the two 350°F cure adhesives showed that temperature differences between 120° and 160°F had no significant effect on bond performance.

The decision was made to conduct all further tests on the two 350°F cure adhesive systems at 160°F/condensing humidity. The rationale was that these adhesives might be exposed to higher temperature service conditions than the 250°F cure adhesive, therefore, the higher test environment would be justified. Testing of the 250°F cure adhesive systems was continued at 140°F/condensing humidity with the exception of the salt spray corrosion tests at 95°F.

Conclusions that can be drawn from these tests are:

1. Increasing temperature from 120° to 160°F in condensing humidity significantly reduces the crack containment capabilities of FM 123-2 and EA 9628 adhesives (250°F cure).
2. Increasing temperature from 120° to 160°F in condensing humidity does not have any significant effect on the crack containment capabilities of AF 143 and PL 729-3 adhesives (350°F cure).

### **3.4 EFFECT OF DURATION ON SUSTAINED-STRESS TESTS (TASKS 2, 3, 5, and 10)**

The purpose of this test series was to examine the effects of longer term environmental exposure (of more than 6 months). This section describes tests using three specimen configurations: the thick-adherend lap-shear, the thick-adherend DCB, and the thick-adherend SCB for honeycomb durability evaluation.

#### **3.4.1 THICK-ADHEREND LAP-SHEAR TESTS (TASK 2)**

Thick-adherend lap-shear specimens were fabricated as described in section 3.2.1. The specimens represented two alloys (2024-T3 bare and clad) and one surface treatment process (phosphoric acid anodize). The four adhesive/primer systems were represented: FM 123-2/BR 127, EA 9628/BR 127, AF 143/EC 3917, and PL 729-3/PL 728. The specimens were loaded at 1500, 1200, 900, and 600 psi using the modified loading fixture shown in figure 6. Those specimens bonded with the 250°F cure adhesives were placed in 140°F/condensing humidity and those bonded with the 350°F cure adhesive systems were placed in 160°F/condensing humidity cabinets.

Time-to-failure results and residual room temperature lap-shear strengths of those specimens not failed after the 9-month exposure period are shown in table 8. These results again show the FM 123-2 adhesive system to be less durable in this test mode than EA 9628 or the two 350°F cure systems, AF 143 and PL 729-3. However, the average time to failure for FM 123-2 was more than twice that observed in the earlier results (sec. 3.2.1) for the 1500-psi stress level. There was no identifiable reason for this difference, as specimens were cut from the same panels, and the same loading fixtures and environmental facilities were used. Comparison of failure modes showed the same cohesive characteristics as those shown in figure 8 for the same bonded system, except for crevice corrosion in bondlines with the FM 123-2 adhesive system.

No EA 9628 bonded specimens failed during the 9-month exposure period. This is consistent with the test results shown in table 5 for the same alloys. Also, AF 143 and PL 729-3

Table 8.—Long-Term Sustained Stress Test Results ( 9 Months)—Thick-Adherend Lap-Shear Specimens,  
Phosphoric Acid Anodize

Alloy	Sustained stress, psi	140°F/Condensing Humidity					160°F/Condensing Humidity				
		FM 123-2/BR 127			EA 9628/BR 127		AF 143/EC 3917			PL 729-3/PL 728	
		$\bar{x}$ (avg)		Residual strength, psi	Days to failure	$S^a$	$\bar{x}$ (avg)		Residual strength, psi	Days to failure	$S$
		Days to failure	Residual strength, psi				Days to failure	Residual strength, psi			
2024-T3 clad	1500	86.5	—	33.5	—	231	—	4636	137	—	119
	1200	106.3	—	39.1	—	130	—	4870	96	—	143
	900	131.7	—	56.6	—	205	—	4803	86	—	154
	600	—	4170	335	—	245	—	4770	126	—	83
2024-T3 bare	1500	70.0	—	25.1	—	152	—	5066	241	—	140
	1200	192.6 (5) <sup>b</sup>	4280 (1)	63.6	—	152	—	4956	212	—	209
	900	200.8	—	59.1	—	309	—	5033	127	—	259
	600	—	3960	425	—	102	—	5030	112	—	135

<sup>a</sup>Standard deviation, S, days or psi as applicable

<sup>b</sup>( ) represents number of specimens for  $\bar{x}$  if other than 6 specimens

adhesive systems did not experience any failures during this time period, even though the environmental temperature was increased to 160°F at condensing humidity conditions.

Residual shear strengths were almost 2000 psi lower than room temperature controls for FM 123-2, about 350 psi lower for EA 9628, almost 1000 psi lower for AF 143, and slightly increased for PL 729-3. The low residual shear strengths for FM 123-2 may be accounted for in part by the presence of bondline crevice corrosion in many of the clad specimens. None of the specimens bonded with the other three adhesives had any bondline crevice corrosion except for trace amounts along the edges of several bare specimens bonded with EA 9628. The increase in residual shear strength for PL 729-3 adhesive and the decrease for AF 143 was not explained, but probably relates to changes in rheological properties as a result of the stressed test conditions. There was no correlation between the change in residual shear strength and stressed durability performance.

Conclusions that can be drawn from these tests are:

1. The stressed lap-shear test is capable of measuring stressed durability differences between the two 250°F cure systems.
2. To obtain durability data at realistic stress levels, long exposure times are required.

### **3.4.2 THICK-ADHEREND DCB TESTS**

#### **3.4.2.1 Long-Term Exposures (Task 2)**

DCB specimens of 2024 bare and clad alloys with the phosphoric acid anodize surface treatment were fabricated using the four adhesive systems: FM 123-2/BR 127, EA 9628/BR 127, AF 143/EC 3917, and PL 729-3/PL 728. Those specimens bonded with the 250° and 350°F cure adhesive systems were exposed to 140° and 160°F/condensing environments, respectively. The test results are plotted as  $G_I$  vs exposure time in figure 15. Extending the exposure time from 22 to 90 weeks did not result in any change in durability when assessed on the basis of crack growth only.

Assessment of the failure modes in the pretest, test, and posttest fracture areas revealed the same conditions observed after 22 weeks as shown in figures 10 through 13 for the respective specimens, except that extensive crevice corrosion occurred in the bondlines of all specimens bonded with FM 123-2 adhesive during the extended exposure time. However, the  $G_I$  vs exposure time data in figure 15a show no effect of the corrosion. Given enough time the corrosion would eventually affect the  $G_I$  data because less bond would be available to hold the specimen together. If the corrosion occurred in the stressed zone, then this effect would show up sooner, but the corrosion phenomenon is independent of stress and this occurrence would be random.

Conclusions that can be drawn from these tests are :

1. The results agree with the earlier verification test results; i.e., the test method did not discriminate between the two 250°F cure adhesive/primers, FM 123-2/BR 127 and

EA 9628/BR 127, but did discriminate between  $G_I$  for these two systems and the two 350°F cure adhesive/primers, AF 143/EC 3917 and PL 729-3/PL 728.

2. The long-term exposure resulted in bondline crevice corrosion of the FM 123-2/BR 127 adhesive/primer system.

#### 3.4.2.2 Comparison of CIAP Primer and Non-CIAP Primer (Task 3)

DCB specimens were fabricated from two alloys, 2024-T3 bare and clad; two surface treatment processes, phosphoric acid anodize and chromic acid anodize; one adhesive, FM 123-2; and two adhesive primers. BR 127—a corrosion-inhibiting adhesive primer (CIAP), and BR 123—a non-corrosion-inhibiting adhesive primer (non-CIAP). The stressed specimens were exposed to 140°F/condensing humidity for over 80 weeks. Results of the test are shown in figure 16 and 17.

Comparing those specimens with CIAP primer to those with non-CIAP primer on phosphoric-acid-anodized surfaces (fig. 16a), there is an indication that the non-CIAP primer slightly lowers the equilibrium  $G_I$ . There is good agreement between the previous data shown in figure 15a and the data in figure 16a for the additional tests. Failure modes in all specimens were cohesive with the exception of extensive bondline crevice corrosion in the unstressed areas with both primers.

The performance of the two primers on chromic-acid-anodized surfaces is shown in figure 16b. The non-CIAP primer on anodized 2024-T3 clad surfaces failed adhesively on all six specimens in a matter of a few hours resulting in  $G_I$  of less than 1, whereas the same bonded system on 2024-T3 bare alloy and the CIAP primer on the two alloys did not delaminate. Crevice corrosion was evident on all specimens in the unstressed bonded area with both primers. Examples of the failed specimens after posttest fracture are shown in figure 17.

Conclusions that can be drawn from these tests are:

1. The interactions between adherend surfaces and primers in the presence of stress (Mode I) and water can be evaluated by DCB tests.
2. Bondline crevice corrosion with FM 123-2 adhesive is independent of primer type and surface treatment.

#### 3.4.3 HONEYCOMB SCB TESTS (TASKS 5 AND 10)

Honeycomb specimens of the configuration shown in figure 5 were fabricated. Specimens were stressed by torquing two bolts on each end of each specimen to acquire a displacement of 0.08 in. This cantilevered the 1/2-in. face sheet, causing a crack to propagate to an arrest point at the interface between the face sheet and test honeycomb core.

Materials and processes used in the fabrication of these specimens are listed in table 9. The honeycomb cores selected for these tests represent three stages of technology development. The phosphoric-acid anodized core represents the newest concept, with a surface treatment that enhances adhesion and bond durability but requires an organic coating for corrosion

protection. The Dura-Core and CR III core (corrosion-resistant cores) represent the current industry standard technology with good corrosion protection and bondability. The standard core represents the technology of the 1960's.

*Table 9.—Materials and Processes Used for Single Cantilever Beam (SCB) Specimens*

Honeycomb core	Face sheet surface preparation	Adhesive/primer system
Phosphoric acid anodized standard core	Phosphoric acid anodize	EA 9628/BR 127
		FM 123-2/BR 127
		AF 143/EC 3917
	Chromic acid anodize	EA 9628/BR 127
		FM 123-2/BR 127
		AF 143/EC 3917
Dura-Core—Corrosion resistant (American Cyanamid Co.)	Phosphoric acid anodize	EA 9628/BR 127
		FM 123-2/BR 127
		AF 143/EC 3917
	Chromic acid anodize	EA 9628/BR 127
		FM 123-2/BR 127
		AF 143/EC 3917
CR III Core—Corrosion resistant (Hexcel Corp.)	Phosphoric acid anodize	EA 9628/BR 127
Standard core	Phosphoric acid anodize	EA 9628/BR 127

Specimens bonded with EA 9628 and FM 123-2 adhesives (250°F cure) were exposed to 140°F/condensing humidity environment. Specimens bonded with AF 143 adhesive (350°F cure) were exposed to 160°F/condensing humidity environment. Periodically, specimens were removed from the environments and changes in crack length recorded.

Crack extension data for each of the three adhesive systems and combinations of honeycomb core and surface treatments to 1-year exposure are shown in figure 18. Crack extension data for those specimens bonded with the EA 9628/BR 127 system show that phosphoric-acid-anodized core and face sheet produced the shortest crack extensions, hence the best environmental durability. Essentially no adhesive failure of the core-to-fillet bonds occurred in the test zone of these specimens. Failure modes in the pretest and posttest zones were 100% cohesive within the fillets and there was no evidence of moisture penetration into the unstressed area. (See fig. 19a.) (The 140°F/condensing humidity environment causes the color of the EA 9628 to change from a medium green to a light green in the exposed adhesive; therefore, the adhesive sealed in the posttest zone remains a darker green color if it has not been exposed to moisture.

Specimens that had phosphoric-acid-anodized core and chromic-acid-anodized face sheets produced longer crack extensions but with the same failure modes as with the preceding specimens. Examination of the posttest area showed that either the crack had extended farther than the measured crack tip on one of the specimens or moisture had penetrated into the cells of the posttest zone (fig. 19b).

The other EA 9628 bonded specimens representing combinations of standard core, Dura-Core, and CR III core, with the various face sheet surface preparations, exhibited 50% or more adhesive failure of the core-to-fillet bond in the test zone. The standard core resulted in 100% adhesive failure and the longest crack extension. Examination of the EA 9628 adhesive in the posttest zone of all the above combinations showed evidence of complete moisture penetration into this zone. Also, the failure modes in the posttest zone ranged up to 60% adhesive in core-to-fillet bonds. A typical example of the effect of moisture is shown in figure 19c, and a comparison of figure 19c with figures 19a and 19b illustrates this observation.

Crack extension data for those specimens bonded with the FM 123-2/BR 127 system showed the core and face sheet combination of phosphoric acid anodize to have the shortest crack extension accompanied by almost 100% cohesive failure of the core-to-fillet bond. The combination of phosphoric-acid-anodized core and chromic-acid-anodized face sheets resulted in longer crack extensions, but with the same failure modes as the phosphoric-acid-anodized core and face sheets. There was nothing obviously different between the two that would explain the spread between the two sets of data. The combinations of Dura-Core with phosphoric-acid-anodized and chromic-acid-anodized face sheets resulted in about 50% adhesive failure of the core-to-fillet bond in the test area, with slightly longer crack extensions than the specimens with phosphoric-acid-anodized core and face sheets.

Failure modes in the posttest zone of all specimens bonded with FM 123-2 were 100% cohesive in the fillet. Assessment of moisture penetration into this area was not possible since FM 123-2 did not exhibit any obvious color change resulting from exposure to 140°F/condensing humidity.

A general observation of all SCB specimens bonded with the FM 123-2/BR 127 system showed that the adhesive fillets to the cores were very small—much smaller than the fillets formed by the EA 9628/BR 127 system. This may account for the longer initial crack lengths and the tighter grouping of data of the FM 123-2 bonded specimens compared to the data from the EA 9628 bonded specimens.

Crack extension data for the specimens bonded with the AF 143/EC 3917 system show very little spread between the different combinations of core and face sheet surface preparations. Assessment of the failure modes in the test zone revealed that the specimens with phosphoric-acid-anodized core had about 10% adhesive failure of the core-to-fillet bond, but the specimens with Dura-Core exhibited more than 50% adhesive failure of the core-to-fillet bond. Failure modes in the posttest zone of all specimens were 100% cohesive, with no evidence of moisture penetration into this area. AF 143 changes color after exposure to 160°F/condensing humidity, going from light brown to dark brown.

A general comment relating to all the SCB specimens representing all three adhesives tested is that there were no instances of adhesive failure to any of the face sheets.

Conclusions to be drawn from this study are:

1. SCB specimens with phosphoric-acid-anodized standard core and face sheets exhibited the best environmental durability with all three adhesive systems tested.
2. The corrosion-resistant cores (Dura-Core and CR III core) were intermediate and the standard core exhibited the poorest environmental durability with the 250°F cure adhesive systems tested.
3. The thick-adherend SCB specimen offers a semiquantitative and qualitative means of assessing the stressed durability performance of honeycomb core adhesive face sheet bonds.

### 3.5 CYCLIC STRESS TESTS (TASKS 4 AND 8)

#### 3.5.1 THICK-ADHEREND LAP-SHEAR CYCLIC LOAD TESTS

##### 3.5.1.1 Tests at 0.8 cph and 10 cph (Task 4)

Thick-adherend lap-shear specimens were subjected to cyclic loading at two slow frequencies and four stress levels while exposed to 140° or 160°F/condensing humidity. The two cyclic load frequencies used are shown in figure 20. The Bell cycle, 1 hour at maximum load ( $f_{max}$ ) and 1/4 hour at minimum load ( $f_{min}$ ) was developed by the Bell Helicopter Company, Fort Worth, Texas (ref. 3). The Boeing cycle, 4 minutes at  $f_{max}$  and 2 minutes at  $f_{min}$ , was selected as a frequency that would be significantly faster than the Bell cycle, yet allow enough time for some polymer relaxation at  $f_{max}$  and  $f_{min}$  and still be compatible with the test equipment. The four stress levels of  $f_{max}$  were 1500, 1200, 900, and 600 psi. The  $f_{min}$  stress equaled zero for all cases. The rate of load application and release was rather fast in all cases, less than 2 seconds from  $f_{min}$  to  $f_{max}$ .

The test machine, shown in figure 21, functioned by raising and lowering a dead weight cantilevered on a beam. The test specimens were stressed individually in chambers that provided condensing humidity at the specified temperatures.

These tests evaluated EA 9628/BR 127 and AF 143/EC 3917 adhesive systems, 2024-T3 clad and bare aluminum alloys, and phosphoric acid anodize (BAC 5555) surface treatment. The specimens were exposed to 140°F/condensing humidity and 160°F/condensing humidity for the EA 9628/BR 127 and AF 143/EC 3917 adhesive systems, respectively.

Data for those specimens bonded with the EA 9628/BR 127 adhesive system and tested at the two loading frequencies are shown in table 10. Data for the specimens bonded with AF 143/EC 3917 adhesive system are shown in table 11. The data are presented as cycles and time to failure for those specimens that failed or as residual shear strength at cumulative cycles for those specimens that did not fail during the test period.

Table 10.—Slow Cyclic Stress Test Results—Thick-Adherend Lap-Shear Specimens, Phosphoric Acid Anodize

EA 9628/BR 127, 140° F/Condensing Humidity

Alloy	Cyclic frequency, cph	f <sub>max</sub> , psi (R = 0)	Cycles to failure	Hours to failure	S <sup>a</sup> , hr	Residual shear, psi	Cumulative cycles	S, psi
2024-T3 clad	0.8	1500	564	705	204	—	—	—
		1200	819	1024	608	—	—	—
		900	Not tested	—	—	—	—	—
		600	Not tested	—	—	—	—	—
	10	1500	3 150	315	11	—	—	—
		1200	5 460	546	152	—	—	—
2024-T3 bare	0.8	900	—	—	—	5310 (2) <sup>b</sup>	45 784	98
		600	—	—	—	5200 (1)	36 620	—
		1500	797	996	367	—	—	—
		1200	1 322 (4) <sup>c</sup>	1652 (4)	328	—	—	—
		900	2 454 (4)	3068 (4)	1950	6060 (1)	6 600	—
		600	4 533 (1)	5666 (1)	—	5970 (4)	5 910	186
	10	1500	1 600	160	31	—	—	—
		1200	14 240 (3)	1424 (3)	599	5500 (2)	45 784	480
		900	—	—	—	5533 (3)	45 784	493
		600	—	—	—	5450 (2)	45 784	127

<sup>a</sup>Standard deviation, S

<sup>b</sup>( ) represents number of specimens if other than 5

<sup>c</sup>One specimen not included because of premature failure due to void in bondline

Table 11.—Slow Cyclic Stress Test Results—Thick-Adherend Lap-Shear Specimens, Phosphoric Acid Anodize

AF 143/EC 3917, 160° F/Condensing Humidity

Alloy	Cyclic frequency, cph	f <sub>max</sub> , psi (R = 0)	Cycles to failure	Hours to failure	S <sup>a</sup> , hr	Residual shear, psi	Cumulative cycles	S, psi
2024-T3 clad	0.8	1500	2 427	3034	386	—	—	—
		1200	—	—	—	4200 (2) <sup>b</sup>	3 896	—
		900	—	—	—	4315 (4)	3 534	370
		600	—	—	—	—	6 652	—
2024-T3 bare	10	1500	20 400	2040	442	4620 (1) <sup>c</sup>	696	—
		1200	—	—	—	4667 (3) <sup>c</sup>	35 320	395
		900	—	—	—	4676 (2)	76 864	21
		600	—	—	—	4690 (1)	54 648	—
2024-T3 bare	0.8	1500	1 855	2318 (4)	635	—	—	—
		1200	—	—	—	4968	2 486	140
		900	—	—	—	—	3 218	—
		600	—	—	—	—	—	—
2024-T3 bare	10	1500	26 920	2692 (1)	—	4767 (2) <sup>c</sup>	20 830	443
		1200	—	—	—	5130 (2) <sup>c</sup>	27 200	14
		900	—	—	—	4940 (3)	21 093	255
		600	—	—	—	5420 (1)	42 863	—

<sup>a</sup>Standard deviation, S

<sup>b</sup>( ) represents number of specimens if other than 5

<sup>c</sup>Metal fatigue failure at loading holes

Failure modes of all specimens were 100% cohesive in the center of the bondline, as shown in figure 22. Several specimens fabricated with 2024-T3 clad alloy had some crevice corrosion undercutting the bondline of both adhesives (e.g., fig. 22a); however, the amount of corrosion apparently did not affect the time-to-failure data. The same filiform corrosion phenomenon was observed in the bondlines of DCB specimens bonded with FM 123-2/BR 127 adhesive system after extended exposure to 140°F/condensing humidity, as reported in sections 3.2.2 and 3.4.2.

A summary of the failure data of tables 10 and 11 is shown in figure 23. This shows the spread between the failures at 0.8 and 10 cph for the two adhesive systems. The slower Bell cycle, 0.8 cph, is much more damaging than the faster 10-cph cycle. Failures occurred only at 1500 psi with the AF 143/EC 3917 system tested at 0.8 and 10 cph. This comparison with the EA 9628/BR 127 system demonstrates the improved stressed durability characteristics of the 350°F curing AF 143.

The following conclusions may be drawn:

1. The slow Bell cycle, 0.8 cph, is more damaging per cycle for the two adhesive systems tested than is the 10-cph Boeing cycle.
2. The AF 143/EC 3917 adhesive system is more durable in cyclic tests than the EA 9628/BR 127 adhesive system.
3. Cyclic loading produces failures much faster than does static load testing.

#### 3.5.1.2 Tests at 1800 cpm (Task 8)

The thick-adherend lap-shear specimens used in this series of tests differed only in that the ends of the specimens were not notched, which facilitated mounting in the SF-1-U Wiedemann Baldwin fatigue machines. All tests were run at 1800 cpm at a stress ratio,  $R$ , of 0.06 ( $R = f_{\min}/f_{\max}$ ). Maximum stresses,  $f_{\max}$ , ranged from 2000 to 3300 psi. Specimens were tested in four environments: 75°F/laboratory humidity (20% to 30%), 75°F/wet, 140°F/dry (less than 10%), and 140°F/wet. Specimens were not preconditioned before testing in the wet environments.

Specimens tested in the four environments were 2024-T3 bare alloy bonded with the EA 9628/BR 127 adhesive system. Two surface treatments were incorporated: phosphoric acid anodize (BAC 5555) and chromic acid anodize (Bell process). Additional specimens of 7075-T6 bare alloy using the same adhesive and surface preparations were tested in the 140°F/wet environment.

The specimen arrangement in the SF-1-U fatigue machine with the chamber for producing the 140°F/wet environment surrounding the specimen is shown in figure 24. The test results for the four environments and specimen combinations are shown in figure 25. High stress levels were used to develop the S-N curves within reasonable time periods. Comparing these data with the slow cyclic data of figure 23 shows that far less damage occurs per cycle at 1800 cpm than at the slow cyclic rates.

Failure modes are different when compared to the slow cyclic rates, as shown in figures 26 and 27. The fingernail-shaped area is the crack front that propagates from the load transfer edge until the remaining bond fails. The failure mode within the fingernail area is very near the metal oxide surface and appears to be at the adhesive-primer interface. This is schematically shown in figure 26a. This failure mode is different from those observed with the slow cycle tests, which were all in the center of the bond suggesting a creep-rupture-type failure. The fast-cycle fatigue-induced failure shows evidence of what could be termed fatigue striations (fig. 28).

Some of the specimens that were chromic acid anodized failed early. (See figs. 25b and 25e.) These specimens were characterized by a different failure mode (fig. 26b). In these cases, the fingernail-shaped area had substantial areas of an oxide-oriented failure.

Conclusions drawn from these tests are:

1. The high-frequency cyclic load tests, 1800 cpm, are much less damaging to the bondline per cycle than the low-frequency tests.
2. Bonds to chromic-acid-anodized surfaces result in occasional oxide failures at the stress levels and cyclic load frequency used.
3. Increasing the test temperature from 75° to 140° F shortens the fatigue life of the bonded systems tested. The presence or absence of water did not seem to have an effect at either temperature. (The test duration was less than 2 days, possibly not allowing sufficient time for the water to affect the mechanical properties of the adhesive. Had specimens been preconditioned to a moisture equilibrium condition, results might have been different.)
4. Failure modes suggest a fatigue failure of the adhesive at or near the adhesive-primer interface. In contrast, the slow cyclic tests, 0.8 and 10 cph, suggest a creep-rupture-type failure where the failure is entirely in the center of the bond. There was no evidence that phosphoric acid anodized surfaces adversely influenced the fatigue behavior of lap shear specimens. However, there was some evidence that chromic acid anodized surfaces did influence the specimen fatigue behavior. When tested at 1800 cpm, some specimens with chromic acid anodized surfaces exhibited decreases in fatigue life apparently as a result of oxide-initiated failures.

### **3.5.2 THICK-ADHEREND DCB CYCLIC LOAD TESTS (TASK 8)**

Thick-adherend DCB specimens were stressed under cyclic loads by alternating the displacement at the load points from 0 to 0.20 in. To acquire the dynamic aspects of cyclic loading, clevises were pinned through the end of the specimens using 1/4-in. pins instead of the torqued bolts shown in figure 3. This loading arrangement is shown in figures 29 and 30 for the two different test apparatus used.

Specimens were fabricated of 2024-T3 and 7075-T6 bare aluminum alloys; phosphoric acid anodize, chromic acid anodize, and FPI etch surface treatments; and EA 9628/BR 127 adhesive system. Bonded specimens consisting of 2024-T3 bare alloy surface treated with

phosphoric acid and chromic acid anodize were tested in four environments: 75°F/wet and dry and 140°F/wet and dry. Those specimens of 2024-T3 bare alloy and FPL etch, as well as those of 7075-T6 surface treated with phosphoric acid and chromic acid anodize, were tested in 140°F/wet environment only. The reason for this was that surface treatment interactions were most important for these specimens, and a warm, wet environment is the most discriminating.

Tests were conducted at three cyclic frequencies: 1800 cpm, 10 cpm, and 0.8 cph. The 1800-cpm frequency was sinusoidal in nature to simulate the standard fatigue test frequency and was obtained using an electric motor turning a flywheel with an eccentrically located pin.

The 10-cpm frequency represented 3 seconds at full load or displacement and 3 seconds at zero load. The 0.8-cph frequency was the Bell cycle described earlier: 1 hour at full load and 1/4 hour at zero load. The two latter frequencies and load profiles were obtained by a timer operating pneumatic cylinders. Environmental exposures in this case were obtained by immersing the specimens in water for the wet environment or in an oven for the 140°F/dry environment.

For each test condition, specimens were opened to 0.20 in. and closed at the prescribed frequency. Specimens were removed from test at intervals dictated by load frequency and crack growth rate, and the change in crack growth was marked and recorded. These data provided crack growth vs cycle information from which plots of  $da/dN$  vs  $\Delta G$  were obtained. Calculation of  $\Delta G_I$  is done in the same manner as described in section 3.2.2, using equation (1):

$$G_I = \frac{y^2 E h^3 [3(a + 0.6h)^2 + h^2]}{16 [(a + 0.6h)^3 + ah^2]^2} \quad (1)$$

Since the displacement,  $y$ , is being cycled between 0.20 and 0 in.,  $\Delta G_I$  varies between  $G_{I\max}$  and  $G_{I\min}$ , where  $G_{I\min} = 0$  and  $G_{I\max}$  is incrementally reduced with each increase in crack length.

The incremental change in crack length per cycle,  $da/dN$ , is obtained from the data by plotting crack length vs cycles on log-log paper and determining the slope,  $m$ , of the curve at significant points. The slope,  $m$ , is determined from the relationship:

$$\log a = m \log N + \log C \quad (2)$$

where  $m$  is the slope,  $a$  is the crack length,  $N$  is the number of cycles, and  $C$  is the intercept crack length at  $\log N = 0$  ( $N = 1$ ). From equation (2):

$$a = C(N)^m \quad (3)$$

Differentiating yields:

$$\frac{da}{dN} = m C(N)^{m-1} \quad (4)$$

Then  $da/dN$  is determined from equation (4) and plotted vs  $\Delta G_I$  on log-log paper.

The results for the different alloy, surface treatment, cyclic frequency, and environment combinations are shown in figure 31. From the 1800-cpm frequency tests, it was possible to determine a threshold point,  $\Delta G_{ITH}$ , which is that point at which a crack no longer propagates.

The plots show characteristic S-shaped curves. This shape is also typical for monolithic metallic materials. In these curves, the upper right-hand section of the curve (i.e., high  $\Delta G_I$  and high crack growth rate) represents the point where the initial crack is generated in the specimen and it comes to some arrest point,  $G_{Ia}$ , at zero cycles.

As the load is reduced to  $y = 0$  and back to  $y_{max} = 0.20$  in, the crack will move forward by some incremental amount. With each cycle,  $G_{I_{max}}$  becomes less as the crack grows until the crack growth per cycle approaches zero or  $\Delta G_{ITH}$ , which is represented by the bottom left portion of the curves;  $G_{I_{min}}$  is equal to zero in all tests.

In all of the tests run at 1800 cpm, a threshold was established which was between a  $\Delta G_I$  of 1.0 to 1.5 for tests run at room temperature/dry and wet, and between a  $\Delta G_I$  of 0.5 and 0.75 for tests run at 140°F/dry and wet.

The tests run at 10 cpm were in general agreement with the 1800-cpm curves. However, thresholds were not established at 10 cpm because of time constraints.

The test run at 0.8 cph produced longer cracks per cycle than either of the faster cyclic rates at the same  $\Delta G_I$ . Less data were collected for these tests because of the very slow cycle and the long test times involved. In all the plots of  $da/dN$  vs  $\Delta G_I$ , the response in fatigue followed trends similar to those observed by Mostovoy and Ripling for bonded joints (ref. 4), even though Mostovoy used a different specimen configuration, as well as a different method of obtaining data. His threshold  $\Delta G_{ITH}$  values ranged from 0.3 to 2.8 in-lb/in<sup>2</sup> for several different commercial adhesives tested in several environments, as compared to 0.5 to 1.6 for EA 9628 tested in this program.

Failure modes, with few exceptions, were 100% cohesive failure. The  $da/dN$  plots are therefore representative of adhesive properties and not system properties. Figure 32 shows typical failure modes for several environments, load frequencies, and bonded systems. Two exceptions are noted:

1. One of the chromic-acid-anodized specimens showed a rapid drop in crack containment capability ( $\Delta G_I$  of 0.65 in-lb/in<sup>2</sup>) after having reached an apparent  $\Delta G_{ITH}$  of about 1.5 (fig. 31a). Examination of the failure showed adhesive or intra-oxide failure in the area where rapid crack growth had occurred (fig. 32d).
2. Another chromic-acid-anodized specimen exhibited the same adhesive failure in the same area of the specimen (fig. 32e). However, in this case there was no obvious increase in crack growth rate or decrease in  $\Delta G_{ITH}$  due to this change in failure mode.

Conclusions that may be drawn from these tests are:

1. Cyclic loading of DCB specimens is more damaging to the stressed bondline than is static stress loading at the same stress level.
2. There is a threshold level,  $\Delta G_{I\text{TH}}$ , at which the crack no longer propagates;  $\Delta G_{I\text{TH}}$  at 140°F is 0.5 to 0.75, which is about half of  $\Delta G_{I\text{TH}}$  at 75°F (1.0 to 1.6) for the adhesive system examined.
3. The Bell cycle (0.8 cph) is more damaging per cycle than the 10 and 1800-cpm cyclic rates.
4. Testing in a water environment at 75° or 140°F, without preconditioning of the specimens, produced the same results as dry conditions for the test durations involved.
5. The test method is of value in that it can identify a property of an adhesive,  $\Delta G_{I\text{TH}}$ , which relates to its behavior under dynamic loading.
6. The magnitude of  $\Delta G_{I\text{TH}}$  for the adhesive tested is in the same range as that observed for aluminum alloys.
7. There was no evidence that phosphoric acid anodized surfaces adversely influenced the fatigue behavior of DCB specimens. However, there was some evidence that chromic acid anodized surfaces did influence the fatigue behavior. When tested at 1800 cpm, some specimens with chromic acid anodized surfaces exhibited a 50% reduction in  $G_{I\text{TH}}$ , apparently as a result of oxide-initiated failures.

### 3.6 DURABILITY TESTING IN SALT SPRAY (TASK 9)

The purpose of this task was to identify the effects of a very corrosive environment on bondlines of different bonded systems. These system variations included clad and bare alloys, surface treatments, adhesive primers, and adhesives. The various combinations are shown in table 12. The test specimen configuration used for these tests is shown in figure 4.

*Table 12.—Bondment Variables for Salt Spray Tests*

Surface treatments	Alloys	Adhesive/primer system
Phosphoric acid anodize	2024-T3 clad	FM 123-2/BR 127
Chromic acid anodize		FM 123-2/BR 123
		EA 9628/BR 127
FPL etch	2024-T3 bare	FM 123-2/BR 127
		FM 123-2/BR 123
		EA 9628/BR 127
	7075-T6 clad	EA 9628/BR 127
	7075-T6 bare	EA 9628/BR 127

Five specimens were fabricated for each of the bonded systems. The specimens were then placed in a salt spray environment of 5% NaCl at 95°F. The change in crack length of each specimen was recorded periodically. At the end of 1 month, one specimen was randomly selected from each bonded system and opened for visual inspection of the bondline condition both in the stressed zone (crack tip zone) and in the unstressed zone. This same procedure was carried out after 2, 3, 6, and 12 months when the last specimen was removed from test.

The average crack lengths and the bondline appearance at the end of each time period are shown in tables 13, 14, and 15, and figure 33. The data in the tables are the averages of five wedge specimens for intervals to 30 days and the averages of the remaining specimens for each interval thereafter. This procedure sometimes resulted in a decrease in the average crack length.

Two basic differences in durability of the bonded systems tested were apparent in these tests. First, the crack growth data showed that some of the bonded systems resulted in poor stressed durability performance as characterized by large crack growths after relatively short exposure times (1 to 30 days). These specimens also showed adhesive failure modes in the crack growth zone. These systems were (1) the FM 123-2/BR 123 system bonded to 2024-T3 clad and bare alloys which were chromic acid anodized or FPL etched, and (2) the EA 9628/BR 127 system bonded to chromic-acid-anodized 2024-T3 clad alloy and FPL etched 7075-T6 clad alloy.

The second basic difference in durability performance was the corrosion phenomenon which occurred randomly in the bondline, stressed or unstressed, starting at an edge. This difference was not apparent in the crack growth rate data. The crevice corrosion was dominated by clad dissolution because of the sacrificial nature of cladding. Although bondline crevice corrosion occurred in all the clad alloy bonded systems tested, the prebond surface treatment has a definite effect on the progress of clad dissolution; i.e., the anodize surface treatments retard the dissolution rate significantly, which is particularly true in those systems that use BR 127 (CIAP) primer. The phosphoric acid anodize performed slightly better than the chromic acid anodize in this regard.

Bondline crevice corrosion was also evident with the bare alloys, but to a far lesser degree than with the clad alloys. Most bondline corrosion of bare alloys occurred with those that were FPL etched, and was more pronounced on 7075-T6 bare. There was essentially no bondline crevice corrosion of bare alloys that were phosphoric acid anodized.

Conclusions that can be drawn from these results are as follows:

1. The phosphoric acid anodize process provides markedly improved stressed bond joint durability and retards bondline crevice corrosion in severely corrosive environments when compared to two other state-of-the-art surface preparation processes.
2. Stressed bond joint durability is markedly affected by the adherend prebond surface treatment and the adhesive/primer system in contact with it. This is evidenced by the poor performance of FM 123-2/BR 123 (non-CIAP) adhesive/primer system on FPL etched and chromic-acid-anodized 2024-T3 clad and bare and the better performance of the same systems when BR 127 (CIAP) is substituted for BR 123 (non-CIAP).

Table 13.—Durability Testing in Salt Spray, Surface Preparation—Phosphoric Acid Anodize

Adhesive system	Alloy	$a_0$ , in. (a)	$a_0 + \Delta a_1$ 1 day (a)	$a_0 + \Delta a_2$ 7 days (a)	$a_0 + \Delta a_3$ 30 days (a)	$a_0 + \Delta a_4$ 60 days (b)	$a_0 + \Delta a_5$ 90 days (c)	$a_0 + \Delta a_6$ 183 days (d)	$a_0 + \Delta a_7$ 365 days (e)
FM 123-2/BR 123	2024 clad	1.32	1.38	1.38	1.49	1.53	1.50	1.62	1.84
	2024 bare	1.43	1.43	1.50	1.54	1.57	1.56	1.68	1.64
FM 123-2/BR 127	2024 clad	1.33	1.36	1.36	1.52	1.53	1.43	1.48	1.48
	2024 bare	1.40	1.40	1.51	1.55	1.60	1.56	1.55	1.73
EA 9628/BR 127	2024 clad	1.37	1.37	1.44	1.44	1.46	1.46	1.47	1.47
	2024 bare	1.48	1.50	1.53	1.58	1.59	1.59	1.64	1.62
	7075 clad	1.44	1.51	1.56	1.63	1.65	1.54	1.53	1.66
	7075 bare	1.47	1.50	1.55	1.60	1.58	1.59	1.57	1.57

<sup>a</sup>Averages of five specimens

<sup>b</sup>Averages of four specimens

<sup>c</sup>Averages of three specimens

<sup>d</sup>Average of two specimens

<sup>e</sup>One specimen

Table 14.—Durability Testing in Salt Spray, Surface Preparation—Chromic Acid Anodize

Adhesive system	Alloy	$a_o$ in. (a)	$a_o + \Delta a_1$ 1 day (a)	$a_o + \Delta a_2$ 7 days (a)	$a_o + \Delta a_3$ 30 days (a)	$a_o + \Delta a_4$ 60 days (b)	$a_o + \Delta a_5$ 90 days (c)	$a_o + \Delta a_6$ 183 days (d)	$a_o + \Delta a_7$ 365 days (e)
FM 123-2/BR 123	2024 clad	1.31	2.68	2.68	2.78	2.80	2.77	2.84	3.48
	2024 bare	1.41	2.66	3.06	3.06	3.38	3.52	3.97	3.66
FM 123-2/BR 127	2024 clad	1.33	1.34	1.44	1.49	1.47	1.40	1.45	3.86
	2024 bare	1.42	1.47	1.56	1.71	1.73	1.73	1.86	2.16
EA 9628/BR 127	2024 clad	1.42	1.45	1.80	2.37	2.63	2.47	2.48	2.44
	2024 bare	1.47	1.52	1.53	1.69	1.79	1.76	2.10	2.82
	7075 clad	1.40	1.43	1.43	1.45	1.46	1.45	1.42	1.42
	7075 bare	1.46	1.48	1.54	1.59	1.67	1.58	1.59	1.64

<sup>a</sup>Averages of five specimens

<sup>b</sup>Averages of four specimens

<sup>c</sup>Averages of three specimens

<sup>d</sup>Average of two specimens

<sup>e</sup>One specimen

Table 15.—Durability Testing in Salt Spray, Surface Preparation—FPL Etch

Adhesive system	Alloy	$a_o$ , in. (a)	$a_o + \Delta a_1$ 1 day (a)	$a_o + \Delta a_2$ 7 days (a)	$a_o + \Delta a_3$ 30 days (a)	$a_o + \Delta a_4$ 60 days (b)	$a_o + \Delta a_5$ 90 days (c)	$a_o + \Delta a_6$ 183 days (d)	$a_o + \Delta a_7$ 365 days (e)
FM 123-2/BR 123	2024 clad	1.40	2.64	3.26	3.56	3.50	3.66	Total disbond	Total disbond
	2024 bare	1.43	2.95	3.23	3.53	3.74	3.66	Total disbond	Total disbond
FM 123-2/BR 127	2024 clad	1.35	1.35	1.45	1.48	1.50	1.53	1.53	2.20
	2024 bare	1.37	1.41	1.50	1.57	1.65	1.63	2.08	2.31
EA 9628/BR 127	2024 clad	1.40	1.40	1.54	1.62	1.76	1.77	2.20	2.47
	2024 bare	1.45	1.46	1.52	1.62	1.72	1.73	1.94	2.46
	7075 clad	1.43	1.52	1.73	3.55	3.42	3.03	Total disbond	Total disbond
	7075 bare	1.49	1.53	1.69	1.90	1.88	1.88	1.94	2.10

<sup>a</sup>Averages of five specimens

<sup>b</sup>Averages of four specimens

<sup>c</sup>Averages of three specimens

<sup>d</sup>Average of two specimens

<sup>e</sup>One specimen

3. The wedge test method is discriminating and provides a relative ranking for many of the parameters that affect bond joint durability.
4. The data confirm that clad aluminum in the bondlines is undesirable under severely corrosive conditions.

### 3.7 LAB TEST/INSERVICE CORRELATION (TASK 7)

The purpose of this task was to attempt to establish a correlation between test results derived from laboratory-prepared specimens and service performance. Two groups of bonded aircraft details were used in this study. The first group was from commercial aircraft and the second from Air Force aircraft. Most of the details employed in this study had demonstrated poor bond durability resulting from service operations; i.e., bondlines had varying degrees of delamination and corrosion. Test specimens were fabricated from those areas of the bonded details where the original bond was still intact.

#### 3.7.1 DURABILITY TESTING OF COMMERCIAL AIRCRAFT

Details consisting of metal-to-metal bonds representing skin, doubler, and tripler configurations from four commercial aircraft were examined in the first part of this task. They were identified as aircraft A, B, C, and D, where aircraft A and C had delamination and varying degrees of corrosion, and aircraft B and D had panels that did not exhibit any bond problems in service. Fracture tests (wedge type), lap-shear tests (sustained-stress and room-temperature controls), porta-shear tests, and peel tests were conducted on specimens prepared from these bonded details.

Table 16 lists the materials of each aircraft detail, the total flight-hours accumulated at the time of removal from the aircraft, and the visual condition of the detail.

*Table 16.—Commercial Aircraft Bonded Details*

Aircraft	Alloy	Surface preparation	Adhesive/primer	Flight hours	Comments
A	2024-T3 clad	FPL etch	AF 126/EC 2320	5000+	Extensive delamination of skin-doubler bond. Some in doubler-tripler bond. Mild corrosion.
B	2024-T3 clad	FPL etch	AF 126/EC 2320	5000+	No bond delamination or corrosion.
C	2024-T3 clad	FPL etch	FM 123-2/BR 123	9000+	Extensive delamination of skin-doubler. Extensive corrosion.
D	2024-T3 clad	FPL etch	FM 123-2/BR 123	3000+	No bond delamination or corrosion.

Specimen configurations for the specific tests for each aircraft are shown in figures 34 through 37. Specimen configurations varied from the standard test specimen configurations depending on detail configurations and whether or not stiffening doublers were required for specimen symmetry. In those cases where stiffening doublers were used, the doublers were bonded to the aircraft details as wide-area bonds using a 250°F cure modified epoxy, and the test specimens were then cut to the configuration shown.

Table 17 presents results of lap-shear, porta-shear, peel and wedge tests for the aircraft details, along with a description of the associated failure modes. Even though the details from two aircraft had exhibited delamination in service, the conventional test results indicated that the remaining bonded areas were still acceptable in terms of mechanical properties.

Time-to-failure results of stressed lap-shear specimens machined from details of aircraft A and B are shown in figure 38. The test results do not predict the inservice performance of either structure, since the two details from aircraft A had experienced delamination in service and the two from aircraft B had not.

The wedge test results for these two aircraft, shown in figure 39 clearly show that aircraft B had a more durable bond. (Note, however, that the wedge test specimen configuration is different between the skin-doubler bond and the doubler-tripler bond, and between aircraft A and B, figs. 34 and 35, which accounts for the difference in initial crack lengths.) The specimen configurations are nonconventional and the results cannot be compared on a one-to-one basis with results from conventional wedge test specimen configurations.

A bonded metal-to-metal section cut from aircraft C detail is shown in figure 40. The photo identifies the areas where various tests were conducted, as well as an area where delamination and corrosion occurred.

The panel was first inspected using ultrasonic through-transmission C-scan to confirm the boundaries of delamination. Next, an electrodynamic proof load test to 2000 psi was conducted in an area adjacent to the delamination and in another area well away. Porta-shear tests were conducted in and around the doughnut-shaped proof-loaded areas, as well as at other random spots on the panel. The large areas for wedge test specimens and peel specimens were cut from the panel and appropriate doublers bonded to one or both sides as shown in figure 36. Test specimens were then cut from these areas as indicated.

Porta-shear and peel results are shown in table 17 and wedge test results are shown in figure 41. A typical wedge test specimen and a typical peel test specimen after completion of testing are shown in figure 42. The wedge test specimen exhibited cohesive failure in the pretest and posttest fracture zones, whereas in the test area extensive adhesive failure occurred. With the particular specimen shown, the porta-shear button which had first seen a 2000-psi proof load followed by the 5100-psi porta-shear attempt without failing has easily delaminated under the combination of stress and 120°F/condensing humidity environment. The peel specimen exhibited excellent peel strength plus 100% cohesive failure. However, when water was introduced at the bondline, the failure immediately went to the interface, and adhesive failure occurred.

Table 17.—Test Results—Commercial Aircraft

Detail	Bondline <sup>a</sup>	Lap shear—thin adherend				Porta shear				Peel, in.·lb			Wedge tests										
		$\bar{x}$ , psi	n	S <sup>b</sup>	Failure mode <sup>c</sup>	$\bar{x}$	n	S	Failure mode	$\bar{x}$	n	Failure mode	$a_o$ , in.	$\Delta a$ , in.				Failure mode					
														1 hr	4 hr	24 hr	72 hr						
Commercial aircraft A (poor service performance)																							
1	SD	4828	5	230	A-C	4198	5	741	A-C	—	—	—	1.66	3.50	3.50	3.50	—	A					
	DT	4734	5	120	A-C	4872	5	132	A-C	—	—	—	1.08	2.00	2.08	2.27	—	A					
2	SD	4795	4	85	C-A	4428	6	387	—	—	—	—	1.53	3.97	3.97	3.97	—	A					
	DT	4790	4	142	A-C	4850	4	107	C-A	—	—	—	0.93	1.97	2.15	2.15	—	A					
Commercial aircraft B (good service performance)																							
1	SD	4415	2	21	C-A	4118	5	822	C	—	—	—	0.48	0.48	0.48	0.48	—	C					
	SD	4425	2	50	C-A	4762	5	112	C	—	—	—	0.33	0.33	0.33	0.33	—	C					
Commercial aircraft C (poor service performance)																							
1	SD	—	—	—	—	5033	17	162	C	71.5	2	C	1.39	2.82	3.13	—	3.22	A					
Commercial aircraft D (good service performance)																							
1	SD	NO TESTS																1.18	1.22	1.29	—	—	C
2	SD	NO TESTS																1.28	1.36	1.41	—	—	C

<sup>a</sup>SD = Skin-doubler bond

DT = Doubler-tripler bond

<sup>b</sup>Standard deviation

<sup>c</sup>Failure modes:

AC = Mostly adhesive, less cohesive failure

CA = Mostly cohesive, less adhesive failure

C = 100% cohesive

A = 100% adhesive (in stressed zone)

Only wedge test specimens were fabricated from aircraft D. These results are shown in table 17 and figure 42. The failure modes were all 100% cohesive in the pretest, test, and posttest fracture zones, confirming the lack of bondline delamination and corrosion after several years of service exposures.

Conclusions from these tests are:

1. Conventional state-of-the-art tests (e.g., lap-shear, peel, porta-shear) do not predict service durability performance.
2. The wedge test shows a good correlation between the service performance of aircraft panels and related wedge test specimen performance in the laboratory.
3. Sustained-stress lap-shear time-to-failure tests do not correlate with the related aircraft details and their service performance.

### 3.7.2 DURABILITY TESTING OF AIR FORCE AIRCRAFT

Bonded panels representing C-141, C-5A, F-5, and T-38 aircraft were collected from scrap bins at McClellan, Travis, and Nellis Air Force Bases. Two types of panels were selected: (1) panels that had obvious bondline delamination and (2) panels that visually had good bonds and were scrapped for other reasons. The aircraft type, a description of each panel, and the materials of construction are identified in table 18. Of the three adhesive systems identified, two were 250°F cure systems (AF 111 and FM 123-2) and one was a 350°F cure system (FM 61).

No service history was available nor were part numbers present on most of the parts, so their identify is based on the type of part (e.g., spoiler, access door, etc.) and its location on the aircraft.

Most of the panels were of honeycomb construction with tapered closeouts. A typical example is shown in figure 43 and a sketch of a typical cross section is shown in figure 44.

Test specimens were fabricated from the metal-to-metal closeout areas or any suitable metal-to-metal faying surface where the bond still appeared to be in good condition. Stiffening doublers of appropriate thicknesses were bonded to the selected metal-to-metal areas, so that specimens of the desired configurations could be cut from them. The test specimen configurations are shown in figure 45.

Because of the poor condition and lack of much metal-to-metal bonded areas on most of the panels, not all the desired specimens could be obtained. The wedge test configuration took priority over the others because of its simplicity when only a few test specimens could be fabricated from a panel. Therefore, only the wedge test results represent all of the panels listed in table 18.

Durability test environments were 140°F/condensing humidity for the 250°F curing AF 111 and FM 123-2 adhesive systems and 160°F/condensing humidity for the 350°F curing FM 61 adhesive. Wedge test, thick-adherend DCB, and thick-adherend lap-shear specimens under

Table 18.—Air Force Aircraft Bonded Details

Aircraft	Part description	Alloy	Surface preparation	Adhesive system	Comments
C-141	Upper wing panel outboard of life raft	2024-T3 clad	FPL etch	AF 111	Panels had obvious delamination and corrosion
	Upper wing panel 1				
	Upper wing panel 2				
	Upper wing life raft door	2024-T3 clad	FPL etch	AF 111	Questionable bond in areas, but no obvious delamination
F-5	Wing panel	2024-T3 clad	FPL etch	AF 111	No obvious indication of poor bonds
	Upper wing panel between spoilers 5 and 6				
	Outboard trailing edge 1				
	Outboard trailing edge 2	2024-T3 clad	FPL etch	FM 61 FM 61	No obvious indication of poor bonds
T-38	Outboard wing trailing edge	2024-T3 clad	FPL etch	FM 61	Some delamination and corrosion
	Landing gear strut door				
	Aileron closeout door	2024-T3 clad	FPL etch	FM 123-2 FM 123-2	No obvious indication of delamination
C-5A					No obvious indication of delamination

sustained stresses were exposed to these environments. The sustained-stress level for lap-shear specimens was 1500 psi. Climbing drum peel and thick-adherend lap-shear specimens for residual bond strengths were conducted at room temperature.

Room-temperature climbing drum peel and thick-adherend lap-shear results are shown in table 19. The peel results for AF 111 are variable, which is characteristic of AF 111. The lowest strength of 42 in-lb/in suggests a possible durability problem with the wing panel. This was verified in the wedge test results where extensive crack extension occurred (fig. 46a).

*Table 19.--Residual Room Temperature Peel and Shear Strength--  
Air Force Aircraft Bondments*

Aircraft	Part description	Adhesive system	Peel strength <sup>a</sup> , in.-lb/in.	Shear strength <sup>a</sup> , psi
C-141	Upper wing panel outboard of life raft	AF 111	78	<sup>c</sup> 2420
	Upper wing panel 1	AF 111	78	<sup>c</sup> 2186
	Upper wing life raft door	AF 111	144	<sup>c</sup> 2240
	Wing panel	AF 111	42	<sup>c</sup> 2442
	Upper wing access door	AF 111	123	1730
F-5	Outboard trailing edge 1	FM 61	12	1078
	Outboard trailing edge 2	FM 61	--	1960
T-38	Outboard wing trailing edge	FM 61	9	4766
C-5A	Aileron closeout door	FM 123-2	<sup>b</sup> 60	<sup>c</sup> 1920

<sup>a</sup>Specimen replication is 1

<sup>b</sup>Specimen replication is 12

<sup>c</sup>Metal failure

FM 61 typically has low metal-to-metal peel strengths, but the 9 and 12 in-lb/in values are about half of typical. The average peel of 60 for the FM 123-2 is normal for this material.

Wedge test results for AF 111 bondments are shown in figures 46a and 46b. The low durability results, figure 46b, correlate well with the panel condition since disbond was evident. The wedge test crack growth area failed adhesively.

The results shown in figure 46a do not correlate as well since the crack extensions of specimens from the wing panel and upper wing liferaft door indicate that poor service performance could be expected. However, the panels had not yet disbanded in service.

Specimens from the third panel (upper wing panel between 5 and 6 spoilers) showed marginal but slow crack extension over the test period, which may show a correlation with its satisfactory service performance to the time of panel removal. All specimens exhibited adhesive failure in the test area.

Wedge test results for those details that were bonded with the FM 61 adhesive are shown in figure 46c. The one detail from the T-38 had evidence of delamination and corrosion in the metal-to-metal bonded areas, and the wedge test specimens correlated well with the poor bond durability in service. The two F-5 trailing edge details had no apparent bond service problems, and the wedge test results showed a marked improvement in bond durability as compared to the T-38 detail. This difference must account for the differences in service durability performance. The failure modes in the  $\Delta a$  crack growth zone for the F-5 specimens were adhesive, however --an undesirable condition. The relative inservice times for these components are not known.

Wedge test results from a C-5A detail and a T-38 detail bonded with FM 123-2 adhesive are shown in figure 46d. The C-5A detail appeared to have never been on an airplane and had no bond delamination, whereas the T-38 detail had obviously been in service but had no bond delamination. The wedge test results indicated that both details should have inadequate service durability.

Sustained-stress lap-shear results for those details bonded with AF 111 and FM 61 adhesives are shown in figure 47. A correlation between the as-received detail condition, wedge test results, and the results shown in figure 47 is not obvious. Large voids were present in the specimen from the wing panel detail, possibly causing early failure of the lap-shear specimen. Only one specimen represents each of the aircraft details; therefore, there is no indication of scatter for each. Based on the sustained-stress results presented in sections 3.2.1 and 3.4.1, one would normally expect considerable scatter. In comparing the FM 61 adhesive sustained-stress shear results to the respective wedge test results, there seems to be a consistent trend; however, the question of scatter would be present here also. The failure mode would be the best indicator. This was the situation with the test results from the commercial airplane (see, 3.7.1).

Thick-adherend DCB test results are shown in table 20. The results are expressed in terms of  $G_I$ , strain energy release rate. For the AF 111 adhesive, the initial crack length varied considerably, resulting in  $G_I$  initial values between 18 and 1.7 in-lb/in<sup>2</sup>. It seems to be a characteristic of this adhesive system that a broad range of  $G_{I0}$  values is produced. A value of 18 in-lb/in<sup>2</sup> is near but less than  $G_{Ic}$ , whereas 1.7 in-lb/in<sup>2</sup> is at or near the lower bounds of  $G_{Ic}$ . Upon exposure to 140°F/condensing humidity,  $G_I$  dropped to relatively low values, consistent with the wedge test results. The large variation in  $G_{I0}$  may be in part a characteristic of AF 111, as demonstrated in the variable peel results shown in table 19.

DCB specimens with FM 61 adhesive again yielded results consistent with the detail condition and the wedge test results.

Table 20.—Thick-Adherend DCB Test Results—Air Force Aircraft Bonded Details

140° F/Condensing Humidity for AF 111 Adhesive  
160° F/Condensing Humidity for FM 61 Adhesive

Adhesive	Panel identification and condition	Strain energy release rate, $G_I$ , in.-lb/in. <sup>2</sup>											
		Initial	1 hour	1 day	1 week	2 weeks	3 weeks	4 weeks	7 weeks	10 weeks	13 weeks	23 weeks	
AF 111	A <sup>4</sup>	1.7	1.45	1.4	1.1	0.9	0.9	0.9	0.9	0.8	0.7	0.7	
	C-141 upper wing panel outboard of life raft												
	C-141 upper wing panel 2	15.0	4.0	2.1	1.4	1.2	1.1	1.1	1.1	0.9	0.8	0.8	
	B	1.8	1.8	1.0	0.9	0.9	0.9	0.9	0.8	0.6	0.4	0.4	
	C												
FM 61	C-141 wing panel	13.5	9.3	1.9	0.8	0.4	0.3	b0.2	Test terminated				
	C-141 upper wing panel between spoilers 5 and 6	4.1	3.6	2.9	2.9	2.9	2.9	2.0	1.7	Test terminated			
	C-141 upper wing access door	18.0	18.0	18.0	6.7	5.0	3.9	3.0	2.1	1.7	1.1	1.1	
	A	1.0	0.3	0.3	0.3	0.3	0.3	0.2	0.2	0.2	0.1	0.1	
	C												
FM 61	F-5 outboard trailing edge 1	4.8	4.4	3.5	1.9	1.2	1.2	1.0	1.0	1.0	1.0	1.0	
	F-5 outboard trailing edge 2	4.4	4.0	3.0	1.7	1.7	1.7	1.7	1.7	1.7	1.7	1.7	

<sup>a</sup>Visual assessment of aircraft part conditions:

A = poor bond; B = questionable bond; C = good bond

<sup>b</sup>Fell apart

Conclusions are as follows:

1. Conventional state-of-the-art tests (e.g., lap-shear, peel, porta-shear) do not predict service durability performance.
2. The Mode I fracture tests (i.e., wedge test and DCB test) show a reasonable correlation between service panels that have delaminated interfacially (adhesive failure) and poor test specimen exposure performance.
3. Sustained-stress lap-shear tests do not correlate well with the related aircraft detail and its service performance.

#### 4.0 PHASE IV, SPECIMENS FOR OUTDOOR EXPOSURE

The purpose of Phase IV was to use the information generated in this program to provide test specimens representing the most durable bonded metal-to-metal and sandwich construction for Air Force use. These specimens are to be tested by the Air Force in long-term outdoor testing at locations to be determined.

The materials and processes selected for the Phase IV specimens and bonded panels are shown in table 21.

*Table 21.—Materials and Processes for Phase IV Specimens*

Adherends	Surface preparation	Core material	Adhesive/primer
2024-T3 bare	Phosphoric acid anodize per Boeing process specification BAC 5555	Phosphoric acid anodize and/or Dura-Core/CR III core	250°F Cure EA 9628/BR 127  350°F Cure AF 143/EC 3917

## 5.0 DISCUSSION

The preceding sections provided the experimental information for the various test methods used in this program, the test results, an interpretation of the results, and conclusions based on the specific tests. The following discussion is intended to make broader assessments and to provide a means of tying together the significant results of the program.

### 5.1 STRESSED DURABILITY TEST METHODS

The primary objective of this program was to determine a sound method of evaluating stressed durability of adhesively bonded structural materials. This objective was achieved, but a single method is not sufficient to evaluate the relative durability performance of the total system. At least two different types of test specimens are necessary to develop the information needed to make a judgment concerning relative durabilities of materials and processes incorporated in a bonded joint.

Two basic loading modes were studied, Mode I and combined Mode I and Mode II, each under a sustained or cyclic stress. Each loading mode measured different aspects of durability. For example, combined Mode I and Mode II loading (lap shear specimens) demonstrated a significant difference in durability between the two 250°F cure adhesive systems, FM 123-2 and EA 9628, whereas Mode I loading results did not suggest this difference. Both loading modes did show a difference in durability behavior between the 250°F cure adhesive systems and the 350°F cure adhesive systems.

The reasons for these differences in loading mode dependent results are not clearly understood. However, Mode I loading concentrates strains in a relatively small volume of adhesive. This is compounded by the constraints placed on this volume when a thin low-modulus material, the adhesive, is sandwiched between higher modulus materials, the aluminum. Mode I loading emphasizes interfacial weaknesses by concentrating strains at that interface.

Mode II loading spreads the strains over a much larger volume, which results in lower unit strains. The use of combined loading modes, with Mode II as primary, is more characteristic of actual designs.

A warm, wet environment is common in aircraft service. This program verified that testing in warm, wet environments is mandatory to assess environmental durability of the 250°F cure systems. The situation with the 350°F cure systems is not as clear, since generally those systems showed excellent durability in all of the tests.

Two environmental interactions need to be considered—the interface reaction between the adhesive-adherend with the environment (i.e., adherend surface treatment influence) and the adhesive bulk property effects. The interface weakness when subjected to stress and water has been identified as a major contributor to bonding problems experienced in service, whereas environmental effects on adhesive bulk properties has not been a problem in current design applications.

Bulk properties of adhesives in this discussion relate primarily to their rheological properties. For instance, an adhesive being cycled at a given strain level may experience viscoelastic behavior in a dry environment, but may revert to viscous flow behavior when exposed to a wet environment. The behavior of adhesives under a sustained or cyclic strain is time dependent, and the critical behavior will relate to the time under a critical strain level as has been shown by the creep-rupture-type failures observed in the stressed durability tests of lap shear specimens. This means that the standard mechanical properties tests, e.g., lap shear and peel, which are routinely conducted, will not be indicative of the stressed durability behavior of that material.

For future applications, the durability aspects of adhesive bulk properties must be understood, but not at the expense of understanding the adhesive/adherend interface durability sufficiently. A much higher reliability factor of bonded joints is necessary for primary structural applications, particularly when mechanical fasteners are eliminated as the alternate load path.

For the maximum reliability of a bonded joint, it is preferable that the adhesive bulk properties be the controlling factor in determining the limitations of the joint, i.e., the weakest link in the joint should be the adhesive rather than the adhesive/adherend interface. This is for the benefit of the designer, who should be able to use his design manual to select the adhesive with those bulk properties best suited for his needs without having to be concerned with the effects of surface preparation, oxide structure, and alloy on the bond durability of his design. The necessity to understand the durability aspects of the adhesive bulk properties is obvious. The question remains, however, as to what are the most realistic ways to determine these properties.

Cyclic loading is characteristic of service, and the cyclic loads imposed on specimens in this program proved to be far more damaging to the bond than the static loads. This was true, for both loading modes.

For combined Mode I and Mode II loading, the failure modes were the same for steady-state and the two slow cycles evaluated (10 and 0.8 cph). The nature of the failure (cohesive) and the conditions under which they were loaded (i.e., warm/wet environments), as well as being under a sustained stress long enough for some amount of creep deformation of the adhesive to occur, suggest the failure mechanism to be one of creep-rupture. Water that has diffused into the polymer matrix plasticizes it to the extent that relaxation under stress occurs as the matrix molecules slip past each other and in doing so causes some breakage of crosslinking bonds. With each cycle, more damage occurs until gross rupture occurs.

The specific cyclic load profile affects the amount of damage that occurs with each cycle. Work done by Bell Helicopter Company (ref. 3), describes their rationale for selecting the cyclic load frequency of 1 hour loaded, 1/4 hour unloaded. Briefly, their findings were that it typically takes longer for the adhesive to creep under load than to relax when load is removed. Some adhesives reach creep equilibrium quickly (e.g., 15 minutes) and some require longer times (e.g., 2 hours). One hour under load was selected as a time element that would encompass most of the observed adhesive creep deflections. The shorter, unloaded period was established using the same criteria, since most relaxation occurs within a 15-minute period.

By increasing the frequency to 10 cph, or 4 minutes loaded and 2 minutes unloaded, the amount of damage per cycle was less, indicating that the amount of creep and/or relaxation was not sufficient to induce maximum damage. Had the specimens been presaturated in their respective environments, it is quite possible that the damage per cycle would have been greater. Stress level will also affect the degree of damage, and there should be a threshold stress for any temperature/humidity condition below which no damage would occur during a loading cycle.

Another important factor to be considered is the rate at which load is applied and removed. For instance, a cycle for pressurization of a fuselage would take several minutes and a similar time period to depressurize. The effect of load application rate was not evaluated in this program.

The high-frequency load cycle, 1800 cpm, caused failures to occur in a manner different than the two slow frequencies. Whereas the slow-frequency failure modes suggested a creep-rupture-type failure, the 1800-cpm cycle failure modes suggested a fatigue crack propagation mechanism. The crack initiated at the load transfer edge and propagated at a 45° angle through the bondline until it was stopped by the higher modulus surfaces on the opposite side (fig. 26). Subsequent propagation was at or near the primer-adhesive interface, and fatigue striations appeared to be present. This crack growth behavior appears analogous to Stage I and Stage II fatigue crack propagation in aluminum alloys.

The 1800-cpm loading rate apparently does not allow the creep-relaxation phenomenon to occur, thereby not allowing a creep-rupture failure to take place. This indicates that the environmental aspects are dominating for the slow load frequencies and that mechanical aspects of fatigue dominate the fast loading frequency.

Test conditions that could have enhanced the mechanical fatigue aspect were (1) stress levels were much higher for 1800-cpm tests (2200 to 3300 psi vs 1500 psi maximum for the slow cycles) and (2) water absorption into the adhesive matrix was probably not significant because of the very short test periods involved (e.g., 1 to 2 days), not allowing the same degree of plasticization to occur as with the slow cycle tests. Future tests of this type should include presoaking the specimens 4 to 6 months in the respective environments.

Mode I cyclic loading caused cracks to grow within the bondlines at much lower loads than under noncyclic conditions. The slow Bell cycle resulted in faster crack growth rates than did the intermediate (10-cpm) and the fast (1800-cpm) cycles. Failure modes for all three frequencies were 100% cohesive in the center of the bond. These specimens were not presoaked in the respective test environment.

A threshold,  $G_{TH}$ , was established at the 1800-cpm frequency, which was about one-tenth of that observed for noncyclic conditions;  $G_{TH}$  is the point at which a crack will no longer grow. This point was not established at the slower frequencies because of the short test duration. Further work should be carried out to establish  $G_{TH}$  for the slow cycles as well as for different adhesive systems (e.g., the more brittle 350°F cure systems).

This same effect occurs in metals such as aluminum. Mostovoy showed a comparison of  $da/dN$  vs  $\Delta G_I$  results for other commercial adhesives bonded to aluminum to  $da/dN$  vs  $\Delta K_I$  results for aluminum alloys by converting  $\Delta G_I$  of the adhesives to  $\Delta K_I$  by using the relationship:

$$\Delta K_I = \sqrt{\Delta G_I E}$$

where  $E$  is the elastic modulus for aluminum,  $\text{psi} \times 10^6$ .

This comparison showed that the fatigue resistance of adhesives in a joint is comparable to that of aluminum alloys at low values of  $da/dN$ . A similar comparison is shown in figure 48 where the nominal range of  $da/dN$  vs  $\Delta K_I$  for the aluminum alloys presented in Mostovoy's work (ref. 4) is plotted as  $da/dN$  vs  $\Delta G_I$  and compared to the room-temperature  $da/dN$  vs  $\Delta G_I$  results for those bonded specimens tested in this program. Also on the same plot are data from Hartman, et al.; Wei, et al.; and Hyatt (ref. 5), where  $\Delta K_I$  was converted to  $\Delta G_I$  using the relationship described above.

The establishment of  $G_{I\text{TH}}$  for bonded joints is important because it should be possible to relate this parameter to the fracture characteristics of combined Mode I and Mode II loading. The existence of this threshold point in Mode I loading suggests that if the Mode I load was less than  $G_{I\text{TH}}$ , then a flaw would never grow. This also suggests that there should be a Mode II threshold or  $G_{II\text{TH}}$  for cyclic loading. However, as previously mentioned, most typical bond joints are eccentrically loaded and have combined Mode I and Mode II loads. The combined effect of Modes I and II may result in thresholds that are different than they are by themselves; e.g.,  $G_{I\text{TH}}$  possibly could be less when in the presence of  $G_{II}$  shear. This is an area that warrants further research since it could lead to some practical design considerations.

## 5.2 LONG-TERM ENVIRONMENTAL EFFECTS

Exposures greater than 6 months are necessary to evaluate bond durability. Both the stressed and corrosion aspects of durability are time dependent. Stressed durability evaluations require time for moisture diffusion and stress relaxation to occur. Corrosion is time dependent both in initiation and progression of the corrosion reaction. Attempts to reduce test time by using high stress levels and/or testing in more aggressive environments often produce misleading information.

## 5.3 STRESSED DURABILITY OF CLAD AND BARE ALLOYS

The adherend plays a role in two basically different types of durability. (These are independent of the adhesive physical properties when characterized by cohesive failures.) One type is the adhesive failure phenomenon that occurs only in the presence of combined stress and water (particularly under Mode I loading). This phenomenon is an interaction between the adhesive primer and the adherend surface (or within this interfacial zone), which is a function of the adherend surface physical and chemical structure and the physical and chemical characteristics of the adhesive primer. After delamination by this mechanism, crevice corrosion will occur to varying degrees depending on the environmental conditions. The second type is crevice corrosion, which is independent of stress.

Crevice corrosion initiated by clad dissolution was obvious in the salt spray tests where all the bonds to cladding experienced bondline corrosion. The cut edges of all the test specimens in the program were unprotected; i.e., the cross-section of the composite bond was directly exposed to the different environments, thereby accelerating the initiation of corrosion. The presence of the salt electrolyte sets up a galvanic cell due to a difference in EMF between the cladding and the core alloy. These  $\Delta E$  differences for 7075 and 2024 alloys are listed in table 22. Even though the absolute values are different and may also be significant, it is the  $\Delta E$  between the clad and core which provides the driving force. Once the cell is set up and corrosion proceeds into the bondline, a complex crevice corrosion mechanism continues the corrosion reaction. Very little corrosion was evident on the bare alloys, occurring mostly with FPL etch (7075), less with chromic acid anodize, and virtually none with phosphoric acid anodize. Surface treatment also affected the degree of clad corrosion in the same order.

*Table 22.—Comparisons of Potential Differences  
Between Cladding and Core for 2024 and 7075*

Alloy	Solution potential cladding, mV	Potential difference Cladding/core, mV	Sheet thickness, in.
2024-T3	-800	100	0.040
7075-T6	-920	100	0.125

The second corrosion phenomenon occurred in the bondlines of both clad and bare alloys (i.e., 7075 and 2024) in 140° and 160°F/condensing humidity environments, almost entirely with FM 123-2 adhesive in the bondline. The appearance of the crevice corrosion was that of filiform corrosion (a worm-like path, figs. 12 and 17) which is commonly observed under paint films. Again, surface treatment influenced the rate of progression, with the FPL-etched surfaces producing the most corrosion and phosphoric-acid-anodized surfaces the least.

To look at the problem of bondline corrosion realistically, several questions need to be answered:

1. Under what conditions can the bondline edge be adequately protected; i.e., paint and/or sealant?
2. Where fastener holes are present through the bondline, how susceptible is the structure to bondline corrosion and what means are available to minimize or eliminate the problem?
3. What environments may be encountered under what application conditions?

This is an area where more work has to be done so proper judgments can be made.

Many bonds have been made to clad surfaces with bondline edges painted, and with rivets through the bondlines. Only a small percentage of these bonds have delaminated in service.

#### 5.4 INSERVICE BEHAVIOR AND STRESSED DURABILITY TEST CORRELATIONS

The most significant aspect about inservice disbonds is that almost all the failures have been a delamination of the joint at the adhesive/adherend interface. This is also true of honey-comb disbonds, but adhesive failure to the core also occurs. Very rarely is there a failure of the adhesive itself (i.e., a cohesive failure with adhesive on both adherend surfaces) except as an aftereffect when the remaining bond cannot take the load.

This is a significant point to make, because in this program FM 123-2 exhibited the lowest stressed durability of the four systems tested. FM 123-2 and other similar 250° F cure systems have been used extensively in commercial and military aircraft without significant problems relating to the durability of the adhesive.

With the current design philosophy and applications, these materials have worked adequately; however, with more emphasis on making bonded joints more efficient (e.g., fewer fasteners, or none) and having the adhesive work at higher stress levels, the element of bond reliability becomes more critical. The use of the new technology adhesives (which include EA 9628 and several other vendors' materials) with improved stress/durability therefore reduces the environmental durability risk.

The inservice behavior of adhesively bonded aircraft assemblies correlated very well with the Mode I loading stressed durability tests, particularly for the commercial aircraft assemblies. Perhaps a better correlation could have been made relating to the military aircraft structures had more metal-to-metal bonded areas been available, since most of the structures were of sandwich construction. The Mode I durability test (wedge test specimens and thick DCB specimens) was the only method that effectively demonstrated the correlation, because the inservice problems are primarily adhesive/adherend surface interface oriented.

#### 5.5 OPTIMUM TEMPERATURE FOR STRESSED DURABILITY TESTS

An optimum temperature or environment for adhesive durability testing is difficult to determine. Much would depend on the application and type of adhesive. Subsonic aircraft would not generally experience temperature above 160°F except around engines and on camouflaged military aircraft, which can approach 200°F. A military supersonic fighter will periodically see temperatures greater than 200°F. All these aircraft can see a variety of environmental conditions just sitting on the runway.

Elevated temperatures affect the physical properties of polymers, and the temperature at which a polymer starts losing most of its strength is the glass transition temperature,  $T_g$ . The presence of water will reduce the  $T_g$ . For instance, water will plasticize a typical 250°F cure material to lower the  $T_g$  from approximately 200° to 210°F to approximately 160° to 175°F. Therefore, if one tested this material at 160°F in a wet environment, its durability performance would be low. Another vendor's product with a slightly higher  $T_g$  (wet) could show significantly better durability. The selection of 140°F/condensing humidity for testing of 250°F cure adhesives in this program may be near the  $T_g$  (wet) for some adhesives, but it is felt that this is a realistic temperature level in terms of possible service exposure.

Higher temperature cure adhesives are typically intended for higher temperature service. The  $T_G$  (wet) of a typical 350°F cure epoxy would be about 250° to 300°F, thereby implying good durability performance below these temperatures. The question remains as to what would be the optimum test environment for a 350°F cure adhesive—a high dry temperature or a lower wet temperature. A lower wet temperature may be the most severe for long-term durability tests for two reasons. (1) water still has a plasticizing effect on the polymer and while under stress the water may still induce some creep within the polymer matrix, thereby breaking molecular bonds, and (2) the presence of water over long exposure periods will enhance any bondline corrosion effects. Consequently, the selection of 160°F/condensing humidity environment represents an environment that is more severe than the 140°F environment, but more work should be conducted to better define optimum test environment for higher temperature cure adhesives.

### 5.6 DOCUMENTING TEST METHODS

A test method using the thin-adherend DCB specimen (wedge test specimen) has been written up in ASTM test method format (app. C). This test method has considerable background within The Boeing Company and elsewhere, and the tests conducted in this program further confirmed the method. It has been particularly useful in ranking surface treatment processes, for evaluating polymer interactions with the adherend surfaces, for investigating bondline crevice corrosion, and as a process control specimen.

No attempt was made to document the other test methods used in this program because of the lack of definitions of test parameters and details such as test specimen configurations, environments, and cyclic load profile.

The best test method for stressed lap-shear durability testing would include cyclic loading, with the Bell cycle being the most desirable load profile at this time. Several factors should be resolved, however, before preparing a recommended test procedure. These would include: (1) the rate of loading and unloading specimens, (2) definition of the optimum test environment for different generic adhesive types, and (3) definition of an optimum specimen configuration (i.e., thinner adherends may be more applicable).

The thick-adherend DCB specimen has had considerable use in characterizing adhesive fracture toughness, but in a noncyclic stressed condition. This is now a recommended ASTM test method, reference 6. The results of cyclic test indicate that more work has to be done to understand the fracture characteristics of adhesives in bondlines. A variant of the DCB specimen used by Mostovoy (ref. 4) may be more useful in establishing  $G_{IHH}$  parameters particularly for very slow cyclic frequencies.

The thick-adherend SCB specimen for honeycomb bond durability is also a promising test method; however, the specimen configuration, as well as the test conditions, needs more study.

## 5.7 GENERAL DISCUSSION

### 5.7.1 DURABILITY OF HONEYCOMB SANDWICH CONSTRUCTION

The durability performance of honeycomb sandwich construction is a function of both the face sheet and honeycomb core. The bond durability with respect to the face sheet is the same as in metal-to-metal bonds. The bond to the core, however, is strongly dependent on the filleting action of the adhesive and the durability of that bond with respect to the core surface. If no filleting occurs, then mechanical pullout of the core may occur at low stresses. In addition to the fillet geometry/core interaction, it is possible for a weak interface to exist between the core and fillet bond. In this case, stressed environmental durability will be low, regardless of fillet height.

Three distinct levels of core-to-fillet bond durability were observed, which were related to the three areas of core technology. The older technology, standard core, performed poorly. The current technology cores, Dura-Core and CR III core, showed a marked improvement, and the phosphoric acid anodize surface treatment applied to the core added another level of durability improvement.

Moisture migration into cells was evident with both older and current technology cores. This was measurable with the EA 9628 adhesive because of color changes. FM 123-2 does not change color with moisture exposure; therefore, moisture ingress could not be assessed. The combinations of phosphoric-acid-anodized core with all three adhesives and current technology cores with AF 143 did not exhibit moisture ingress into bonded cells (standard core was not evaluated with AF 143).

Perhaps a better environmental exposure would be a ground-air-ground (GAG) cycle (e.g., the Weber chamber), which would provide a cyclic pressure differential for the pumping action which is probably most damaging to sandwich structure in service. This environment would be applicable only to sandwich structure because of the differential pressure between the cell void and the outside. Metal-to-metal bonds would not respond to this pumping action since diffusion is the primary driving force.

More work should be done in this area with the SCB specimen. Further refinement of the test method is necessary in order to obtain the maximum amount of useful information from the test; e.g., introducing cyclic loading. Also, further refinement of the specimen configuration would be worthwhile, particularly to reduce the mass if GAG testing is to be conducted.

### 5.7.2 CORROSION-INHIBITING ADHESIVE PRIMERS

Corrosion-inhibiting adhesive primers (CIAP) provide benefits from both manufacturing and durability standpoints. CIAP is beneficial to durability in those cases where non-CIAP results in poor stressed durability of the adherend/adhesive interface. However, if applied to a poorly treated surface, it will not prevent delamination resulting from stress and water.

Non-chromate-containing curing primers can probably be developed which would be superior to the current CIAP primers in terms of bond durability. Primer development with this concept in mind should be encouraged.

### 5.7.3 ADHEREND SURFACES

The role that adherend surfaces play in the durability of the total bonded joint cannot be overemphasized. The polymer bond to the surface oxide must provide good adhesion and stress durability. In addition, the oxide must be cohesively strong enough for the applied loads. The oxides formed on aluminum can vary considerably depending on the conditions under which they are formed. In this program the anodic oxides gave the best durability results with the phosphoric-acid-anodized surfaces rating highest.

The improved stressed durability performance of anodic oxides is probably related to the specific structures of the oxide; i.e., highly porous, great surface area, high surface activity, and high cohesive strength. However, formation of the oxide structure desirable for bonding is influenced by the alloy composition. Cladding will form an oxide structure which differs from that formed by the bare alloy. Therefore, it is important that the means of forming the proper oxide structures be compatible with the variety of alloys used for bonding.

### 5.7.4 ADHESIVES

The two 350°F cure adhesives studied consistently performed better in the stressed durability tests than did either of the 250°F cure systems. This improved performance does not necessarily mean that these systems are the best choice for bonding. The brittle nature of the 350°F cure systems creates a question as to their ability to contain a crack under Mode I loading conditions. The PL 728 primer showed a variable brittle behavior on the anodized surfaces. The reason is not known, but it was an interaction between oxide structure and primer with failures oriented in the primer.

Further investigation into the brittle behavior of these 350°F cure adhesives is necessary to understand the significance in terms of real applications. The application of cyclic Mode I loads and combined Mode I and Mode II cyclic loading at low and high frequencies and several wet and dry environments would be appropriate for comparison with the 250°F cure systems.

## 6.0 CONCLUSIONS

Specific conclusions relating to individual tasks have been presented in section 3.0 with the test results. The following conclusions are of a more general nature and consider the overall results of the program.

### 6.1 STRESSED DURABILITY TEST METHODS

1. Sound methods of evaluating stressed durability of adhesively bonded structural materials were established. Two basically different test specimens are required: (1) a specimen that includes Mode I and Mode II loading (e.g., the lap-shear specimen for metal-to-metal bonds or the SCB specimen for metal-honeycomb) and (2) a specimen that includes only Mode I loading (e.g., the wedge test or DCB test). In addition, testing must be accomplished under appropriate environmental conditions, which include elevated temperature and the presence of water.
2. The lap-shear specimen is capable of rating the stressed environmental durability performance of *adhesives* by comparison of the times to failure.
3. The thick-adherend DCB and wedge test specimens are capable of evaluating the *influence of interface variables* on stressed environmental durability.
4. The thick-adherend DCB specimen is capable of establishing the critical threshold crack containment capabilities of adhesives under cyclic loads.
5. Cyclic loading of bonded joints in Mode I or combined Mode I and Mode II is more damaging to the bond than is static loading. The slow Bell cycle (1 hour stressed, 1/4 hour unstressed) was more damaging per cycle than the intermediate and fast cycles (10 cph and 1800 cpm).
6. The thick-adherend SCB specimen is capable of evaluating the relative stress durabilities of the core bond in sandwich structure.
7. The older technology standard core provides poor adhesive fillet-to-core bond durability with the 250°F cure adhesive, EA 9628. Newer technology cores (e.g., Dura-Core and CR III core) are a major step forward in providing durable core bonds. There is still room for improved core bond durability (e.g., phosphoric-acid-anodized surfaces coated with a bondable organic).

### 6.2 LONG-TERM ENVIRONMENTAL EFFECTS

Exposures greater than 6 months are necessary for high-confidence durability evaluations of bonded joints. This is because failure times are long at low stress levels, and the secondary corrosion interactions that may occur in the bondlines require long exposure times for the effects to be evident.

### **6.3 STRESSED DURABILITY OF CLAD AND BARE ALLOYS**

1. The presence of cladding in bondlines promotes bondline crevice corrosion in corrosive environments, particularly if the edge of the bondline is unprotected.
2. The corrosion mechanism is independent of the stressed durability characteristics of the joint and can occur regardless of the adhesive system and adherend surface treatments involved. However, the adhesive system and the adherend surface treatment do affect the initiation and rate of corrosion.
3. In general, the alloy, clad or bare, has little influence on the stressed durability performance of the bonded joint when the optimum adhesive primer/adherend surface treatment is used. However, the alloy does control the oxide formation mechanism/surface preparation interaction.

### **6.4 INSERVICE BEHAVIOR AND STRESSED DURABILITY TEST CORRELATIONS**

1. With Mode I loading (DCB specimens), a correlation was shown to exist between in-service behavior of adhesively bonded aircraft assemblies and stressed durability testing where assembly disbond in service correlated with poor wedge test performance.
2. Traditional test methods (e.g., lap-shear and peel) do not predict inservice durability performance.
3. Sustained-stress lap-shear durability tests also do not correlate with inservice performance.

### **6.5 OPTIMUM TEMPERATURE FOR STRESSED DURABILITY TESTS**

The optimum temperature for performing stressed durability tests of all structural aerospace adhesives has not been defined. A realistic environment for testing of 250°F cure adhesive systems was established as 140°F/condensing humidity. An appropriate test environment for 350°F cure adhesives was not clearly established and requires additional evaluation.

### **6.6 DOCUMENTING TEST METHODS**

1. The wedge test specimen has demonstrated a discriminating capability in durability testing. The test method has been written in the ASTM test method format and submitted to ASTM for consideration (app. C).
2. Test methods using the thick-adherend lap-shear SCB specimens were not sufficiently evaluated to warrant writing ASTM test procedures at this time.
3. The thick-adherend DCB specimen is now described as a recommended ASTM test method, but this test method does not include environmental testing nor cyclic load testing. Cyclic load testing of DCB specimens is not sufficiently defined to write an ASTM test procedure at this time.

## 6.7 GENERAL CONCLUSIONS

1. The more brittle 350°F cure and modified epoxy adhesives consistently demonstrated superior environmental durability at 160°F/100% RH over the 250°F cure modified epoxies at 140°F/100% RH.
2. The new technology 250°F cure modified epoxy demonstrated improved stressed durability compared to the older technology 250°F cure adhesive.
3. Of the three surface treatments evaluated, phosphoric acid anodizing showed the best overall performance.
4. Durability tests should be conducted to verify the stressed durability performance of any untested adherend/adhesive/primer/surface preparation system.
5. CIAP primer (BR 127) in the bondline improved the stressed durability of wedge test specimens compared to a non-CIAP primer (BR 123).
6. CIAP primer did not prevent crevice corrosion in the bondline.
7. There was no evidence that phosphoric acid anodized surfaces influenced the fatigue behavior of lap shear and DCB specimens. However, there was some evidence that chromic acid anodized surfaces did influence the fatigue behavior of both specimen types. When tested at 1800 cpm, some lap shear and DCB specimens with chromic acid anodized surfaces exhibited decreases in fatigue performance, apparently as a result of oxide-initiated failures.

## 7.0 RECOMMENDATIONS

### 7.1 STRESSED DURABILITY TEST METHODS

1. Continue the evaluation of the lap-shear and the SCB sandwich specimens for stressed durability testing to the point that proposed test methods in ASTM format can be prepared.
2. Further refine the lap-shear specimen configuration, particularly the adherend thickness. The thick adherends as described in this report may not be the optimum for fabricating and testing large numbers of specimens. Adherends of 0.125 in. or less should be evaluated.
3. Adopt the slow Bell cycle, 1 hour stressed and 1/4 hour unstressed, as a baseline frequency for cyclic stress durability testing of lap-shear specimens.
4. Conduct a program to study the involvement of Mode I loading in bonded joints and its interaction with Mode II shear loads, and to identify  $G_{ITH}$  and  $G_{IITH}$  for several types of adhesives and loading frequencies.
5. Continue cyclic stress durability tests of lap-shear and DCB specimens, assessing the effects of preconditioning the specimens in water prior to test and the effect of strain rate.
6. Further refine the SCB test method for honeycomb core bond durability with emphasis placed on specimen configuration, testing in a cyclic humidity and cyclic pressure environment, and testing under cyclic loading.

### 7.2 STRESSED DURABILITY OF CLAD AND BARE ALLOYS

1. Further assess the effects of cladding in bondlines when exposed to various environments to define conditions when clad could be used and when clad in the bondline should be prohibited.
2. Include protection of the cut edges using common finishing practices and the application of new technology adhesives, primers, and surface preparations, as well as an examination of the effect of fasteners through bondlines.
3. Evaluate different clad alloys, as well as the effect of heat treatments, e.g., 2024-T3 clad vs 2024-T81 clad.

## 8.0 REFERENCES

1. J. A. Marceau and W. M. Scardino, *Durability of Adhesive Bonded Joints*, Boeing Company Interim Report AFML-TR-75-3, February 1975.
2. S. Mostovoy and E. J. Ripling, *Factors Controlling the Strength of Composite Structures*, Materials Research Laboratories Final Report, Contract No. N00019-69-C-0231, 1 March 1969 through 28 February 1970.
3. T. B. Frazier and A. D. Lajoie, *Durability of Adhesive Bonded Joints*, Bell Helicopter Co. Final Report AFML-TR-74-26, March 1974.
4. S. Mostovoy and E. J. Ripling, "Flaw Tolerance of a Number of Commercial and Experimental Adhesives," *Adhesion Science and Technology*, Vol. 9B, pp 513-562, 1975.
5. M. V. Hyatt, *Program to Improve the Fracture Toughness and Fatigue Resistance of Aluminum Sheet and Plate for Airframe Applications*, Boeing Company Technical Report AFML-TR-73-224, September 1973.
6. Part 22, Designation D3433-75, Standard Recommended Practice for "Fracture Strength in Cleavage of Adhesives in Bonded Joints," *Annual Book of ASTM Standards*, p. 908.

## GLOSSARY

**Adhesive failure:** the failure mode where separation occurs at the interface between the adhesive primer and oxide (adherend surface).

**Adhesive bulk properties:** the mechanical and physical properties of adhesives that define their performance.

**Adhesive/primer system:** the combination of an adhesive and adhesive primer used in a bonded joint.

**Bonded system:** the composite bonded joint which consists of metal alloy adherend, metal oxide produced in the surface preparation step, adhesive primer, and adhesive.

**Bondments:** aluminum details joined together by adhesive bonding, e.g., test specimens, aircraft structure, etc.

**Cohesive failure:** the failure mode where separation occurs within the adhesive matrix (center of bond).

**Posttest zone:** the area of bond fracture produced after test termination by opening the specimens for inspection.

**Pretest zone:** the area of bond fracture produced prior to any test or environmental exposure, especially on double cantilever beam (DCB) specimens and single cantilever beam (SCB) specimens. This area is also known as the precracked area.

**Rheology:** the science treating the deformation and flow of matter.

**Test zone:** the area of bond fracture produced as a result of environmental exposure.

PRECEDING PAGE BLANK-NOT FILMED

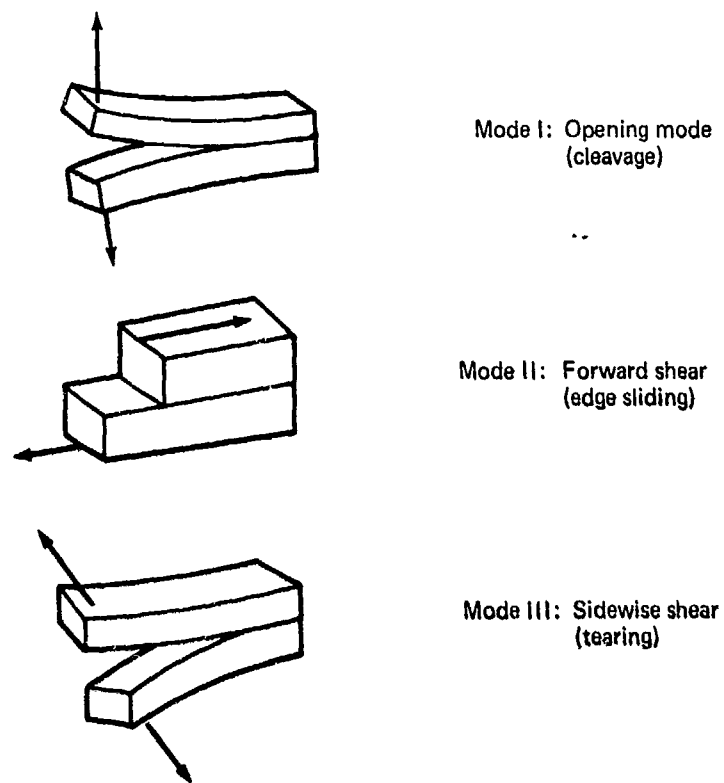


Figure 1.—Loading Modes Possible in Bonded Materials

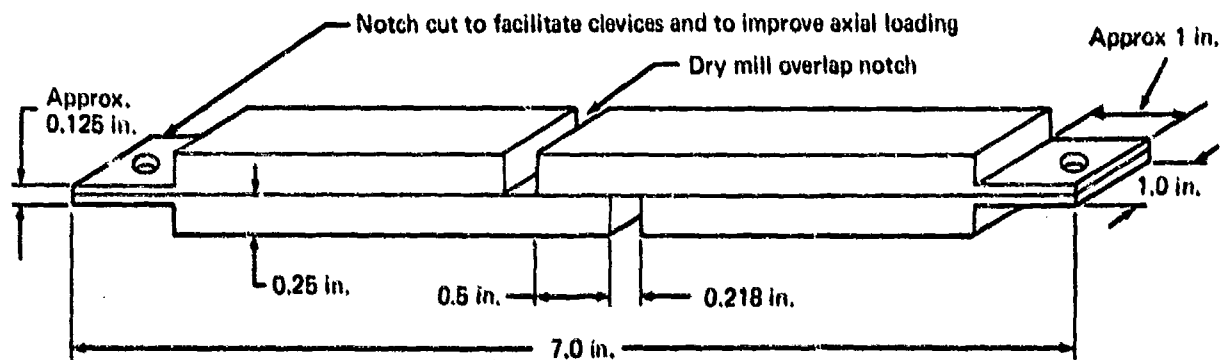
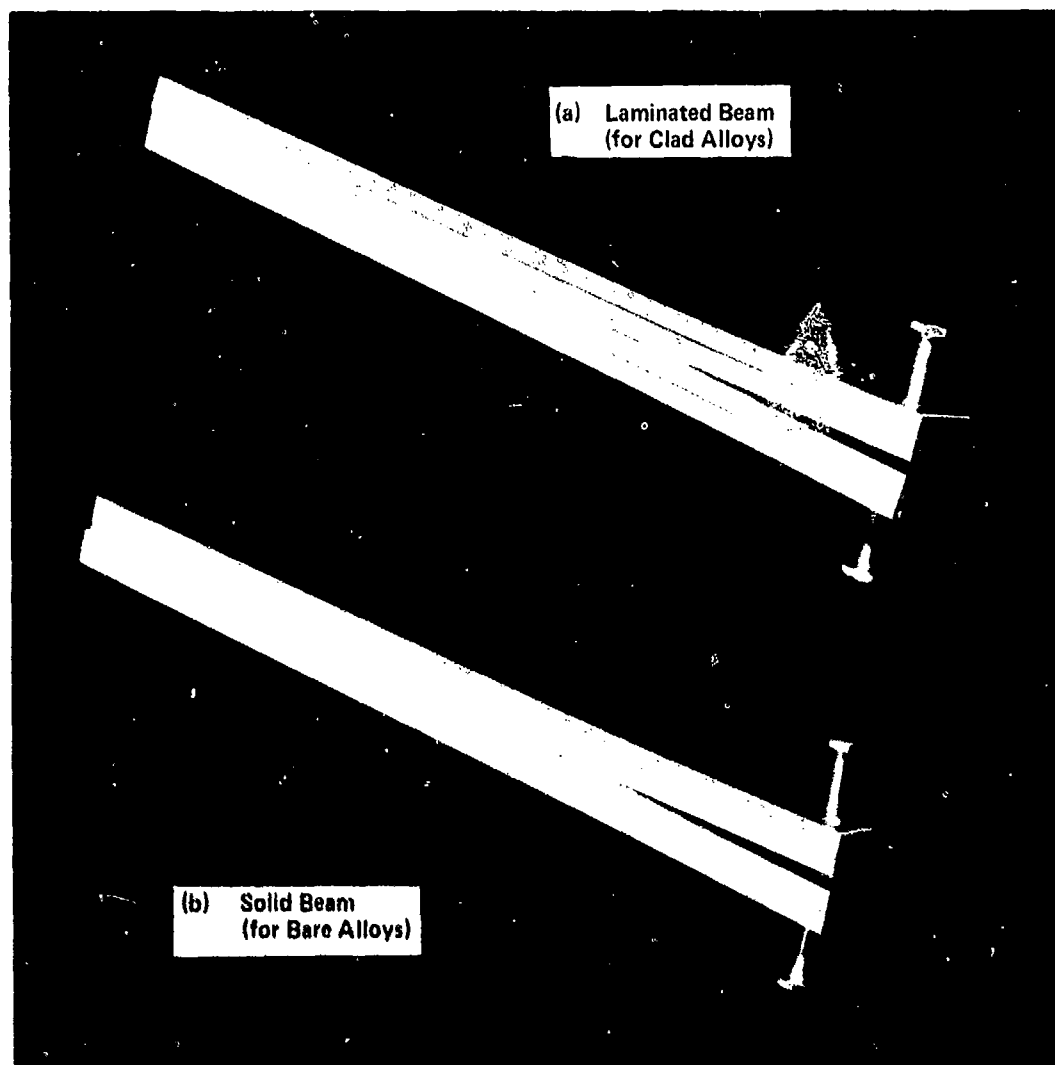
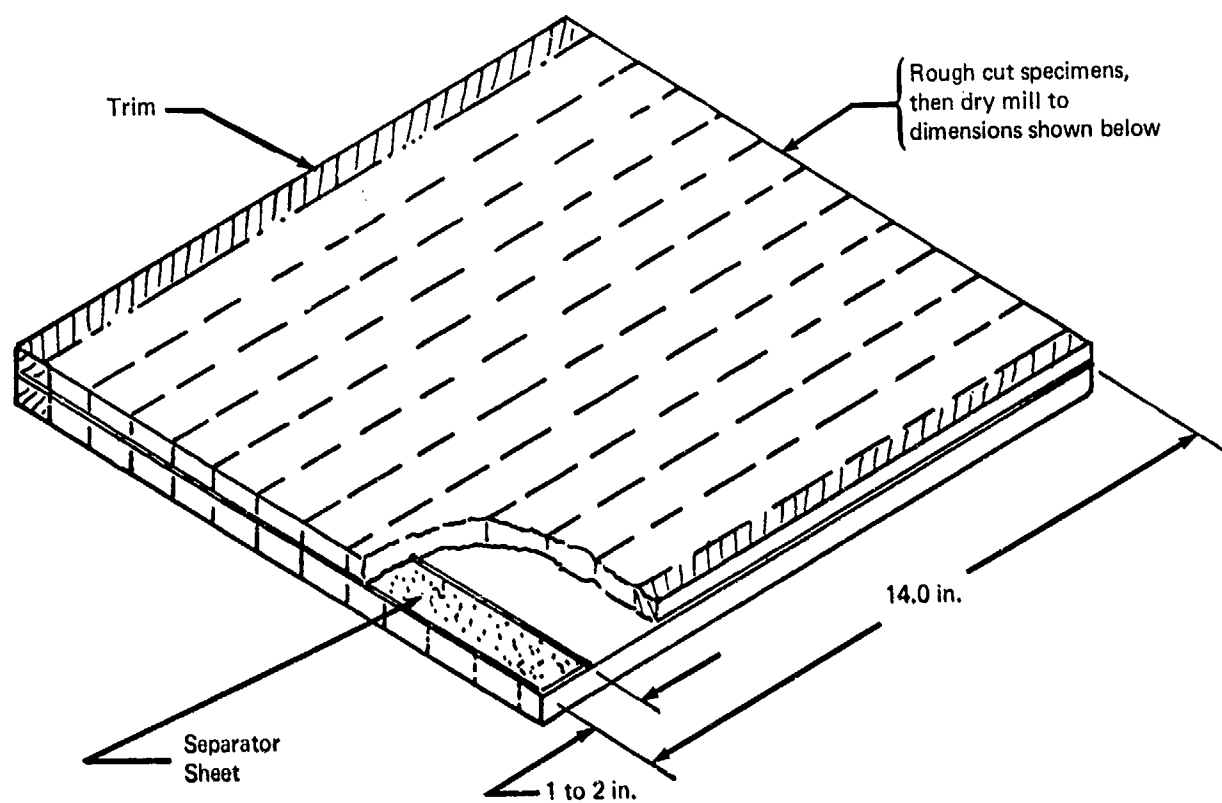


Figure 2.—Thick-Adherend Machined Lap-Shear Specimen

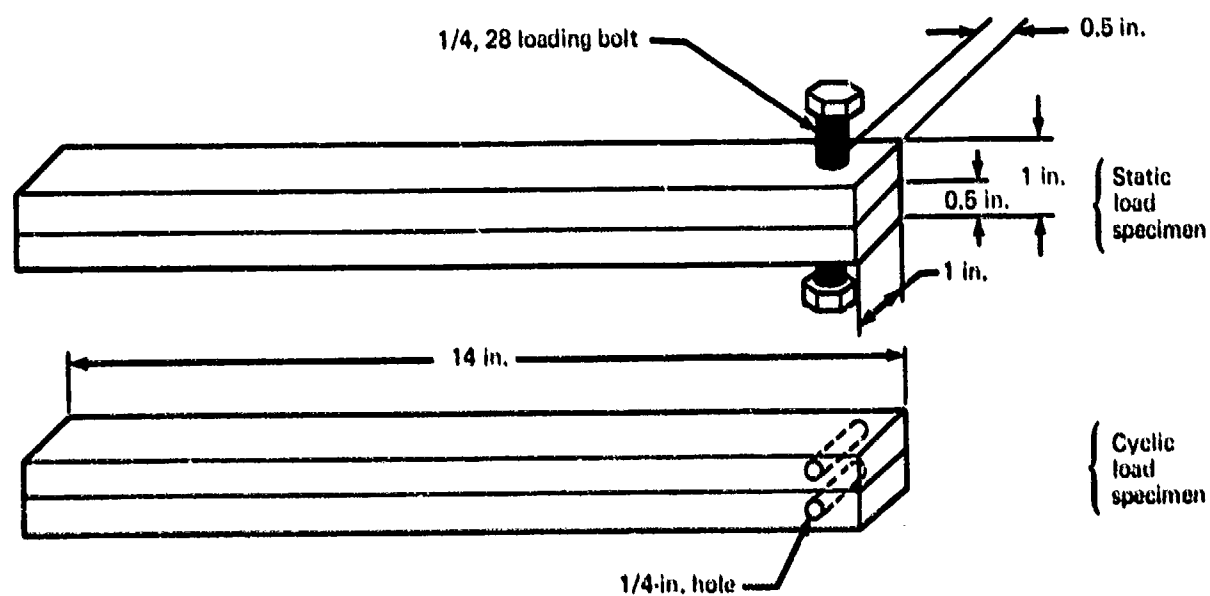
PRECEDING PAGE BLANK NOT FILMED



*Figure 3.—Thick-Adherend DCB Specimens*



(c) Typical DCB Specimen Bonded Assembly



(d) Details of Thick-Adherend DCB Specimens

Figure 3.—(Concluded)

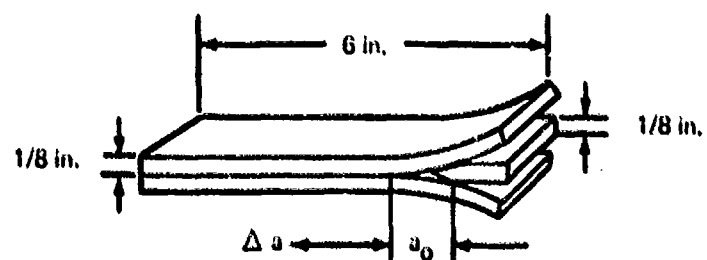
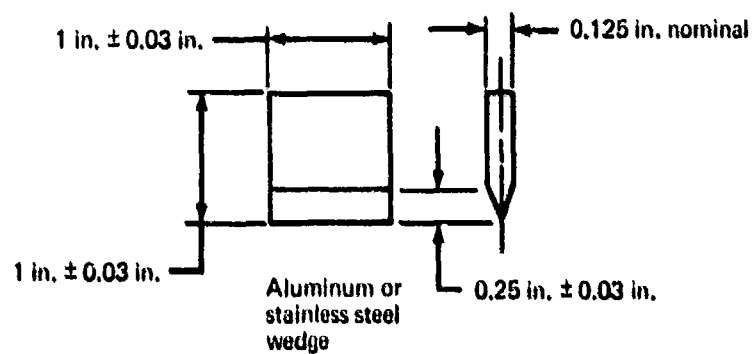
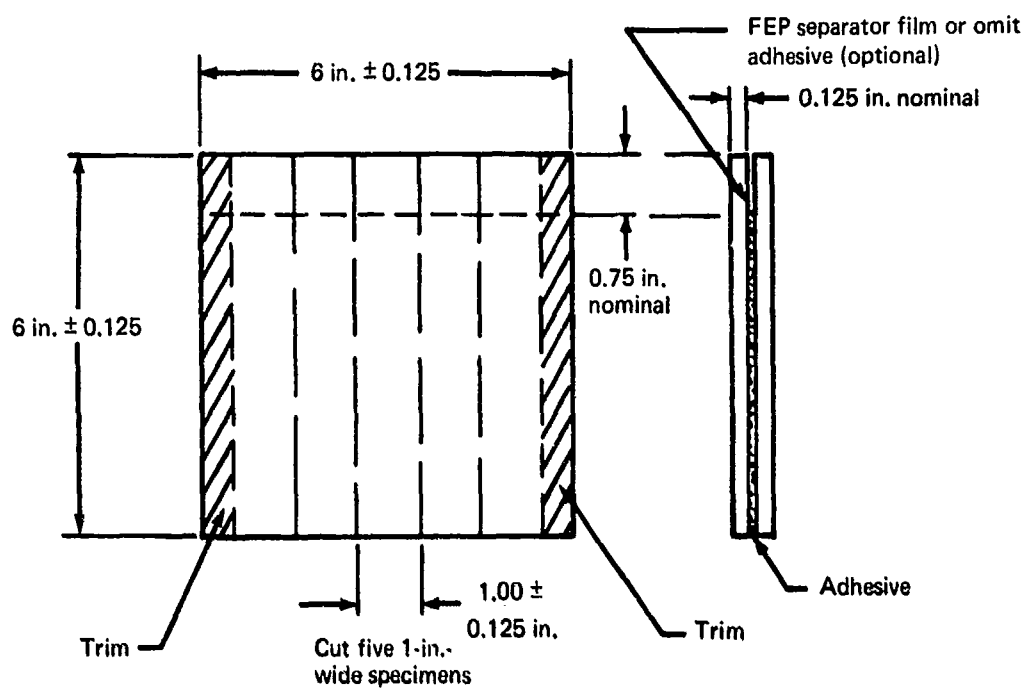
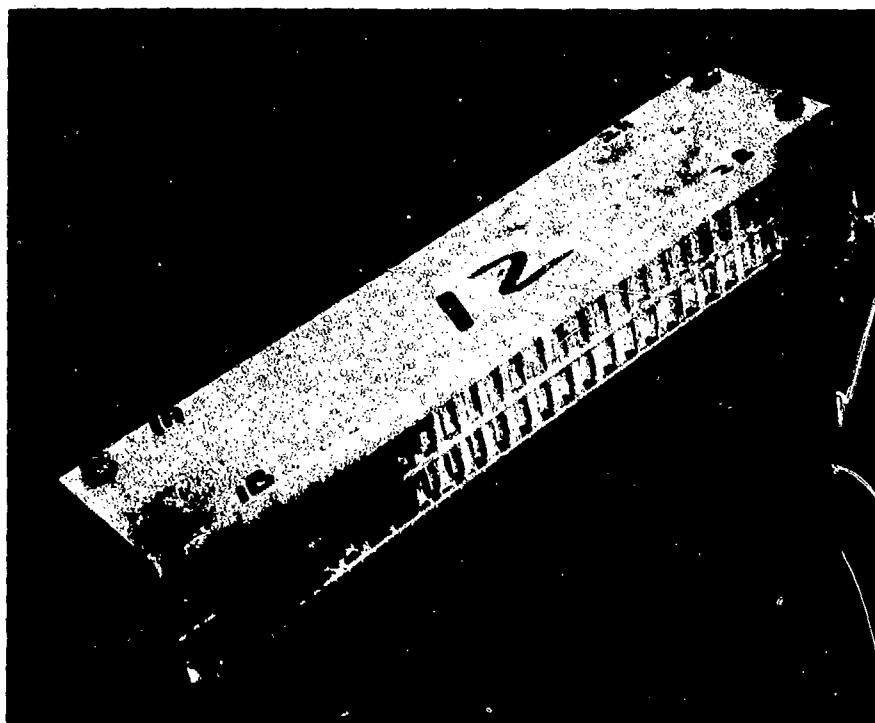
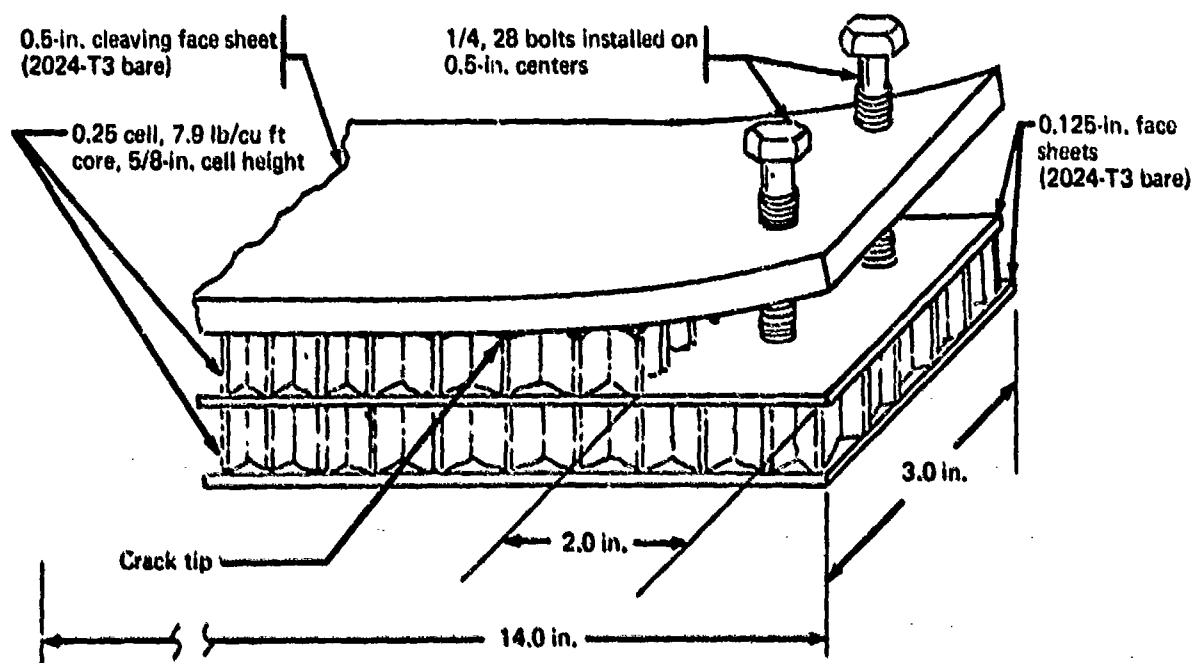


Figure 4.—Thin-Adherend DCB Specimen (Wedge Test)



(a) Stressed SCB Specimen



- Notes: 1. Opposite end of specimen identical  
2. Specimens saw cut from bonded panels 14 x > 3 in.

(b) Details of SCB Specimen Configuration

Figure 5.—Thick-Adherend SCB Specimen

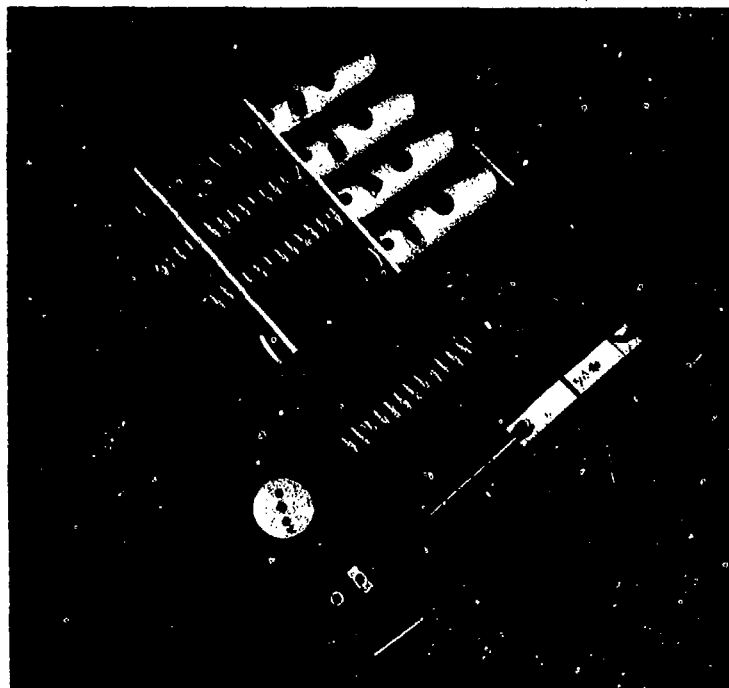


*Figure 6.—Thick-Adherend Lap-Shear Modified Loading Fixture*

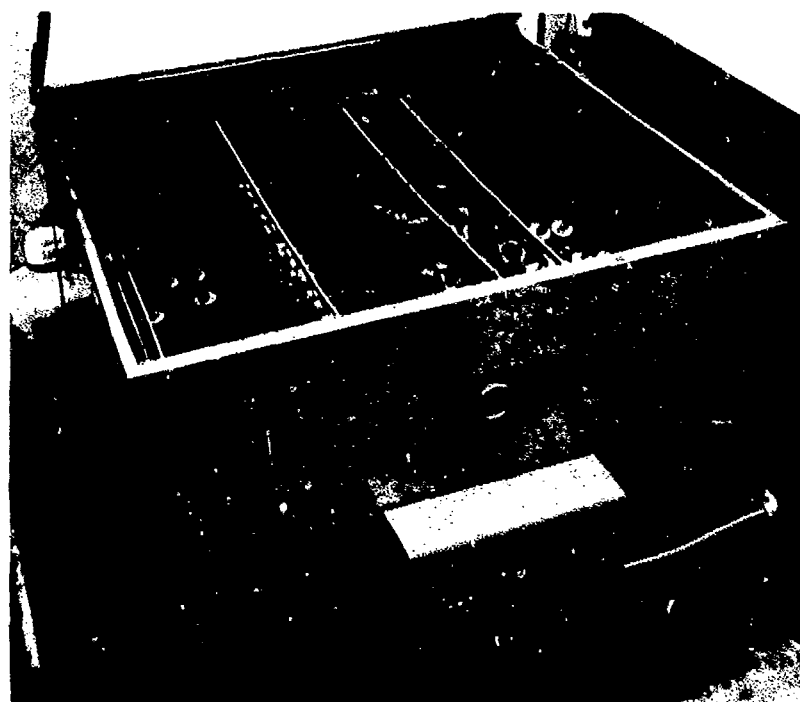
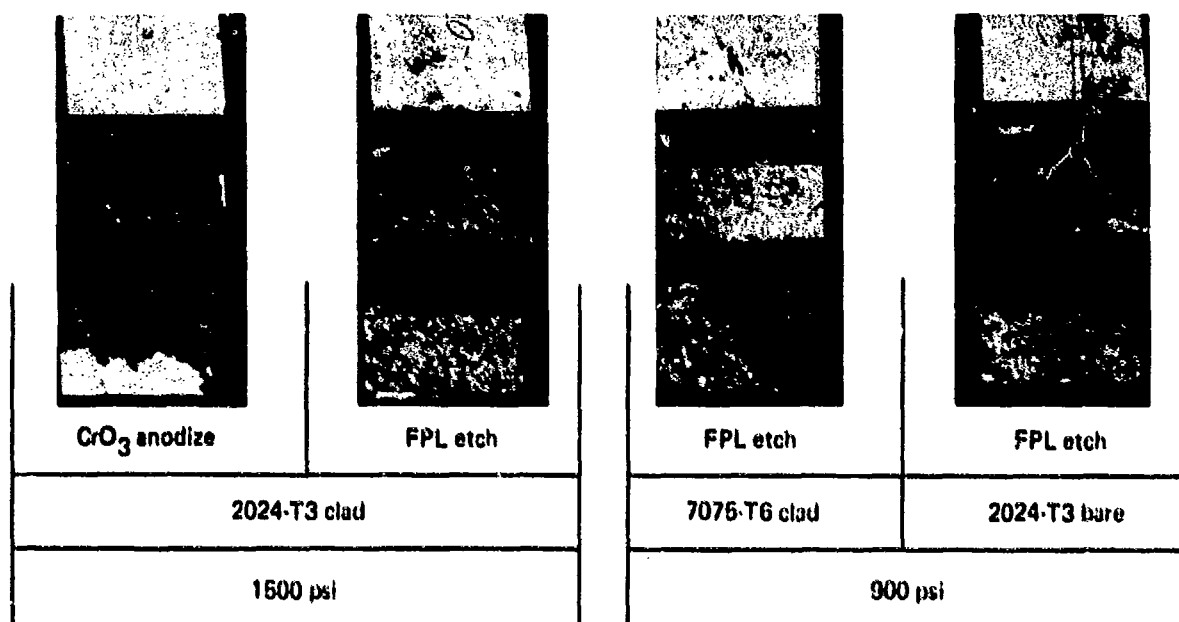
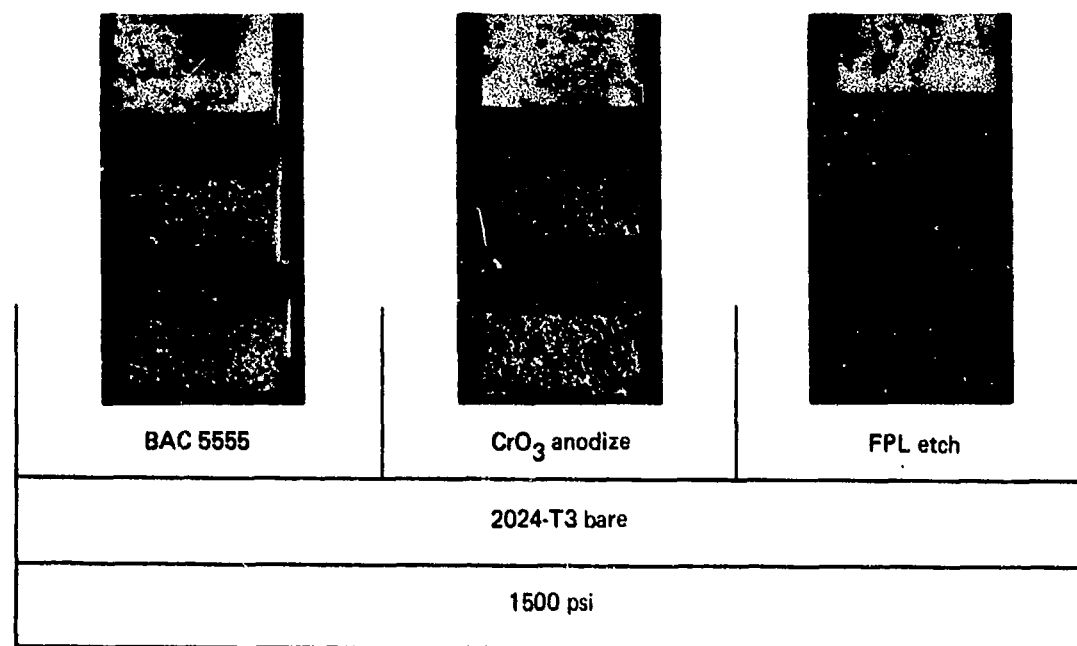
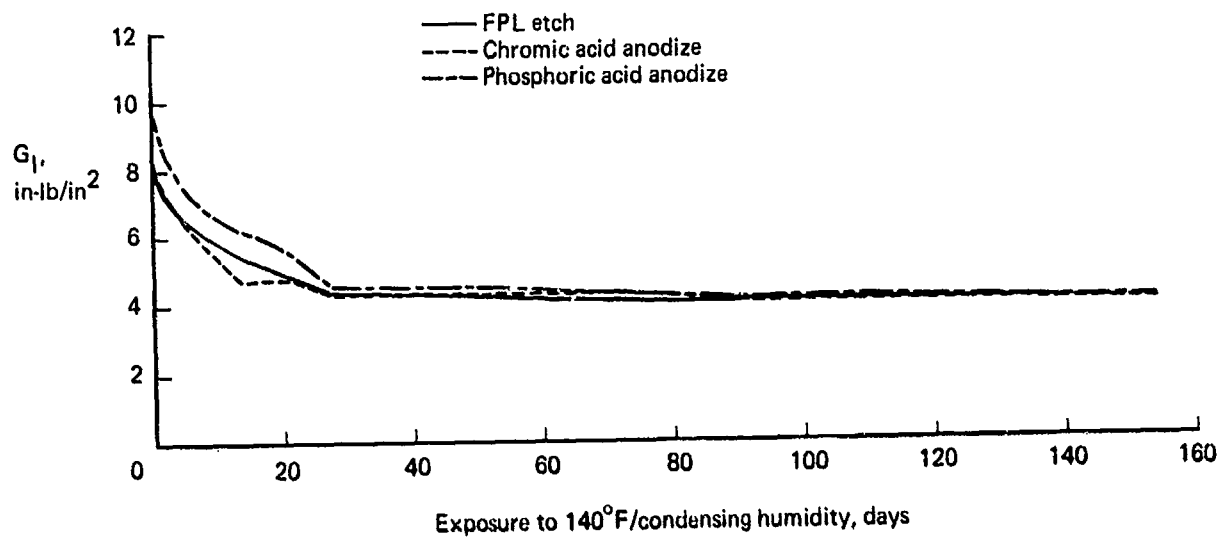


*Figure 7.—Environmental Exposure Chamber for 140° F/Condensing Humidity, Showing Arrangement of DCB and Stressed Lap-Shear Specimens*

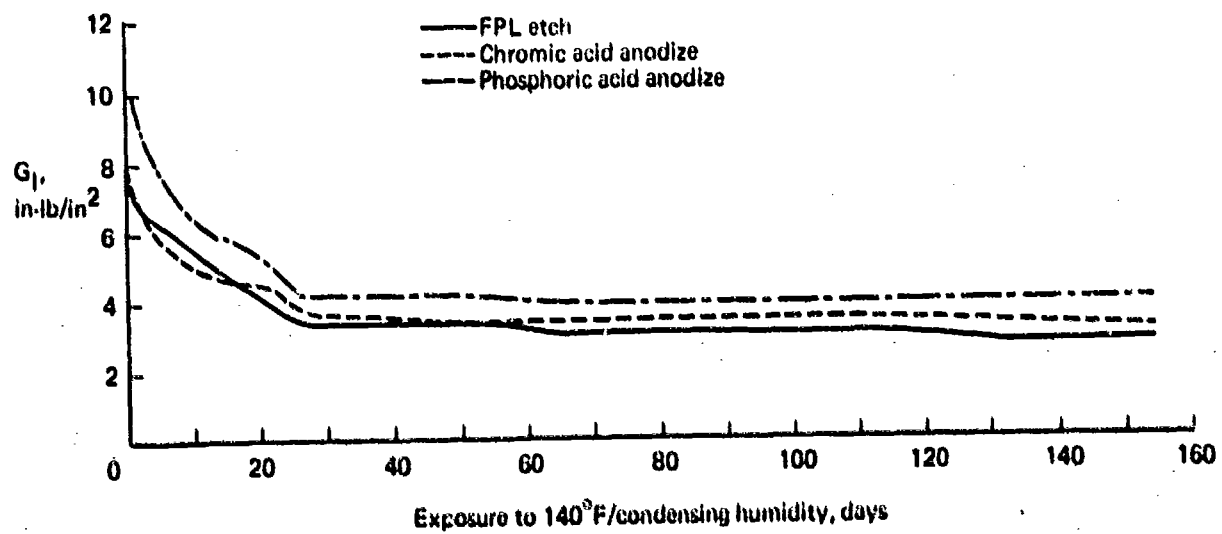


Adhesive System: FM 123-2/BR 127

Figure 8.—Typical Thick-Adherend Lap-Shear Specimen Failures for Sustained-Stress Tests Exposed to 140° F/Condensing Humidity

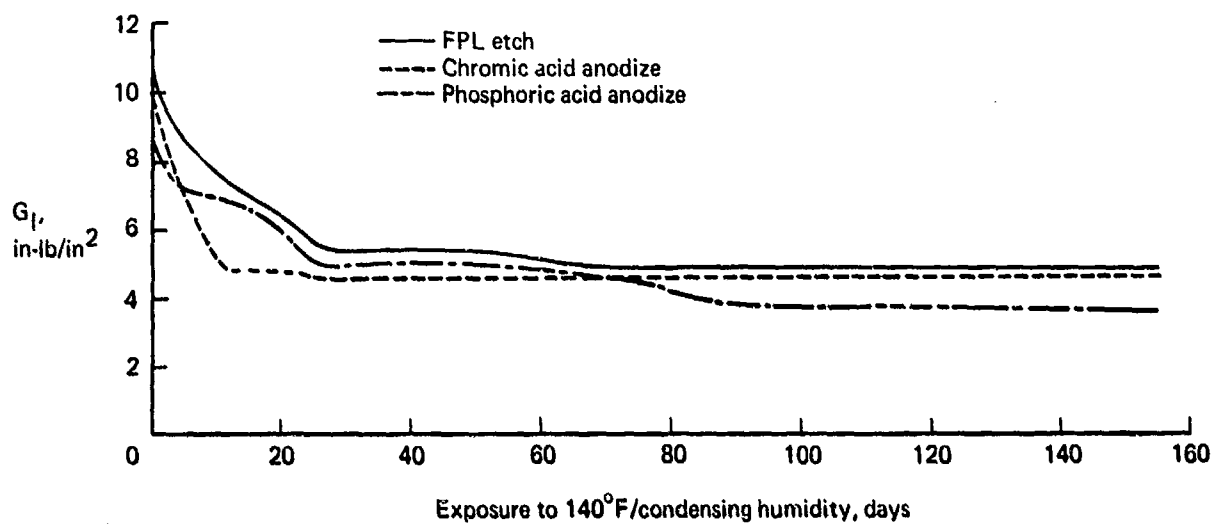


(a) FM 123-2/BR 127, 2024-T3 Clad

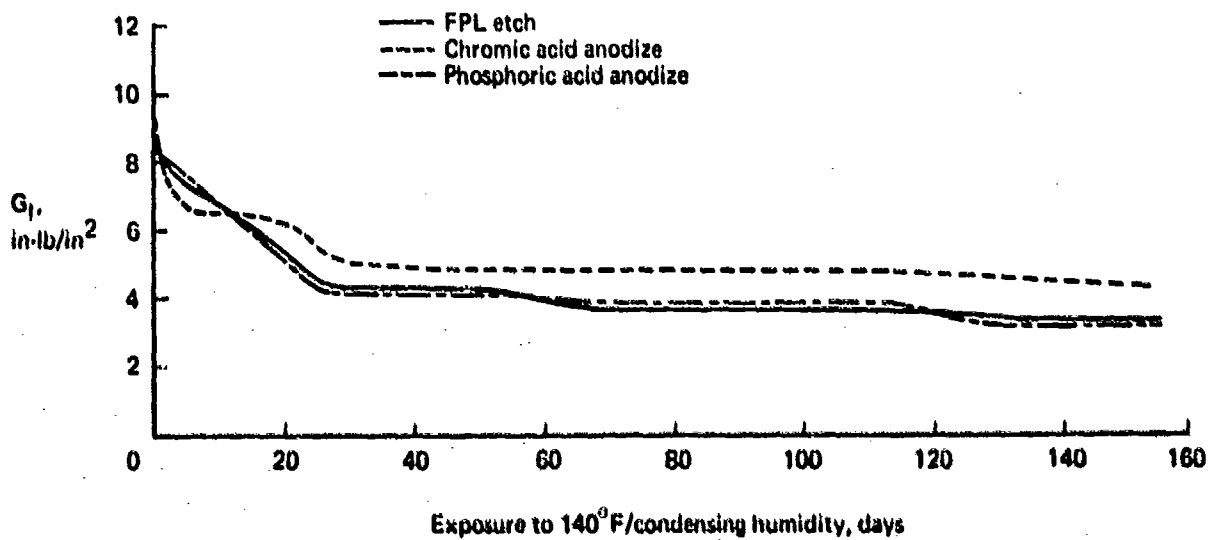


(b) FM 123-2/BR 127, 2024-T3 bare

Figure 9.—DCB Specimen Exposure Results

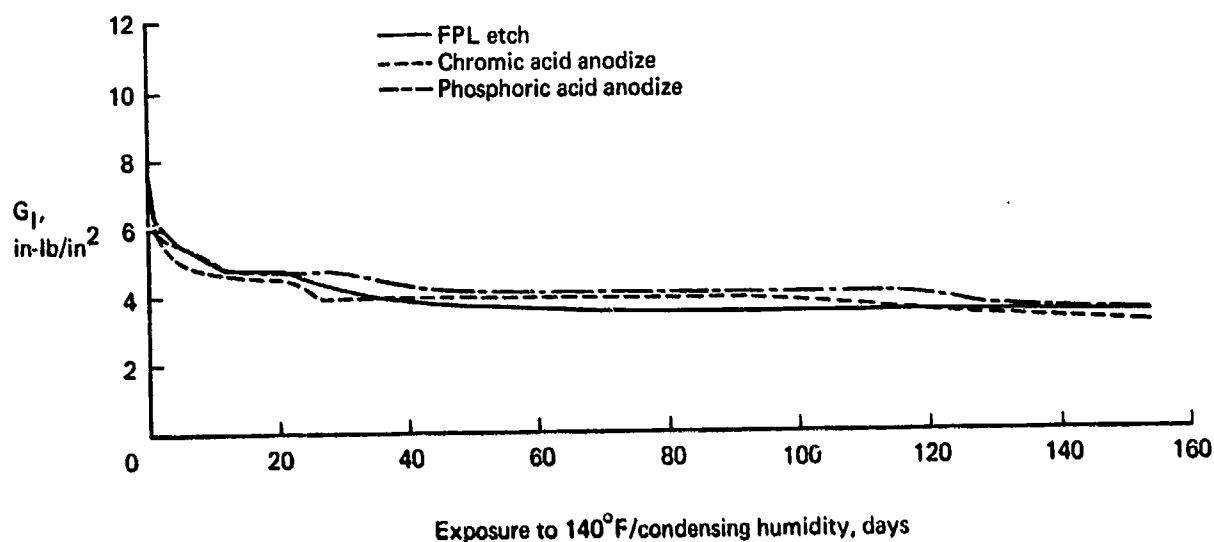


(c) FM 123-2/BR 127, 7075-T6 clad

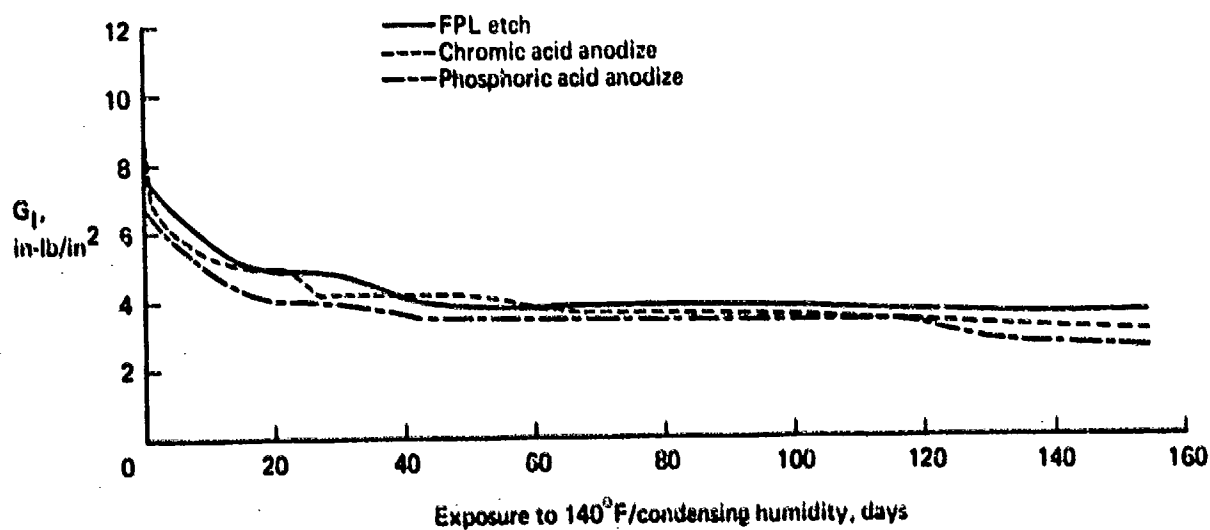


(d) FM 123-2/BR 127, 7075-T6 bare

Figure 9.—(Continued)

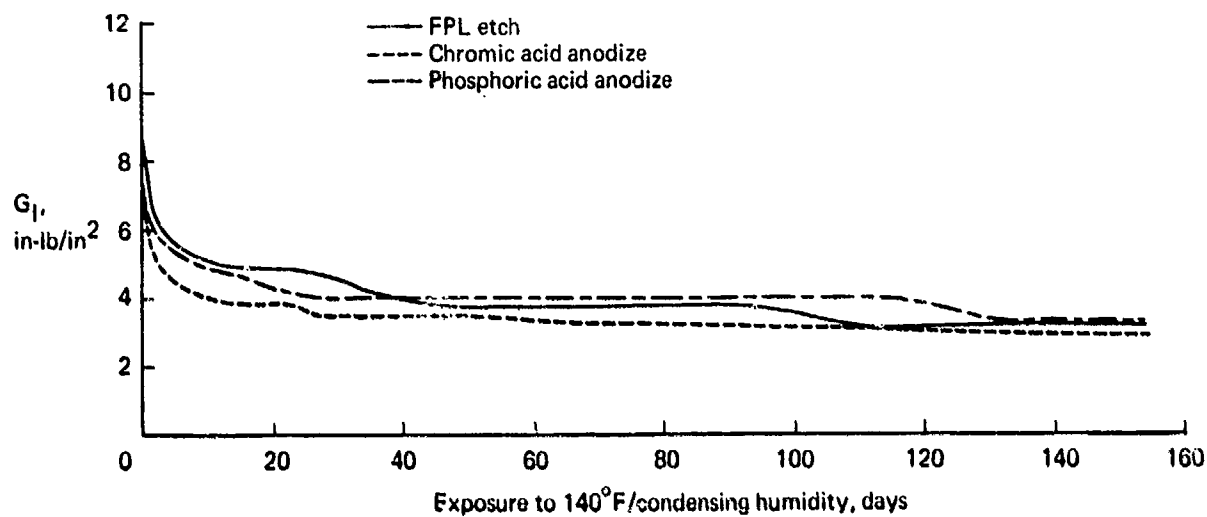


(e) EA 9628/BR 127, 2024-T3 clad

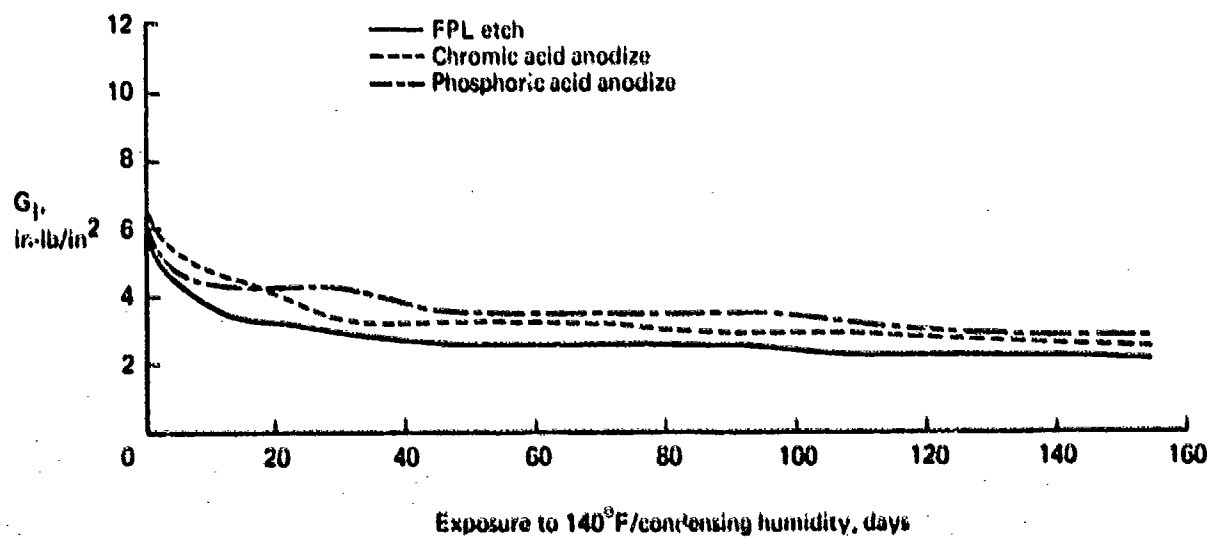


(f) EA 9628/BR 127, 2024-T3 bare

Figure 9.—(Continued)

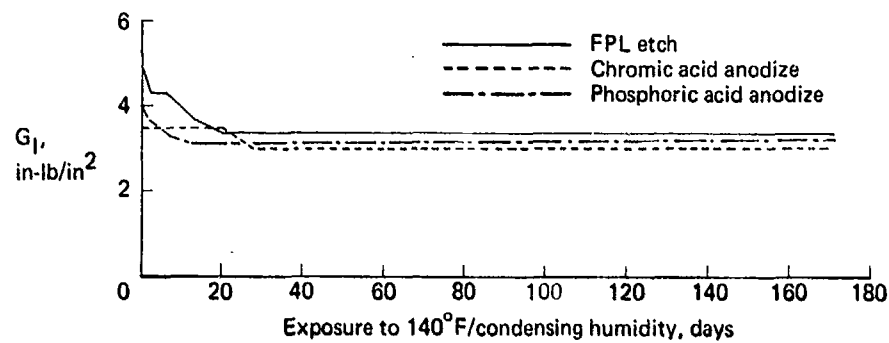


(g) EA 9628/BR 127, 7075-T6 clad

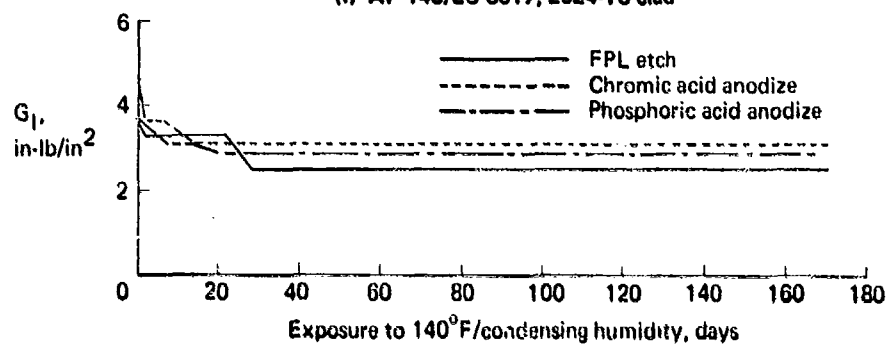


(h) EA 9628/BR 127, 7075-T6 bare

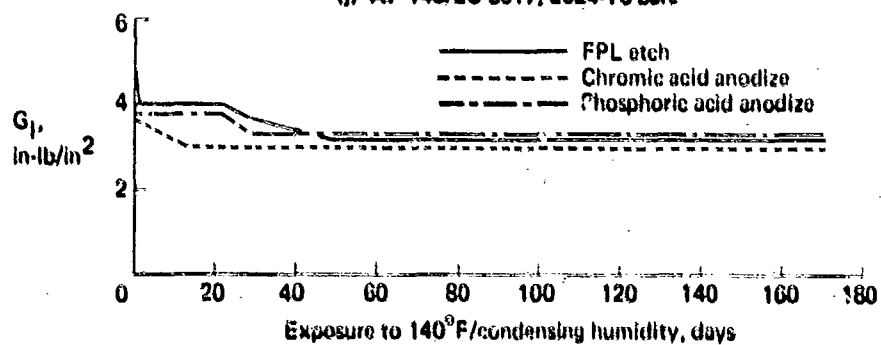
Figure 9.--(Continued)



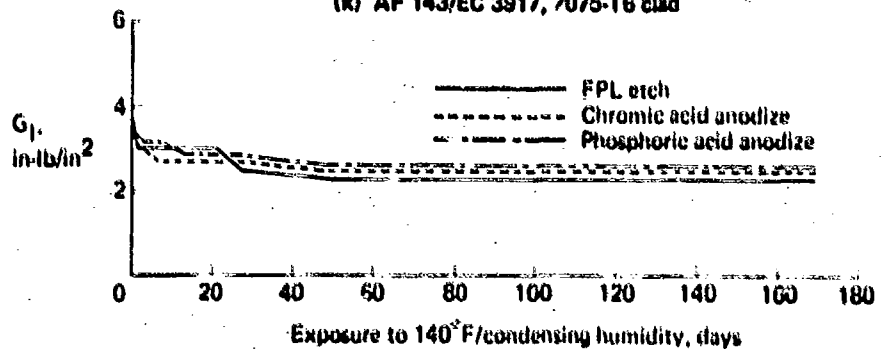
(i) AF 143/EC 3917, 2024-T3 clad



(j) AF 143/EC 3917, 2024-T3 bare

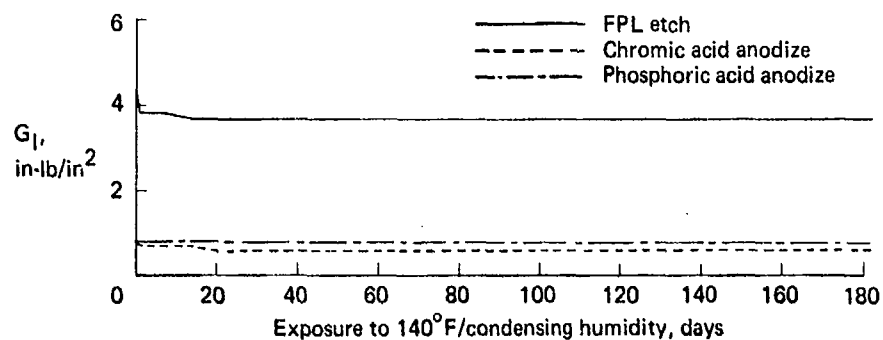


(k) AF 143/EC 3917, 7075-T6 clad

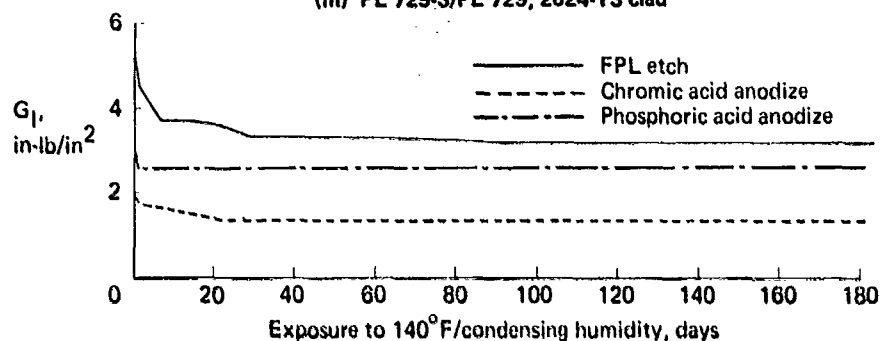


(l) AF 143/EC 3917, 7075-T6 bare

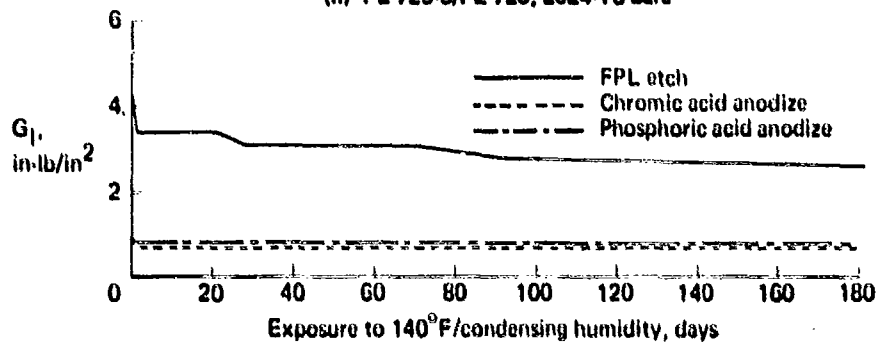
Figure 9.—(Continued)



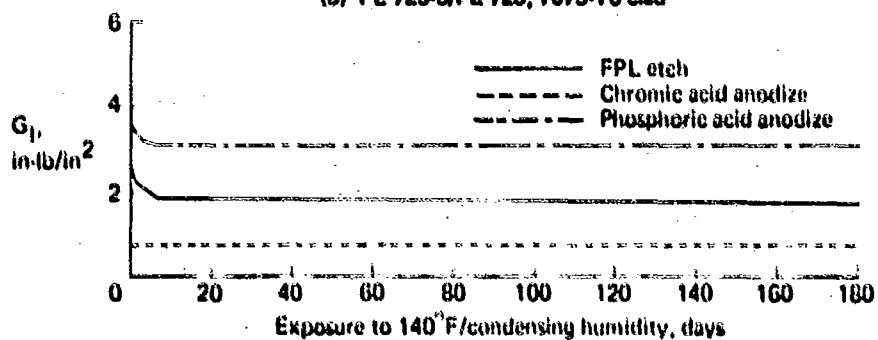
(m) PL 729-3/PL 729, 2024-T3 clad



(n) PL 729-3/PL 728, 2024-T3 bare

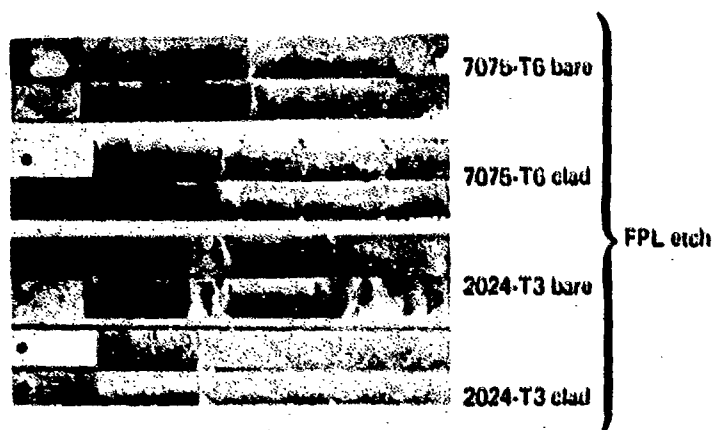
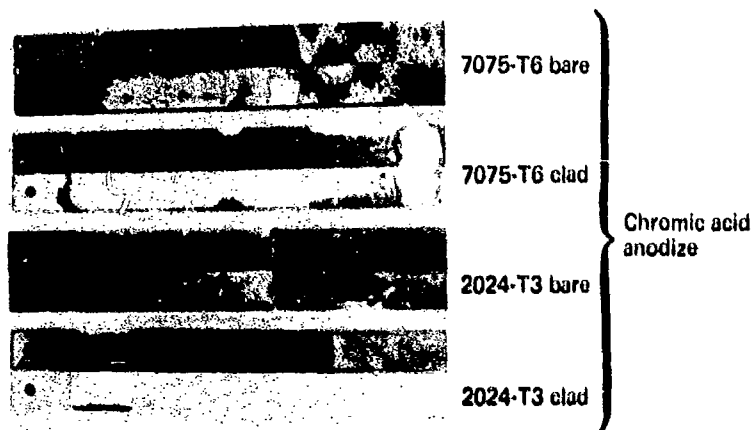
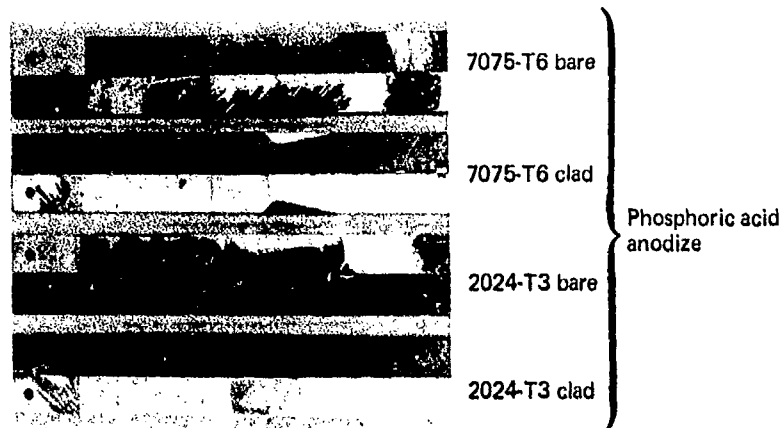


(o) PL 729-3/PL 728, 7075-T6 clad



(p) PL 729-3/PL 728, 7075-T6 bare

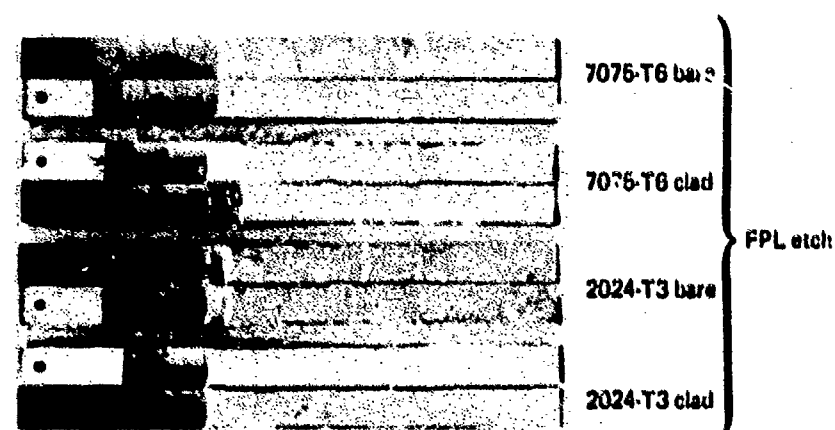
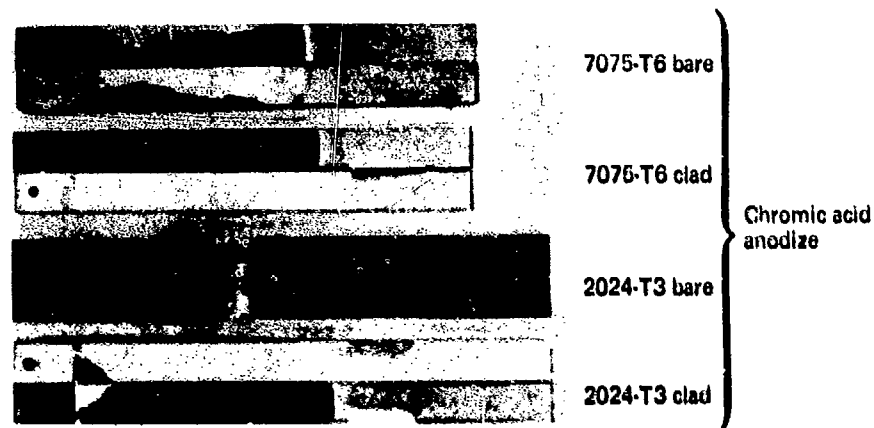
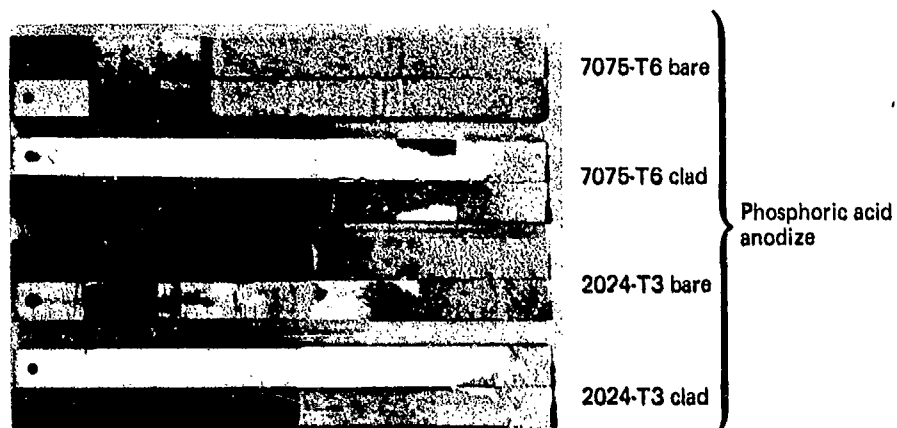
Figure 9.—(Concluded)



→ Crack growth

(a) With 20 Weeks' Exposure to 140°F/Condensing Humidity

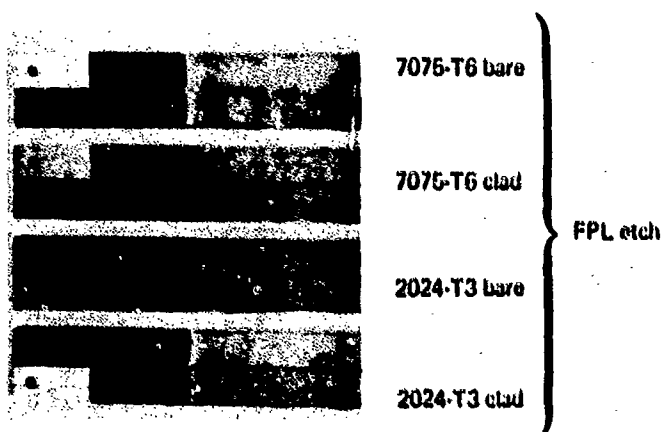
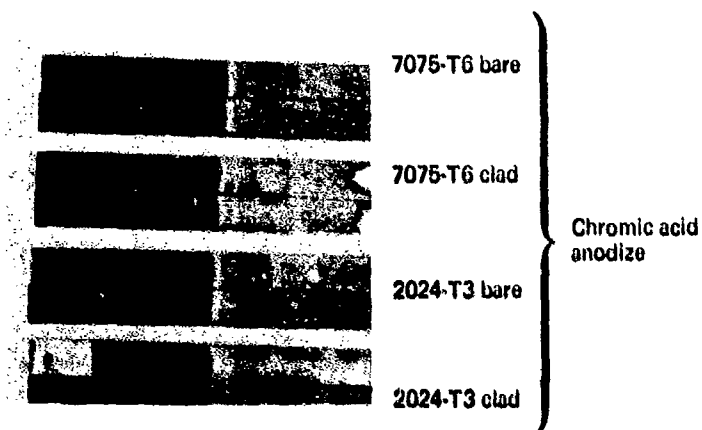
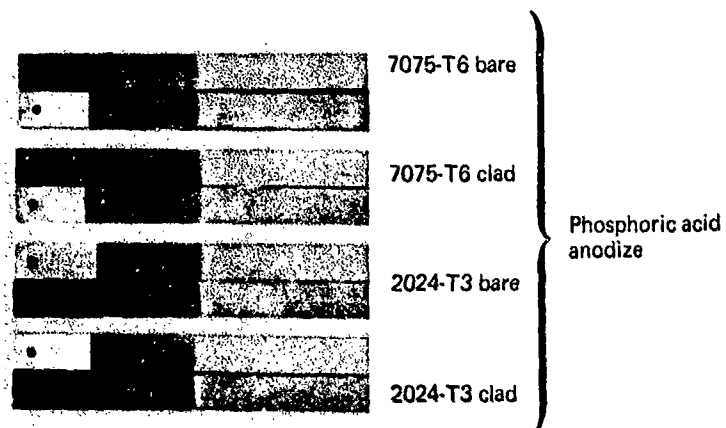
Figure 10.—Opened DCB Specimens Bonded with PL 729-3/PL 728



→ Crack growth

(b) With 77 Weeks' Exposure to 140°F/Condensing Humidity

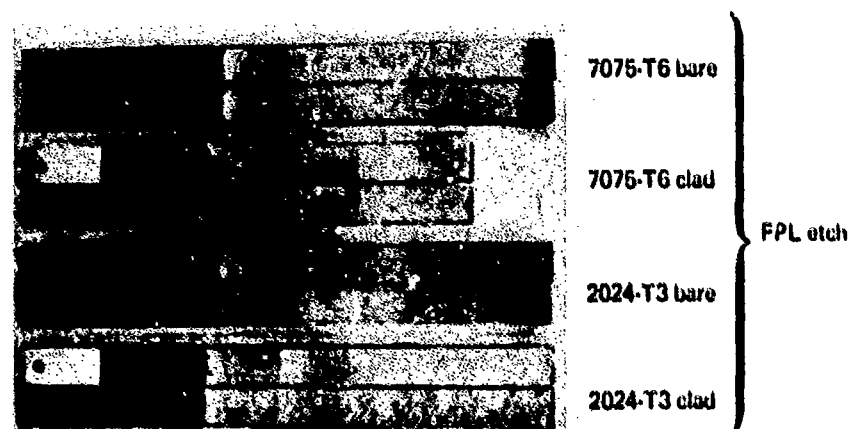
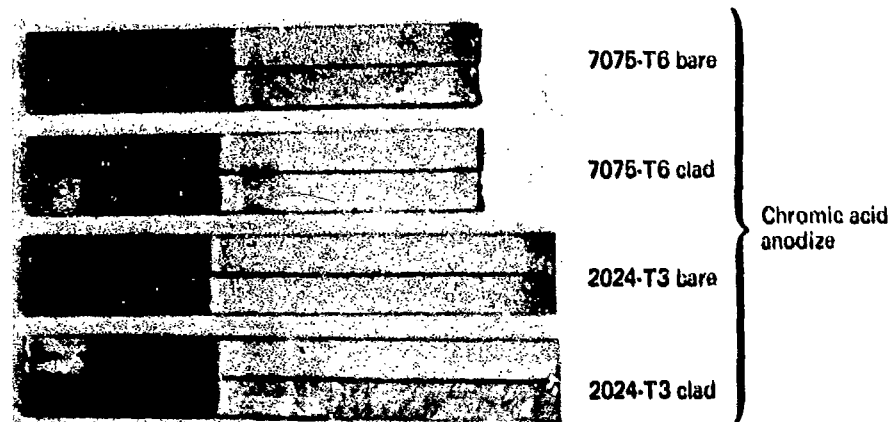
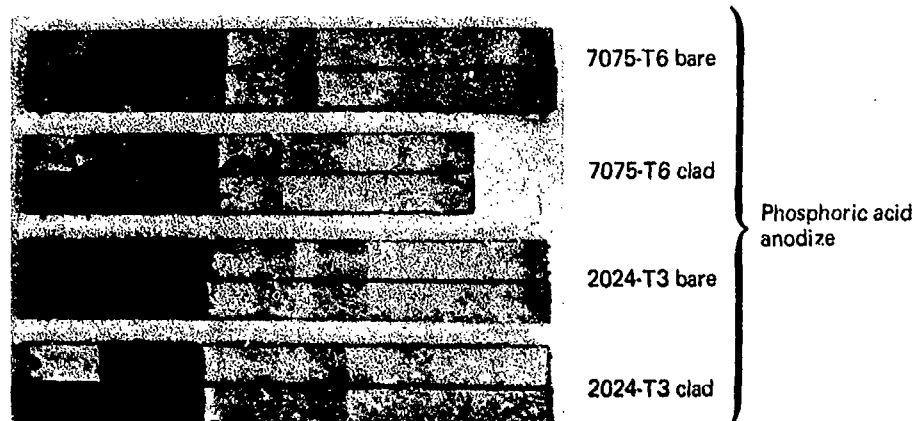
Figure 10.—(Concluded)



→ Crack growth

(a) With 20 Weeks' Exposure to 140°F/Condensing Humidity

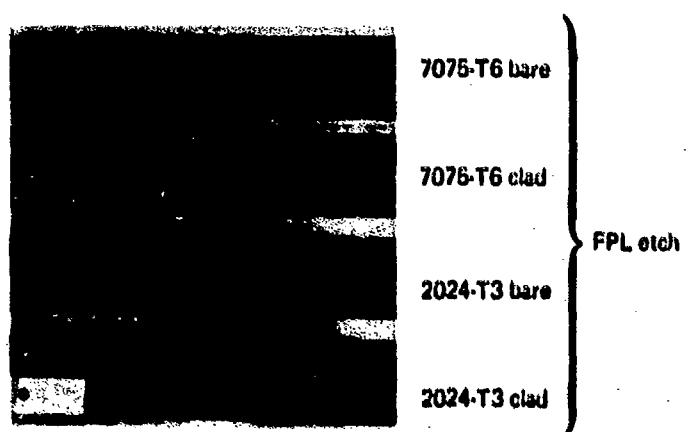
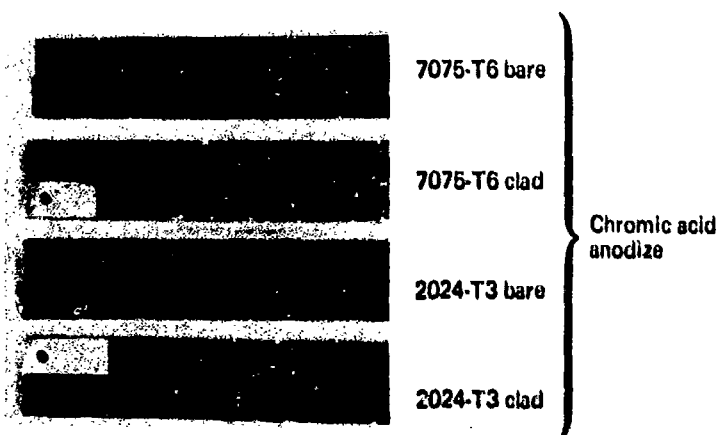
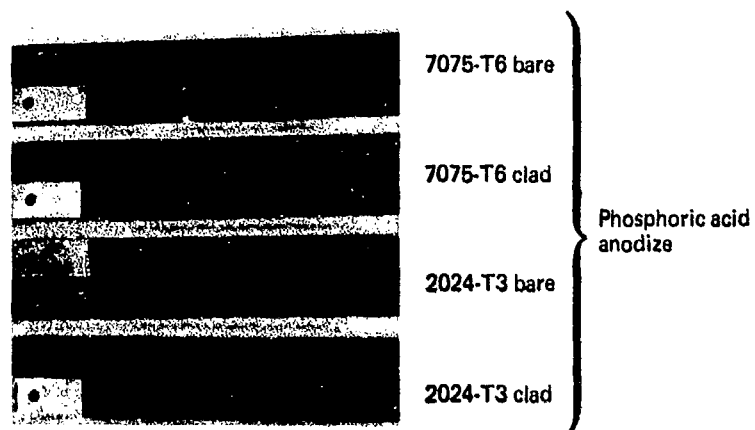
**Figure 11.—Opened DCB Specimens Bonded With AF 143/EC 3917 System**



→ Crack growth

(b) With 77 Weeks' exposure to 140°F/Condensing Humidity

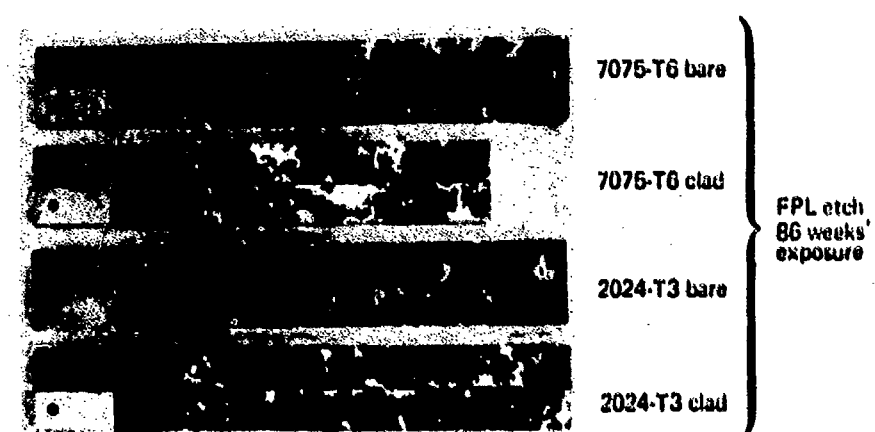
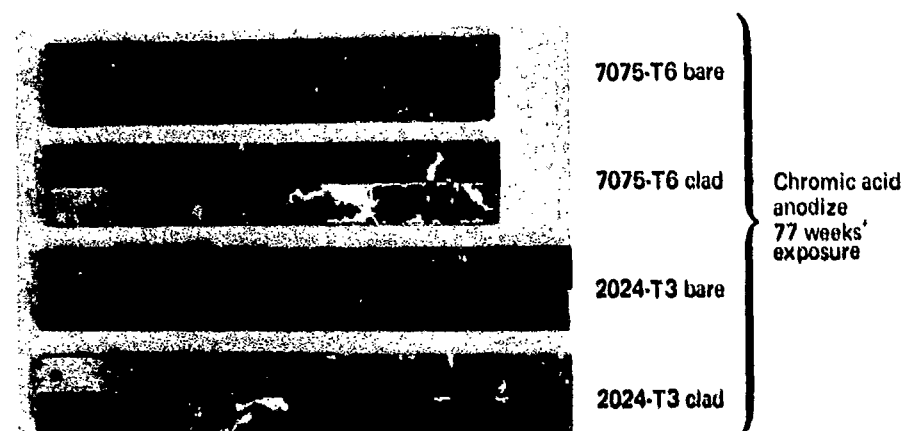
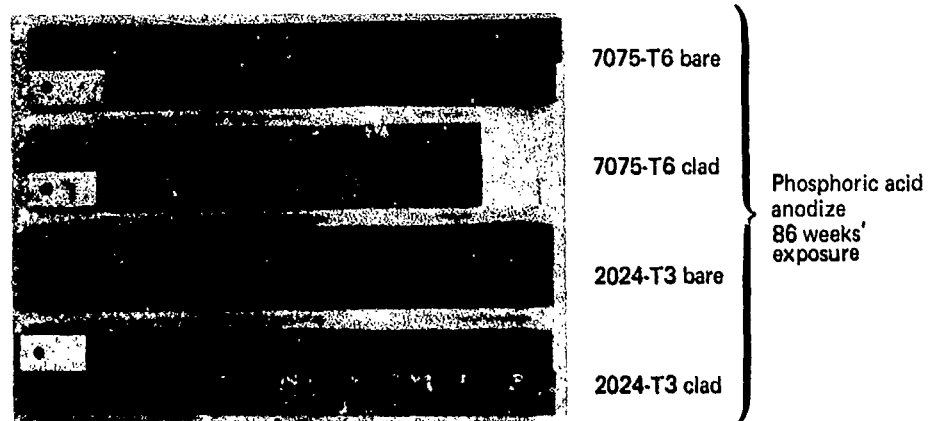
Figure 11.—(Concluded)



→ Crack growth

(a) With 20 Weeks' Exposure to 140°F/Condensing Humidity

**Figure 12.—Opened DCB Specimens Bonded With FM 123-2/BR 127 System**



→ Crack growth

(b) With up to 86 Weeks' Exposure to 140°F/Condensing Humidity

Figure 12.—(Concluded)



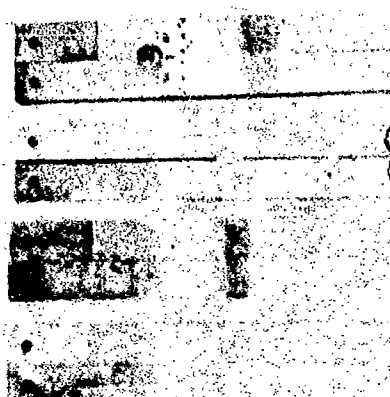
7075-T6 bare

7075-T6 clad

2024-T3 bare

2024-T3 clad

Phosphoric acid  
anodize



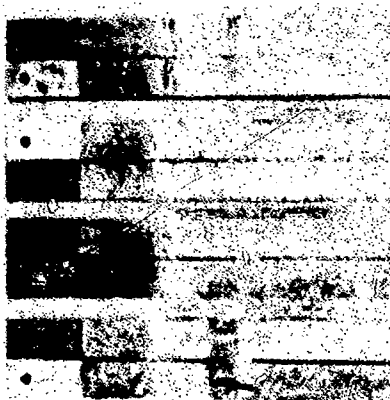
7075-T6 bare

7075-T6 clad

2024-T3 bare

2024-T3 clad

Chromic acid  
anodize



7075-T6 bare

7075-T6 clad

2024-T3 bare

2024-T3 clad

FPL etch

→ Crack growth

(a) With 20 Weeks' Exposure to 140°F/Condensing Humidity

Figure 13.—Opened DCB Specimens Bonded With EA 9628/BR 127 System



7075-T6 bare

7075-T6 clad

2024-T3 bare

2024-T3 clad

Phosphoric acid  
anodize  
86 weeks'  
exposure



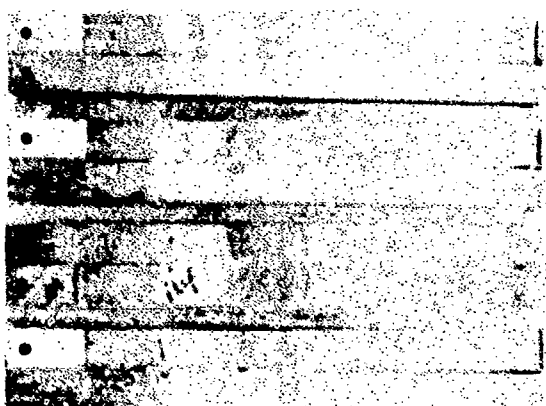
7075-T6 bare

7075-T6 clad

2024-T3 bare

2024-T3 clad

Chromic acid  
anodize  
77 weeks'  
exposure



7075-T6 bare

7075-T6 clad

2024-T3 bare

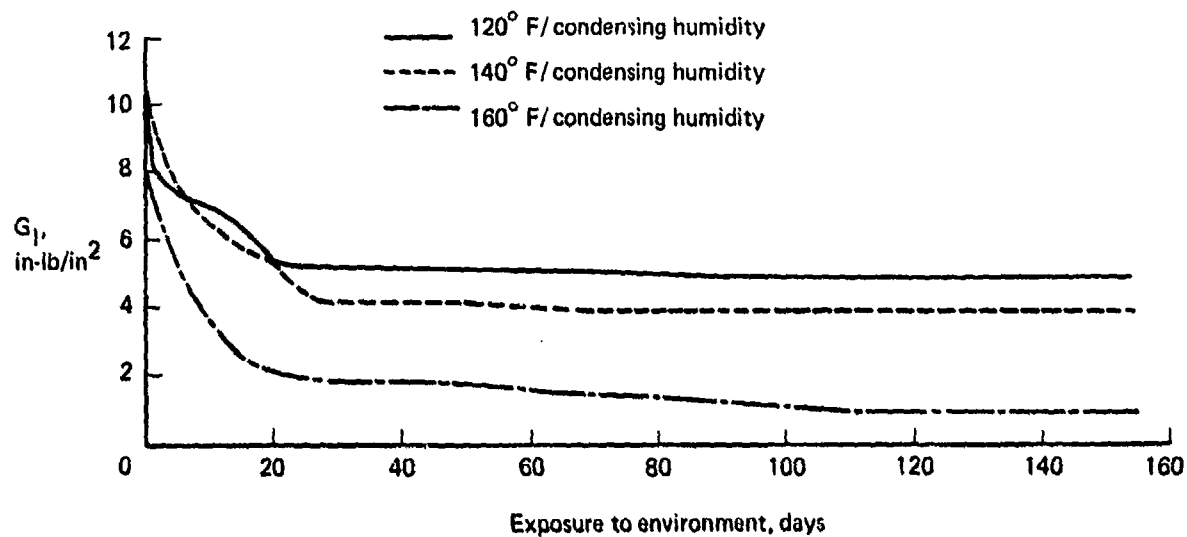
2024-T3 clad

FPL etch  
86 weeks'  
exposure

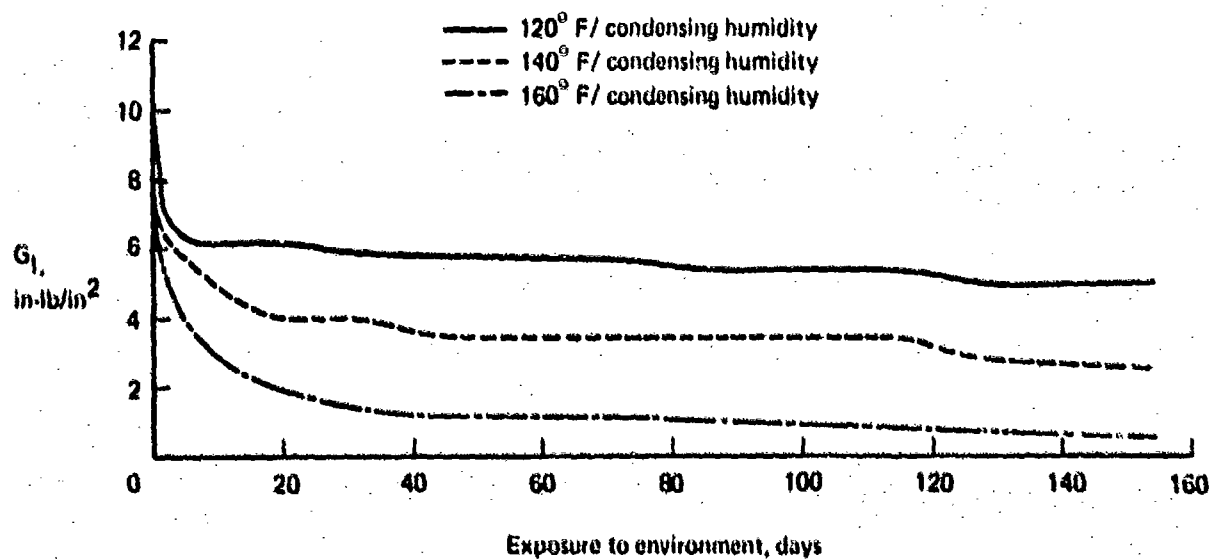
→ Crack growth

(b) With up to 86 Weeks' Exposure to 140°F/Condensing Humidity

Figure 13.—(Concluded)

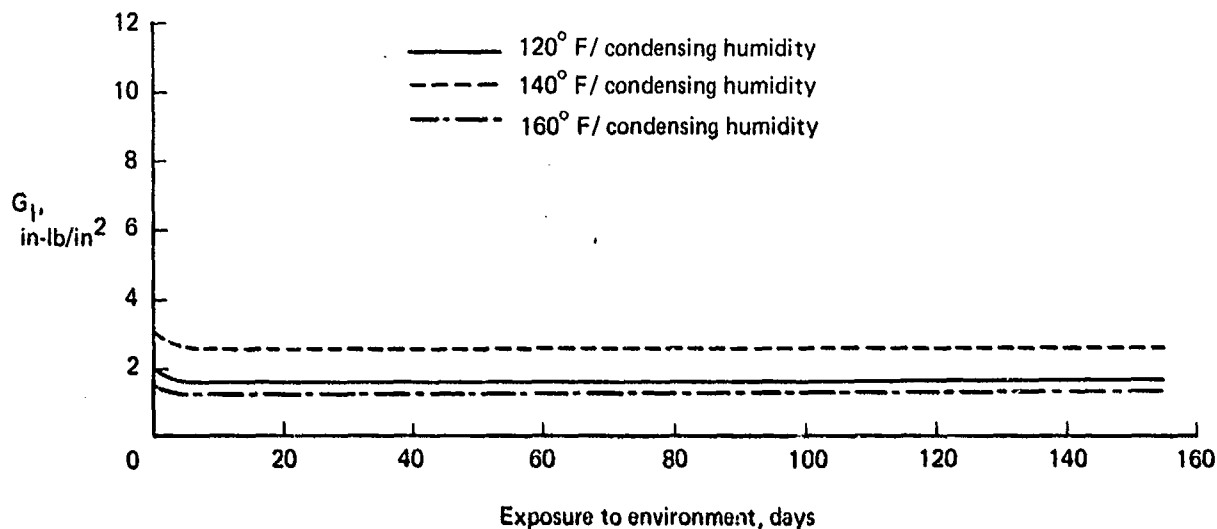


(a) Exposure Results: FM 123-2/BR 127, 2024-T3 Bare, Phosphoric Acid Anodize

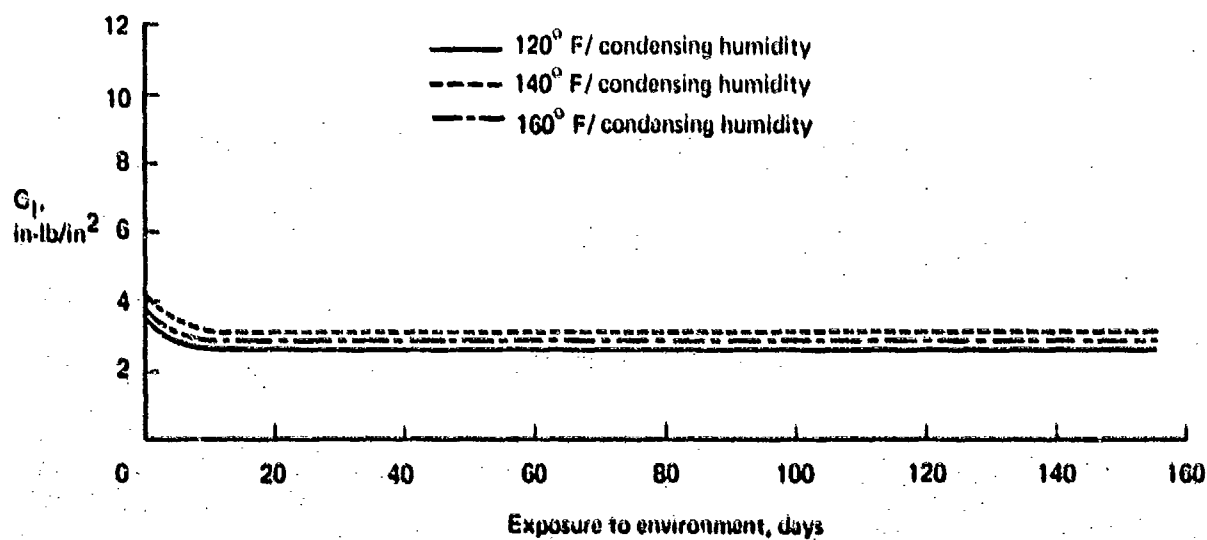


(b) Exposure Results: EA 9628/BR 127, 2024-T3 Bare, Phosphoric Acid Anodize

Figure 14. —Influence of Test Temperature on DCB Specimen

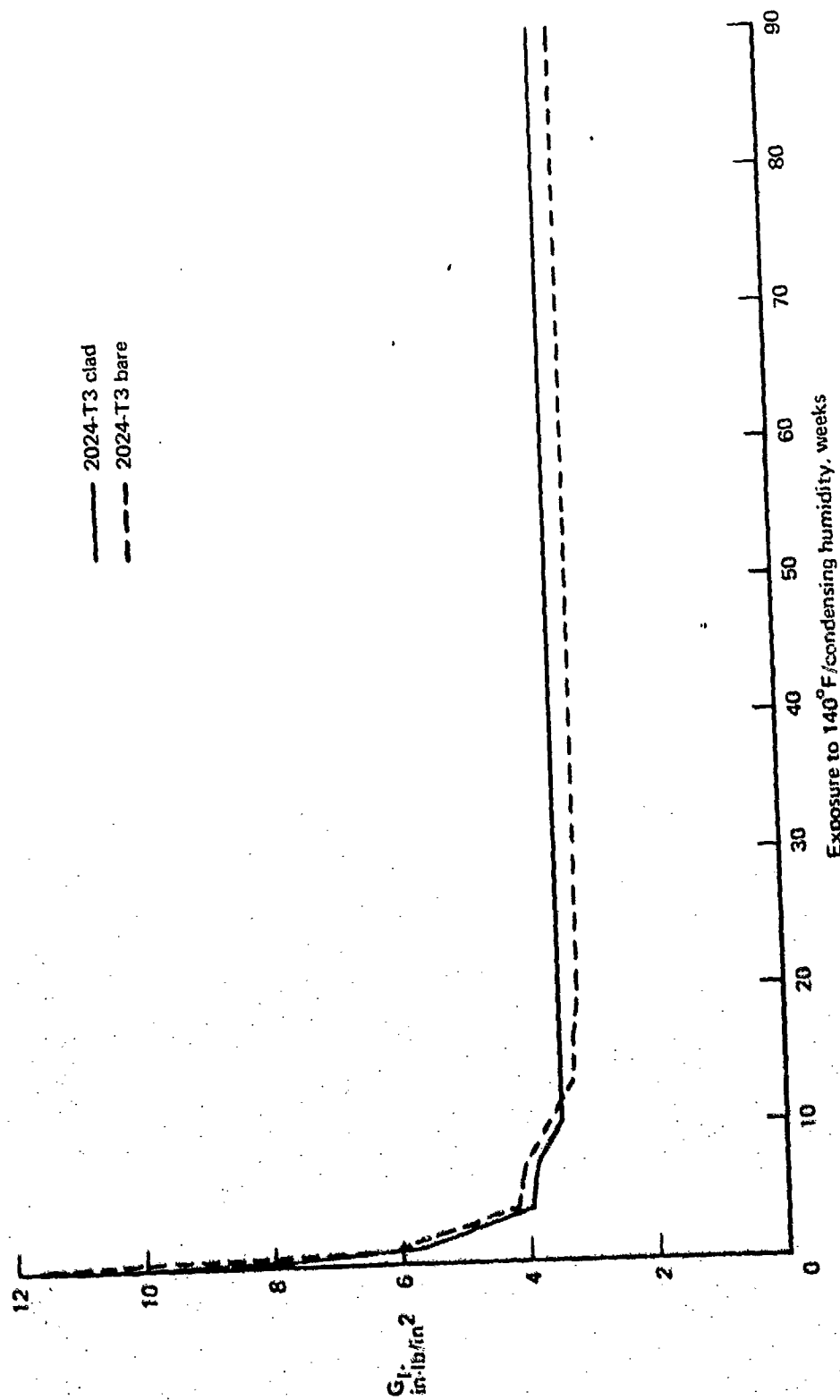


(c) Exposure Results: PL 729-3/PL 728, 2024-T3 Bare, Phosphoric Acid Anodize



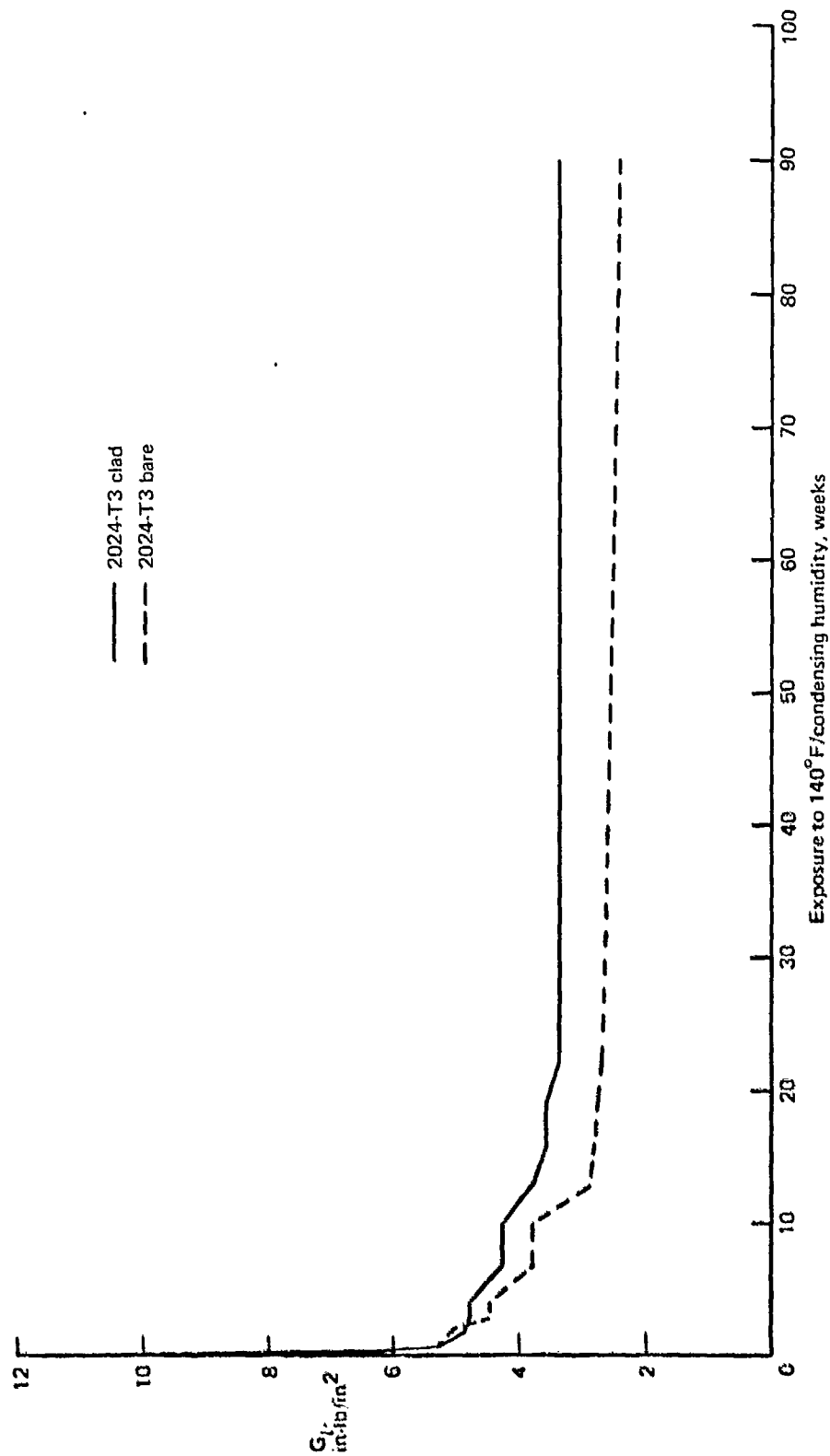
(d) Exposure Results: AF 143/EC 3917, 2024-T3 Bare, Phosphoric Acid Anodize

Figure 14.—(Concluded)



(a) Exposure Results: FM 123-2/BR 127, 2024-T3 Bare and Clad, Phosphoric Acid Anodize

Figure 15.—Influence of Long-Term Exposure on DCB Specimen



(b) Exposure Results: EA 9628/BR 127, 2024-T3 Bare and Clad, Phosphoric Acid Anodize

Figure 15.—(Continued)

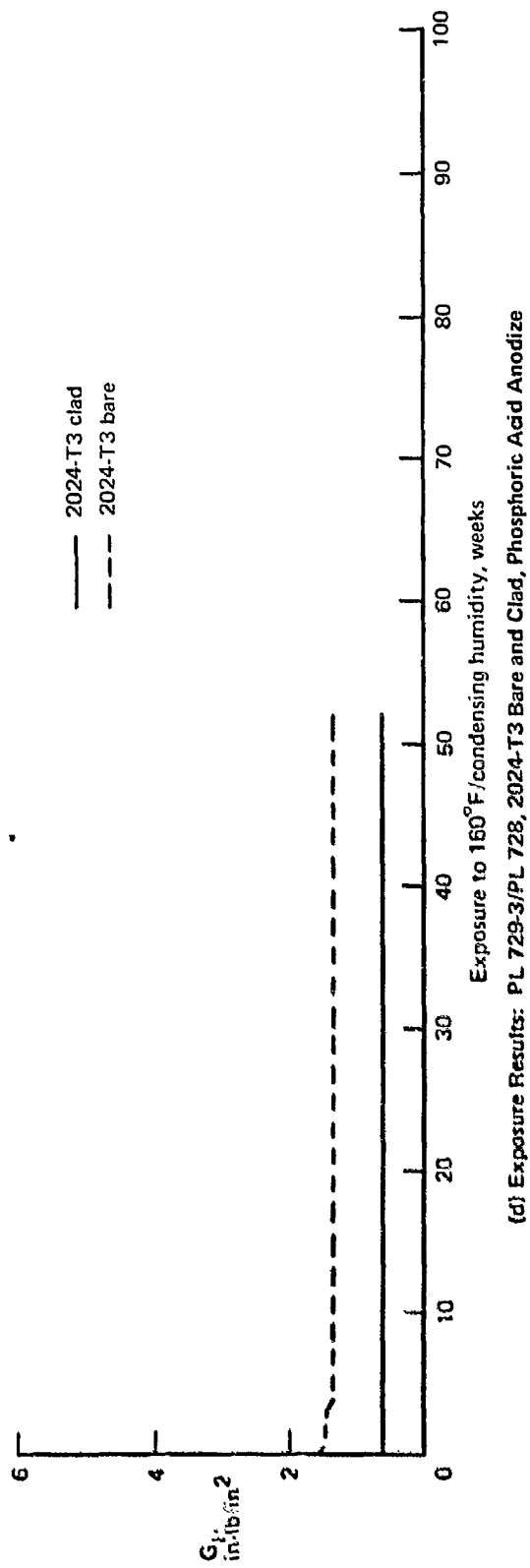
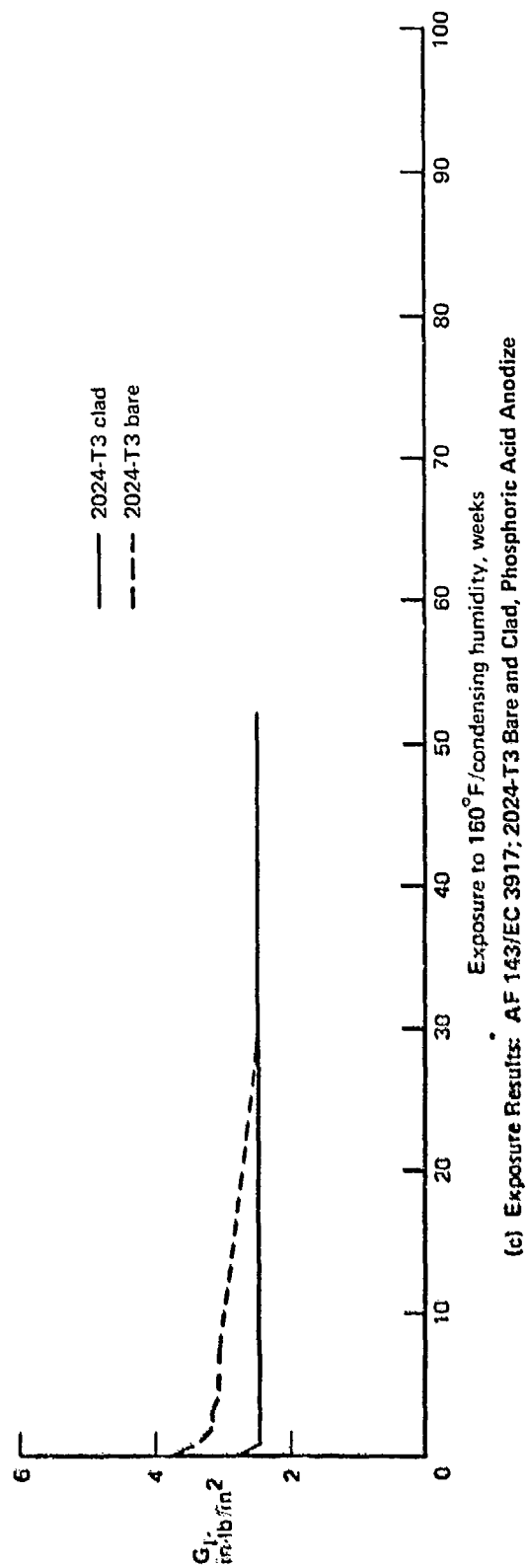
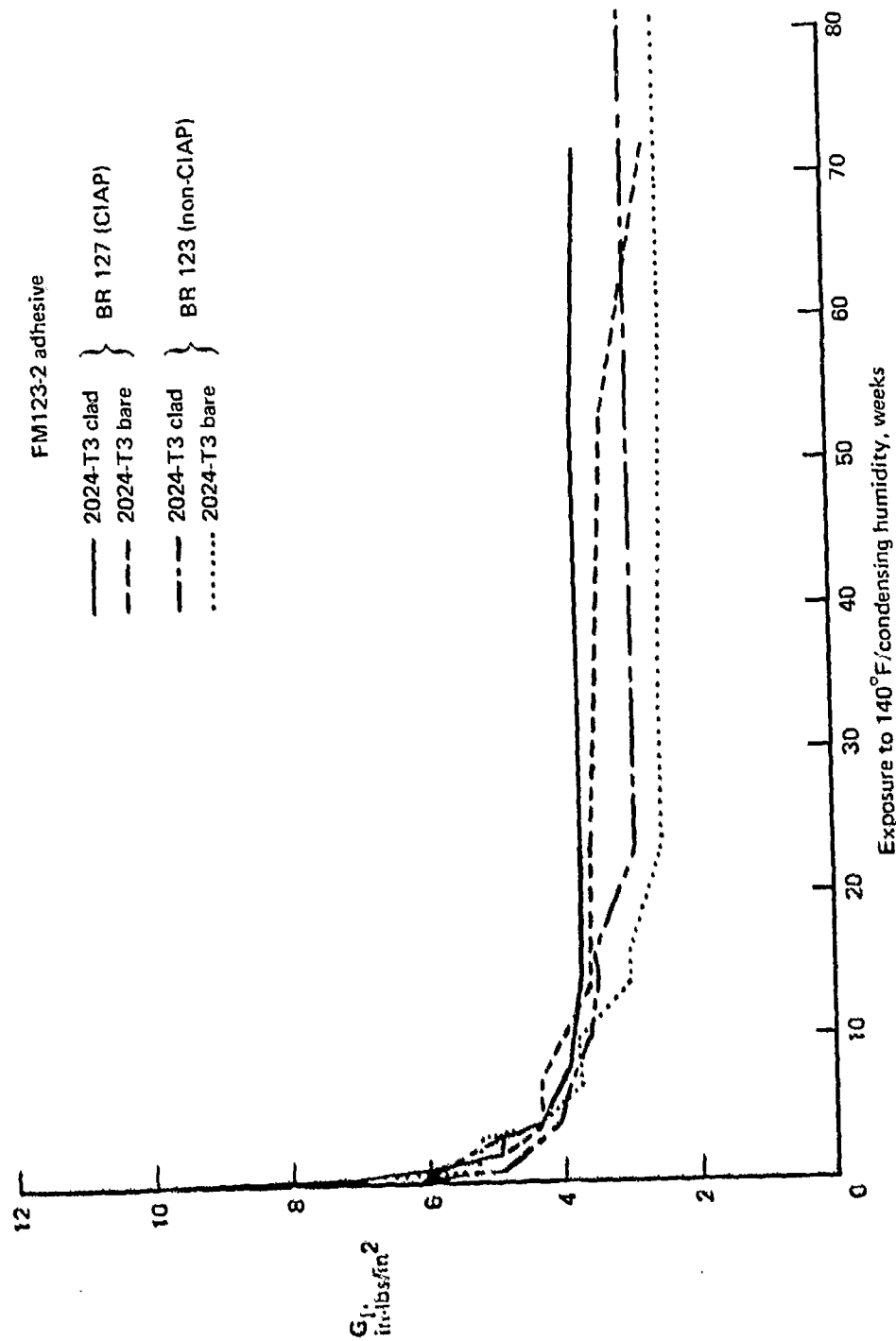
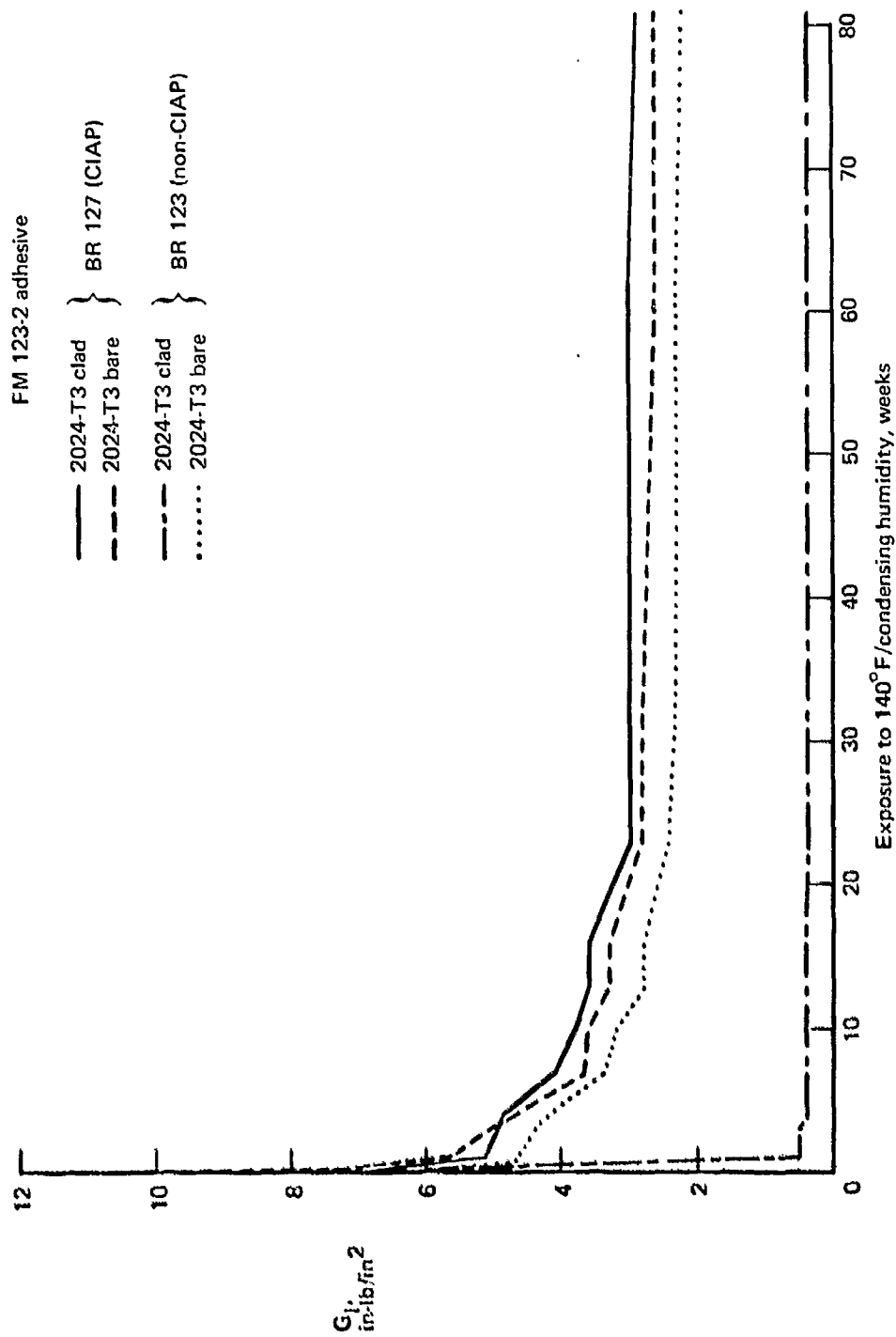


Figure 15.—(Concluded)



(a) Exposure Results, Phosphoric Acid Anodize Surface Preparation on 2024-T3 Bare and Clad with BR127(CIAP) and BR123(Non-CIAP) Primers

Figure 16.—Influence of Adhesive primers on DCB Specimen



(b) Exposure Results—Chromic Acid Anodize Surface Preparation on 2024-T3 Bare and Clad with BR 127 (CIAP) and BR 123 (Non-CIAP) Primers

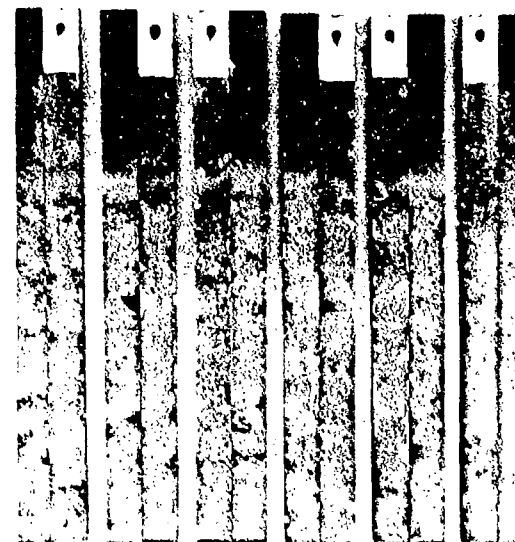
Figure 16.—(Concluded)

Chromic acid anodize

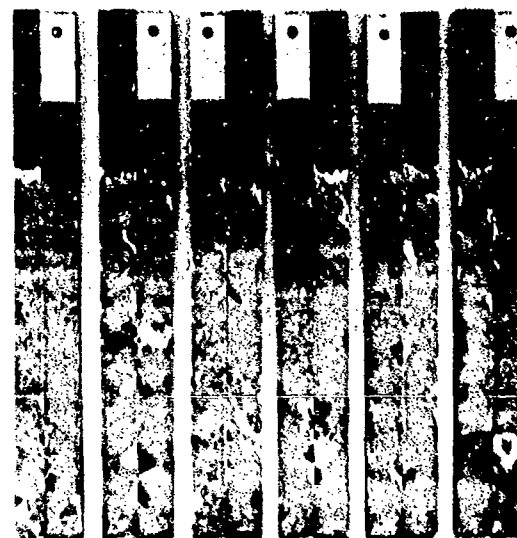
Phosphoric acid



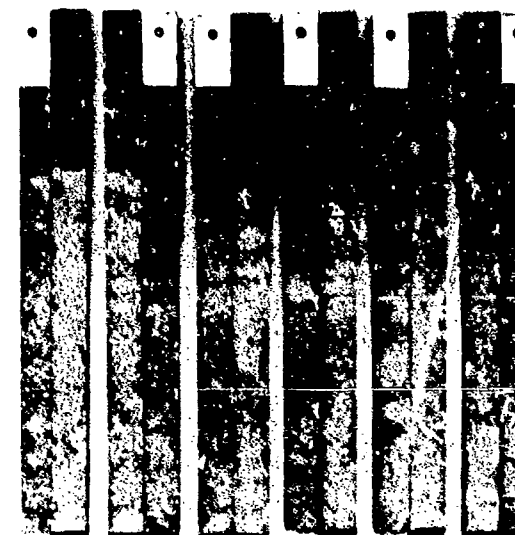
BR 123 (non-CIAP)



BR 123 (non-CIAP)



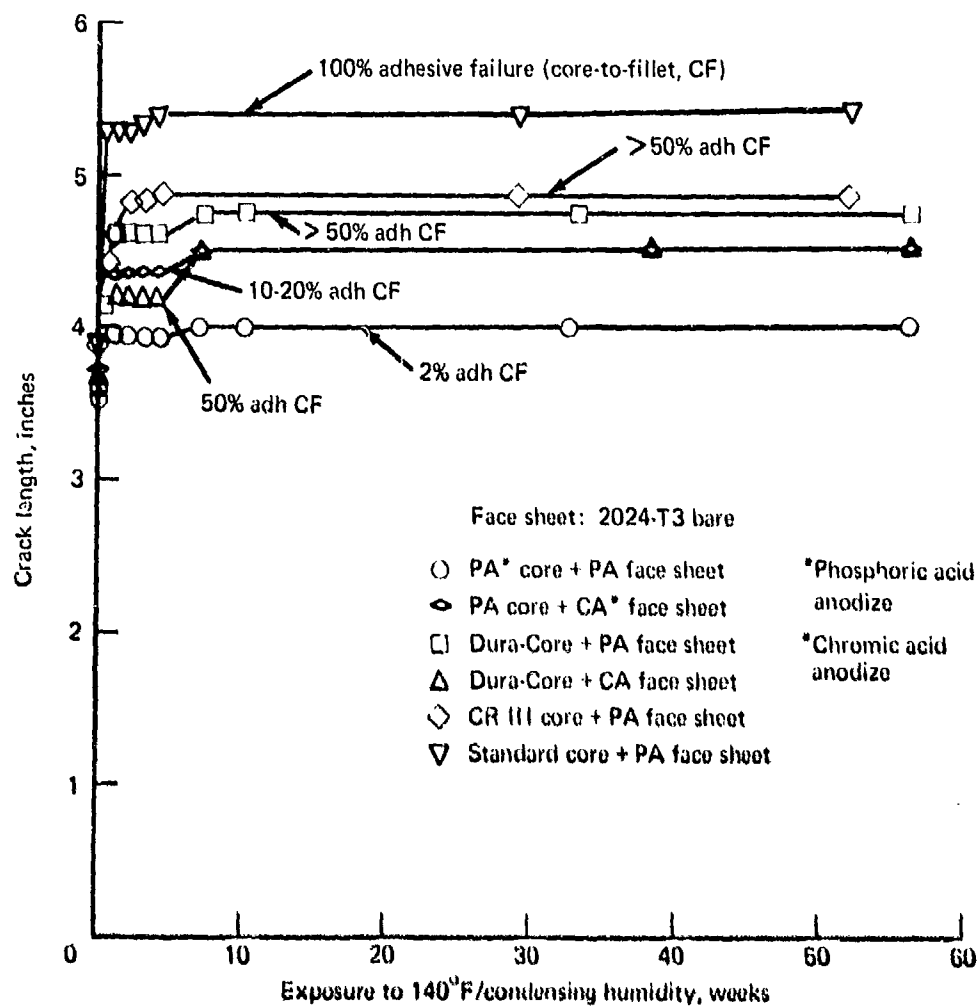
BR 127 (CIAP)



BR 127 (CIAP)

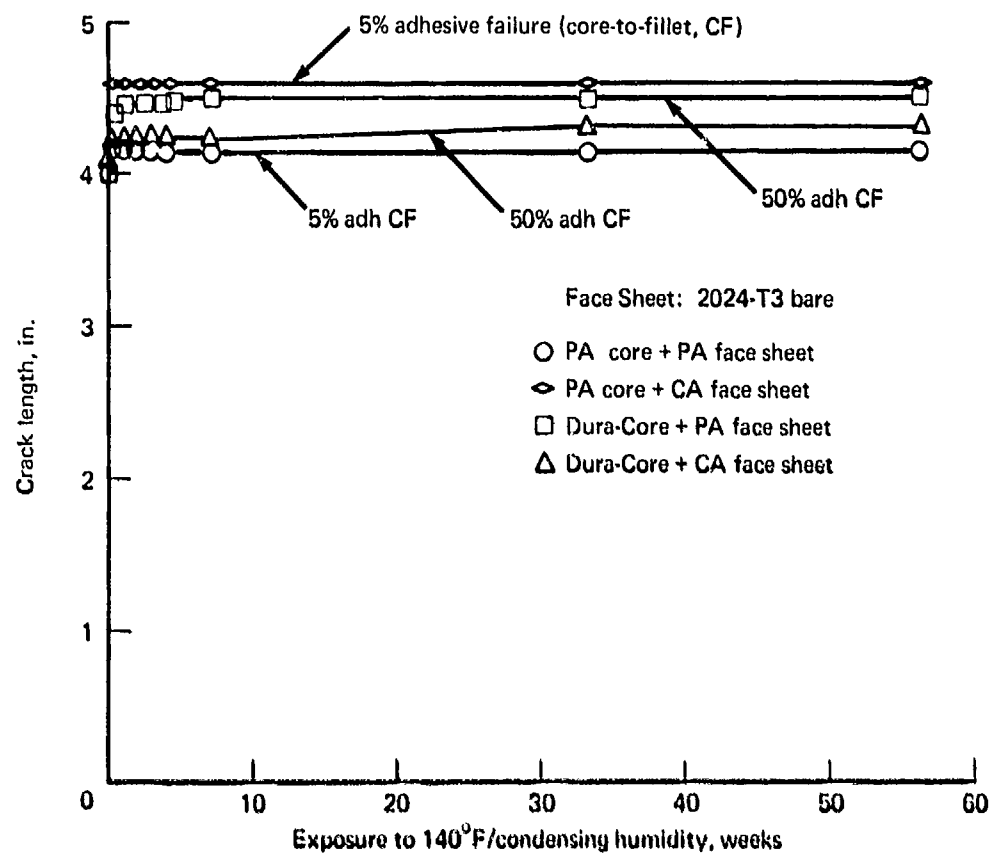
FM 123-2, 2024-T3 Clad

*Figure 17.—Typical Failure Modes and Filiform Corrosion in Bondlines of DCB Specimens Comparing CIAP and non-CIAP Primers After 82 Weeks Exposure to 40° F/Condensing Humidity*



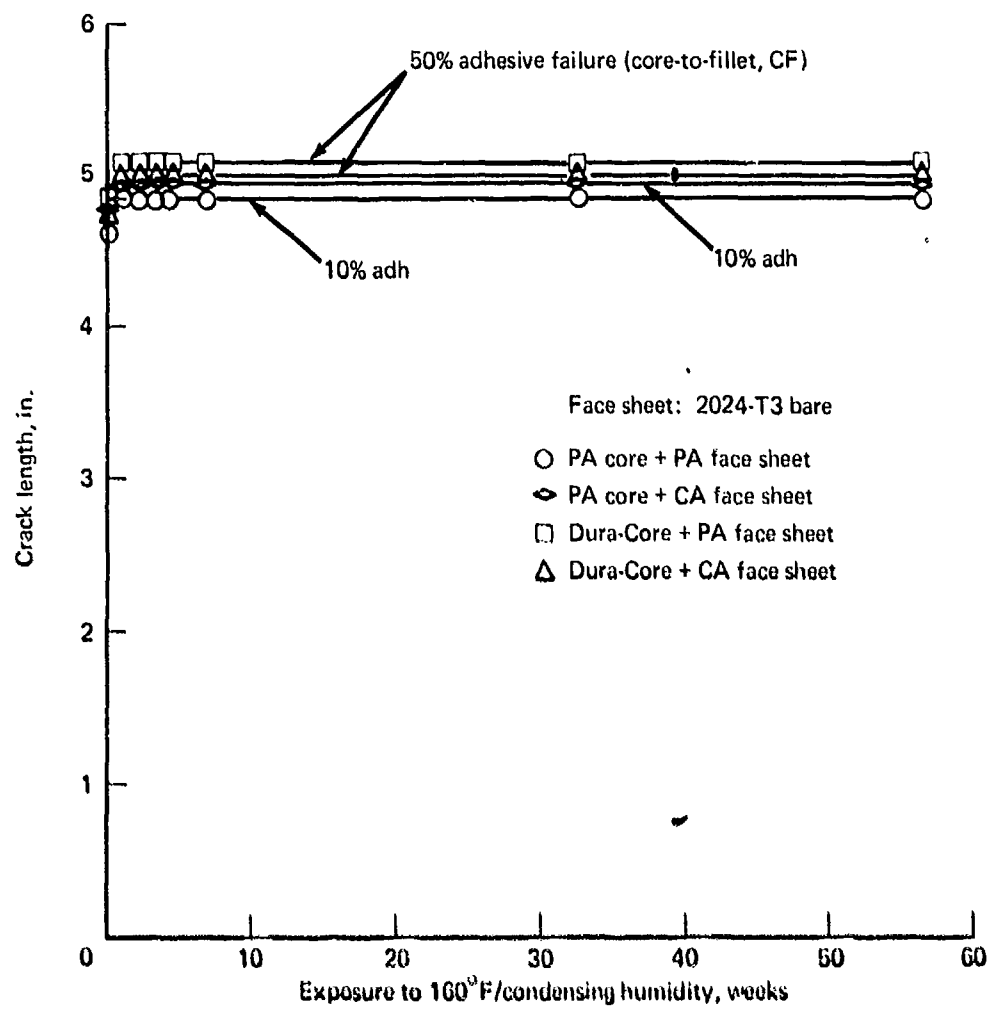
(a) SCB Specimens, EA 9628/BR 127

Figure 18.—Influence of Honeycomb Core and Face Sheet Surface Treatments on Environmental Durability



(b) SCB Specimens, FM 123-2/BR 127

Figure 18.—(Continued)



(c) SCB Specimens, AF 143/EC 3917

Figure 18.—(Concluded)

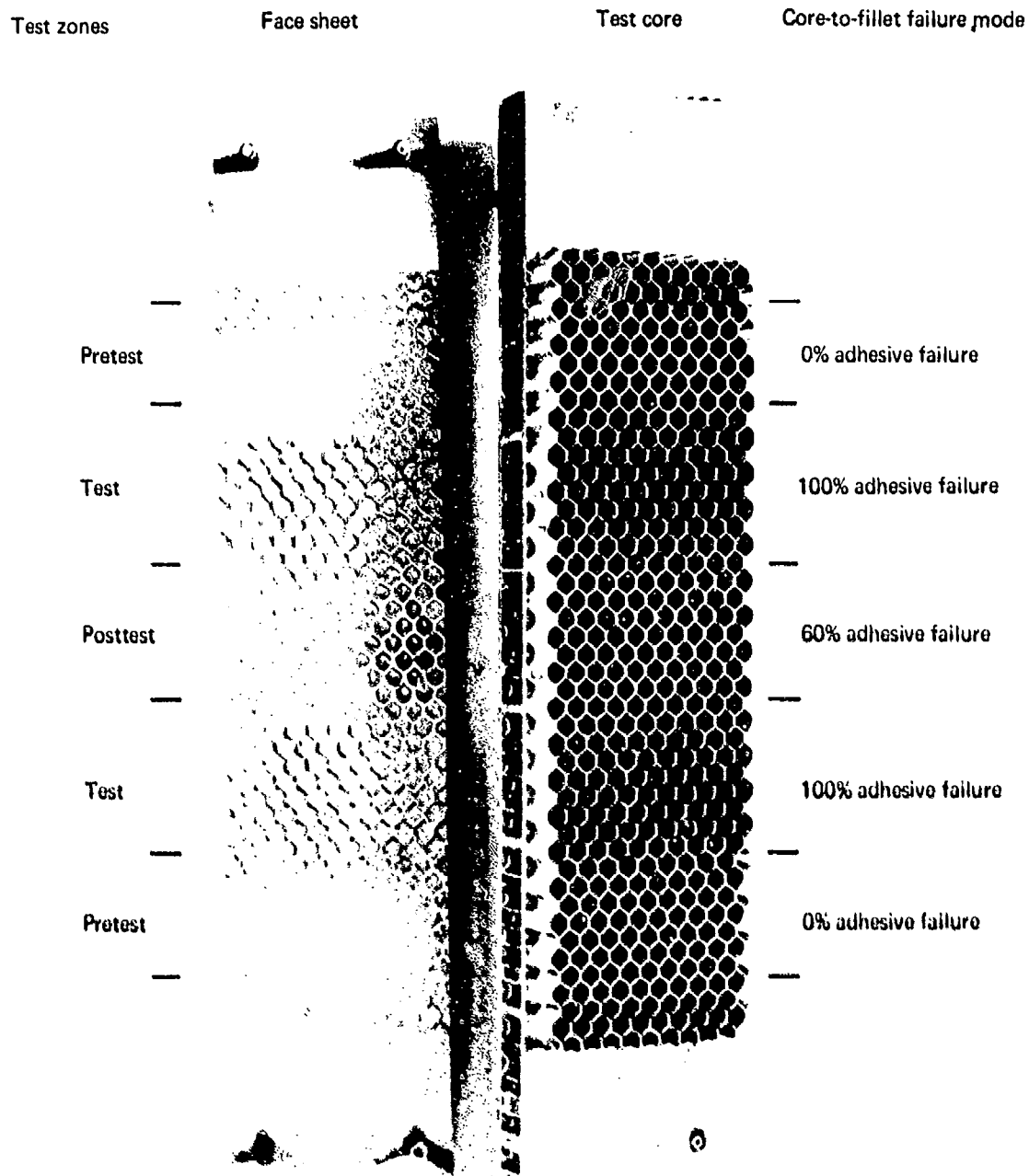
Test zones	Face sheet	Test core	Core-to-fillet failure mode
Pretest			0% adhesive failure
Test			2% adhesive failure
Posttest			0% adhesive failure
Test			2% adhesive failure
Pretest			0% adhesive failure

(a) Phosphoric Acid Anodize Core and 2024-T3 Bare Face Sheet

Test zones	Face sheet	Test core	Core-to-fillet failure mode
Pretest			0% adhesive failure
Test			10% - 20% adhesive failure
Posttest			0% adhesive failure
Test			10% - 20% adhesive failure
Pretest			0% adhesive failure

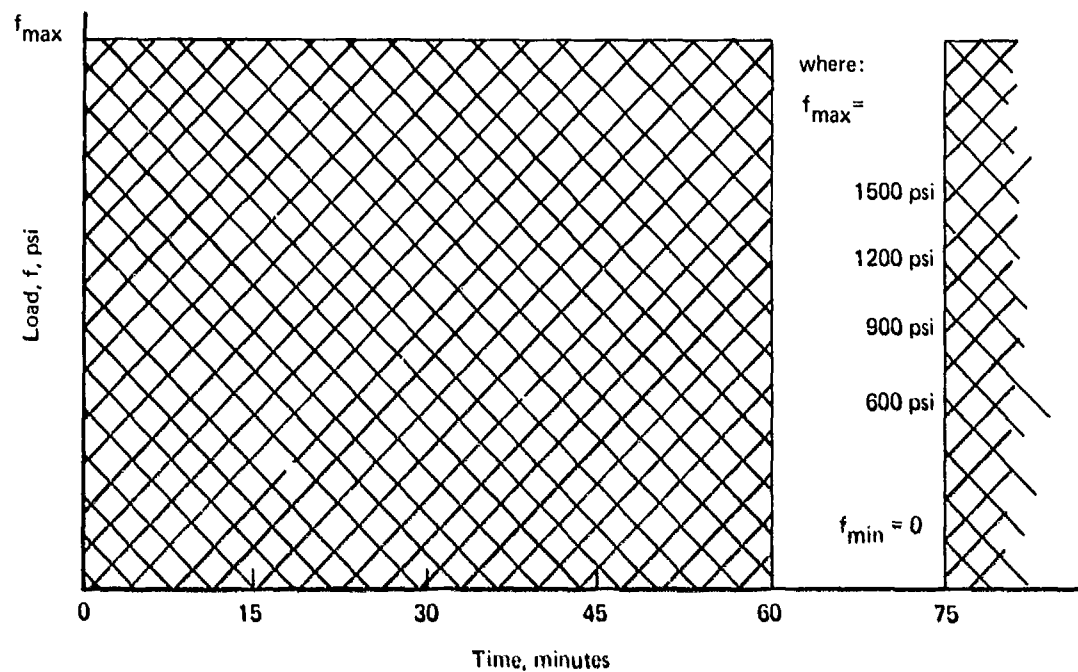
(b) Phosphoric Acid Anodize Core, Chromic Acid Anodize 2024-T3 Bare Face Sheet

Figure 19.—Failure Modes in the Pretest, Test, and Posttest Areas of SCB Specimens Bonded with EA 9628 and Exposed to 140° F/Condensing Humidity

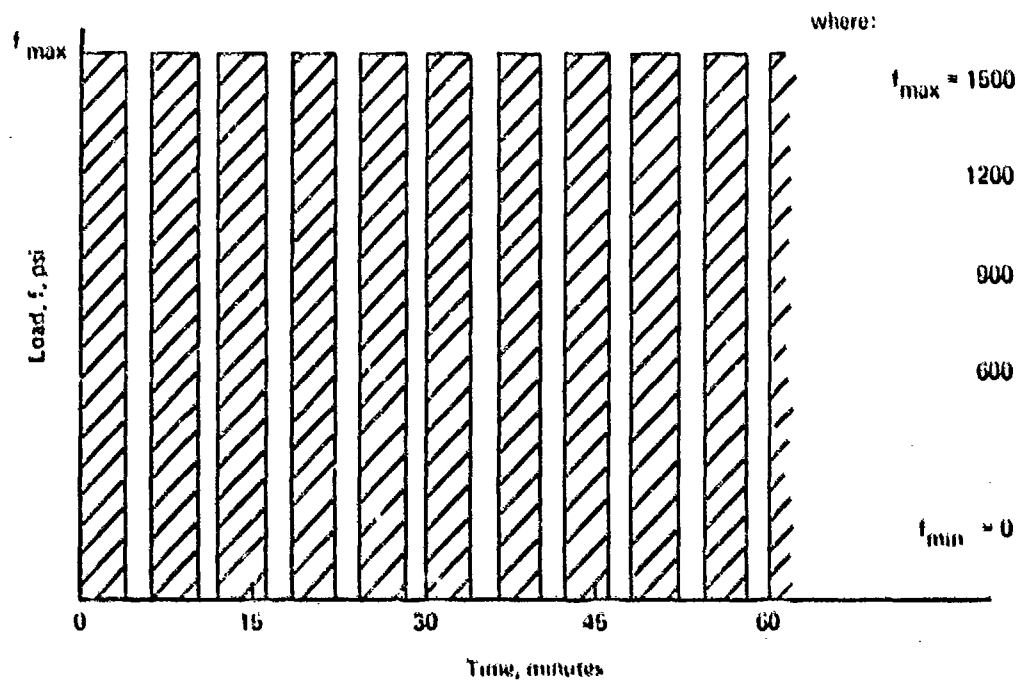


(c) Standard Core, Phosphoric Acid Anodize Face Sheet

Figure 19.—(Concluded)



(a) Bell Cycle: 1 hour at  $f_{\max}$ , 15 minutes at  $f_{\min}$



(b) Boeing Cycle: 4 minutes at  $f_{\max}$ , 2 minutes at  $f_{\min}$

Figure 20.—Load Profiles for Slow Cyclic Loading of Lap-Shear Specimens

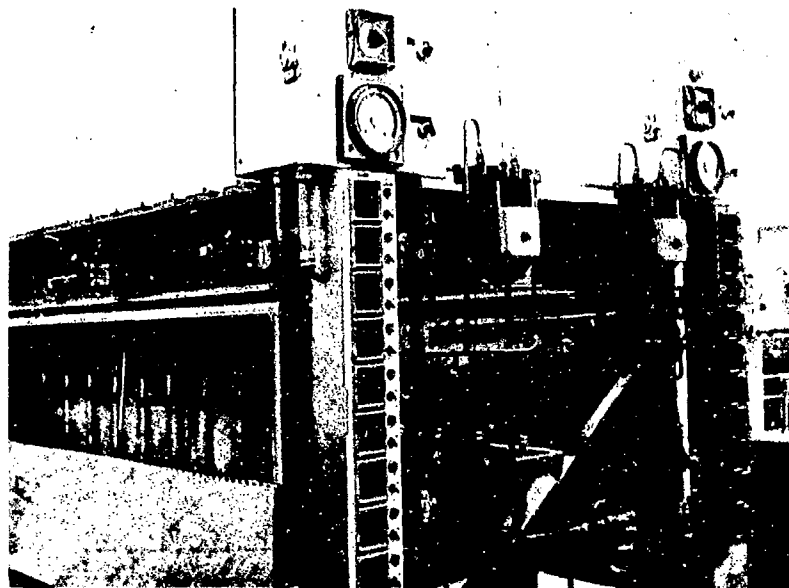


*Figure 21.—Cyclic Load Machine for Lap-Shear Durability Testing*

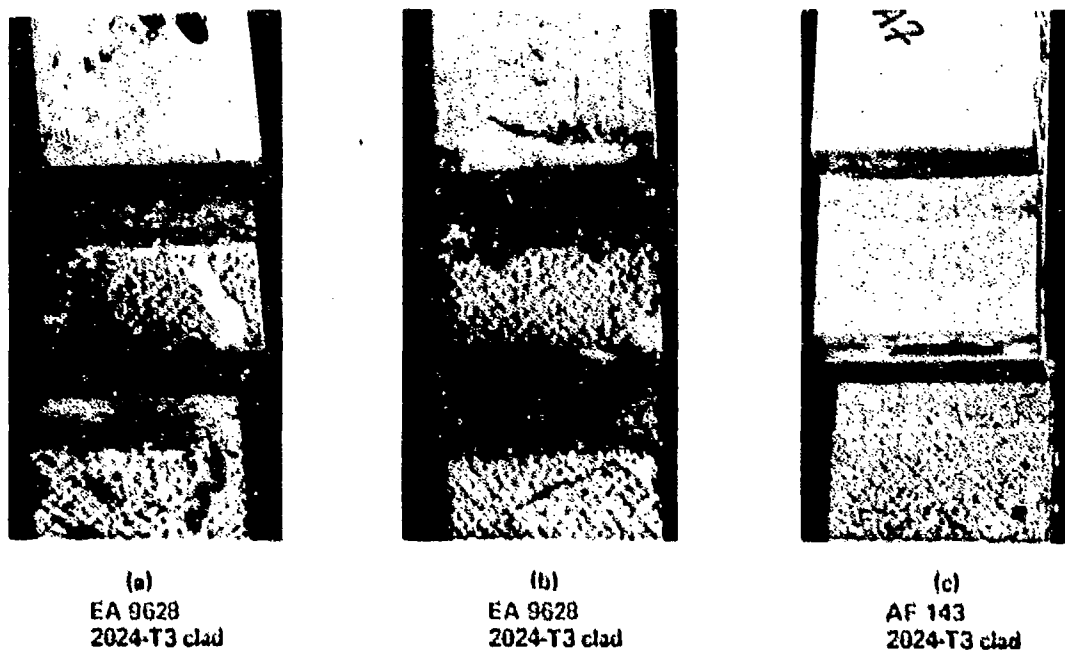


*Figure 22.—Typical Examples of Failure Modes for Slow Cycle Fatigue (0.8 and 10 cph)*

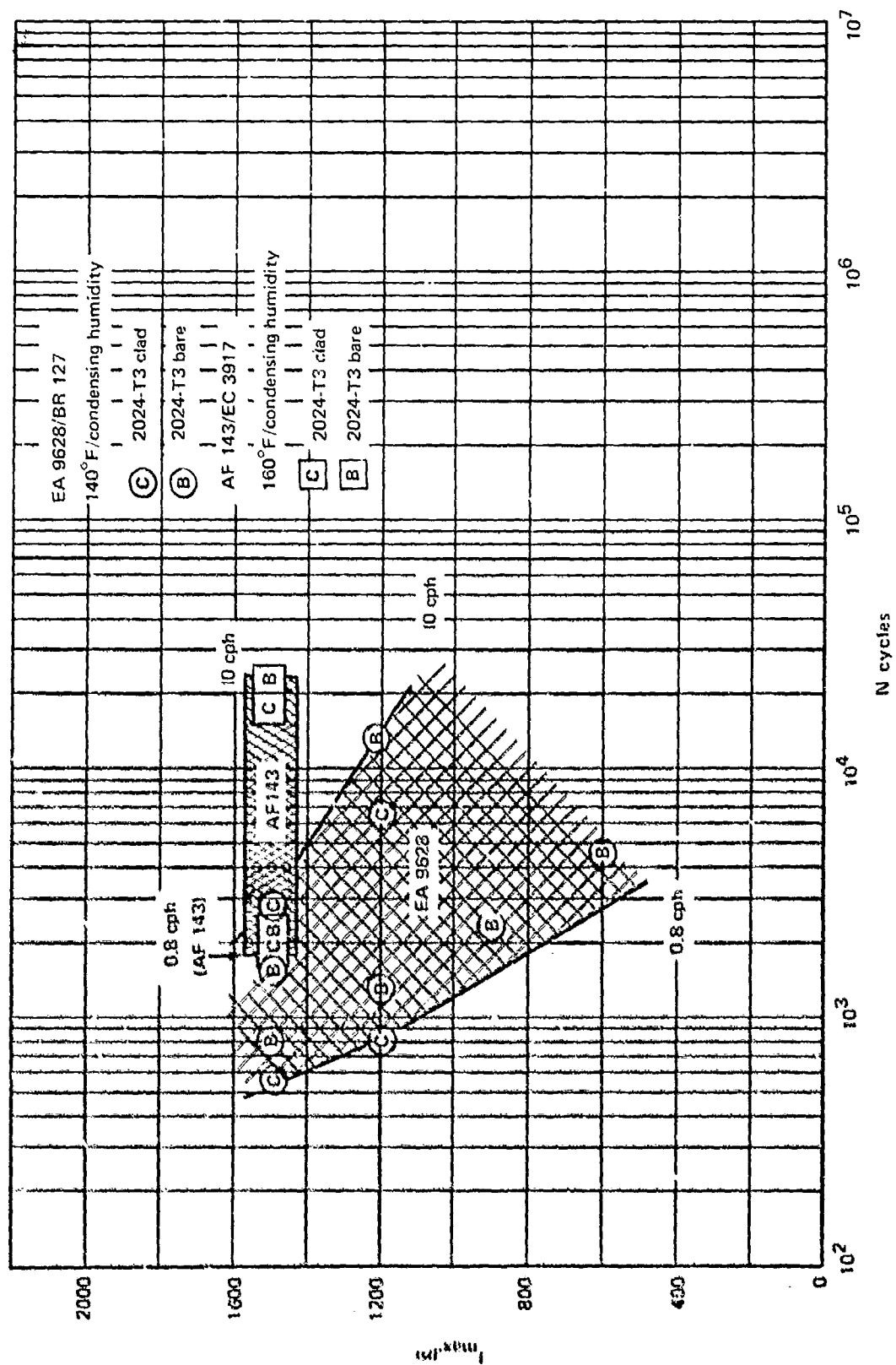
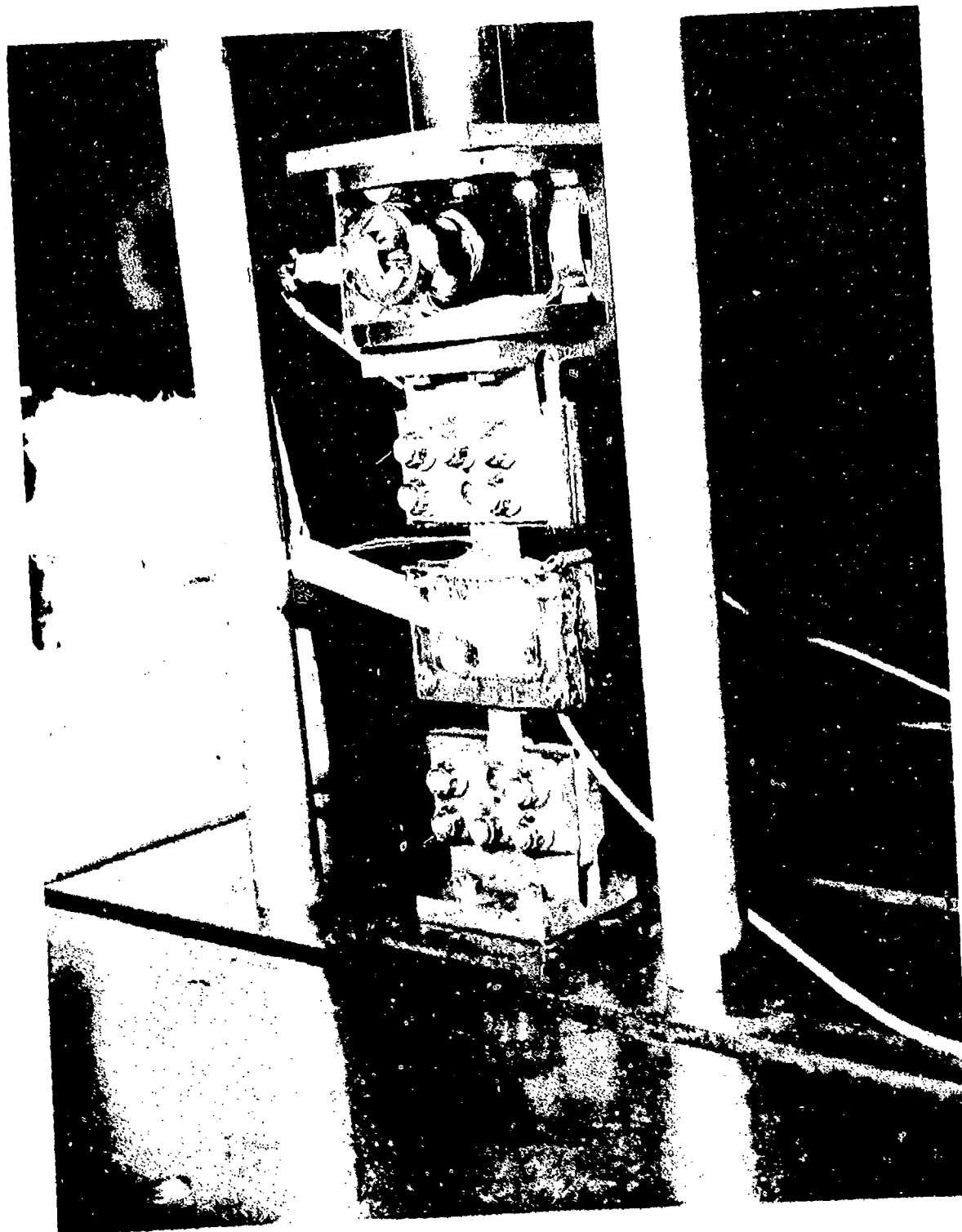
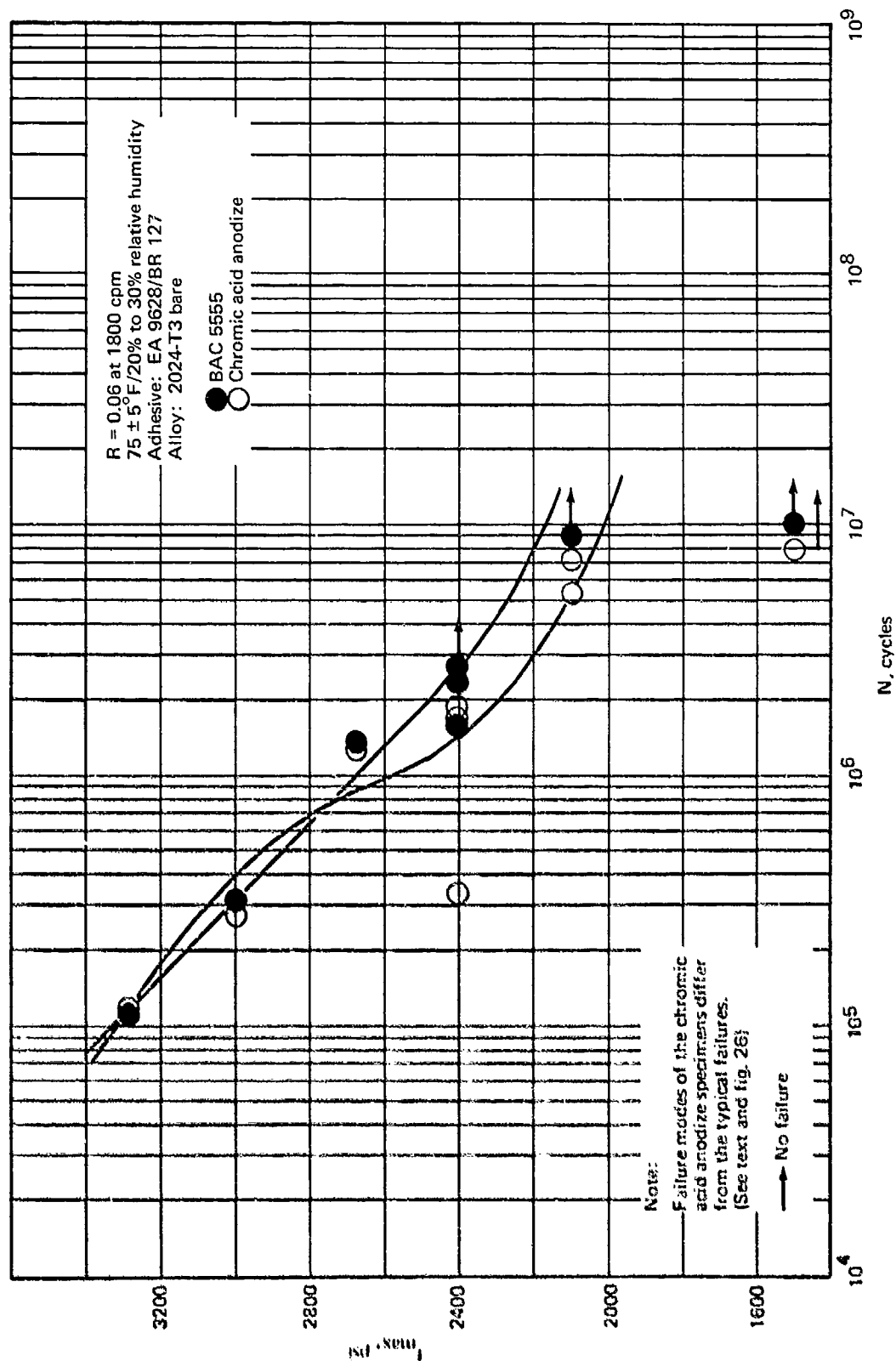


Figure 23.—Comparisons of Slow Cyclic Fatigue for 0.8 cph (Bell) and 10 cph for EA 9628/BR 127 and AF 143/EC 3917 Adhesive Systems

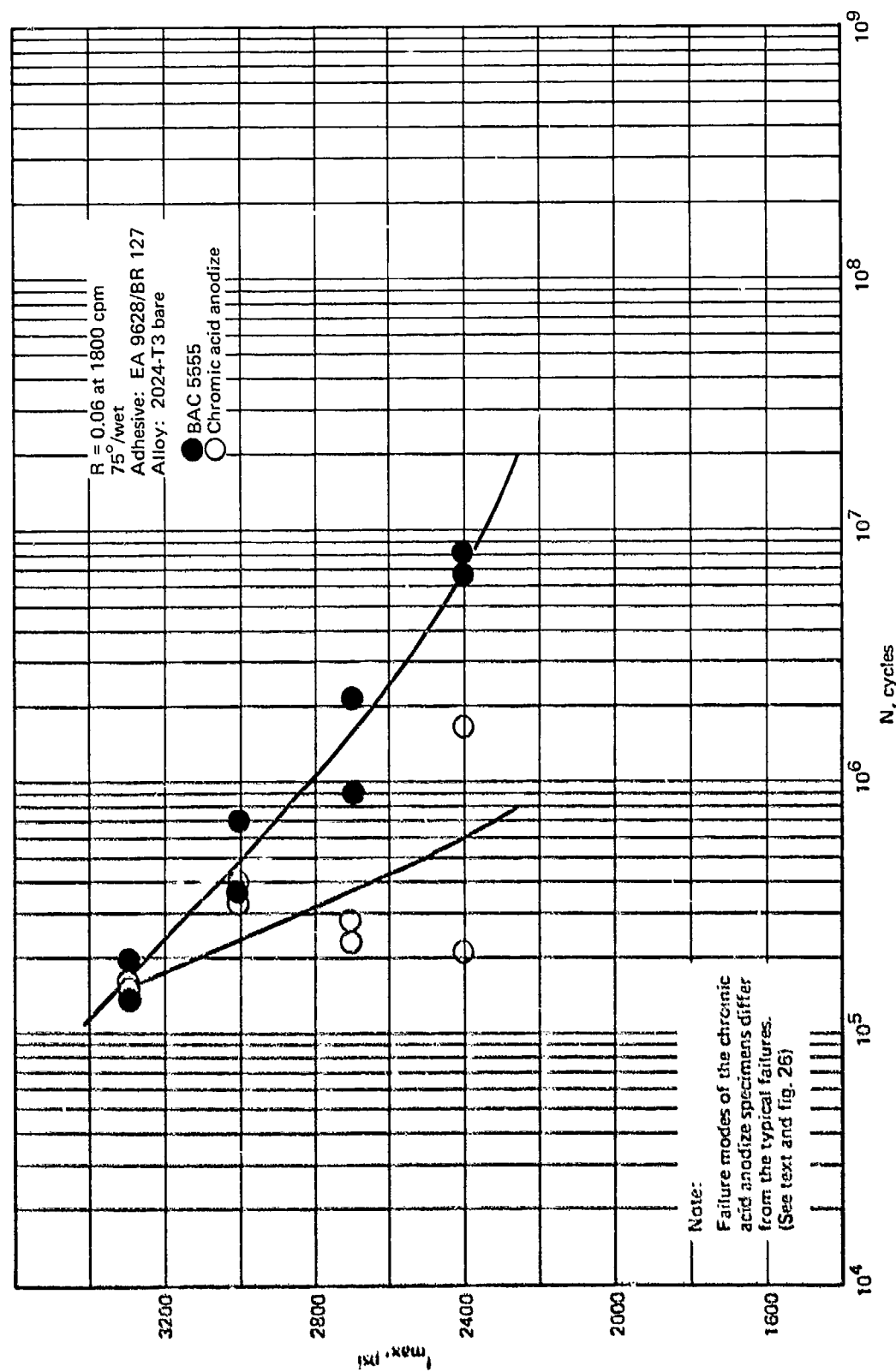


*Figure 24.—Fatigue Test Arrangement for Thick-Adherend Lap-Shear Specimens  
(Environmental Chamber Surrounds the Specimen.)*

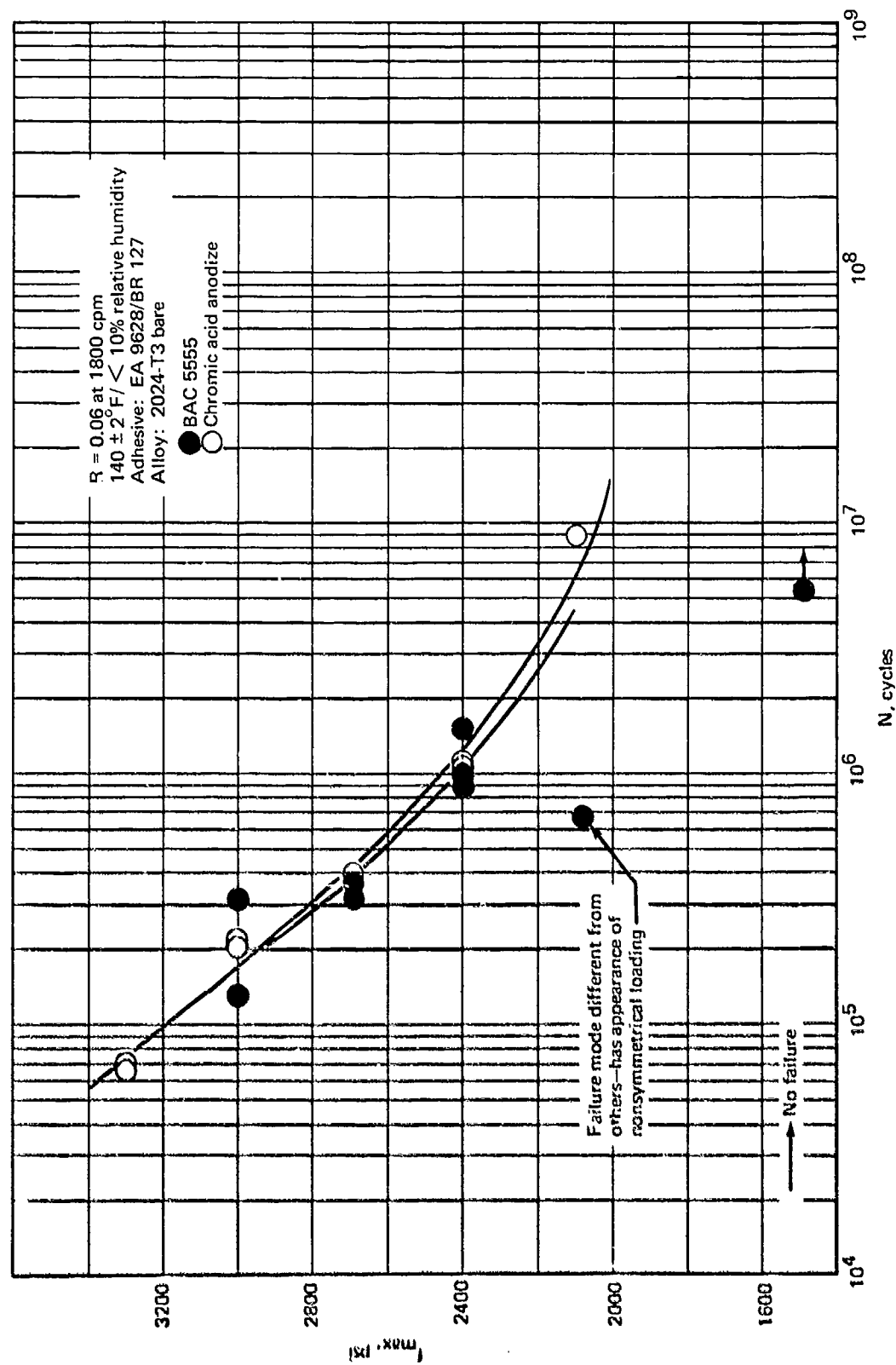


(a) 75°F Dry Environment

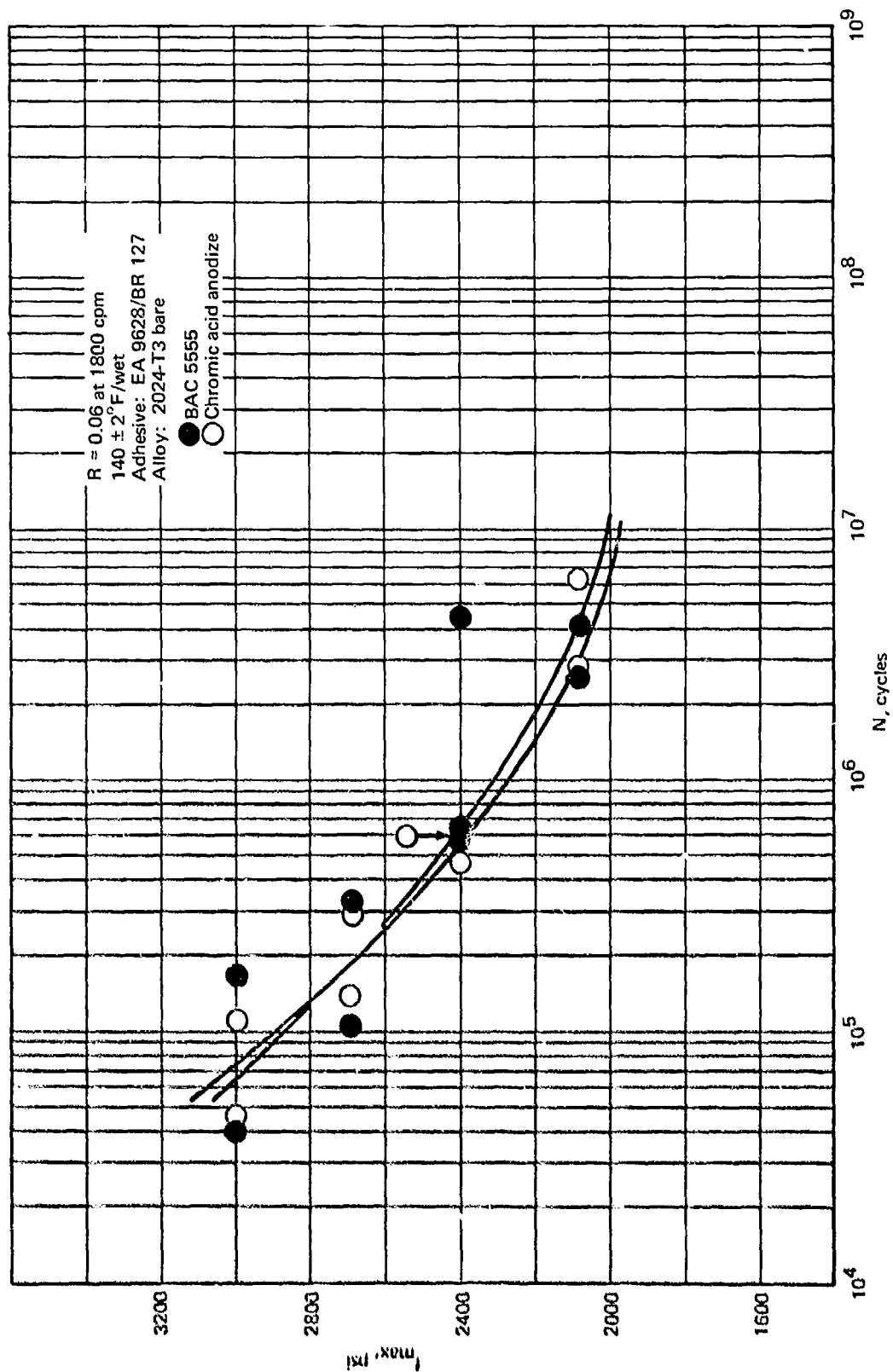
Figure 25.—Fast Cycle Stress Results



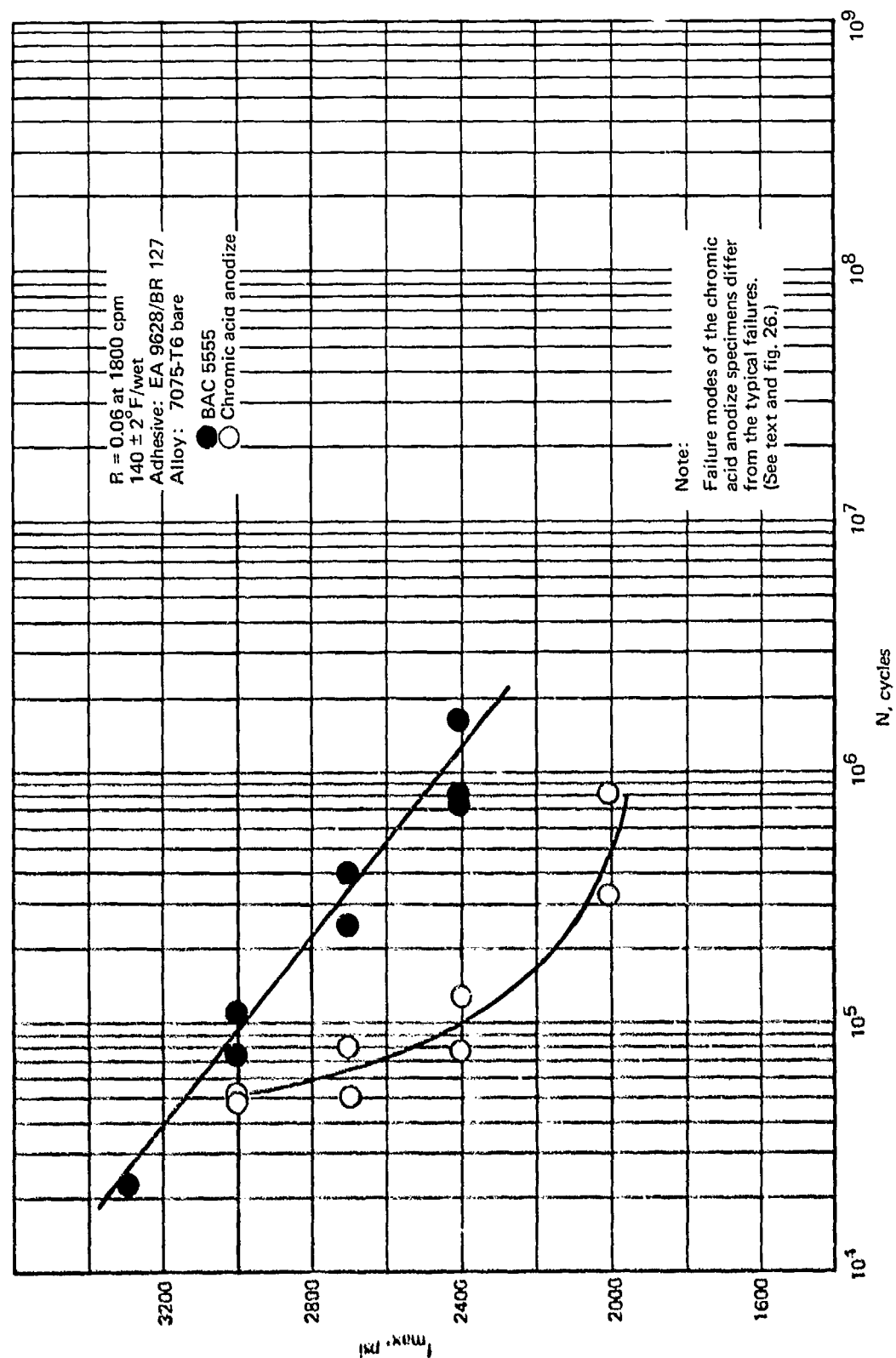
(b) 75°F Wet Environment  
 Figure 25. — (Continued)



(c)  $140^\circ\text{F}$  Dry Environment  
 Figure 25.—(Continued)

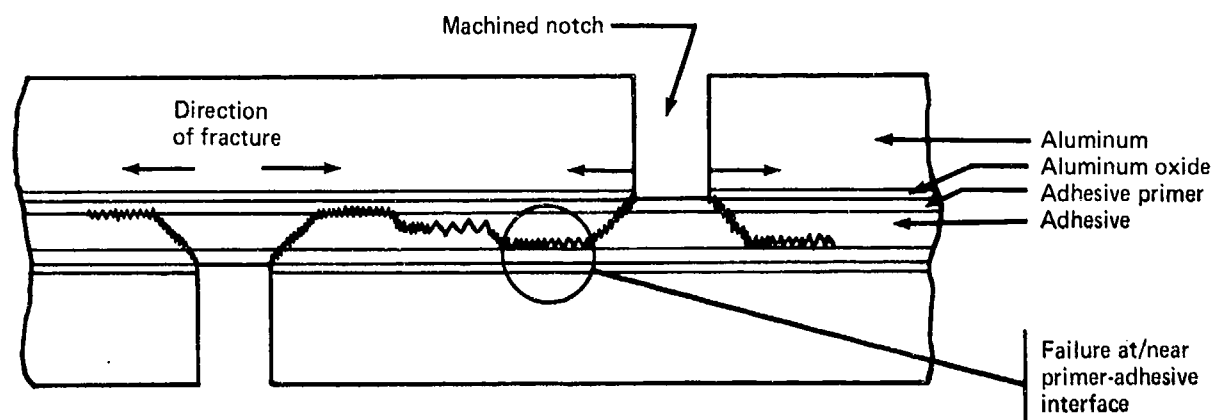


(d) 140°F Wet Environment  
Figure 25.—(Continued)

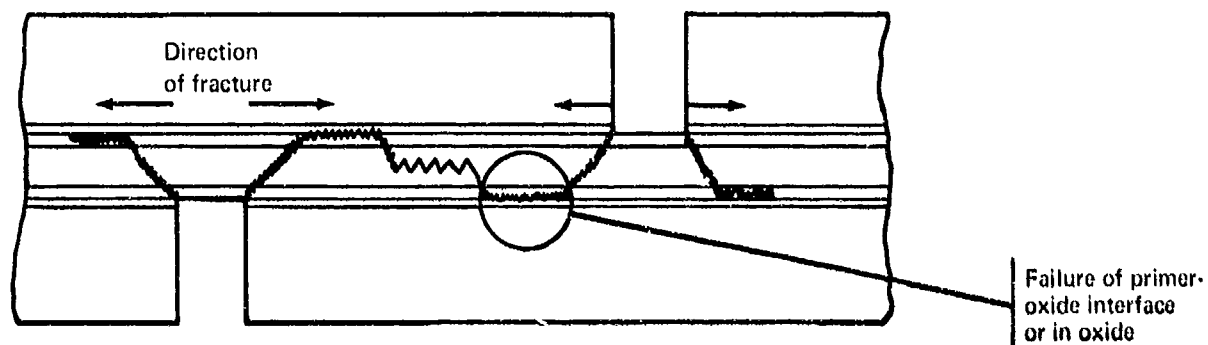


(e)  $140^\circ\text{F}$  Wet Environment, 7075-T6 bare

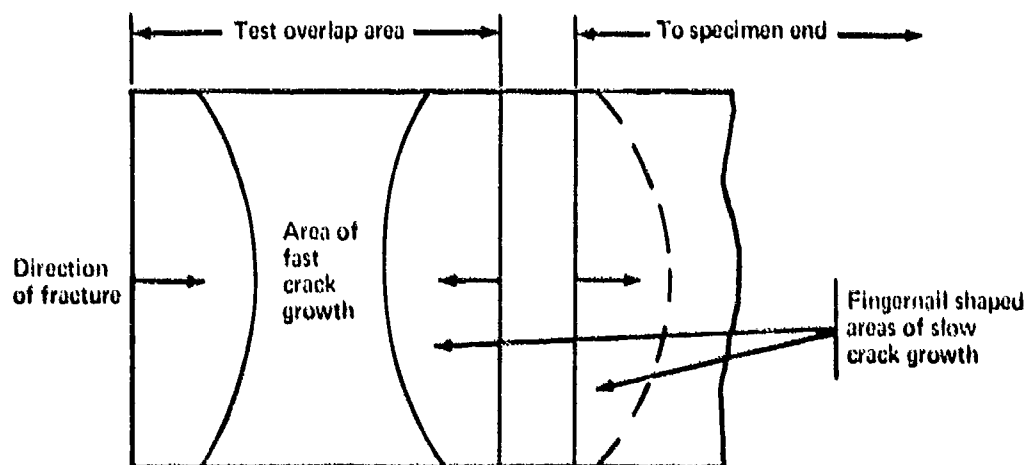
Figure 25.—(Concluded)



(a) Side View of "Typical" Failure

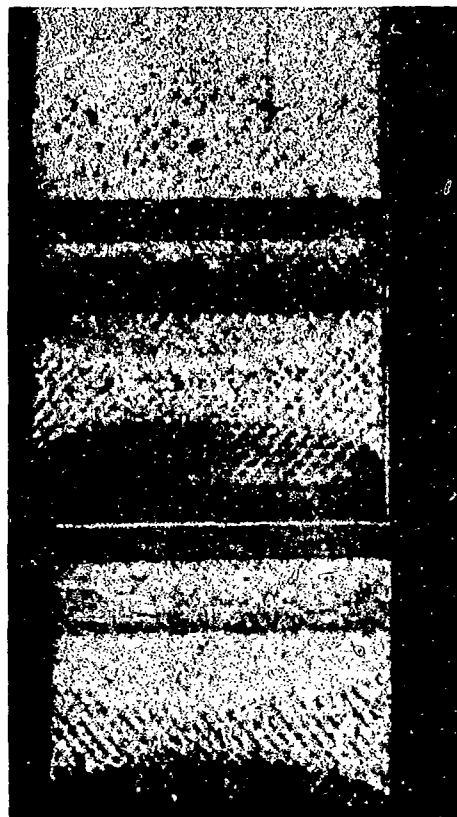


(b) Side View of "Adhesive" Failure

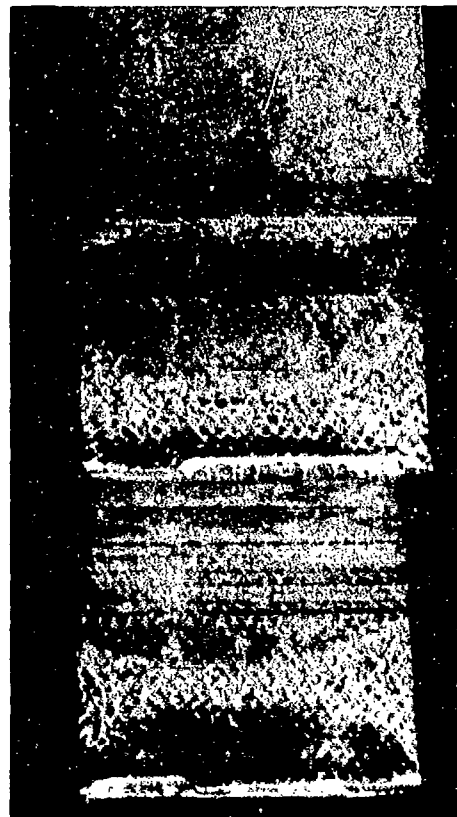


(c) Top View of Fracture Surfaces

Figure 26.—Failure Mode Characteristics of Thick Adherend Lap Shear Specimens Tested at 1800 cpm,  $R = 0.06$ .

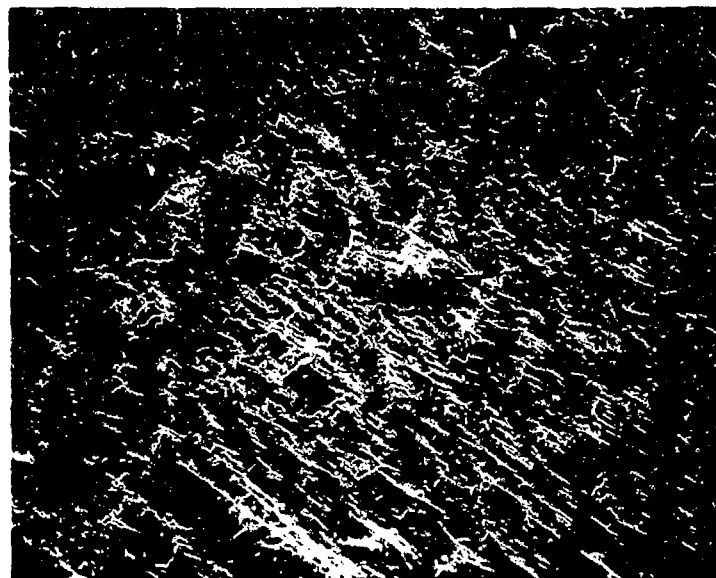


Phosphoric acid  
anodize

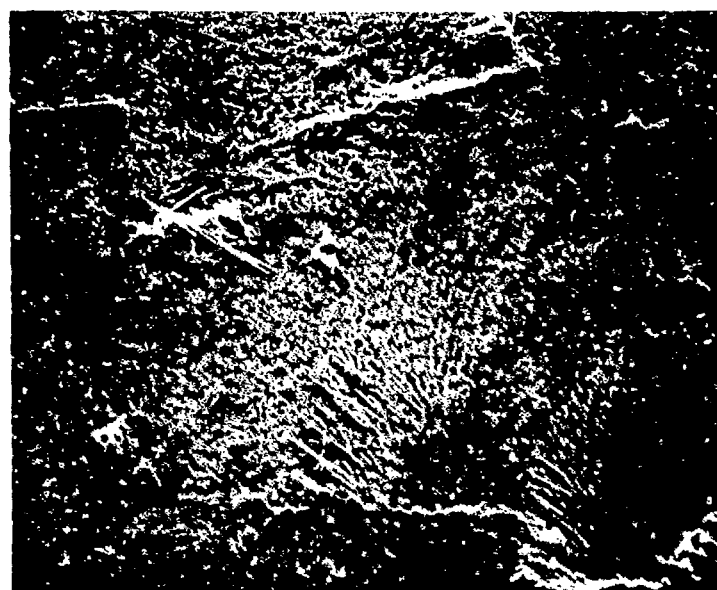


Chromic acid  
anodize

*Figure 27.—Typical Lap-Shear Failures at 1800 cpm, 2024-T3 Bare Bonded  
With EA 9628/BR 127.*

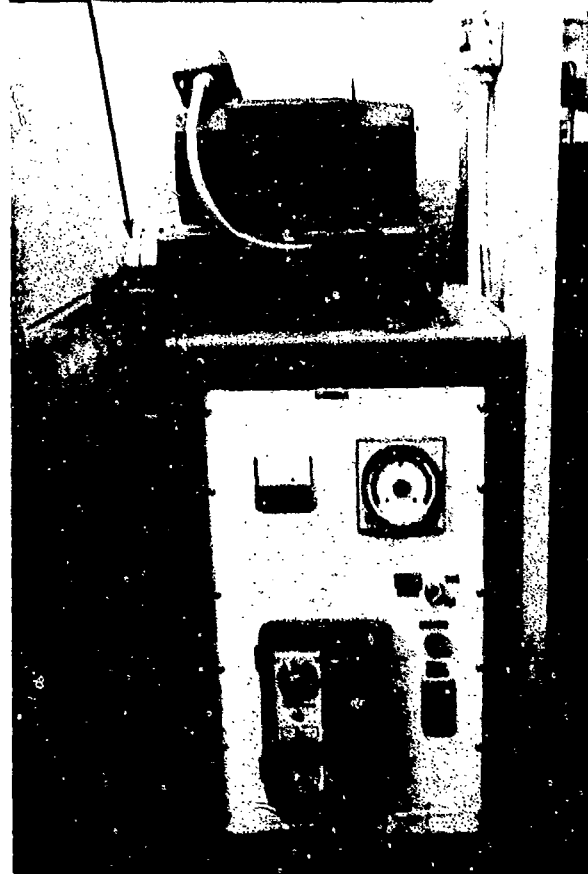
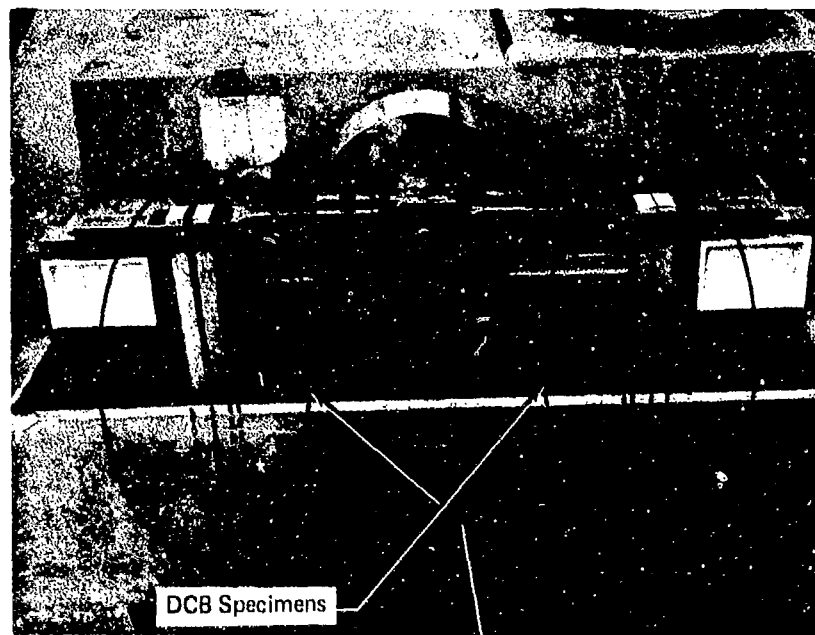


450X

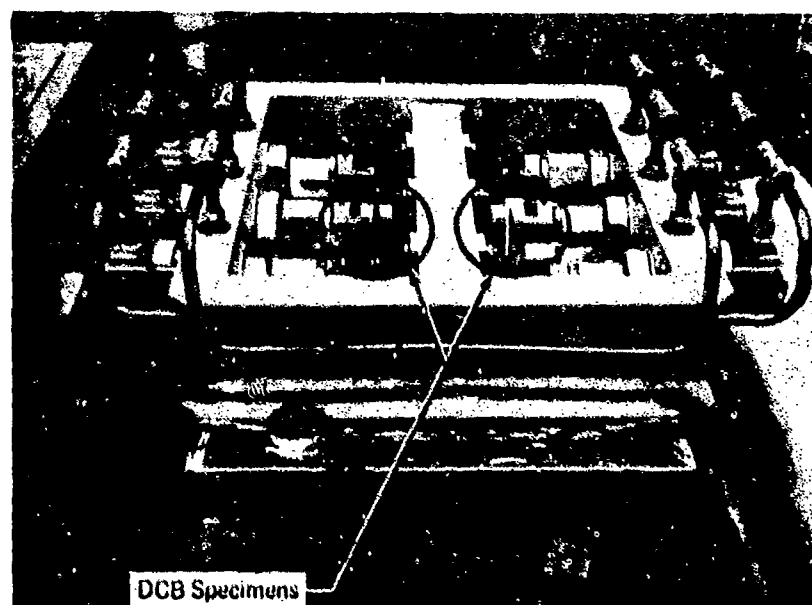
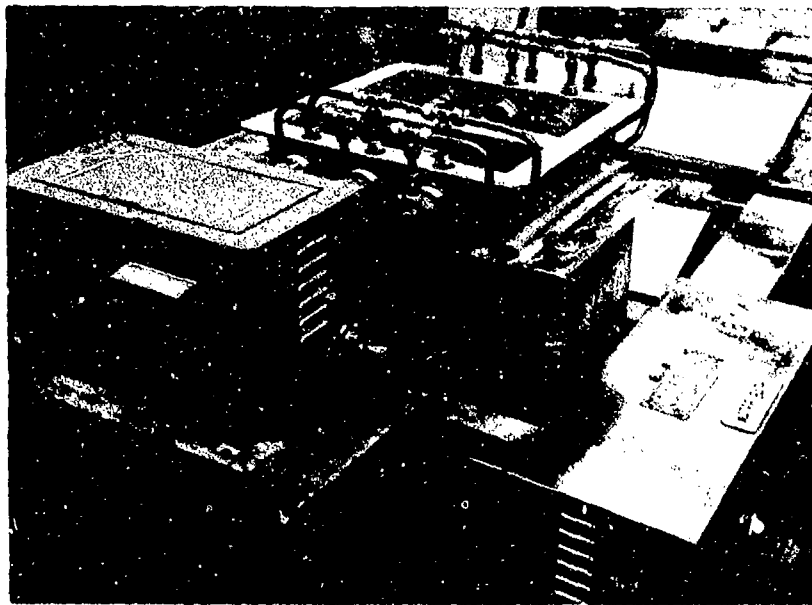


90X

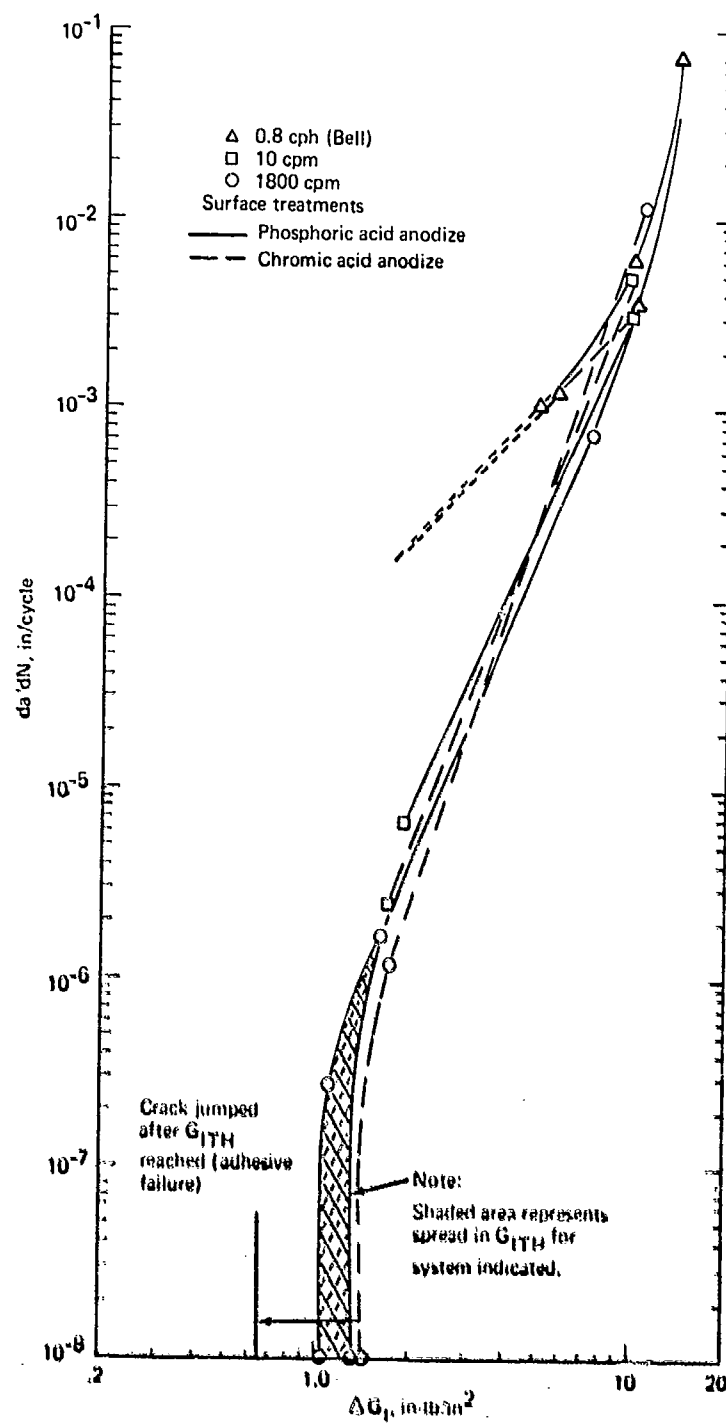
*Figure 28.—Topographical Features Which Appear To Be Fatigue Striations  
at Adhesive-Primer Interface Zone*



*Figure 29.—Fast Cyclic Load Machine for DCB Specimens*

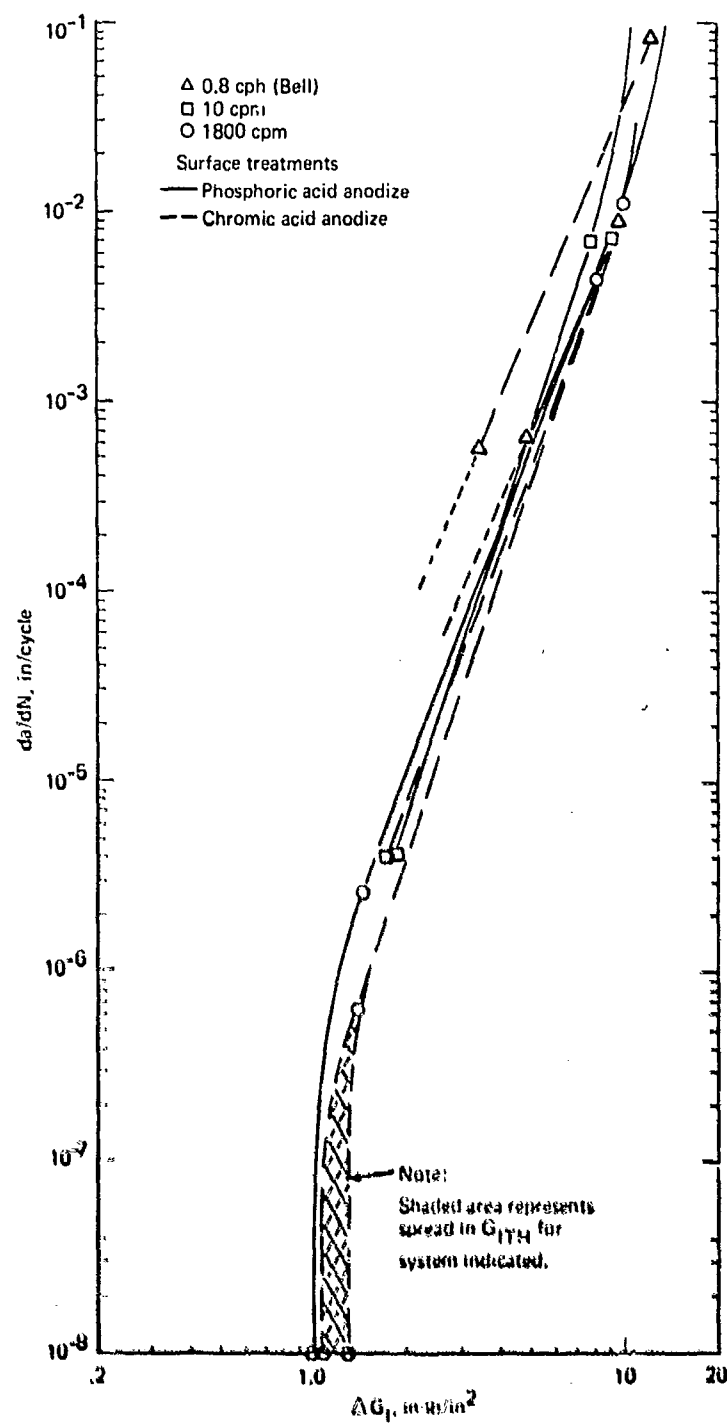


*Figure 30.—Slow Cyclic Load Machine for DCB Specimens*



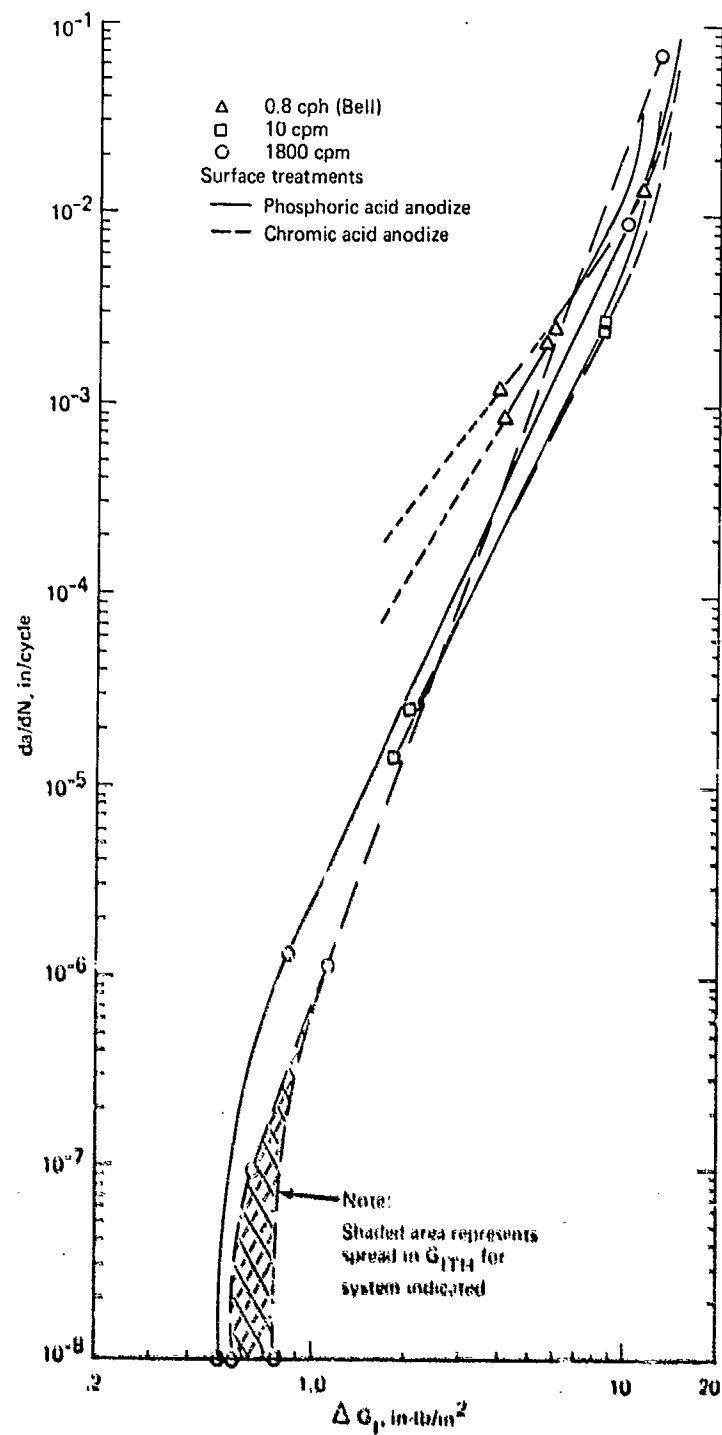
(a) Specimens Tested at Room Temperature, Humidity < 50%, EA 9628/BR 127, 2024-T3 Bare

Figure 31.—Cyclic Crack Growth Rate Data



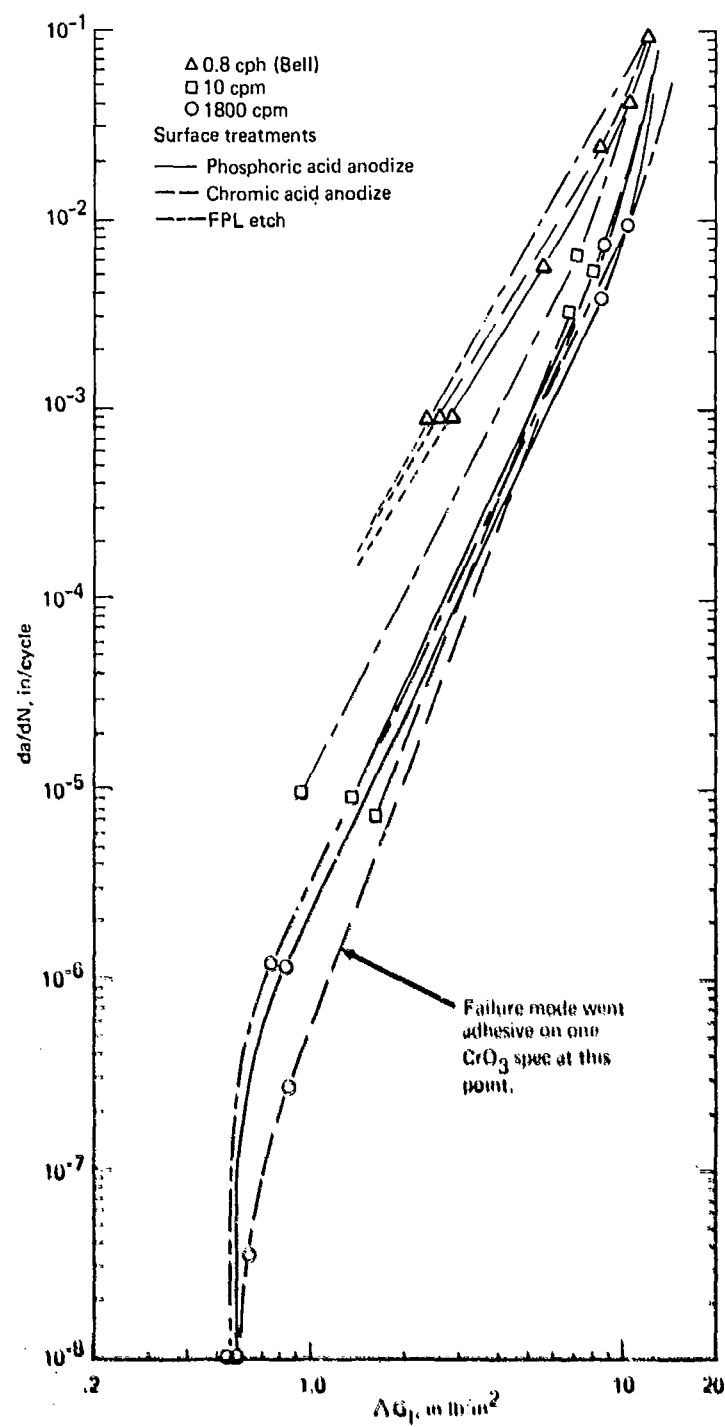
(b) Specimens Tested at Room Temperature, Wet, EA 9628/BH 127, 2024-T3 Bare

Figure 31.—(Continued)



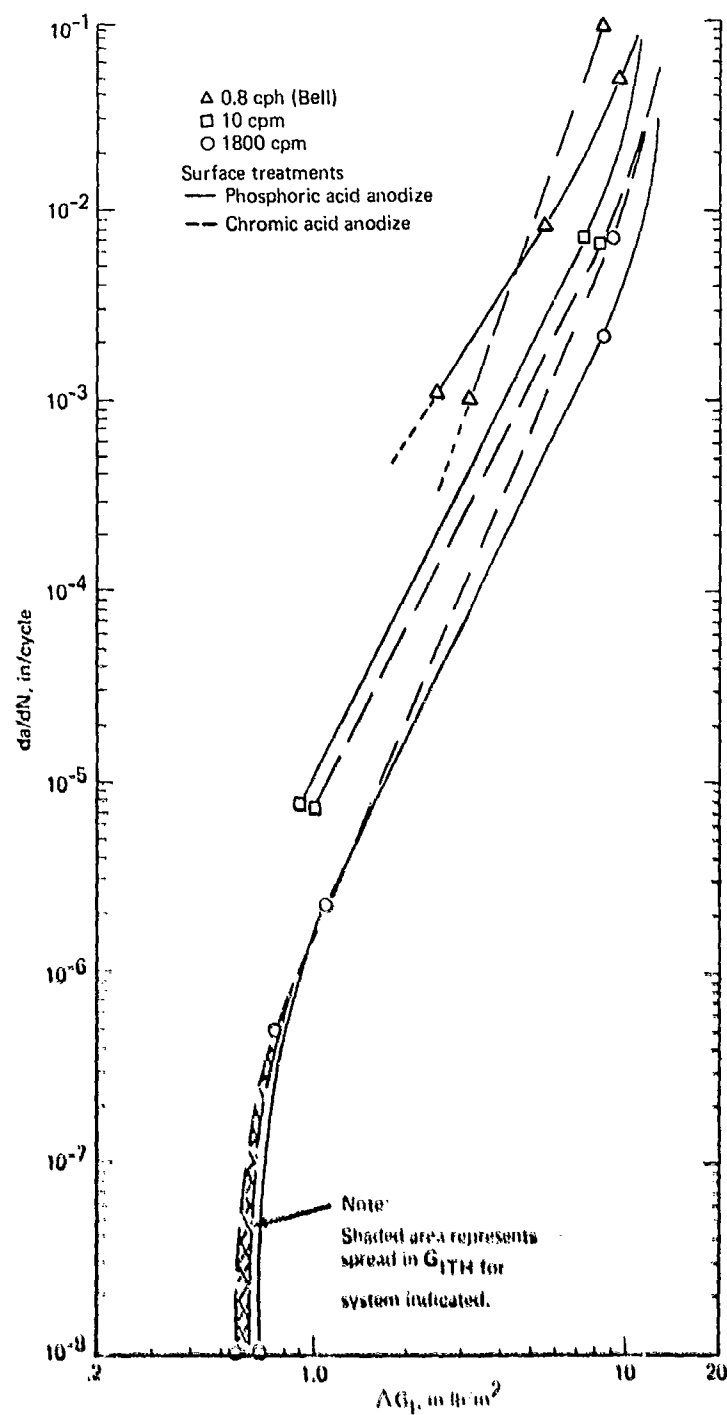
(c) Specimens Tested at 140°F, Dry (<20% RH), EA 9628/BR 127, 2024-T3 Bare

Figure 31.—(Continued)



(d) Specimens Tested at 140°F, Wat, EA 9628/BR 127, 2024-T3 Bar

Figure 31.—(Continued)



(e) Specimens Tested at 140°F. Wet, EA 9628/BR 127, 2024-T3 Bare

Figure 31.—(Concluded)

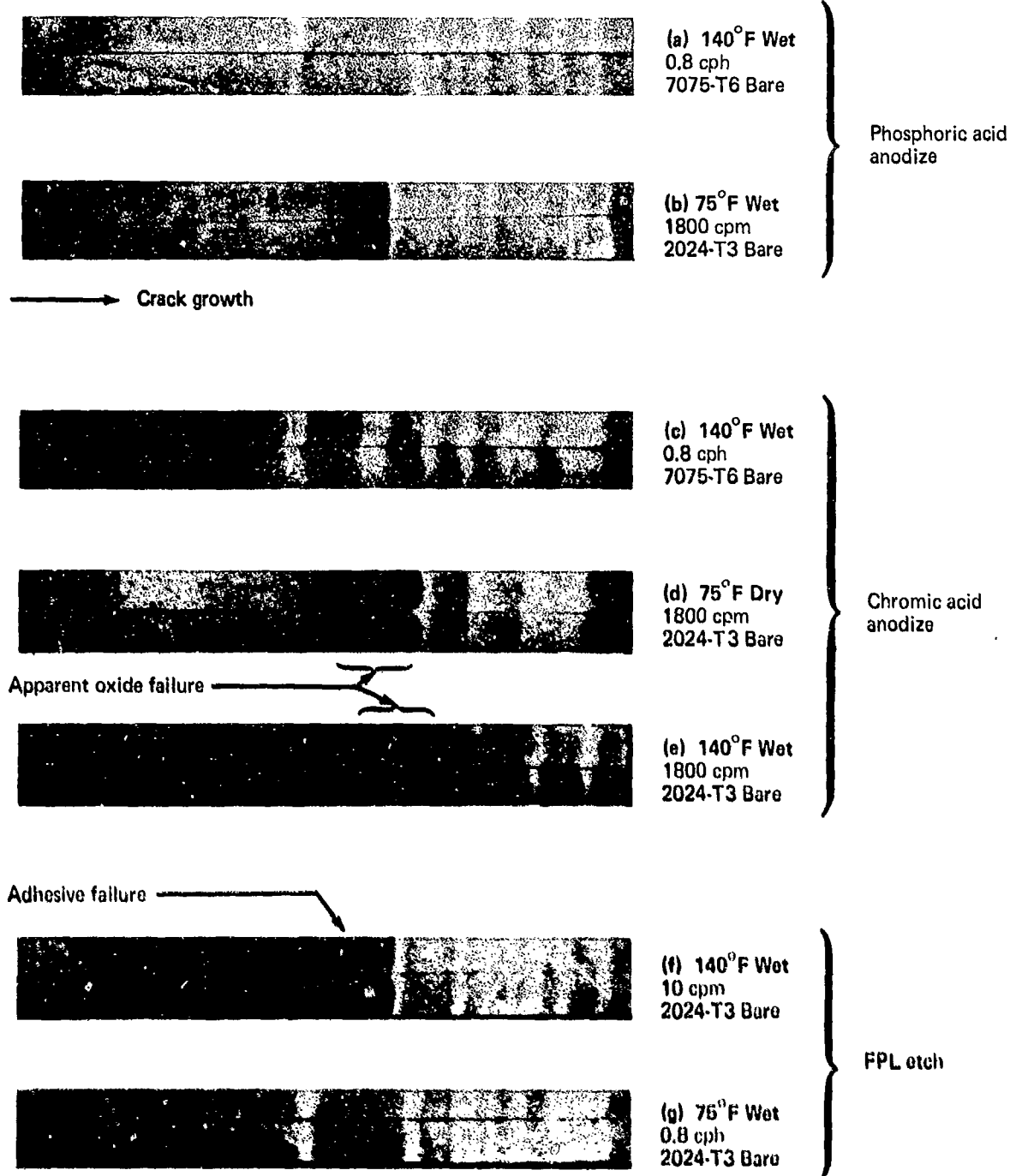
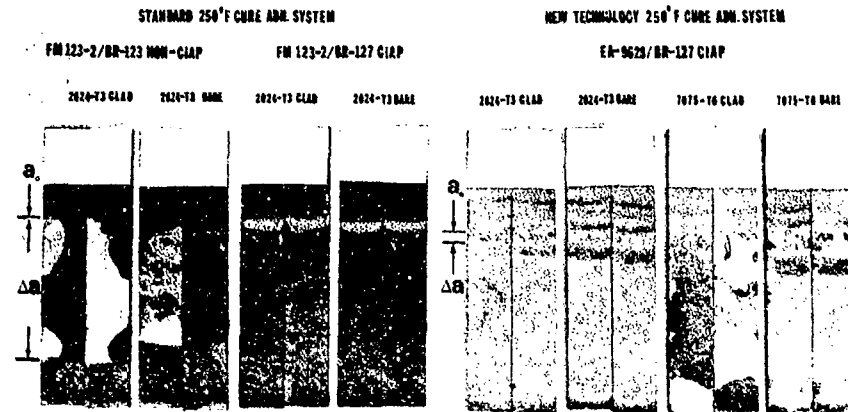
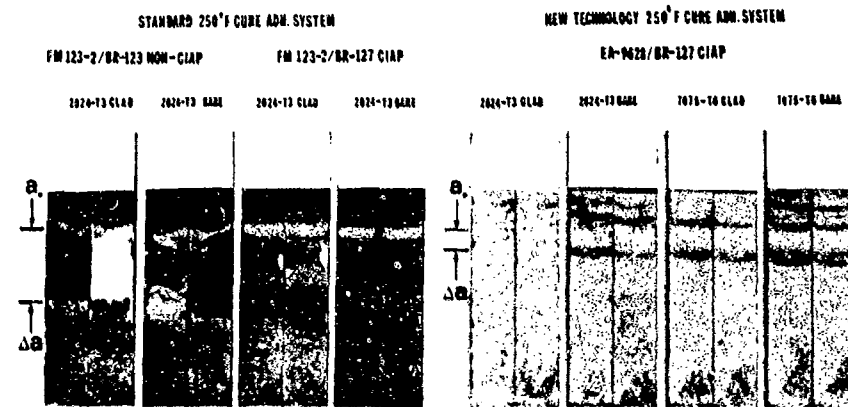


Figure 32.—Fracture Appearances From Cyclic Loading of DCB Specimens  
EA 9628/BR 127 Adhesive Primer System.

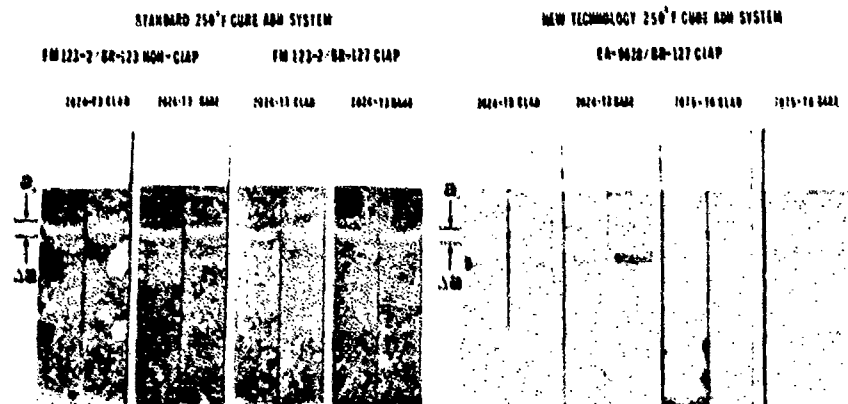
FPL



CrO<sub>3</sub> ANODIZE



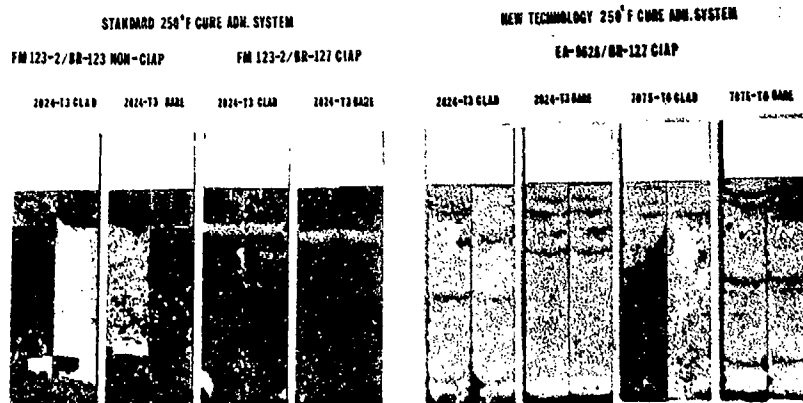
BAC 5555



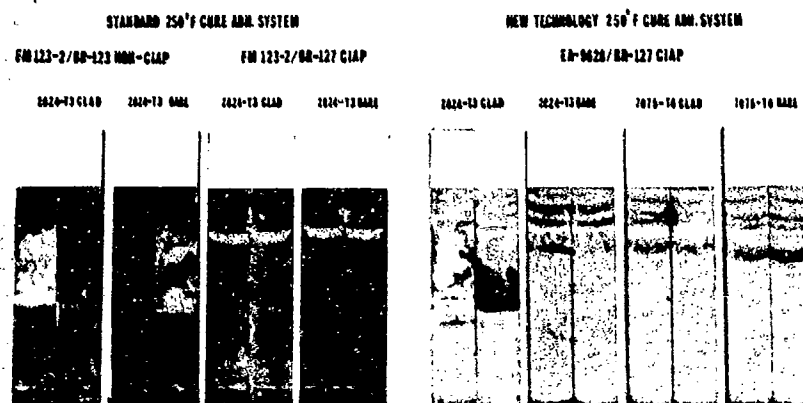
(a) 30-Day Exposure

Figure 33.—Wedge Test Specimens Exposed to 5% Salt Spray

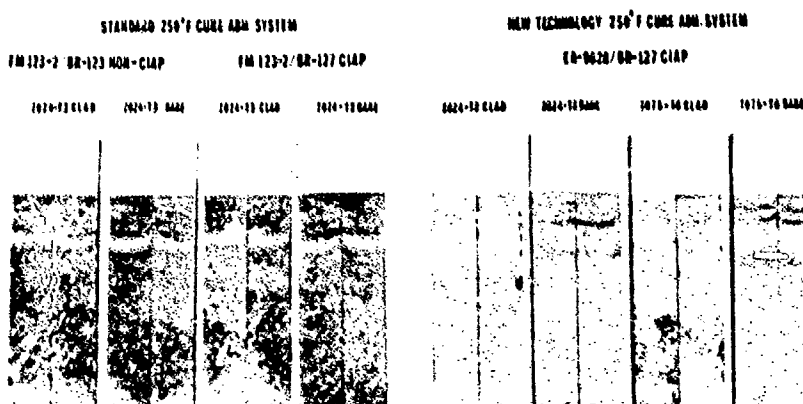
FPL



CrO<sub>2</sub> ANABRIZE



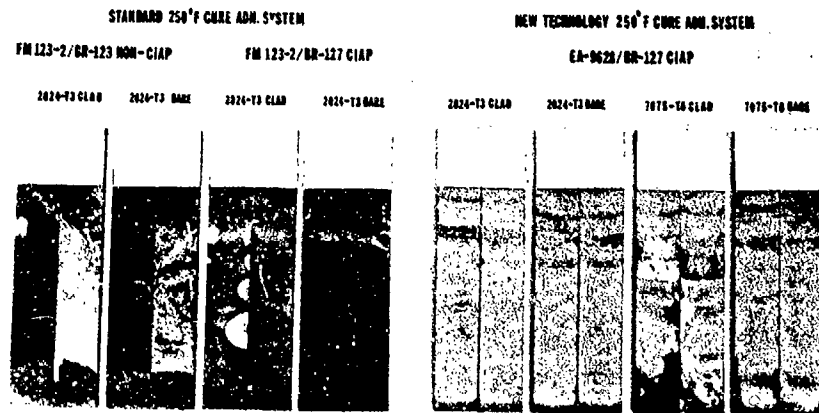
BAC5555



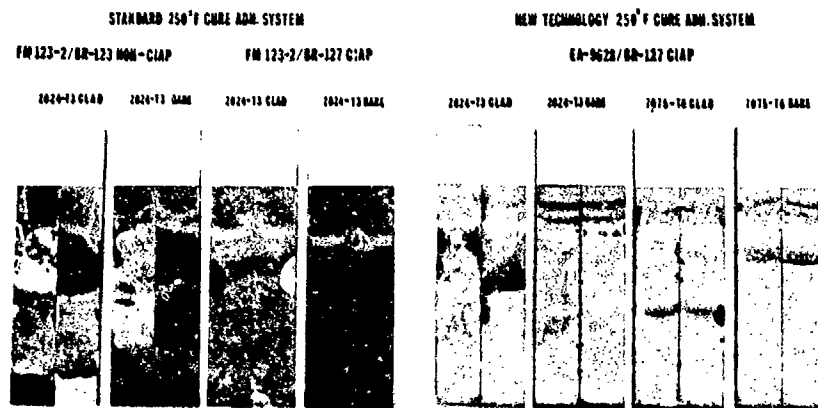
(b) 60-Day Exposure

Figure 33.--(Continued)

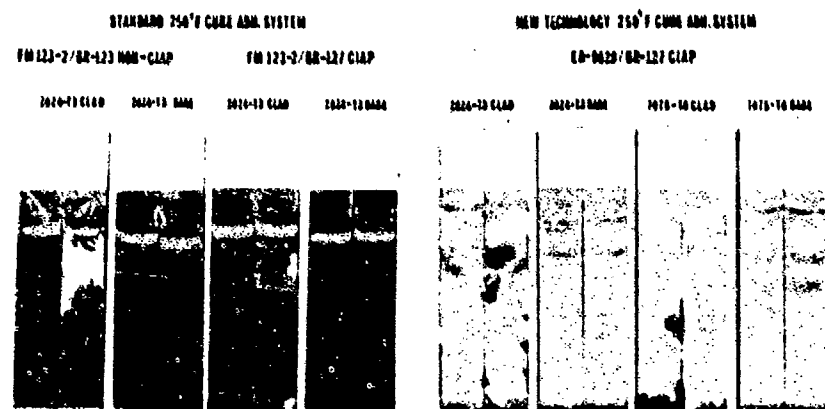
FPL



CrO<sub>3</sub> ANODIZE



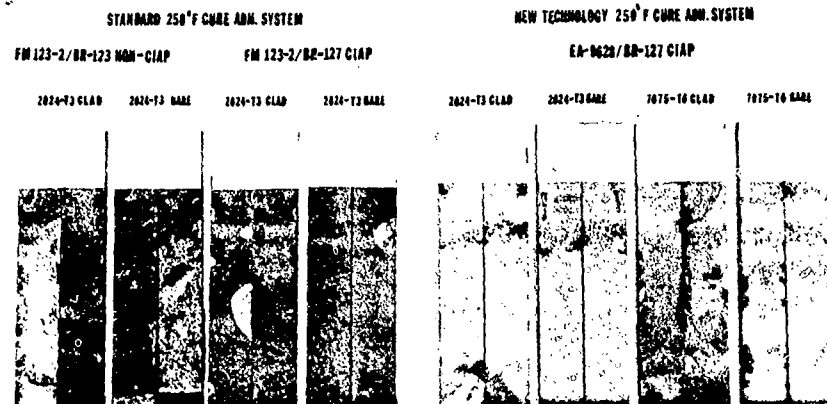
8AC5555



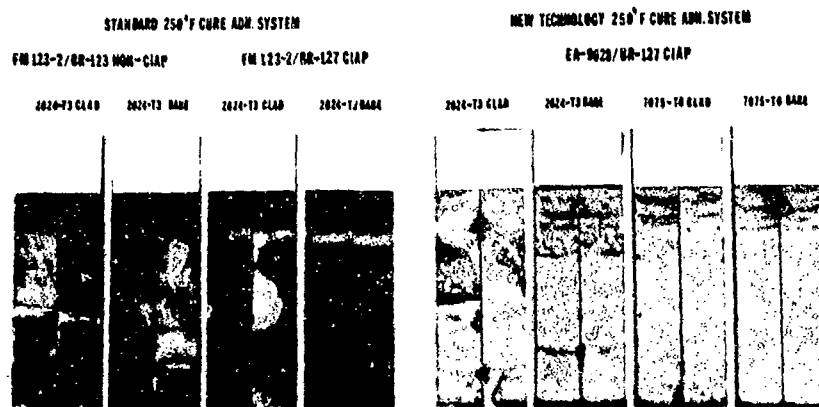
(c) 90-Day Exposure

Figure 33.—(Continued)

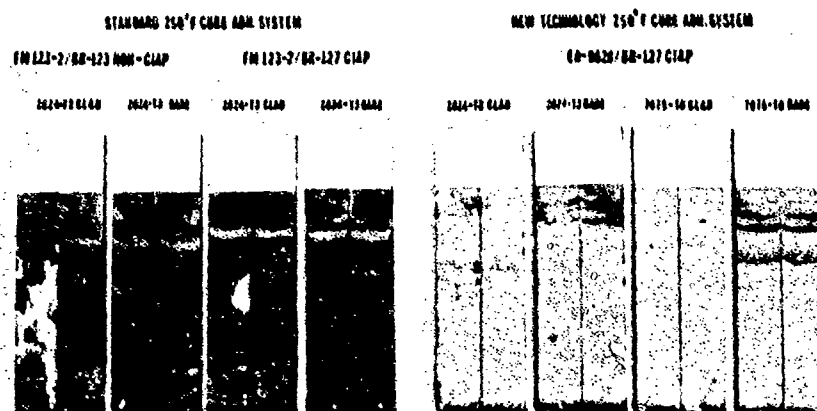
FPL



CrO<sub>3</sub> ANGIOIZE



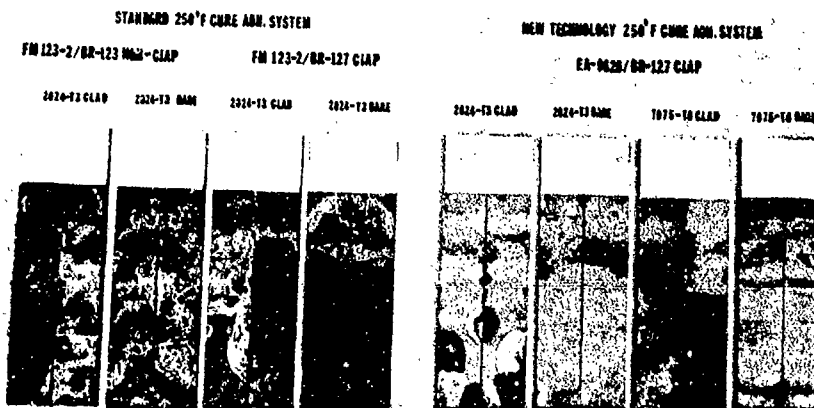
BAC5555



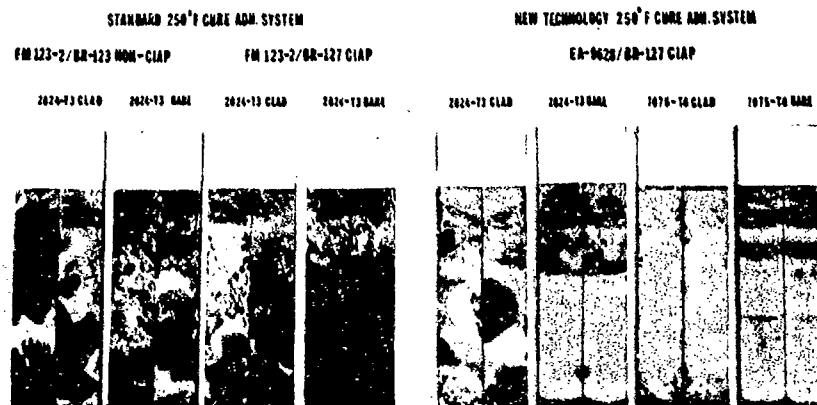
(d) 180-Day Exposure

Figure 33.—(Continued)

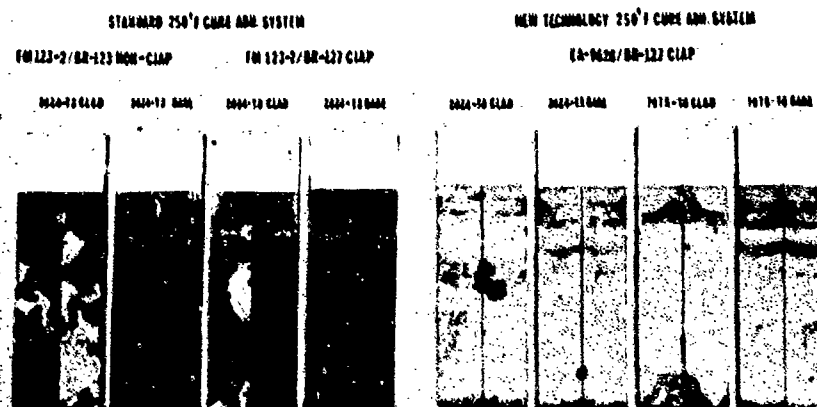
FPL



CyO, ANDRIZE

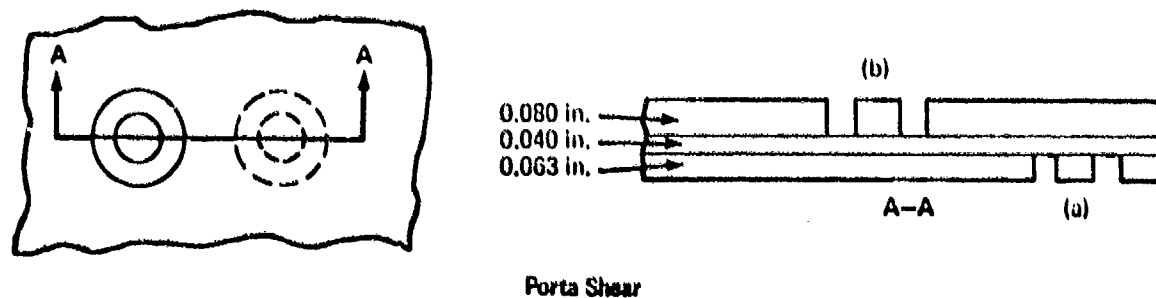
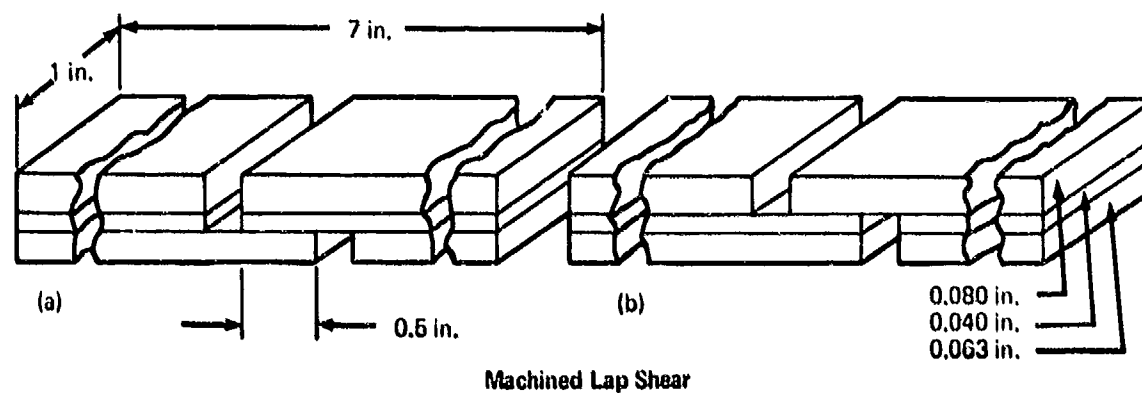
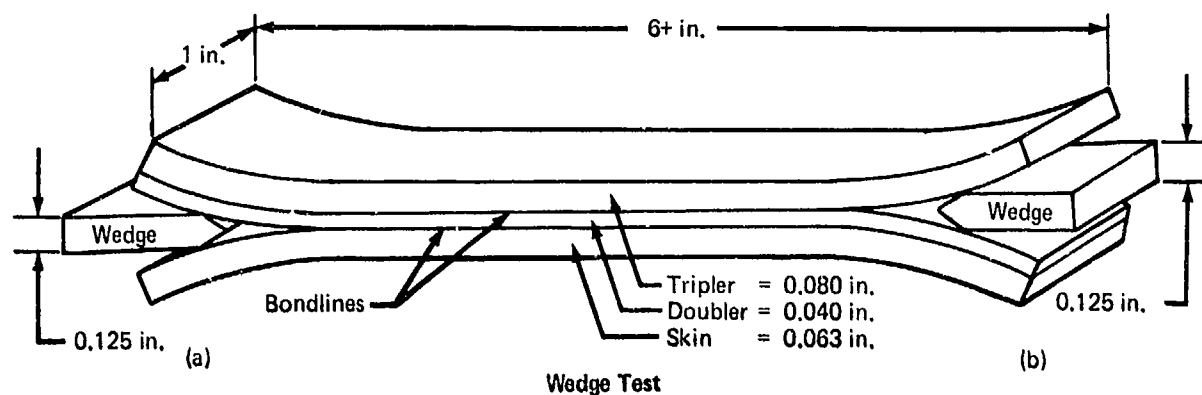


BAC6555



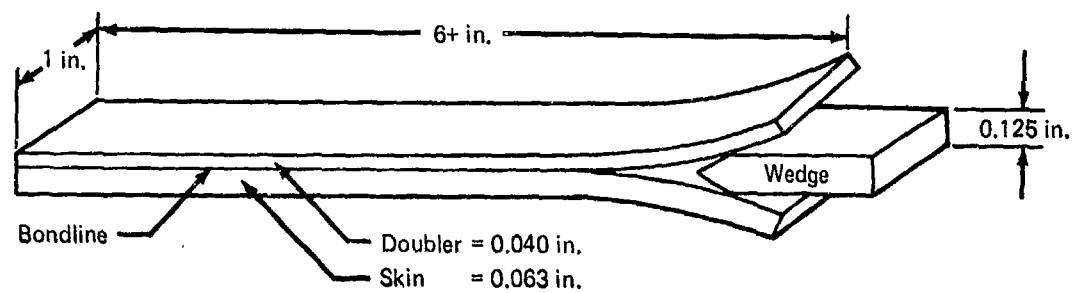
(e) 365-Day Exposure

Figure 33.—(Concluded)

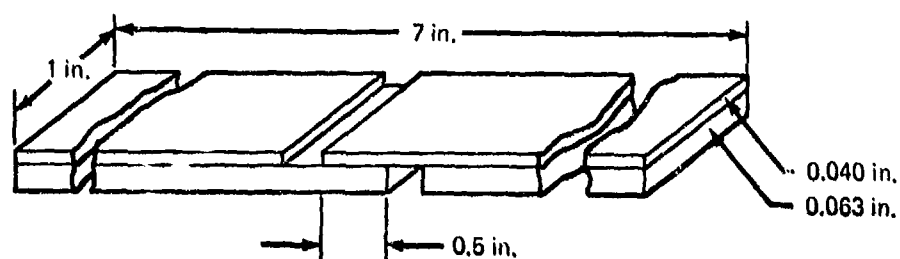


Note:  
 (a) Skin-doubler bond (SD)  
 (b) Doubler-tripler bond (DT)

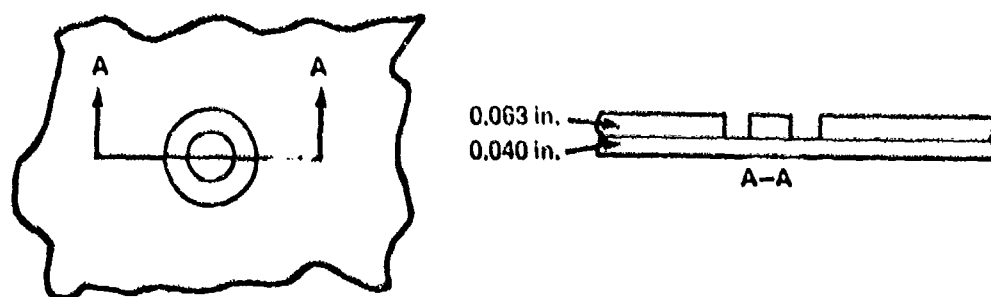
Figure 34.—Specimen Configuration for Commercial Aircraft A



Wedge Test



Machined Lap Shear



Porta Shear

Figure 35.—Specimen Configuration for Commercial Aircraft B

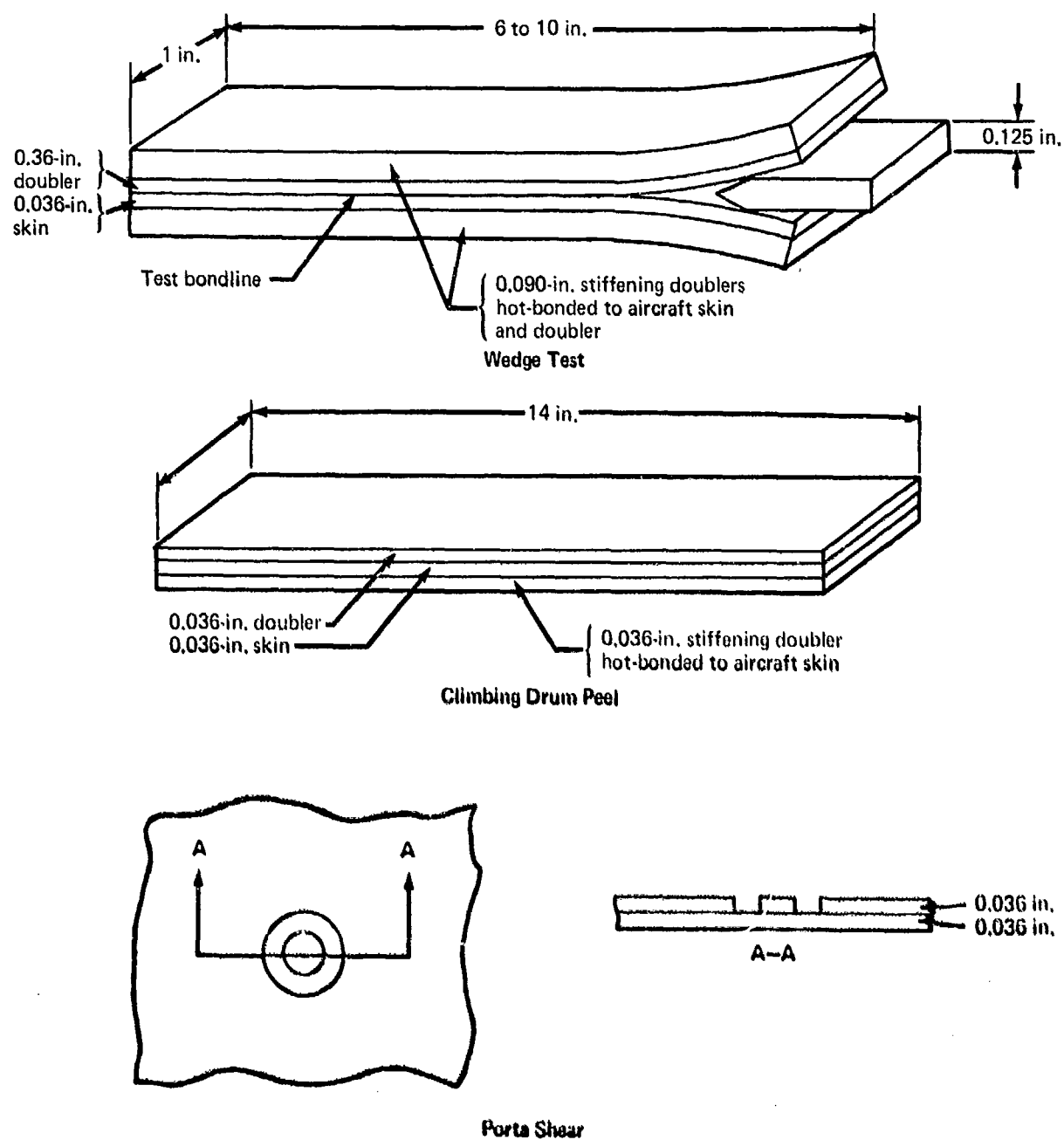
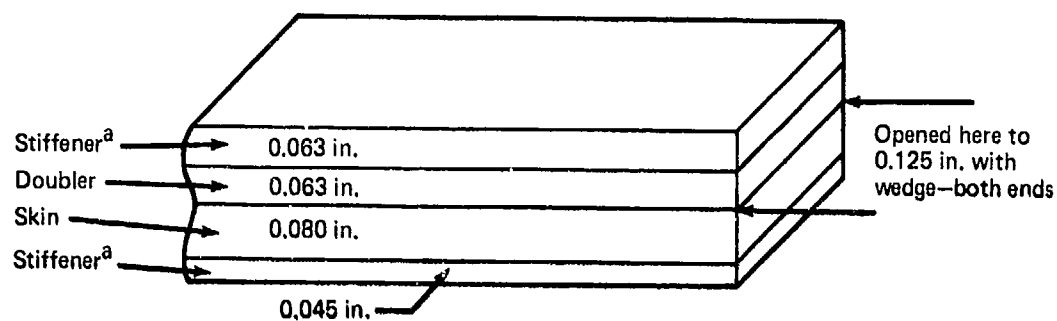
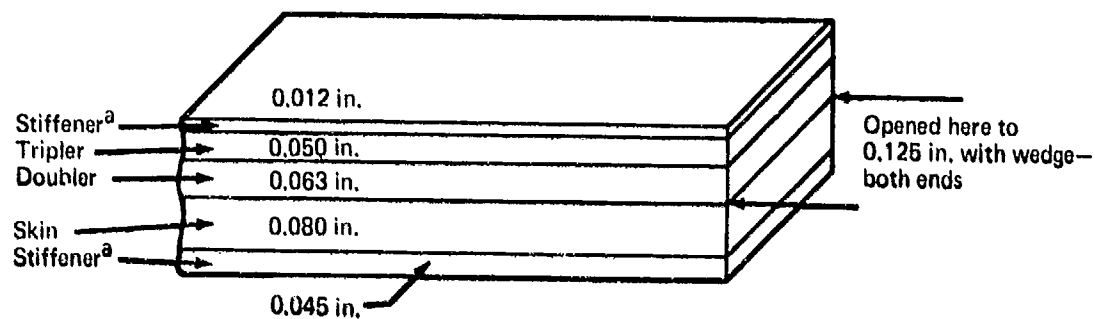


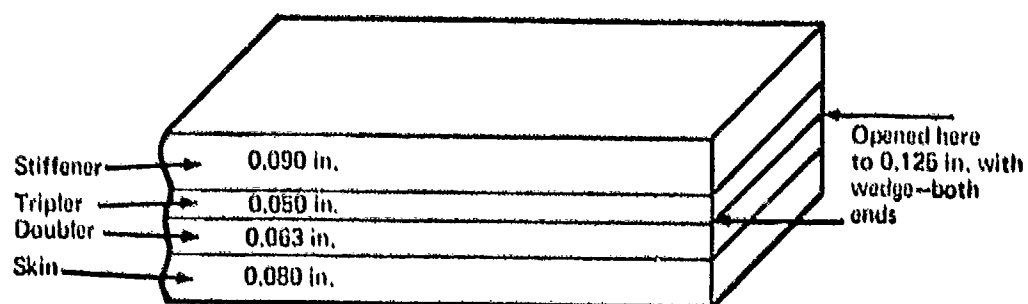
Figure 36.—Specimen Configuration for Commercial Aircraft C



Detail 1D: Specimens 1 and 2



Detail 2D: Specimen 3a



Detail 2D: Specimens 3b and 3c

Note:

All specimens 1 in. wide and 6 in. long

<sup>a</sup>Stiffening doublers hot-bonded to aircraft details

Figure 37.—Specimen Configuration for Commercial Aircraft D

AF 126/EC 2320, 2024-T3 clad

f = 300 psi

Environment: 140°F/condensing humidity

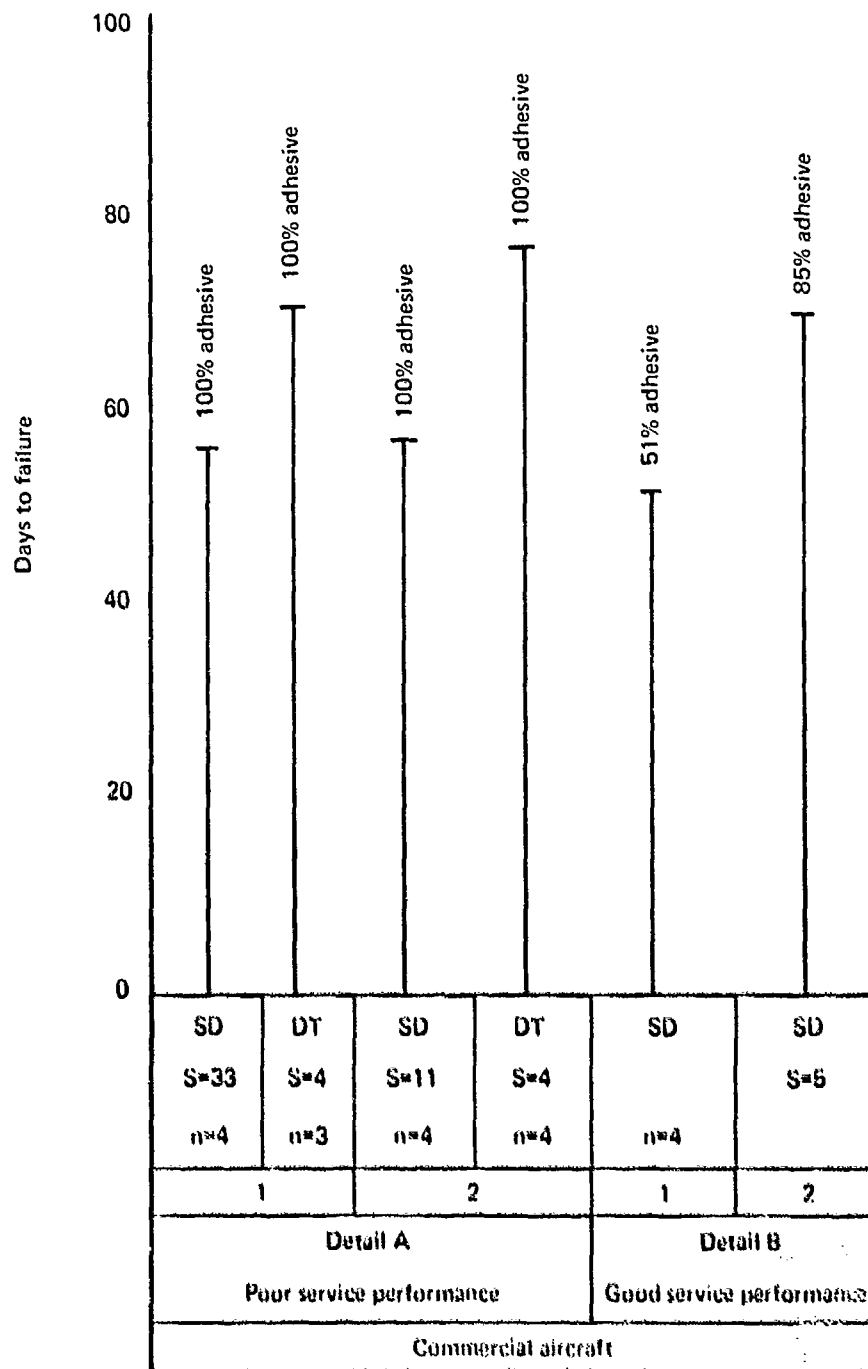


Figure 38.—Sustained-Stress Lap-Shear Results of Specimens Machined From Aircraft A and B Components

AF 126/EC 2320,  
2024-T3 clad

Environment: 140°F/condensing humidity

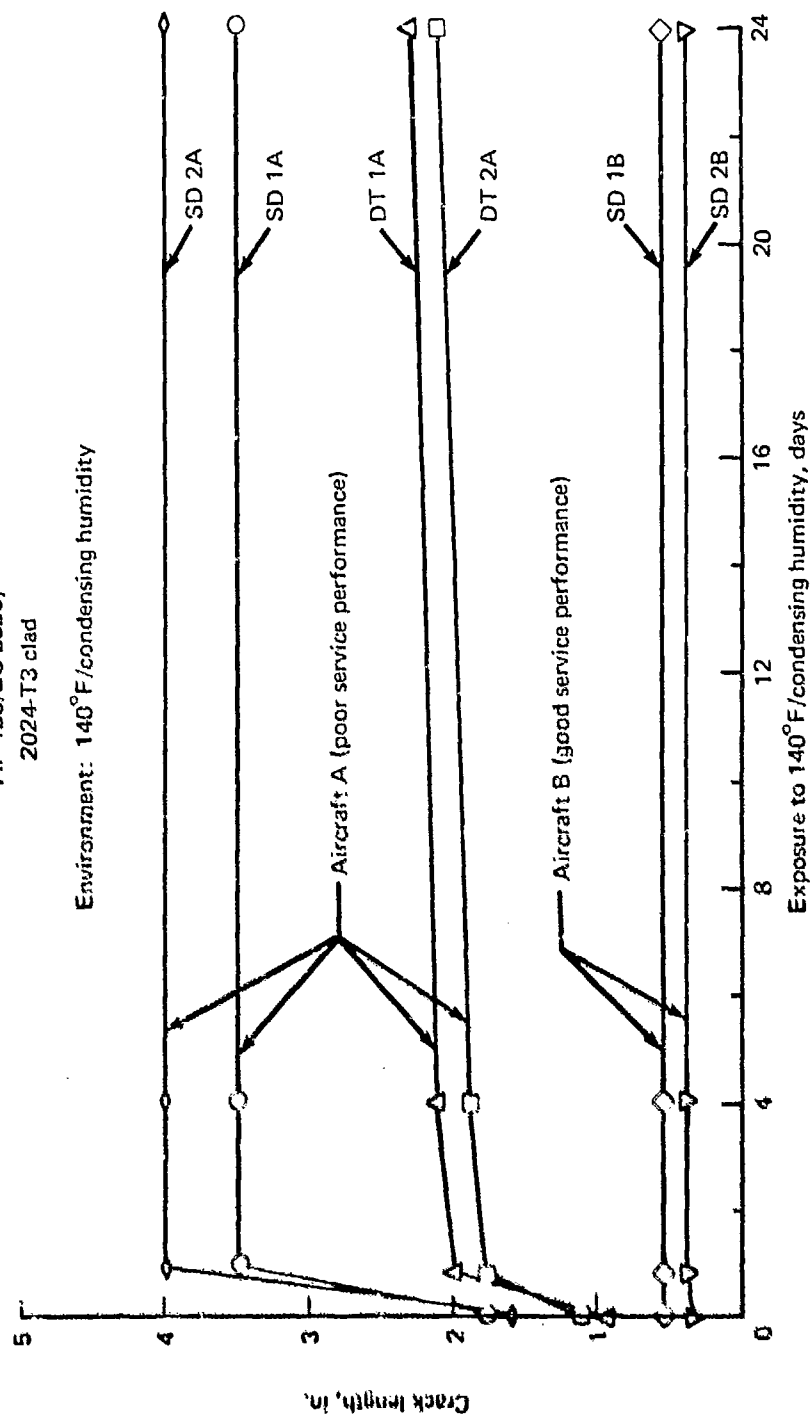


Figure 39.—Wedge Test Results of Specimens Machined From Aircraft A and B Components

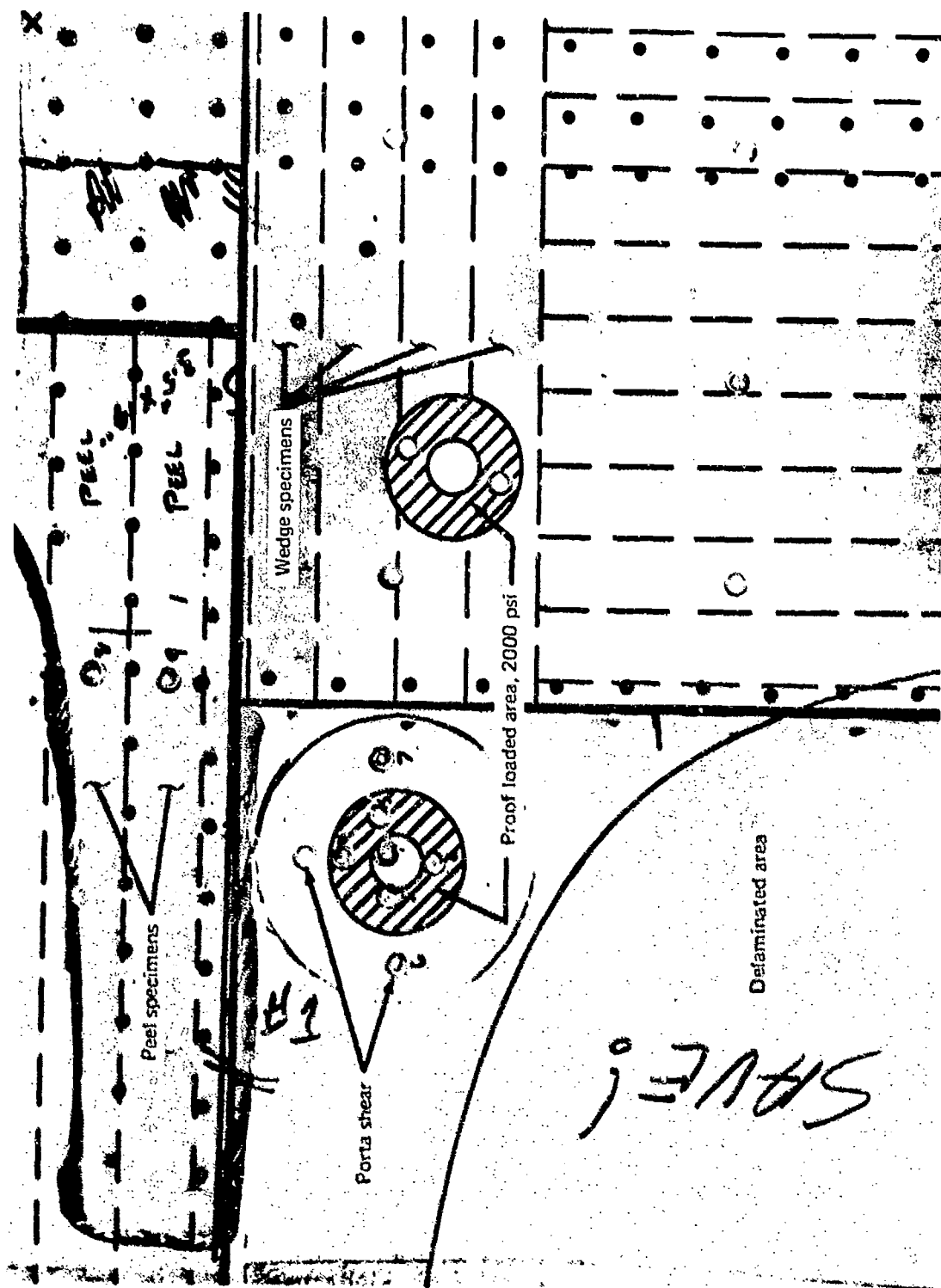


Figure 40.—Section of Aircraft C Component Showing Areas Where Test Specimens Were Taken

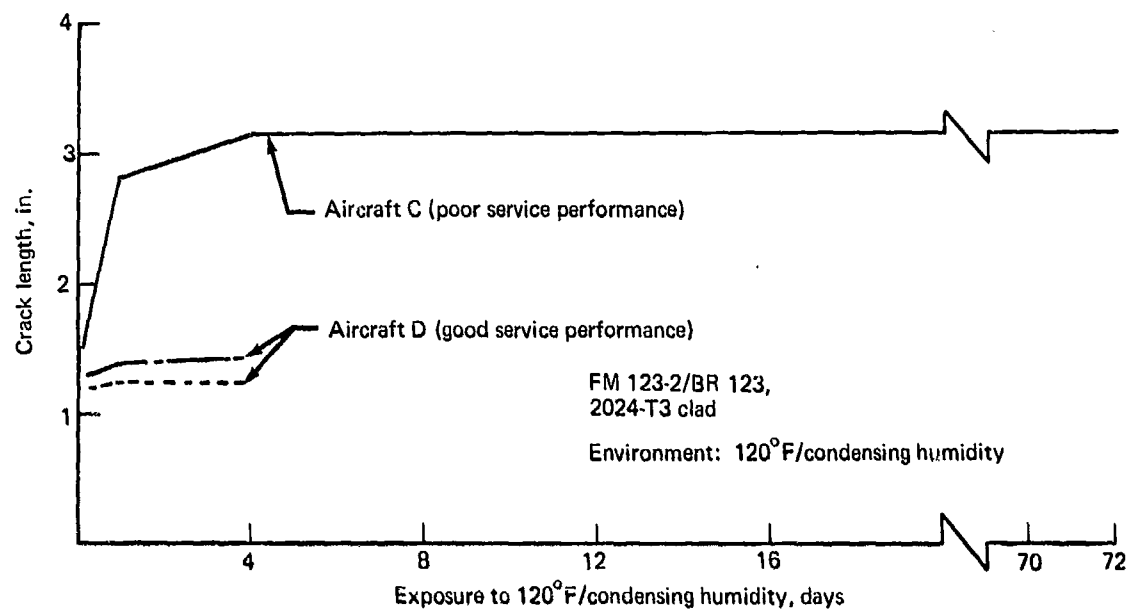


Figure 41.—Wedge Test Results of Specimens Machined From Aircraft C and D Components

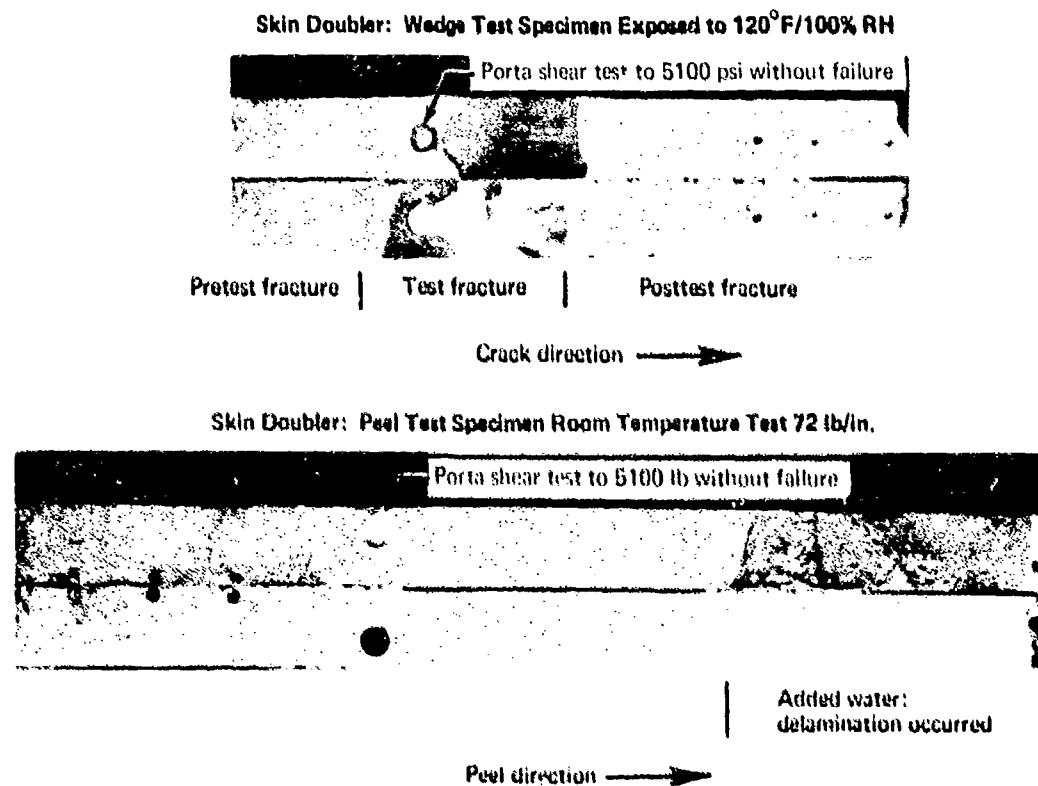
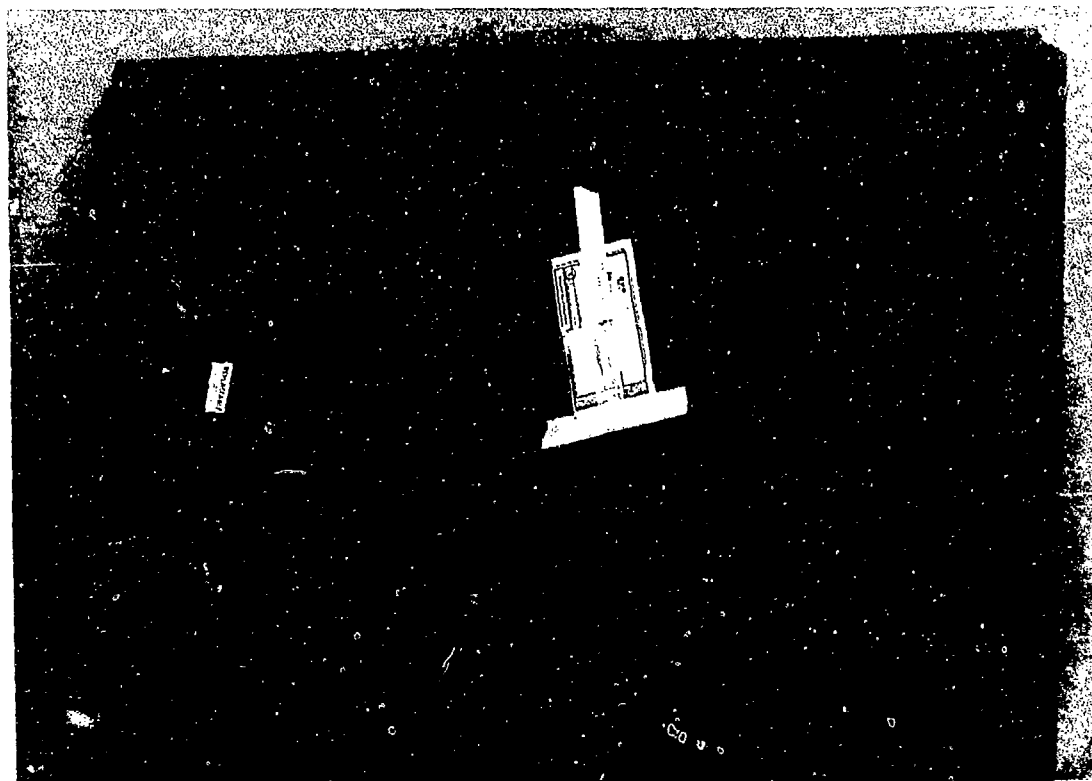
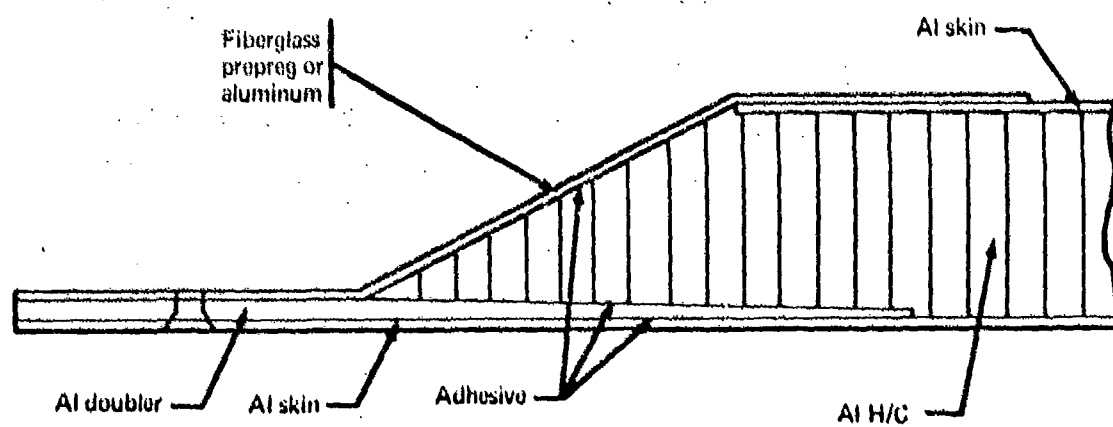


Figure 42.—Typical Wedge Test and Peel Test Specimens From Aircraft C



*Figure 43.—Typical Bonded Honeycomb Panel With Closeouts From Air Force Aircraft*



*Figure 44.—Typical Cross Section of Honeycomb Structure With Tapered Closeout*

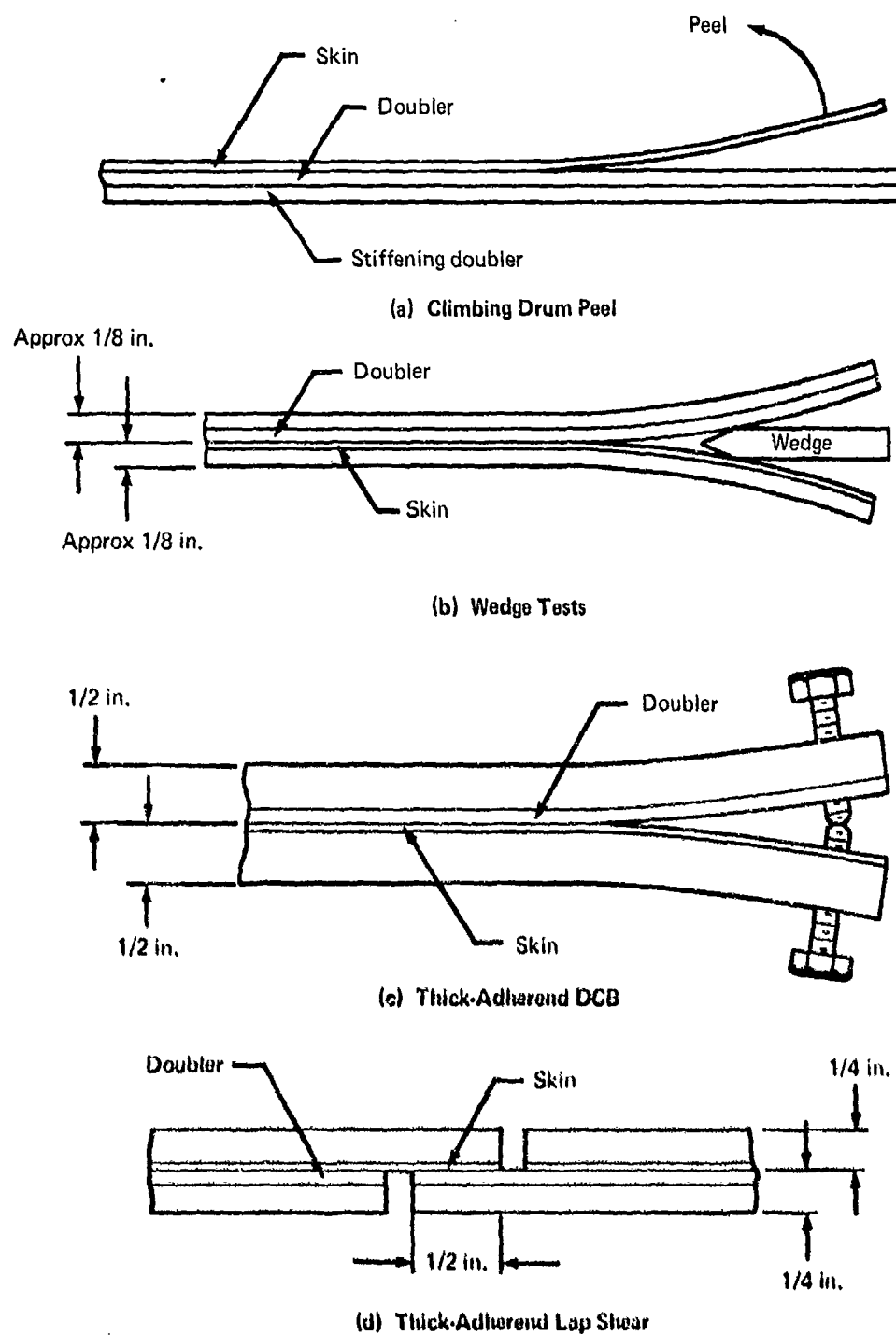
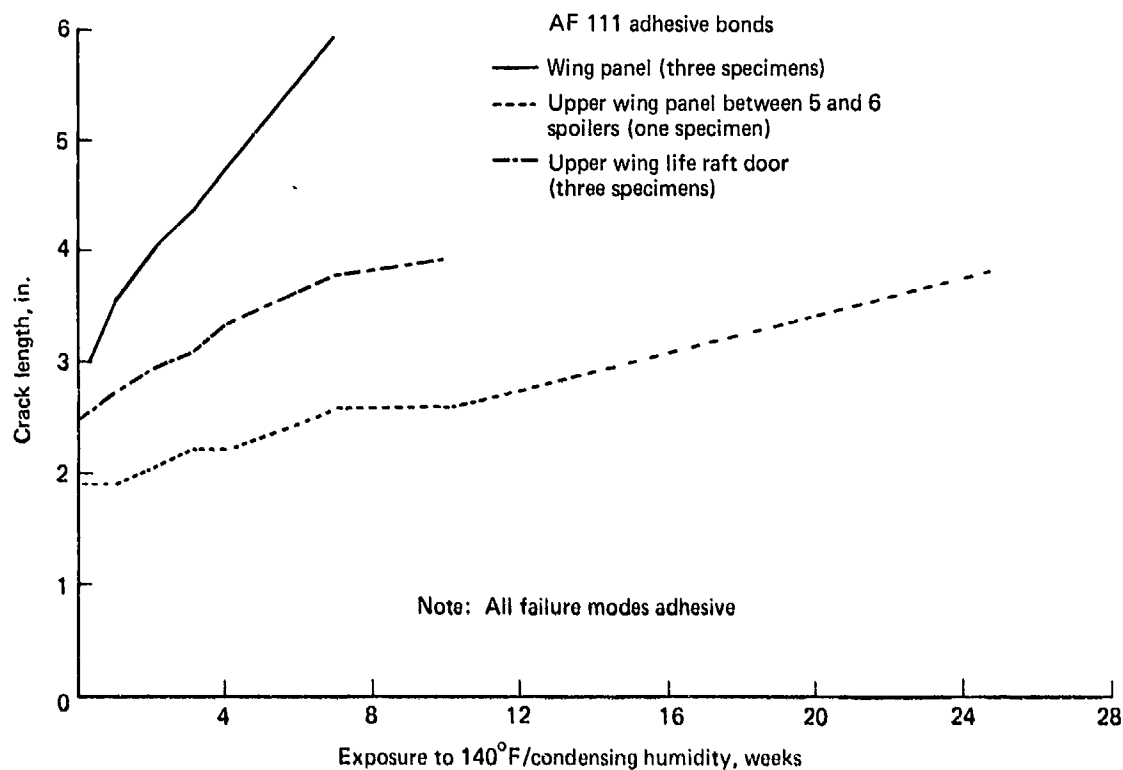
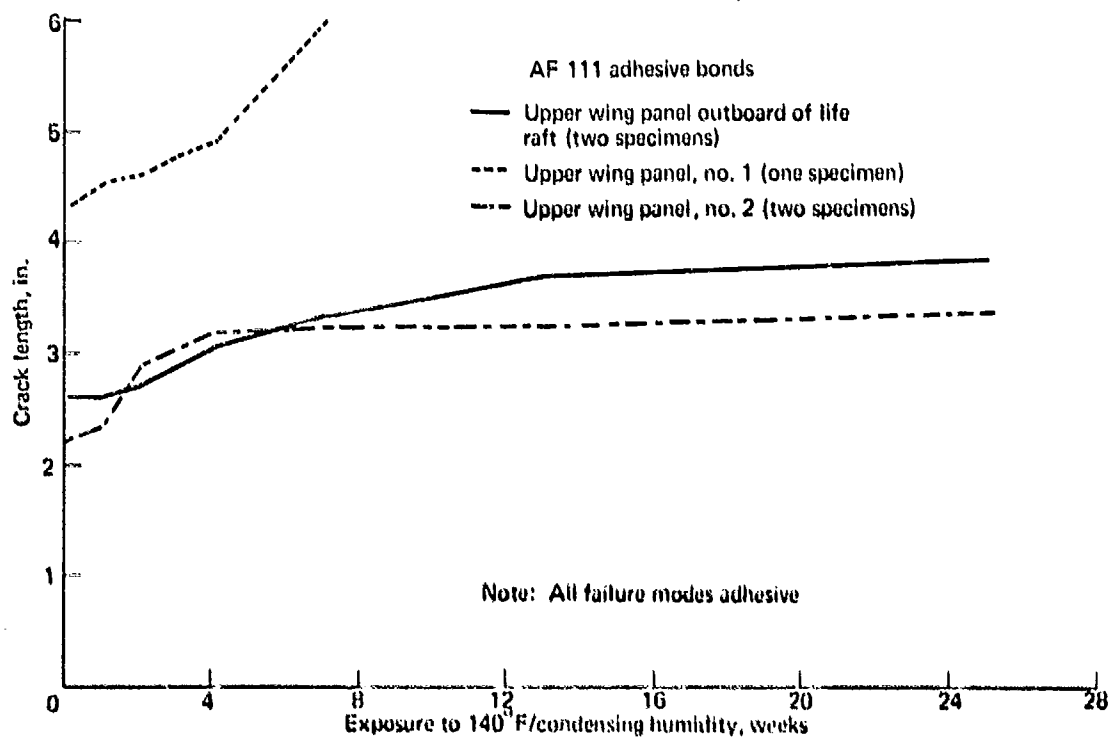


Figure 45.—Configurations of Specimens Fabricated From Air Force Aircraft Details

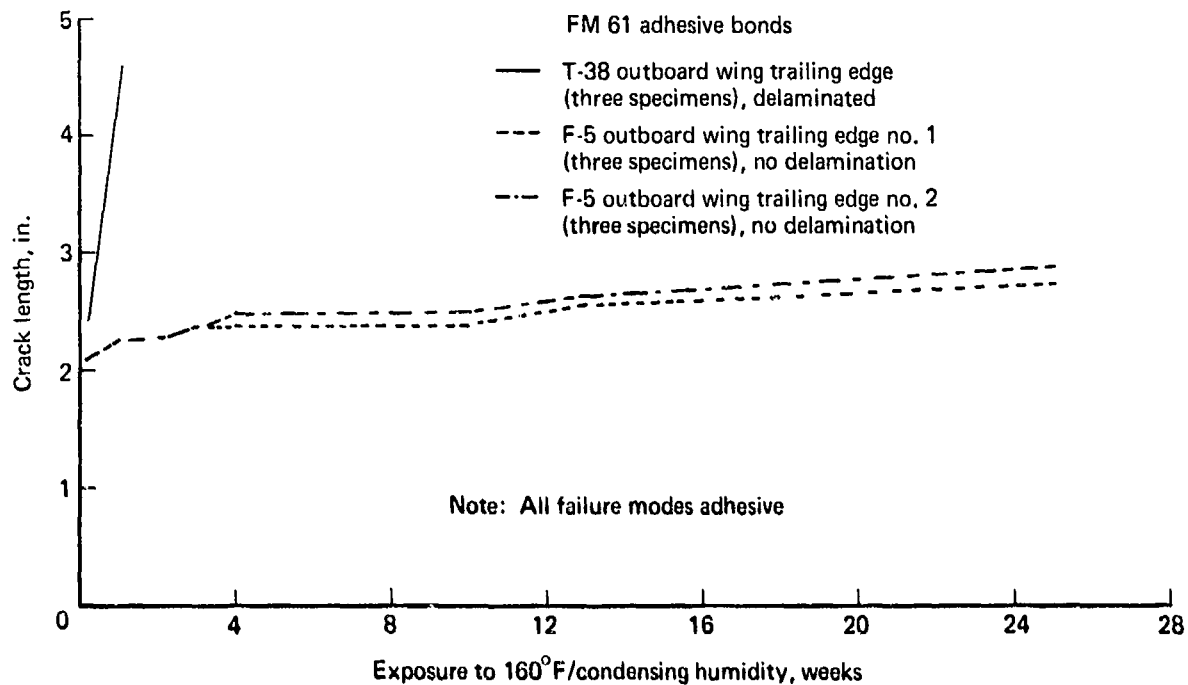


(a) C-141 Bonded Panels Which Were Not Obviously Delaminated

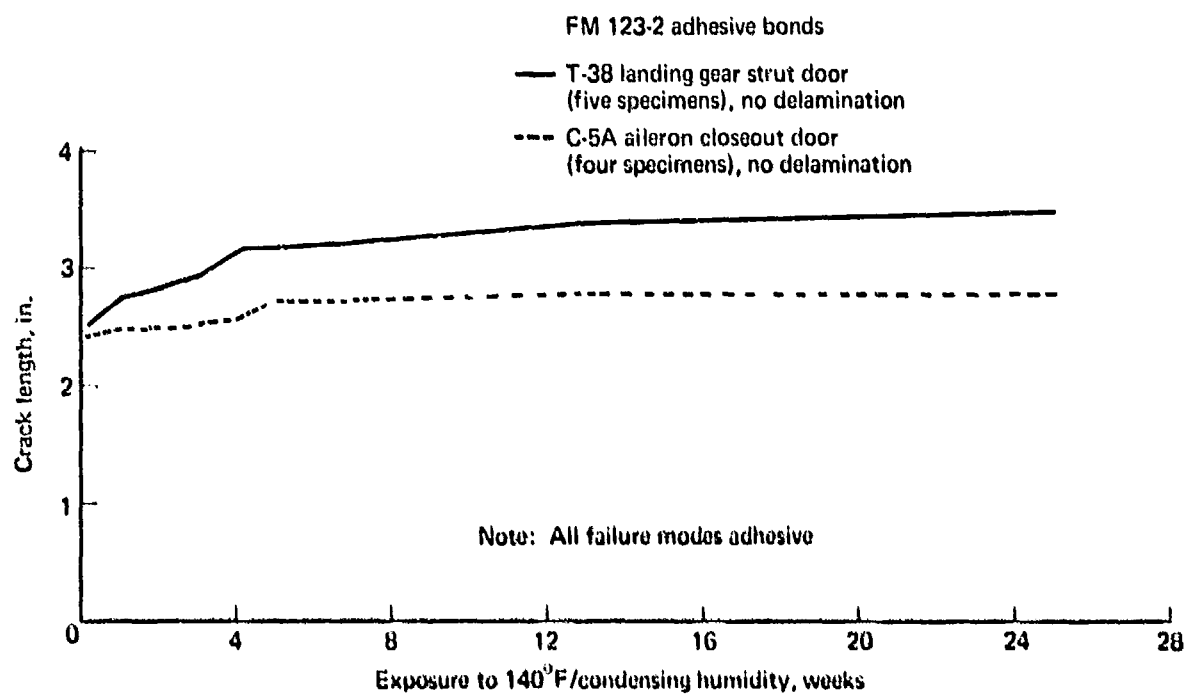


(b) C-141 Bonded Delaminated Panels

Figure 46.—Wedge Test Results of Specimens Machined From Air Force Aircraft



(c) T-38 and F-5 Bonded Panels



(d) T-38 and C-5A Bonded Panels

Figure 46.—(Concluded)

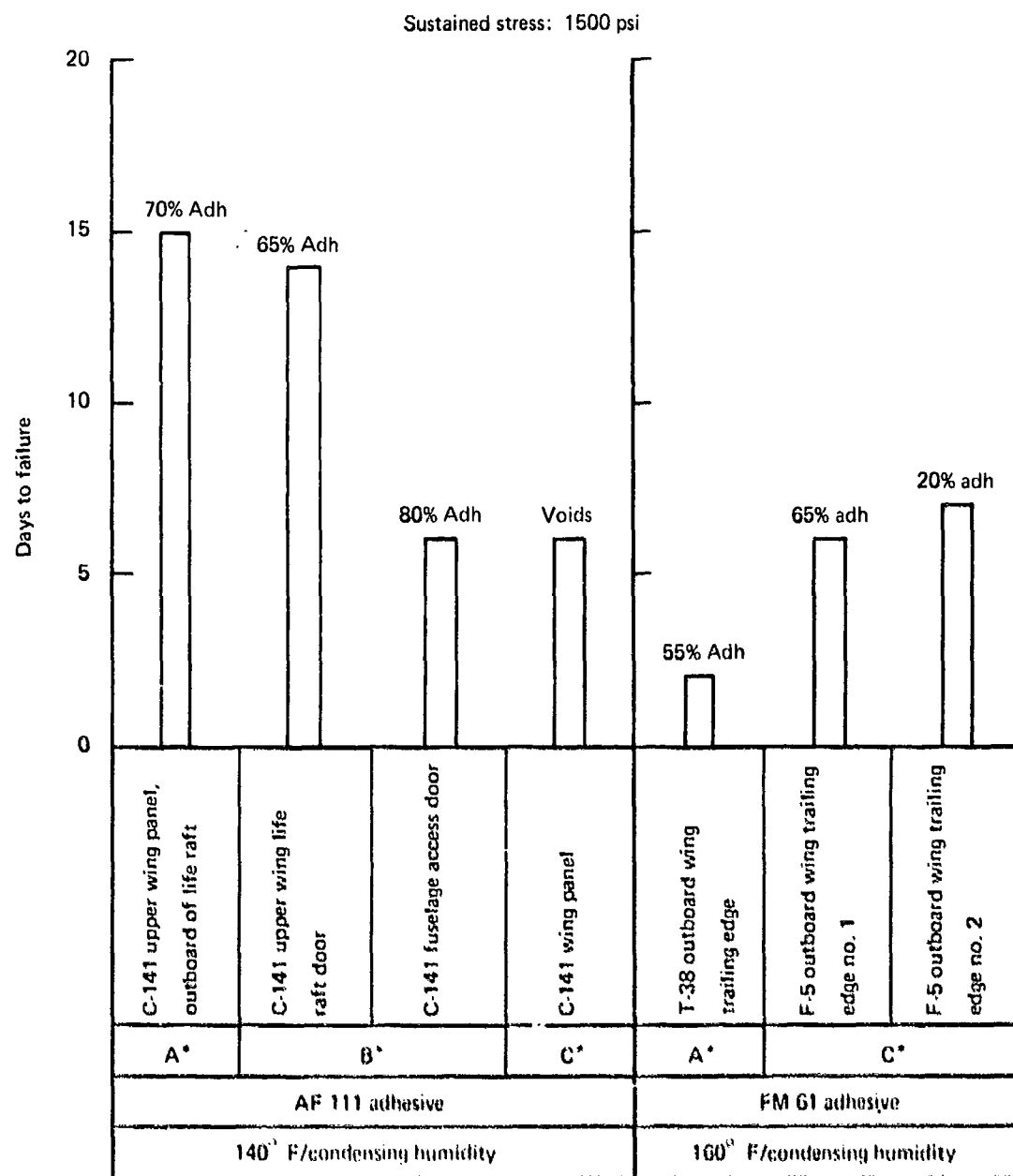


Figure 47.—Sustained-Stress Thick-Adherend Lap-Shear Time-to-Failure Results

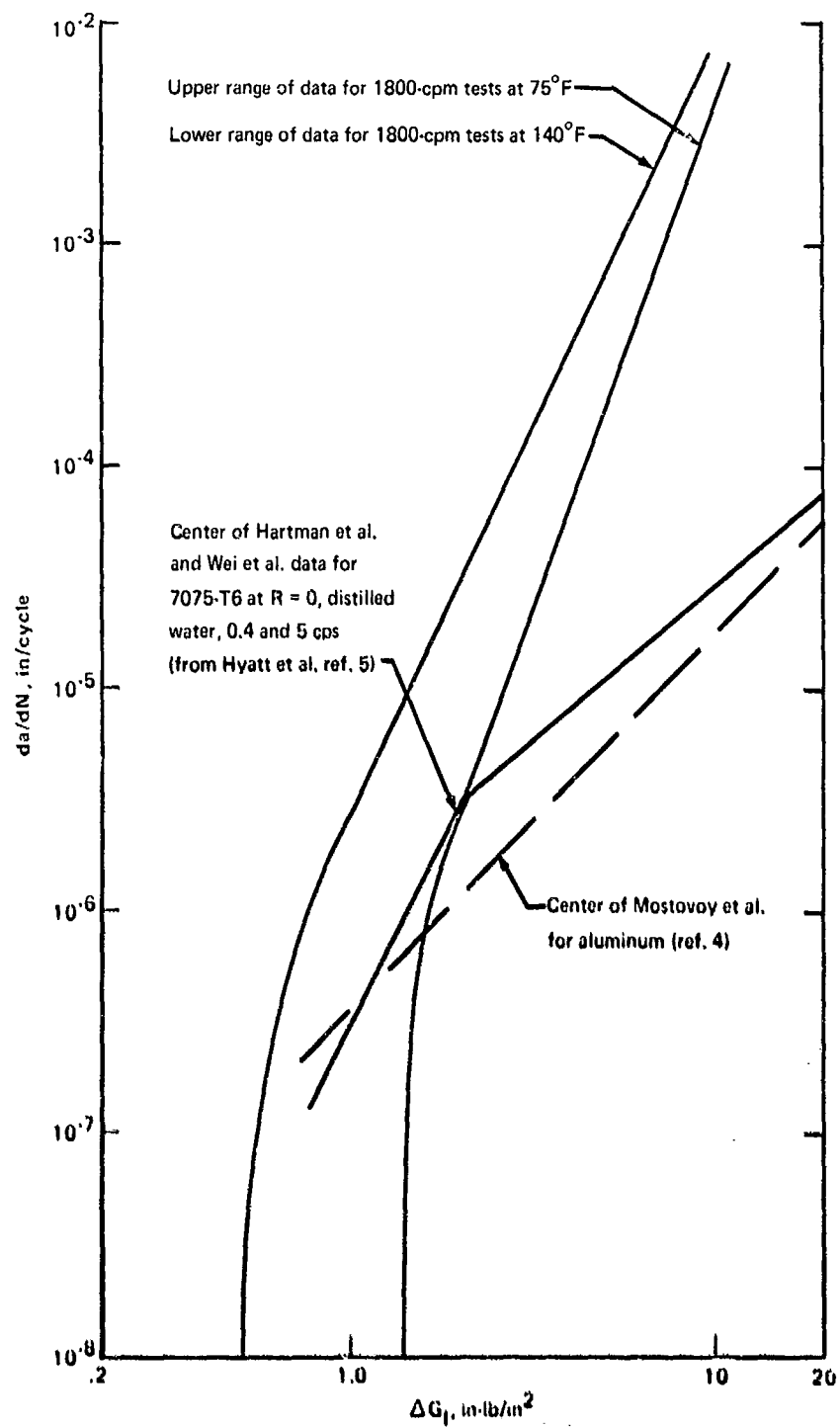


Figure 48.—Comparison of Bonded Aluminum Fatigue Crack Growth Data With Published Data for Fatigue Crack Growth in Aluminum Alloys

## APPENDIX A

### NONDESTRUCTIVE INSPECTION (NDI) OF BONDED TEST ASSEMBLIES

All bonded test assemblies fabricated for this program were nondestructively inspected (NDI) before fabricating test coupons. Ultrasonic through-transmission inspection with single-level and/or multilevel C-scan recording and low-voltage X-radiography (25 to 50 kV) were used on all bonded assemblies. Neutron radiography was used on most of the honeycomb sandwich and on selected metal-to-metal assemblies. Results of these NDI evaluations are shown in tables A-1 and A-2.

Low-voltage X-radiography, and especially neutron radiography, proved more definitive in identifying voids and porosity than did the ultrasonic through-transmission for metal-to-metal assemblies. An example of neutron radiography showing some of the largest and most numerous voids and porosity is shown in figure A-1.

The ultrasonic through-transmission data did not clearly show the same pattern of voids and porosity as did the radiographic methods, and in most cases did not suggest this condition. See table A-1. Part of this problem could have been due to bondline thickness variations which made it difficult to set the proper gates for the C-scan recorder, particularly when single-level recording was used.

Interpretation of NDI results for the honeycomb sandwich specimens was even more difficult, because of the double honeycomb sandwich and multiple bondlines. Again, neutron radiography gave the most definition, but complete interpretation of the indications was not achieved. See table A-2.

Two examples can be cited where voids were responsible for reduced specimen performance: 1) A 3/8-in. to 1/2-in. diameter void resulted in a premature stressed lap shear test failure (table 10 of text), and 2) several baseline lap shear results were lower than expected (table 4 of text). None of the bonded assemblies from which the specimens were taken showed evidence of voids or porosity on the X-radiographs or C-scan recordings.

Voids and/or porosity were evident in numerous DCB and lap shear specimens after posttest fracture, with some of these bondline discontinuities showing up in the NDI evaluation. However, there was no evidence that these discontinuities contributed to reduced durability.

It appears that the only effect of voids and porosity is to increase the local stress in the confined test area.

Conclusions drawn from the assessment of NDI results and subsequent durability tests are:

1. The radiographic NDI methods, particularly neutron radiography, are the most definitive means of identifying voids and porosity.
2. Voids and porosity that did not show up in either of the NDI methods were present in bondlines of test specimens.
3. There was no correlation between NDI-observed voids and porosity in bonded assemblies and adverse stressed durability test results.



Note: Area shown represents approximately 20% of the AF 143 Bonded Assembly.

*Figure A-1.—Neutron Radiograph of Laminated 2024-T3 Clad Panel Section for Thick-Adherend DCB Specimens Showing Voids in One or More Bondlines*

Table A-1.—Nondestructive Inspection (NDI) of Bonded Metal-to-Metal Assemblies

Adhesive/primer system	Alloy	Surface treatment <sup>a</sup>	No. of assemblies	X-ray results	Ultrasonic through-transmission results
FM 123-2/BR 127	2024-T3 clad	F	3	No anomalies ↕	Nothing definitive ↕
		C	3		
		P	4		
	2024-T3 bare	F	3	No anomalies No anomalies (5) Porosity (1)	Nothing definitive Nothing definitive (5) Spots on edge (1)
		C	3		
		P	6		
	7075-T6 clad	F	2	No anomalies ↕ No anomalies	Nothing definitive ↕
		C	2		
		P	2		
	7075-T6 bare	F	2	No anomalies (1) Adhesive gap (1) No anomalies No anomalies (1) small porosity (1)	Nothing definitive ↕
		C	2		
		P	2		
FM 123-2/BR 123	2024-T3 clad	F	1	No anomalies ↕	Nothing definitive ↕
		C	2		
		P	2		
	2024-T3 bare	F	1	No anomalies ↕	Nothing definitive ↕
		C	2		
		P	2		
EA 9628/BR 127	2024-T3 clad	F	3	No anomalies ↕	Nothing definitive Nothing definitive Nothing definitive (4) Three 1/2- to 1-in-spots (1) One 1 1/4-in. spot (1)
		C	3		
		P	6		
	2024-T3 bare	F	4	No anomalies ↕ No anomalies No anomalies (11) voids or porosity (1)	Nothing definitive (3) Spotty areas (1) Nothing definitive Nothing definitive (11) Spotty areas (1)
		C	7		
		P	12		
	7075-T6 clad	F	3	No anomalies (2) Small voids w/neutrons (1) (not w/x-ray) No anomalies ↕	Nothing definitive ↕
		C	3		
		P	3		
	7075-T6 bare	F	3	No anomalies ↕	Nothing definitive ↕
		C	6		
		P	6		

Table A-1.— (Concluded)

Adhesive/primer system	Alloy	Surface treatment <sup>a</sup>	No. of assemblies	X-ray results	Ultrasonic through-transmission results
AF 143/EC 3917	2024-T3 clad	F	2	Porosity	Nothing definitive ↑
		C	2	Porosity	
		P	5	Porosity (2) No anomalies (3)	
	2024-T3 bare	F	2	Porosity	
		C	2	No anomalies (1) Porosity (1)	
		P	4	No anomalies (3) Porosity (1)	
	7075-T6 clad	F	2	Porosity	Nothing definitive ↓
		C	2	Porosity	
		P	2	No anomalies	
	7075-T6 bare	F	2	No anomalies (1) Voids and porosity (1)	Nothing definitive (1) 9 in. area in center (1)
		C <sup>1</sup>	2	No anomalies (1) Porosity (1)	Nothing definitive
		P	2	No anomalies (1) Adhesive overlap (1)	Nothing definitive
PL 729-3/PL 728	2024-T3 clad	F	2	Porosity	Nothing definitive
		C	3	No anomalies	Nothing definitive ↑
		P	3	No anomalies (2) Small void 1/8 in. dia (1)	
	2024-T3 bare	F	2	Voids and porosity (1) No anomalies (1)	Some discontinuities (1) Nothing definitive (1)
		C	3	No anomalies (2)	Nothing definitive (2)
		P	4	No anomalies (1) Voids and porosity (3)	Nothing definitive (3) Spotty areas (1)
	7075-T6 clad	F	2	No anomalies	Nothing definitive ↑
		C	2		
		P	2		
	7075-T6 bare	F	3		Nothing definitive ↓
		C	1		
		P	2	No anomalies	Nothing definitive

<sup>a</sup>F = FPL etch

C = Chromic acid anodize

P = Phosphoric acid anodize

Table A-2.—Nondestructive Inspection (NDI) of Bonded Honeycomb Sandwich Assemblies

Adhesive/primer system	Honeycomb core treatment	No. of assemblies	X-ray and neutron radiography results	Ultrasonic through-transmission results
FM 123-2/BR 127	Dura-Core (corrosion resistant)	2	No anomalies	Nothing definitive
	Phosphoric acid anodized STD core	2		
EA 9628/BR 127	Dura-Core (corrosion resistant)	2	No anomalies	Nothing definitive
	CR III core (corrosion resistant)	1		
	Phosphoric acid anodize STD core	2		
	Standard (STD) core	1		
AF 143/EC 3917	Dura-Core (corrosion resistant)	2	No anomalies	Nothing definitive
	Phosphoric acid anodized STD core	2		

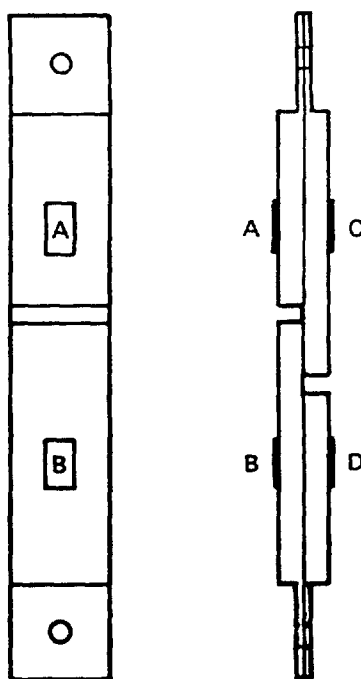


*Figure B-2.—Strain Gage Location on Thick-Adherend Lap-Shear Specimen*

Each of the four specimens was tested on two different tensile test machines to determine strain behavior under conditions of known uniaxial loading. These two machines were a Tinius Olsen 30 000-lb tensile tester and a 20 000-lb Instron Universal. Tests were made by incorporating the clevis tie rods from the jig into the test fixture and substituting wider clevises requiring a longer pin for the jig clevis tie rod.

Each of the strain-gaged specimens was then loaded into the loading fixture in the manner normally used for environmental durability testing. The orientation of the specimens within the fixture is within the tube and partly up into the helical spring, figure B-1.

Several repetitions of this loading were performed, and slight modifications were made on two of the runs. One modification was to install a hemicylindrical washer between the nut and bottom plate; the other was to replace the safety bolt by a cable.

The strains, in microinches per inch, indicated by each of the strain gages from two of the tensile tests and four of the loading fixture tests, are shown in table B-1. These strains are for a nominal applied 750 lb.

In table B-1, the sets of strains from the tensile test machines represent the widest variations between numbers obtained from two different loadings on the machines. These numbers represent practical axial loads obtainable.

**Table B-1.—Strain Gage Measurements of Thick-Adherend Lap-Shear Specimens**

(microinches per inch)

Gage designation <sup>a</sup>	1A	1B	1C	1D	2B	2D	3B	3D	4B	4D
<sup>b</sup> Tensile 1	147	101	110	136	116	143	108	162	139	140
Tensile 2	151	98	119	159	83	168	129	149	121	155
<sup>c</sup> Load 1	90	165	124	133	93	121	114	141	91	195
Load 2	129	97	150	168	90	175	115	147	90	204
Load 3	82	78	198	182	69	183	122	139	75	214
Load 4	90	73	192	181	—	—	—	—	90	175

<sup>a</sup>Gage designation: First character is specimen number  
Second indicates gage position

<sup>b</sup>Tensile 1: Instron with wide clevises  
Tensile 2: Tinius Olsen with fixture clevises

<sup>c</sup>Load 1: Standard loading of fixture  
Load 2: Standard loading of fixture  
Load 3: Installation of hemicylindrical washer  
Load 4: Installation of hemicylindrical washer and  
substitution of safety bolts by cables

By comparing the readings from a given gage (i.e., tensile 1 and 2 vs loads 1, 2, 3, and 4), it is evident that there were indeed nonaxial loads being applied to the specimen by the fixture, making it necessary to modify the fixture.

Since it has been noted with the fixtures that the springs tend to bend considerably out of line when loaded and that there was little clearance inside the spring for the specimen, the fixture design was modified to accomplish the following:

1. Load the specimen outside of the spring
2. Restrain the spring from bending out of line as much as possible
3. Compensate for small amounts of spring bending

In keeping with these objectives, the tube was lengthened to contain the entire specimen, a second alignment plate was added and the distance between the two alignment plates was set to maintain both ends of the spring, a hemicylindrical washer was installed between the nut and bottom plate, and the safety bolt was replaced by a cable. The modified fixture is shown in figure B-3.

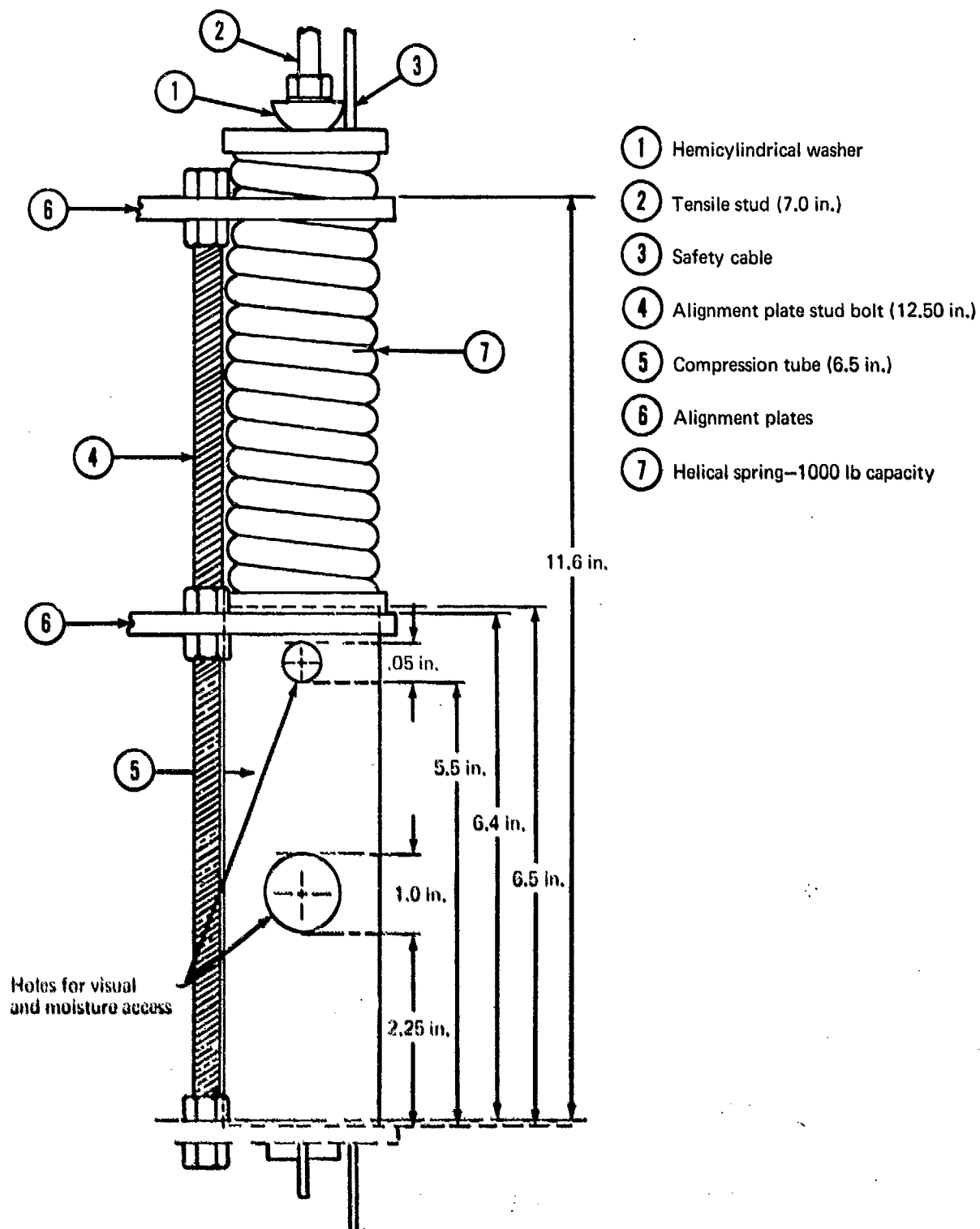


Figure B-3.—Thick-Adherend Lap-Shear Modified Loading Fixture

A prototype of this modified fixture was made as shown in figure B-3 except that two existing tubes were stacked together with a separator plate between in place of the single 6.5-in. tube shown. The gaged specimens were tested in this modified jig, and their orientation within the fixture was equivalent to that shown in figure B1, except for the specimen being contained within the tube. Strains indicated from four separate loadings to a nominal 750 lb in the modified jig are shown in table B-2. Loads 1 through 4 represent loadings of the modified fixture in a manner equivalent to the usual method of loading the fixture.

*Table B-2.—Strain Gage Measurements of Lap-Shear Specimens in Modified Loading Fixture*

(microinches per inch)										
Gage designation	1A	1B	1C	1D	2B	2D	3B	3D	4B	4D
Load 1	154	99	93	140	98	140	107	141	122	134
Load 2	160	104	110	153	99	145	111	143	123	146
Load 3	174	112	120	165	95	158	119	154	133	153
Load 4	140	108	101	150	90	149	100	159	137	152

### B.3 DISCUSSION AND CONCLUSIONS

Based on this program, it was concluded that the modified loading fixture represents a significant improvement in loading reliability over the unmodified fixture. This improvement is shown by bending moments calculated for the tensile test data for both the unmodified and the modified fixtures. Assuming that all bending is uniaxial, the resultant principal strains are shown in tables B-1 and B-2.

Two natural bending moments are produced in the lap-shear specimens under uniaxial tension. These are given by the relations:

$$M_{a-c} = \frac{2\sigma_{a-c} I}{h}, \quad M_{b-d} = \frac{2\sigma_{b-d} I}{h} \quad (B-1)$$

where  $I$  is the moment of inertia of the specimen at an unnotched cross section,  $h$  is the specimen height at an unnotched cross section, and  $\sigma_{a-c}$  and  $\sigma_{b-d}$  are given by:

$$\sigma_{a-c} = \left(\frac{A-C}{2}\right) E, \quad \sigma_{b-d} = \left(\frac{B-D}{2}\right) E \quad (B-2)$$

In equations (B-2), A, B, C, and D are the strains in inches per inch at the points shown in figure B-2 when the specimen is pulled in pure axial tension, and E is the tensile modulus of aluminum. It is obvious that for a specimen of perfect dimensions:

$$M_{a-c} = M_{b-d} \quad (B-3)$$

If it is found under a given loading condition that equation (B-3) does not hold, then there must be some external applied bending moment,  $M_{ex}$ , given by the equation:

$$M_{ex} = \frac{M_{a-c} + M_{b-d}}{2} \quad (B-4)$$

In table B-3, the values of  $M_{ex}$  are shown for specimen 1 loaded in the tensile test machines (the same two tests whose results are shown in table B-1) in the unmodified and the modified fixtures. Values of  $M_{b-d}$  are shown for all four specimens under the same loading conditions.

It is clear, then, from table B-3, that the modified fixture offers a significant improvement over the unmodified fixture. Further, it seems that the modified fixture may produce loading that is as close to uniaxial loading as is possible with the wide-area, thick-adherend, machined lap-shear specimens.

Table B-3.—Bending Moments of Lap-Shear Specimens at 750 lb Load

	Bending moments (in.-lb) at 750 lb					
	Specimen 1			2	3	4
	M <sub>a-c</sub>	M <sub>b-d</sub>	Net	M <sub>b-d</sub>	M <sub>b-d</sub>	M <sub>b-d</sub>
Axial Tinius Olsen with clevis	+ 6.56	-12.5	- 2.97	-17.42	- 4.10	- 6.97
Axial Instron without clevis	+ 7.58	- 7.18	+ 0.20	- 5.54	-11.1	- 0.02
New fixture						
-1	+12.5	- 8.4	+ 2.05	- 8.61	- 6.97	- 0.246
-2	+10.25	-10.15	+ 0.10	- 9.43	- 6.56	- 4.71
-3	+11.07	-10.87	+ 0.10	-12.92	- 5.13	- 4.1
-4	+ 8.0	- 8.61	+ 0.305	-12.10	-12.1	- 3.08
Old fixture						
-1	- 6.97	+ 6.46	- 0.205	- 5.74	- 5.53	-21.3
-2	- 4.31	-14.56	- 9.44	-17.4	- 6.56	-23.4
-3	-23.0	-21.3	-22.2	-23.4	- 3.49	-28.5
-4	-20.9	-22.1	-21.5	—	—	-17.4

## **APPENDIX C**

### **WEDGE TEST FOR ADHESIVE BONDED SURFACE DURABILITY OF ALUMINUM<sup>1</sup>**

#### **C.1 SCOPE**

This test simulates in a qualitative manner the forces and effects on an adhesive bond joint at metal-adhesive/primer interface. It has proved to be highly reliable in determining and predicting the environmental durability of adherend surface preparations. The method has proved to be correlatable with service performance in a manner that is much more reliable than conventional lap-shear or peel tests.

#### **C.2 SUMMARY OF METHOD**

A wedge is forced into the bondline of a flat bonded aluminum specimen, thereby creating a tensile stress in the region of the resulting crack tip. The stressed specimen is exposed to an aqueous environment, usually at an elevated temperature, or to an appropriate environment relevant to the use of the bonded structure. The resulting crack growth with time and failure modes is then evaluated. Variations in adherend surface quality are easily observable when the specimens are opened—forceably, if necessary—at the test conclusion.

#### **C.3 SIGNIFICANCE**

The test is qualitative only but is very discriminating in determining variations in adherend surface preparation parameters and adhesive environmental durability. In addition to determining crack growth rate and assigning a value to it, the failure mode should be evaluated and reported. For example, cohesive, adhesive-to-primer, or primer-to-adherend failures should be noted after opening the specimen at the conclusion of the period.

#### **C.4 APPARATUS**

The following apparatus is used:

1. A 5 to 30 power magnifier (preferably stereo binocular)
2. Sharp, pointed marking stylus and/or triangular file
3. Stainless steel or aluminum wedges
4. Small scale graduated in millimeters or hundredths of an inch

#### **C.5 TEST SPECIMEN**

A minimum of five 2.54- by 15.2-cm (1- by 6-in.) specimens from a single assembly shall be used for each test.

<sup>1</sup>Submitted to ASTM Committee D-14

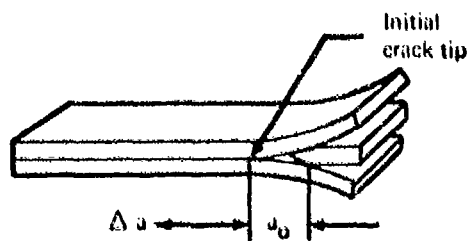
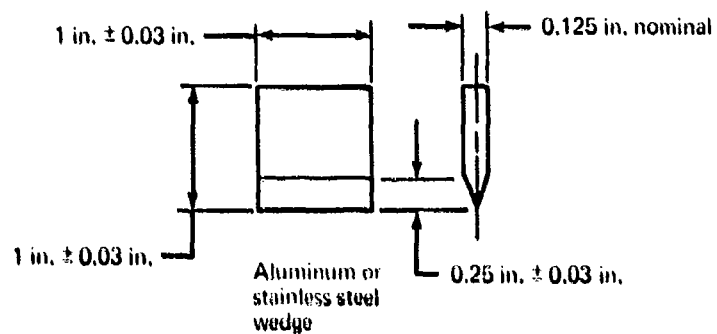
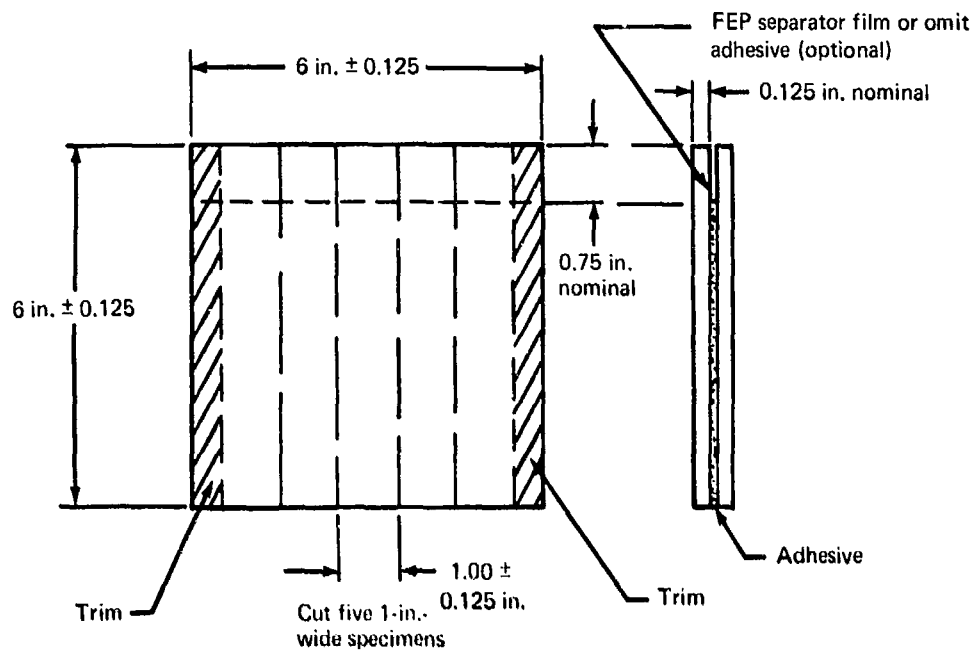
## C.6 CONDITIONING

The specimens may be exposed to any environment appropriate to the bonded structure being represented; e.g. humidity, heat, thermal shock, salt spray, etc. For most applications, however, water is the most deleterious environment to the polymer-adherend interface. A typical environment commonly used is 49°C (120°F) and condensing humidity. If consistency with other stressed durability testing requirements is desired, then the following conditions can be used:

- For 121°C (250°F) curing adhesives: 60°C (140°F) and 95% to 100% RH
- For 177°C (350°F) and higher curing adhesives: 71°C (160°F) and 95% to 100% RH

## C.7 PROCEDURE

1. Prepare the surfaces of a piece of 15.24- by 15.24- by 0.32-cm (6- by 6- by 0.125-in.) aluminum, using a surface treatment process appropriate for the test requirements.
2. Prime the faying surface of each panel, apply the adhesive, assemble the panels, and cure the adhesive as required by the appropriate specification. (For later convenience in inserting a wedge, a separation film may be inserted along one edge of the assembly as shown in fig. C-1, or the adhesive may be omitted along one edge.)
3. Cut the test assembly into five 1-in.-wide test specimens as shown in figure C-1. At least one cut edge of each specimen shall have a surface finish of 125  $\mu$  in. or better. There shall be no burrs or smearing of adherend material onto the bondline. Do not overheat or damage the bond when cutting or finishing.
4. Appropriately identify all test specimens in such a manner that testing in a high humidity environment will not destroy the identification markings. (Appropriately positioned identification markings can be made on the 6- by 6-in. (15.24- by 15.24-cm) panels prior to surface preparation processing.)
5. Crack one end of each test specimen by inserting a wedge as shown in figure C-1. Insert the wedge by using a pushing force or several relatively light taps with a hammering device. *DO NOT* insert the wedge with a single striking blow. When inserting wedge, *DO NOT* hold specimen in any way that will restrain the initial cracking. Position the wedge so that the blunt end and sides are approximately flush with those of the specimen. (In any use of an auxiliary tool to precrack a test specimen to facilitate insertion of a wedge, the extent of precracking must be less than that which is caused by insertion of the wedge.)
6. Using 5 to 30 power magnification and adequate illumination, locate the tip of the crack on the 125- $\mu$  in. finish edge of each specimen. This is the point farthest from the wedge where the specimen (the adhesive, primer, and/or adherends) has separated. Using a fine stylus or scribe, mark the location on one adherend edge. If the specimen is to be used in salt spray or other environment expected to be corrosive and liable to obliterate the mark, deepen the scribe mark with a triangular file.



Wedged Crack Extension Specimen (The end and sides of the wedge shall be approximately flush with specimen end and sides.)

Figure C-1.—Crack Extension Specimen Configuration

7. Expose the wedged specimens to the environment required by the appropriate specification.
8. Remove the specimens from the environment, and within 15 minutes mark the location of the tip of the crack after exposure in the same manner as in step 6.
9. Measure the crack extension of each specimen to (0.025 cm) 0.01 in. or less precision to determine that the crack extension is more or less than the specified amount required by the appropriate specification.
10. At the conclusion of the test, forceably open the specimen and note the failure mode of the test section.

### C.8 INTERPRETATION OF RESULTS

The crack extension  $\Delta a$  and the crack extension failure mode (i.e., adhesive failure at the interface or cohesive within the adhesive) are reported.

The initial crack length  $a_0$ , the crack extension  $\Delta a$ , and the crack extension failure mode are all a function of the adhesive/primer systems being considered and the adherend surface treatment. Because of these variables, the acceptance criteria for a bonded system of interest will have to be established. The following is an example of an acceptance criterion for 121°C (250°F) curing high-peel modified epoxy structural adhesives:

Ten specimens, representing two individual bonded test assemblies, are tested. Typically, good durability surface preparation is evidenced by no individual specimen having a crack length exceeding 19 mm (0.75 in.) and the average of all specimens being not over 6.3 mm (0.25 in.).

### C.9 REPORT ON RESULTS

1. Report the original crack length and the crack extension at the end of various time intervals, such as 1, 4, 8, 24 hours; 7, 30 days.
2. Also report the failure mode as 100% cohesive, 100% adhesive, or 50% adhesive, etc.